UNIVERSITÀ DEGLI STUDI DI PALERMO

Dottorato di ricerca in Energia e Tecnologie dell'Informazione
Dipartimento Energia, Ingegneria dell'Informazione e Modelli Matematici (DEIM)
Settore Scientifico Disciplinare ING-IND/11 – Fisica Tecnica Ambientale

Towards sustainable Net Zero Energy Buildings: life cycle energy performances and environmental impacts of a prefabricated building module

IL DOTTORE
Giovanni Tumminia

IL COORDINATORE
Prof. Ing. Maurizio Cellura

IL TUTOR
Prof. Ing. Maurizio Cellura

I CO TUTOR
Dott.ssa Ing. Sonia Longo
Dott. Ing. Marco Ferraro

CICLO XXXI
ANNO CONSEGUIMENTO TITOLO 2019

ABSTRACT

The impact of prefabrication in the building sector is currently undergoing significant growth. Although prefabricated buildings cannot in any situation replace conventional buildings, they have some characteristics, such as reduced construction time, higher safety during construction if compared to traditional buildings and modularity, that make them competitive in specific applications, that are undergoing substantial increase importance and market relevance. However, in a context where the transition towards a low-carbon energy system is quickly becoming an important target of scientific efforts and research, prefabricated buildings, as well as any other type of building, will have a key role in achieving the decarbonisation of the building sector.

In this contex, this work of thesis explores the energy and environmental performances of a NZEB modular case study: the IDEA (Integrating Domotics, Energy and Architecture) building. The case study is a prototype of a net zero energy housing module, integrating renewable sources energy generation systems (PV system) and innovative materials (fiber reinforced polymers materials) in Messina (Italy) at the “National Research Council of Italy– Institute for Advanced Energy Technologies”. Through the Life Cycle Assessment (LCA) methodology all life cycle stages were included in the study: materials and component production, construction process, use and end-of-life. Monitoring studies were performed during 2 months. The building use stage was simulated through and energy plus model, validated on monitored data.

Abstract

In addition to investigate the overall energy and environmental performances of the existing prefabricated modular unit, another aim of the research is to analyze several building redesign option through a multidisciplinary approach with a view to the entire building life cycle. In this context, the research proposes a multidisciplinary methodological framework which allows to integrate into the building design and investigate at the same time the use stage energy performances, the load matching and the grid interaction issues, the life cycle overall performances and the economic feasibility.

The results show that the materials production stage alone accounted for about 50 - 80% of the total energy and environmental impacts caused by the building. The use stage is the second most impactful stage (about the 31% on average of the total life cycle impacts), while the construction and the end-of-life stages give a marginal contribution to the total impacts. In this context, the findings of the research pointed out the relevance of LCA in the assessment of the building energy and environmental performances. In particular, the study demonstrates that reaching the Net Zero target during the use stage could imply the displacement of the environmental impacts to the other stages, as well with a prevalence towards the production of the building materials. Therefore, a mere focus on the use stage performances cannot give the whole picture that is required in the context of a paradigm shift towards decarbonisation policies. Focusing only on the assessment of the energy consumptions related to the use stage quantifies the reduction of the environmental burdens of this stage but it does not guarantee that the life cycle overall performances will be improved. Thus, the integration of the LCA methodology in the design choices is of paramount importance to support the development of sustainable buildings.

Moreover, the research shows that the design of any type of building requires an integrated and multidisciplinary design approach, covering a number of key aspects such as energy saving, life cycle environmental impacts, economic feasibility and many others, to create the conditions for a significant decarbonisation of the building sector. In this context, the multidisciplinary methodological framework can be used to explore and improve the low sustainability performing areas over the life cycle of new modular building designs. Moreover, the methodological approach can also be adopted for sustainability assessment of other type of constructions.

TABLE OF CONTENTS

LIST OF FIGURES

LIST OF TABLES

NOMENCLATURE

ADP = Abiotic resource Depletion Potential

AFN = Airflow Network

AP = Acidification Potential

CV(RMSE) = coefficient of variation of the root mean square error

EED = Energy Efficiency Directive

EES = electric storage system

EP = Eutrophication Potential

EPBD = Energy Performance of Buildings Directive

EPCs = Energy Performance Certificate

f_{grid} = grid interaction index

FRP = pultruded fiber reinforced material

FU = functional unit

GER = Global Energy Requirement

GWP = Global Warming Potential

Nomenclature

HVAC = Heating, Ventilation and Air Conditioning

LCA = Life Cycle assessment

LCI = Life Cycle Inventory

LCIA = Life cycle impact assessment

LOLP = loss of load probability

MBE = mean bias error

ne = net exported electricity

NMBE = normalised mean bias error

NPV = net present value

NPV_r = relative net present value

nZEB = nearly Zero Energy Building

NZEB = Net Zero Energy Building

ODP = Ozone Depletion Potential

PBT = payback time

PCM = phase change material

$P_{e\approx 0}$ = no grid interaction probability

POCP = Photochemical Ozone Creation Potential

PV = photovoltaic system

R^2 = coefficient of determination

RES = renewable energy sources

RMSE = root mean square error

RSP = reference study period

WWR = window-to-wall area ratio

γ_{load} = load cover factor;

γ_{supply} = supply cover factor

SUMMARY

Building energy renovation is one of the pillars upon which the 2050 European low carbon goals are based (European Commission, 2011). In this context, the concept of NZEBs (Net Zero Energy Buildings) has been developing through policy and research agendas during the last decade throughout the world as practical embodiment of the prototype ideas described, among the others, by Rifkin in its description of the third industrial revolution (Rifkin, 2011). For example, the recast of EU Directive on Energy Performance of Buildings (EPBD) has stated that all new buildings in the member states should be nearly zero energy buildings (nZEBs) by 2020 (EPBD Recast, 2018). In the United States, the Building Technological Program point out the strategic goal toward achieving marketable energy zero homes in 2020 and zero commercial energy buildings in 2025 (US DOE, 2008).

However, both with the definition of the nZEBs and NZEBs, major efforts to achieve decarbonisation of the building sector are inspired to minimize the energy impacts in the use stage, since the primary energy consumption in this stage is the most relevant in the entire life cycle of conventional buildings. On the other hand, fulfilling minimum requirements will not be enough to reach the GHG emission target set for 2050. In detail, as buildings move towards the zero energy target, the impacts of product embodied energy becomes much more important to the building's life cycle.

Moreover, the large-scale deployment of NZEBs will involve multiple interconnected factors. Therefore, the design of future buildings will require the cooperation of different expertise including building physics, economic assessment, energy, life-cycle impact assessment and social sciences, each of them with existing tools adapted to their particular focus.

For all this reasons, this thesis investigates the significance of utilizing multidisciplinary approaches in the context of zero energy building practices within the built environment today. In detail, the aim of this research is to verify if the prefabricated modular buildings can couple use stage energy efficiency with life cycle environmental sustainability through the analysis of an existing case study.

In particular the thesis focuses on a study of the energy performance and the environmental impacts of a NZEB modular case study: the IDEA (Integrating Domotics, Energy and Architecture) building. The case study is a prototype of a net zero energy housing module, integrating renewable sources energy production systems (PV system) and innovative materials (fiber reinforced polymers materials), located in Messina (Italy) at the “National Research Council of Italy– Institute for Advanced Energy Technologies”.

All life cycle stages were included in the study: materials and component production, construction process, use and end-of-life. The LCA methodology, based on the standards of the ISO 14040 (ISO, 2006a) and ISO 14044 (ISO, 2006b) and according to the regulation UNI EN 15978 (UNI, 2011), was used to quantify energy and environmental impacts associated to the entire building life cycle. Monitoring studies were performed during 2 months. The building use stage was simulated in Energy Plus environment (DoE, 2010), validated obtaining limited differences between monitored and simulated data.

In addition to investigate the overall energy and environmental performances of the existing prefabricated modular unit, another aim of this research is to analyze several building redesign option through a multidisciplinary approach with a view to the entire building life cycle. In detail, the redesign options have been selected trying to reduce the use stage energy consumptions. In order to optimize the self-consumption of electricity generated and to reduce the stress on the energy networks, load matching and grid interaction issues were also taken into account. Moreover, since focusing only on the assessment of the energy consumption related to the use stage quantifies the reduction of the environmental burdens of this stage but it does not guarantee that the life cycle overall

performances will be improved, the LCA methodology was used to investigate each of the proposed scenarios. Finally, since to reach the target of NZEBs, the technical feasibility in general is not sufficient to help the diffusion of NZEBs into building current practice, a preliminary analysis of the economic feasibility of the different design option have been conducted.

Each scenario investigates some specific parameters that are closely related through wide applications of parametric analyses by analyzing the combined effects of all of them to the end results. The effect on other parameters not included as main focus of this thesis is also included when deemed necessary (e.g. visual comfort when investigating variation of window to wall ratio).

The material production stage causes the highest impact for almost all the examined impact categories. For the products stage, fiber reinforced polymers material, that it is the main material used in the building envelope (about 77%), accounts for more than 40% of the impacts for almost all environmental and energy indicators, with the exception of the ODP and the ADPe. The use stage is the second most impactful stage. Even though the overall PV energy generation (about 8,000 kWhe) in a year surpasses the electricity consumption (2,700), about 79% of the energy produced is fed into the grid and about 47% of the electricity consumption is supplied by electricity imported from the electricity grid. The construction process and the end-of-life stages give a marginal contribution to the total impacts. Since the main construction works are performed outside the construction site, the construction of the building is done with few easy operations that require a limited amount of inputs. Furthermore, the selective demolition of the building allows to obtain uniform and separated waste and this increases the possibility of recycling the wastes.

In detail, to decrease the risk of overheating in summer and reduce the energy needed for cooling, into the building redesign the window-to-wall area ratios (WWRs) of the north and south façades were reduced to the 15%, the insulation thickness on all the exterior walls was also changed, and a simple ventilation strategy to model occupant reactions to temperature variation was implemented, allowing a reduction of the building energy demand of about 17% if compared to the existing building, with a decrease of the cooling consumption of about 57.3%.

Moreover, in order to optimize the self-consumption of generated electricity, in the redesign the building was equipped with a 3.84 kWh electric storage system, which allows to match the building energy demand with the

PV energy generation, while, in order to reduce the stress on the power grids, the nominal power of the PV system was varied from 5.76 kWp to the 1.92 kWp. The downsizing of the PV system coupled with the sizing of the electrical storage system show that on yearly basis the 81% of the building electric demand is covered by on-site electricity generation.

The LCA results show that, for all the impact categories investigated, if compared to the base case the redesign solution shows a reduction in the environmental and energy impacts between 3.1% (ODP) and 50.5% (ADPe) reaching values above 20% in the case of GWP (24%), AP (22%), EP (20%), POCP (22%), ADPff (24%) and GER (20%). In detail, the operational energy use, due to the reduction of the imported energy, shows the highest impacts reduction followed by the materials end-of-life stage and the materials production stage.

The preliminary results of the cost analysis show that the redesign solution is more cost-effective than the base case. In particular, the difference between the net present value (the combination of the initial investment cost and the difference between the present value of future money inflows and the present value of future money resulting from the initial investment) of the base case and the redesign solution shows that the redesign solution produced a profit between € 700 and € 1500 compared to the base case after 25 year.

In conclusion, although the outcomes of the study are based on the specific conditions of the assessed building, the design of any type of building, even modular building, requires an integrated and multidisciplinary design approach, covering a number of key aspects such as energy saving, life cycle environmental impacts, economic feasibility and many others, to create the conditions for a significant decarbonisation of the building sector.

Generally, the minimization of the use stage energy consumption and related polluting emissions is the main objective of the public perspective. On the other hand, when the optimization of building energy performance is faced, it is fundamental to consider also the cost-effectiveness of the design solutions, which is the principal aim of the private perspective. Moreover, a successful design and construction of a NZEB includes not only energy efficient measures and adoption of renewable energy sources targeting to the minimization of the energy needs, but also an effective grid integration in order to accomplish the appropriate balance between consumption and production. Finally, also a life-cycle oriented approach is particularly needed to assess the environmental impacts associated with all the stages of the building's lifespan. For all this reasons, the optimization of building design is a complex multi-objective problem with a huge domain of design variables and several potential objective functions. Therefore, the need to address multiple and often contradicting objectives emphasizes the necessity of a holistic approach during all stages of the design process.

In context, the research proposes a multidisciplinary methodical framework which allows to integrate into the building design and investigate at the same time the use stage energy performances, the load matching and the grid interaction issues, the life cycle overall performances and the economic feasibility. It can be used to explore and improve the low sustainability performing areas over the life cycle of new modular building designs. Moreover, the methodological approach can also be adopted for sustainability assessment of other type of constructions.

Finally, while energy performance and environmental effects of traditional buildings have been previously studied in detail, limited number of works about prefabricated constructions and more in particular about modular buildings are available in literature. In this context, this research contributes to the current body of knowledge by providing a deeper insight into the environmental performance of modular buildings by investigating the importance of the design of a building to its whole life cycle sustainability performances. The outcomes of this study may help construction industry practitioners, such as decision makers, policymakers, clients, developers, engineers, contractors, and modular manufacturers, to have a better understanding of modular construction and devise appropriate strategies to overcome the identified challenges.

1 INTRODUCTION

1.1 BACKGROUND

During the last Conferences of the Parties held in Paris and in Marrakech (COP21), Member States set out a global plan to put the world on track with two main objectives (Rogelj et al., 2016):

1) to avoid dangerous climate change by keeping global warming well below 2°C above pre-industrial levels;

2) to pursue an effort to limit the temperature rise to 1.5°C.

This ambitious long-term objective will require the start of “zero GHG emission” from a period between 2020 and 2030. The most recent report of Intergovernmental Panel on Climate Change (IPCC) (Allen et al., 2014), published in 2014, estimates that through technical measures approximately 29% of emissions could be avoided in residential and commercial building sector in 2020 and 40% in 2030. Governments are paramount in order to create and coordinate buildings sectors’ responses and must be able to identify and encourage synergies between buildings adaptation to climate change and GHG emissions mitigation. In Europe, the building sector is responsible for huge energy consumption and results as one of the most influent sectors in which reduction action should be regulated. Buildings account for approximately 40% of global energy consumption and 36% of CO_2 emissions (EPBD Recast, 2018). Moreover, considering that almost 70% of the existing building stock will still be used in 2050 and that it is expected a 25% increase in building stock, a long-term vision is needed to align with future challenges because without any reduction regulation CO_2 emission could be double or triple by 2050. From this point of view, the updating of the European directives offers a possibility to develop actions aimed at lower energy consumption and a reinforced use of renewable energy sources (RES).

1 Introduction

After the 2007 Climate and Energy package of 20% reduction of buildings primary energy consumption by 2020, 20% increase of renewable energy production and 20% decrease of greenhouse gas emissions from 1990 levels, new targets have been introduced by the 2030 Climate & Energy framework (Helm, 2014). This package fixes the reduction of greenhouse gas emissions at 40% from 1990 levels, the share for renewable energy at 27% and the improvement in energy efficiency at 27%. Finally, on March 2011, the European Commission adopted a "Roadmap for moving to competitive low carbon economy" with reference to 2050, identifying from this perspective the need for greater attention to energy efficiency (European Commission, 2011). In this document, the European Commission has established a long-term goal of reducing CO_2 emissions for the building sector by 88-91% by 2050 compared to 1990 levels. In order to address climate change issues, the European Parliament has promoted different directives for energy efficiency in the building sector. Regulations involve energy certification of buildings and incentives for the reduction of the operational energy use in buildings through the introduction of minimum energy requirements for new buildings and the promotion of energy retrofitting of existing ones.

In this context, the concept of NZEBs (Net Zero Energy Buildings) has been developing through policy and research agendas during the last decade throughout the world as practical embodiment of the prototype ideas described, among the others, by Rifkin in its description of the third industrial revolution (Rifkin, 2011). For example, the recast of EU Directive on Energy Performance of Buildings (EPBD) has stated that all new buildings in the member states should be nearly zero energy buildings (nZEBs) by 2020 (EPBD Recast, 2018). In the United States, the Building Technological Program point out the strategic goal toward achieving marketable energy zero homes in 2020 and zero commercial energy buildings in 2025 (US DOE, 2008).

Moreover, beyond the contributions in reducing both energy consumption and GHG emissions, the dissemination of NZEBs can contribute to achieving to the Sustainable Development, that has been highlighted as a central idea for our age (Sachs, 2015), and in more detail they can contribute to achieving the Sustainable Development Goals (SDGs), a collection of 17 global goals (Fig. 1.1) set by the United Nations Development Programme to end poverty, protect the planet and ensure prosperity for all (Sachs, 2012; UN, 2015).

Fig. 1.1 - The Sustainable Development Goals (SDGs) (Sachs, 2012; UN, 2015).

The buildings are key in achieving economic, environmental and health benefits (Laski & Burrows, 2017). Insights about the importance of nZEB and how they contribute to achieving the SDGs are provided in a point-by-point manner below (Czerwinska, 2017):

- **SDG 3** – Good health and well-being: Diseases caused by poor indoor environmental quality are common in developing countries. The implementation of onsite renewable technologies and energy efficiency measures in buildings, particularly in cities, would improve the health by improvement of air quality.
- **SDG 7** – Affordable & clean energy: Sustainable energy provides an opportunity to guarantee universal access to modern energy. On-site renewable technologies are technically and economically feasible nowadays.
- **SDG 8** – Decent work & economic growth: Demand for new buildings should grow to cover the housing deficit and to meet the rising population. As a result, more workforce is necessary to deliver them. Deployment of on-site renewable in the future building sector would contribute to the inclusive employment goal.
- **SDG 9** – Industry, innovation & infrastructure: Future building stock design should be resilient and adaptable to the global climate change. In developing countries is even more important because these countries are more vulnerable to the effects of the global climate change. In this sense, the deployment

of nZEB in the coming building stock would be a driver for industrialization and for innovation to face the global climate change.

- **SDG 11** – Sustainable cities and communities: Buildings are the heart of the cities. Then, high performance buildings would contribute to ensure a better quality of life for all.
- **SDG 12** – Responsible consumption e production: The building industry has a major role to play in preventing waste through reduction, recycling and reuse – ‘circular economy’ principles where resources are not wasted.
- **SDG 13** – Climate action: Since building sector is responsible for 32% of the final energy consumption and 19% of the energy-related CO2 emissions (Edenhofer, Pichs-Madruga, Sokona, & Minx, 2014; International Energy Agency, 2017; UN Environment and International Energy Agency, 2017), CO2 emissions mitigation in this sector should be considered in climate action.
- **SDG 17** – Partnerships for the goals: The barriers to a sustainable built environment are not overcame with technical solutions (Laski & Burrows, 2017). Instead of that, the solutions should be related to how effectively the stakeholders collaborate between them, guaranteeing the communal efforts are accurately aligned to achieve much greater impact. In this sense, to strengthening partnership with the institutions involved with the achievement of the rest of the SDG´s is important.

However fulfilling minimum requirements will not be enough to reach the GHG emission target set for 2050. In detail, as buildings move towards the zero energy target, the impacts of product embodied energy becomes much more important to the building’s life cycle, as clarified by many research works stating that the excessive attention paid to the operational energy consumption and the concomitant lack of control on the other stages of the lifecycle involves the reduction of the environmental burden to almost zero of this phase but it may cause relevant increases in use of energy throughout the rest of its life cycle. For these reason, a life-cycle oriented approach is particularly needed to assess the environmental impacts associated with all the stages of the building’s lifespan.

1.2 PREFABRICATED BUILDING HOUSING MODULES

All of the above taken into account, in order to achieve a sustainable future for generations to come, the general building design process will have to adapt to the challenges created by the growth of population and limited energy supply. There are multiple actions that can be undertaken in the sector to achieve those goals. One of the solutions to solve this could be the use of modular prefabricated units.

Due to several causes, ranging from natural disasters to temporary working needs, or as a solution to economic and demographic growth in developing countries, the need for lightweight modular buildings is widespread around the world. The impact of prefabrication in the whole building market is currently undergoing significant growth. For example, in USA modular/prefabricated housing reach 140,000 units in 2017, representing 14% annual growth from 2012 (Gibb, 2007).

Modular construction is not a new concept. Its lineage can be traced to 1837, when Henry Manning developed the Manning Portable Cottage. Built in London, this prefabricated home was shipped to British emigrants scattered across the empire (Bergdoll, Christensen, Christensen, & Oshima, 2008). Almost two centuries after Manning, the benefits of modular construction are clearly defined (Lu, 2007): a reduction in construction time due to efficient scheduling and parallel production activities, increased building quality, increased labour productivity and safety, minimized environmental impact on the construction site, and a quicker return on investment (Schoenborn, 2012).

Although modular buildings, and more in general prefabricated buildings, cannot per se replace conventional buildings, the motivation for using modular construction generally arises because of over-riding client requirements for speed of construction, improved quality, and for early return of investment. Furthermore, there is a noticeable trend to use modular construction in social housing, where speed of construction is allied to economy of production scale, and to reduced disruption in congested inner city sites.

Modular buildings can save around 40% of construction time compared with traditional construction (R M Lawson & Ogden, 2010; Smith, 2010). Manufacturing numerous building components simultaneously can save costs because materials can be ordered in bulk and labor and machinery transportation can be reduced (Quale, Eckelman, Williams, Sloditskie, & Zimmerman, 2012).

1 Introduction

Workplace accidents, congestion, severe weather, dangerous activities, and neighboring construction operations can be reduced by transferring the main construction work to factories with easier and highly repetitive site operations (Cartz & Crosby, 2007; Kamali & Hewage, 2016; R. Mark Lawson, Ogden, & Bergin, 2012; Lu, 2007). According to Lawson et al. (2012), when modular construction is used, on-site reportable accidents can be reduced by 80% compared to on-site construction (R. Mark Lawson et al., 2012).

Several environmental benefits are offered in modular construction. Less waste is one of the most important benefits of more precise purchasing, planning, and cutting of materials and appropriate recycling opportunities (L. C. Jaillon, 2009; R. Mark Lawson et al., 2012; Lu, 2007, 2009; Moon, 2014),

At the end of the modular buildings' life cycle, modules can be disassembled, relocated or refurbished to be used in other projects instead of disposal (Li & Li, 2013). On-site reduction of greenhouse gas (GHG) emissions is another benefit of modular systems (Amiri, Caddock, & Whitehead, 2013; Lu & Korman, 2010). Reduced construction time leads to less energy consumption, fewer workers' trips, fewer trips by suppliers and subcontractors to the construction sites (due to material delivery in bulk to the factory plants) (Kamali & Hewage, 2016).

Finally, higher quality can be achieved with the use of modular construction due to the controlled manufacturing facilities in which the components are built. Repetitive processes and operations, as well as automated machinery, can result in a higher level of product quality (Ambler, 2013; Cartz & Crosby, 2007).

These advantages, can justify the use of modular construction by the construction industry practitioners as an effective alternative, more than in the past. However, despite many reported advantages of modular buildings, its application is still limited when compared to the conventional construction approach (Kamali, Hewage, & Milani, 2018; O'Neill & Organ, 2016; Quale et al., 2012; Steinhardt & Manley, 2016). Prefabrication in US construction has steadily risen over the last two decades, leading to an average use of 35% in new construction in 2016 (Parsons, 2017). The percentage of fully modular new construction, however, is far less significant, limited to around 3% of single family houses and around 1% of multi-family residences between 2000 and 2014 (Kamali & Hewage, 2016).

A key reason for reluctance to accept innovated construction techniques is the difficulty of ascertaining the benefits that they offer (Pasquire & Gibb, 2002). For many of those involved in the construction process, the benefits of using modular buildings were not well understood (Lu, 2007). As a result, decisions surrounding this construction techniques are largely made based on anecdotal evidence rather than rigorous data (Blismas, Pasquire, & Gibb, 2006; Blismas & Wakefield, 2009; Pasquire & Gibb, 2002).

1.3 RESEARCH AIM

The energy performance and environmental effects of traditional buildings have been previously studied in detail, while a limited number of works about prefabricated constructions and more in particular about modular buildings are available. However, for a reliable and convincing case for the improved uptake of the prefabrication technology, there is a need to provide empirical evidence in terms of its quantifiable benefits. This study contributes to filling the existing knowledge gap on the evidence-based and quantifiable benefits of modular technology.

In this context, the aim of this research is to verify if the prefabricated modular buildings can couple use stage energy efficiency with life cycle environmental sustainability through the analysis of an existing case study: the IDEA (Integrating Domotics, Energy and Architecture) building showed in Fig. 1.2. In detail, it is a prototype of a NZE housing module integrating renewable sources energy production systems (PV system) and innovative materials (fiber reinforced polymers materials).

Fig. 1.2 - The IDEA building.

This objective was investigated, combining both the analysis of the use stage and of the whole life cycle, to avoid the shifting of environmental and energy burdens from one stage to others and analyze the hotspots of the building during its life cycle. All life cycle stages were included in the study: materials and component production, construction process, use and end-of-life. The use stage was simulated through dynamic building energy simulation, using data collected during on-site monitoring for model calibration. The LCA methodology, based on the standards of the ISO 14040 (ISO, 2006a) and ISO 14044 (ISO, 2006b) and according to the regulation UNI EN 15978 (UNI, 2011b), was used to quantify energy and environmental impacts associated to the entire building life cycle.

In addition to investigate the overall energy and environmental performances of the prefabricated modular unit, another aim of this research is to analyze several building redesign option through a multidisciplinary approach with a view to the entire building life cycle. In detail, the redesign options have been selected trying to reduce the use stage energy consumptions. In order to optimize the self-consumption of generated electricity and to reduce the stress on the surrounding energy networks, load matching and grid interaction issues were also taken into account. Moreover, since focusing only on the assessment of the energy consumption related to the use stage quantifies the reduction of the environmental burdens of this stage but it does not guarantee that the life cycle overall performances will be improved, the LCA methodology was used to investigate each of the proposed scenarios. Finally, since to reach the target of NZEBs, the technical feasibility in general is not sufficient to help the diffusion of nZEBs into building current practice, a preliminary analysis of the economic feasibility of the different design option have been conducted.

In context, the research proposes a multidisciplinary methodical framework which allows to integrate into the building design and investigate at the same time the use stage energy performances, the load matching and the grid interaction issues, the life cycle overall performances and the economic feasibility. It can be used to explore and improve the low sustainability performing areas over the life cycle of new modular building designs. Moreover, the methodological approach can also be adopted for sustainability assessment of other type of constructions.

Moreover, the research contributes to the current body of knowledge by providing a deeper insight into the environmental performance of modular buildings by investigating the importance of the design of a building to its whole life cycle sustainability performances. The outcomes of this study may help construction industry practitioners, such as decision makers, policymakers, clients, developers, engineers, contractors, and modular manufacturers, to have a better understanding of modular construction and devise appropriate strategies to overcome the identified challenges.

1.4 THESIS STRUCTURE

The thesis comprises ten chapters as follows.

Chapter 1 introduces the research, highlights statement of research problem, study objectives, research propositions, scope of research work and the importance of research findings.

Chapter 2 addresses the EU legal framework on reducing energy consumption of buildings. The provisions, challenges and opportunities of the principal energy efficiency laws - Energy efficiency directive (EED) and Energy Performance of Buildings Directive (EPBD) - and supporting legislation - Renewable Energy Directive (RED) and the Eco-Design Directive are broadly examined.

Chapter 3 focuses on review of related literature on the subject with a view to putting the work in the context of previous studies. In detail, the first part of the chapter shows the concept of Net Zero Energy Buildings (NZEBs) in more detail: it presents the review of different definitions, related technologies and measures to reach NZEB target. Moreover, since the energy performance and environmental effects of traditional buildings have been previously studied in detail, while a limited number of works about prefabricated constructions are available, in the second part of the chapter, literature studies on the energy and environmental performances of prefabricated buildings are discussed.

Chapter 4 is focussed on the case study. In this chapter the case study building will be shown, starting from the design phase and explaining the main features of the building: the IDEA (Integrating Domotics, Energy and Architecture) building.

Chapter 5 outlines the methodology of the proposed framework, used for the integrated life cycle energy and environmental assessment of the building case study, and explains how the detailed analyses are conducted. In detail, the first part of the chapter provides a detailed insight of the modelling and simulation steps followed, while the second part of the chapter describes the life cycle model developed to assess environmental impacts caused by the building.

Chapter 6 focuses on modelling and simulation of energy consumption related to the building case study introduced in chapter 4. In detail, this chapter, to ensure that the building model is an accurate representation of reality and that their data outputs are reliable, shows the calibration and validation results obtained for the case study.

Chapter 7 investigates the energy performances of the existing building case study. In the first part of the chapter, to study the answer of the dynamic model, the temperature trends in some critical days in terms temperature were analyzed. Firstly, free-floating conditions were assumed in order to investigate the natural indoor thermal performance of the spaces. Then, in order to investigate also the energy consumption for heating and cooling, the HVAC system modeled was activated with temperature reference set points in summer and winter. In the second part, monthly and yearly energy consumption and generation were analyzed. Two different energy balances were calculated: LG Balance and Weighted Balance. Finally, to quantify the load-matching levels and Grid Interaction for the case study, quantitative indices, selected in the chapter 5, were presented.

Chapter 8 presents the Life Cycle Assessment results. The first section shows the results for the entire building life cycle. Moreover, according to the European Standard UNI EN 15978 (UNI, 2011) and in order to achieve the goals set in goal and scope definition stage, more details are shown for each life cycle stage. Finally, in order to compare the primary energy use and environmental impacts due to the entire building life cycle to the primary energy use and environmental impacts potentially avoided thanks to the renewable energy produced during the use stage, energy and environmental payback times are shown.

Chapter 9, in order to optimize the design of the module, a redesign results of the building case study are shown. The redesign options were selected trying to reduce energy consumptions and to increase the building energy performances. In order to optimize the self-consumption of generated electricity and to reduce the stress on the energy grids, load matching and grid interaction issues were also taken into account. Moreover, to guarantee coherence and feasibility of all the potential solutions, the LCA methodology and a preliminary analysis of the economic feasibility were used to investigate each scenarios proposed.

Chapter 10 is the closing chapter and summarizes key results, draws conclusions for the dissertation and discusses the implications of the research highlights the contribution of the study to the body of existing knowledge.

2 EU REGULATORY FRAMEWORK ON BUILDINGS

2.1 INTRODUCTION

The EU regulation on reducing energy consumption of buildings is generally based on directives which set minimum requirements, obligations and measures for all Member States to abide by. These directives include specific energy efficiency standards for both new and existing building stocks. The Union law has to be transposed to Member States' legal systems (with equal or more stringent requirements) in order to reduce the energy consumption of this sector.

This chapter will therefore examine the EU principal legislation on energy efficiency (EED, 2012; Recast, 2010) and the EU's growing portfolio of legislation that addresses and promotes reducing energy consumption of buildings. These directives and regulation are relevant in addressing the reduction of the environmental impact of the building sector by targeting different measures, goals and different aspects of energy savings. They also variably influence the consumers behavior and regulate the operations of energy providers.

There are two principal legislative instruments that are designed to address this goal within Member States. These are the Energy Efficiency Directive (EED - Directive 2012/27/EU), and the Energy Performance of Buildings Directive (EPBD - Directive 2010/31/EU) as discussed in the following sections (EED, 2012; Recast, 2010).

In this context, the first section and the second will focus on the EED and EPBD directives, respectively. Bearing in mind that these regulatory instruments cannot be assessed in isolation, the third section further examined the supporting directives namely the RED and the Eco-Design Directive. To conclude, this chapter also focuses on the EPBD legislative updates in the last section.

2.2 ENERGY EFFICIENCY DIRECTIVE (EED)

The EED recast (2012) was developed with the primary objective "to establish a common framework of measures for the promotion of energy efficiency" repealing and merging two directives on energy efficiency to ensure that opportunities for improvements are addressed. The EED was intended to help achieve the target of 20% primary energy savings in 2020, offer a direct response to increased dependence on energy imports, climate change mitigation initiatives, and ensuring energy security within the EU Member States (Burman, Mumovic, & Kimpian, 2014). It is well understood as a key policy instrument to decrease energy consumption of EU buildings and convert national building stocks from energy consumers to energy producers (D'Agostino, Zangheri, & Castellazzi, 2017).

The directive mandates Member States to use energy more efficiently at all stages of the energy chain, from production to final consumption in various sectors of the economy to promote smart use of energy (Schiavo, 2013). The EED promotes the reduction of energy demand compared to the business-as-usual pathway where energy demand is rising rapidly within the EU and globally as a result of rapid industrialization and urbanization in particular. The EED has key Articles and measures on energy efficiency promotion which are directly linked to buildings. Some Articles have cross-sectoral level coverage with great relevance to energy efficiency of buildings. Although the EED is a cross sectoral instrument, this section will address the main components of the directive which is applicable to energy efficiency of buildings. The focus will be on renovations and energy usage by public buildings, energy efficiency supply obligations, efficiency in energy use and horizontal provisions which are geared to drive GHG emissions.

2.2.1 Public buildings

Public buildings renovation is an important driver in reducing GHG emissions from the EU given the special role of the public sector in owning a considerable share of the total building stock (Schiavo, 2013). The higher visibility of public buildings in public life gives the public sector greater responsibilities for meeting the energy efficiency of buildings targets in future (Handbook, 2013). The directive focuses on the EU's long-term strategy on energy efficiency of buildings that addresses cost-effective renovations and procurement of energy-efficient materials of the existing public buildings primarily in Articles 4, 5 and 6. The obligation to renovate central government buildings complements Directive 2010/31/EU, which promotes the improvement on the energy performance of buildings within the Union, taking into account outdoor climatic and local conditions, as well as indoor climate requirements and cost-effectiveness (Parejo-Navajas, 2015).

Member States have an obligation to renovate 3% of public bodies buildings per year (3% of total useful floor area over 500 m2 and lowered to over 250 m2 as of 9 July 2015) showing that the public sector has a responsibility to lead by example (Article 5). The public sector is, "an important driver to stimulate market transformation towards more efficient products, buildings and services, as well as to trigger behavioral changes in energy consumption by citizens and enterprises" (EED, 2012). The mandate also extends to the procurement of products, services and buildings with high energy-efficiency performance which is a sound condition to ensure energy savings and promote energy efficiency (Article 6 (1) as recommended in Annex III). To ensure public accountability and transparency, "public bodies are required to publish an inventory of buildings they own, the floor area of each building and the energy performance of each building" (EED, 2012). One limitation of the procurement provision is the existence of the purchase threshold established in Article 7 of Directive 2004/18/EC (CEU, 2004). The threshold hinders efforts of far-reaching energy efficiency since procurement obligations cannot be enforced for procurements below the stipulated threshold of EUR 162,000.

2.2.2 Energy efficiency obligation schemes, audits and energy management systems

The EED introduces measures to be undertaken by Member States and utility companies for improving energy efficiency and reducing dependency on oil and gas imports by creating an energy efficiency obligation requirement in Article 7. The ways in which these measures are implemented are left to the discretion of the Member States. With the energy savings or reduction obligation to 1.5% per year, the Article lays great responsibility for utility companies (energy distributors or retail energy sales) to be major players in reducing the customers' energy use of buildings and other sectors of the economy. They have control of the infrastructure and customer base which is important to GHG emissions. In this context, the utility companies are turned into service companies rather than simply sellers of energy thus introducing legal obligations that make utility companies key players in the energy efficiency game.

Article 8 outlines the obligations to implement energy audits and energy management systems to be carried after every 3 years. The audits are a critical part of checking progress of goals set towards achieving the broader goals by 2020. Energy audits and management system tools provides additional measures for reducing end-user energy by providing consumers with the necessary information and tools to make more energy efficient decisions. Providing customers with their energy usage information have a potential to encourage a change of behavior towards energy savings. Energy audits are "used to identify, quantify and report existing energy consumption profiles and energy savings opportunities in buildings, industrial or commercial operations or installations, and in private or public services" (EED, 2012).

2.2.3 EED challenges and opportunities

The EED is crucial for achieving energy efficiency goals and targets in the EU although there are still major challenges to be overcome. In 2015, the Commission report on the implementation of the EED heavily criticizes the insufficient implementation of both the EED and the related EPBD, and calls on both Member States and the Commission to improve implementation and enforcement. Despite setting out ambitious goals, the directive has been criticized for following the policy objective of reaching indicative national targets for Member States rather than the binding targets (Schiavo, 2013). Specific Member States binding targets that promote energy efficiency improvements is preferred to indicative targets, however, the failure to focus on binding targets reflects the

Council's relaxed position in accepting 'binding terms' and to ensure that Member States are not overburdened (Schiavo, 2013). Indicative targets are criticized for not sharing the same guarantees of compliance as the binding ones, and they appear problematic to enforce (Schiavo, 2013). According to the Commission's 29th Annual Report, obligations to submit plans and to reach binding targets are quite often neglected, and the infringement procedure is an insufficient deterrent for Member States to avoid non-compliance (EED, 2012).

Efforts to repeal the EED to adapt the directive to meet EU climate and energy targets for 2030 and align it with other aspects of the Clean Energy package have been pursued since November 2016. The revised EED has an upgraded binding target to achieve 30% energy consumption reduction by 2030 beyond the 27% indicative target (Commissie, 2004). The updated EED will ensure Member States upgrade their smart meters to ensure that they are read remotely. This applies to all energy installations and district heating, cooling and domestic hot water thus leading to greater transparency in billing information. A firm commitment to renovations to be counted towards compliance with the mandate for additional savings under an efficiency obligation is incorporated into the proposed amendments (Rosenow, Cowart, Bayer, & Fabbri, 2017). As discussed above, the EED is therefore an important one piece of the EU energy and climate change mitigation puzzle but standing alone it will likely not reduce EU energy demand, reduce GHG emissions and curb climate change.

2.3 ENERGY PERFORMANCE OF BUILDINGS DIRECTIVE (EPBD)

The first EU Directive on the Energy Performance of Buildings (EPBD) was proposed in December 16th, 2002 and became core reference for future studies on energy performance of buildings. Objective of EPBD is to promote the improvement of the energy performance taking into account outdoor climatic and local conditions, as well as indoor conditions. It demonstrates the EU's ambitious efforts to address the interrelated and connected challenges of climate change and energy emanating from the EU's building stocks by making new and existing buildings more efficient. In detail, the EPBD 2002/91/EC included four main aspects (EPBD, 2002):

1) Establishment of a calculation methodology: Member States were to implement a methodology for the calculation of the energy performance of buildings, taking account of all factors that influence energy use.

2) Minimum energy performance requirements: regulations would need to set minimum energy performance requirements for new buildings and for large (>1000m²) existing buildings when they were refurbished.

3) Energy performance certificates: an energy performance certificate would need to be made available whenever buildings were constructed, sold or rented out.

4) Inspections of boilers and air-conditioning: regulations would be needed, requiring inspections of boilers and heating systems (with the possibility of alternative approaches such as providing advice), as well as inspection of air conditioning systems.

Important outcome of EPBD is the necessity of a national energy performance calculation method for buildings covering both new and existing buildings. Performance evaluation is followed by renovation if necessary, certification, and inspection of HVAC equipment. Detailed information about the EPBD and its articles is given in Fig. 2.1.

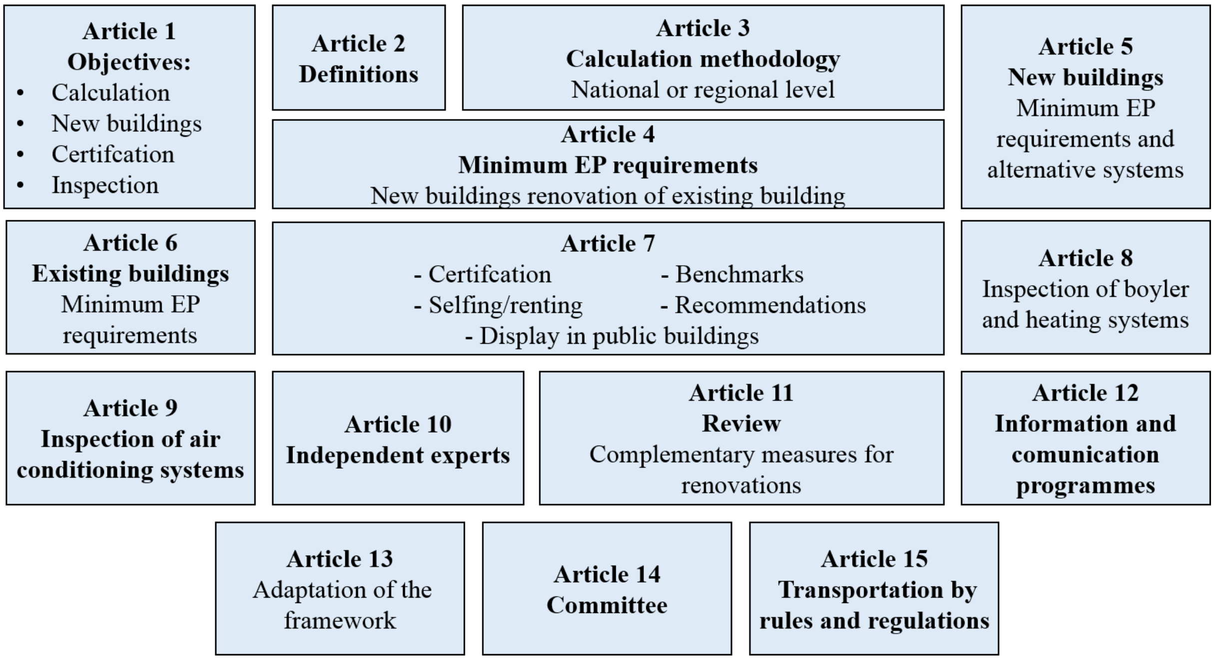

Fig. 2.1 - The EPBD and its articles (EPBD, 2002).

Over subsequent years, the continuously evolving regulatory framework has mobilised significant resources that led to the recasting of the European directive on the energy performance of buildings (EPBD) in 2010. The 2010 recast is considered the EU's main legislation covering the reduction of energy consumption. The directive promotes the reduction of energy requirements through the development of new building designs that reduces energy consumption and ultimately reduce CO_2 emissions and afterwards, promote energy production from renewable resources (Paleari, Lavagna, & Campioli, 2016). The primary focus of the EPBD is therefore to reduce energy usage demand and CO_2 emissions from the building stocks with the central objective of promoting "cost-effective improvement of the overall energy performance of buildings, while taking into account climatic and local conditions as well as indoor climate environment" (EPBD Recital 8) (Maxoulis, 2012). In 2014 it accounted for 48.9 Mtoe final energy savings based on the 2007 baseline (Pinna, Costanzo, & Romano, 2018).

The EU had to tighten Directive 2002/91/EC on the energy performance of buildings to realize the emission reduction potential for the building sector and to maximize its impact since it underperformed (Maxoulis, 2012). Directive 2002/91/EC's real potential in terms of energy reduction in the building sector and mitigating climate change (Mlecnik, Visscher, & Van Hal, 2010) was untapped (Maxoulis, 2012) due to a number of flaws and shortages such as, market failures and inefficiencies in the building sector, the lack of convergence, synergies and coordination between Directives 2002/91, 2001/77 and 2006/32 (Maxoulis, 2012). There was also low level of ambition and political will from Member States and as such, the recast Directive was strengthened to include more ambitious and in some extent more binding measures for Member States (Maxoulis, 2012). The recast EPBD therefore focuses on enhanced quality assurance improvements to ensure the reliability and robustness of energy efficiency that lacked in the 2002 EPBD (Burman et al., 2014). A recast EPBD retained most of the framework of Directive 2002/91/EC and introduced a number of new requirements that will be discussed in this thesis.

The recast EPBD introduced the concept of nearly Zero Energy Buildings (nZEB) and a target of 2018/2020 for their introduction. The EPBD do not settle minimum performance requirements that buildings must comply to be considered as nZEBs. Instead, Member States are responsible for setting those requisites, following a common methodology. These requisites must chase the cost-optimal between investment in the building and energy savings. In addition to this, the different European countries must implement their own national plans for increasing the number of nZEBs. In order that by the 31st of December 2020 all new buildings must be nearly zero-energy buildings. As the public sector should lead the way with more ambitious targets, all new public buildings should be nZEBs by the 31st of December 2018.

Alongside the nZEBs, the EPBD proposes, among others:

- The use of common methodologies for the calculation of buildings energy consumption;
- The adoption of new performance requirements on buildings;
- A new regulation about inspections of heating and air conditioner systems;
- New guidelines about energy performance certificates.

On the 30 November 2016 the Commission proposed an update to the Energy Performance of Buildings Directive, approved on May 14, 2018 and published the Official Journal of the EU On June 19, 2018), to help promote the use of smart technology in buildings and to streamline the existing rules. The Commission also published a new buildings database – the EU Building Stock Observatory – to track the energy performance of buildings across Europe.

2.3.1 Energy Performance Certificates

Energy Performance Certificates (EPCs) are regarded as the cornerstone of the effort to reach the EU's emissions reduction target of the building sector (Ries, Jenkins, & Wise, 2009). EPCs provide useful information to the public which is essential in promoting energy efficiency. They provide enhanced information to a broader network of building owners and occupiers about how to reduce emissions through energy efficiency. Evidence from the UK (Burman et al., 2014) indicates that the results of actual energy performance have been significantly higher than the standardized and theoretical performance determined under Article 3 since actual operating conditions often differ from standardized conditions (Burman et al., 2014). There is always an energy efficiency or performance gap due to the discrepancy of the actual energy performance of a building with its theoretical performance (Burman et al., 2014). In some Member States the discrepancy derived from using the EPBD compliant software is up to 30%.

2.3.2 Technical building systems and renovations

Among major requirements of the directive, the Member States are obliged to promote the implementation of intelligent energy consumption metering systems in new buildings or existing renovated building stocks (Article

8.2). This requirement ensures that building stocks achieve the set cost-optimal levels. The directive ensures that the energy performance of new or existing buildings is calculated.

The EPBD shows the EU's increased attention on buildings renovation quality, rate and efficiency. Member States are encouraged to adopt actions and measures to harness energy savings opportunities in the building sector through deep and major renovations (D'Agostino et al., 2017). Most of the EU building stocks averages 55 years186 with about 35 % over 50 years old. The Union has demonstrated high ambition to tackling the high energy consumption of these old existing buildings as outlined in Article 5 and 7. The rate of renovations has been low ranging from 0.5% to 2.5 % per year across Member States. The Fraunhofer Institute research conducted on behalf of the European Commission indicated variations across EU regions, with rates of 1.2%, 0.9% and 0.5% per year were found for North-Western Europe, Southern Europe and new Member States respectively (Dawes, 2010).

2.3.3 Nearly zero-energy buildings

The Directive introduced the 'nearly zero-energy buildings' (nZEB) requirement. The EU ensures that new buildings are nZEB by 31 December 2020 while new buildings occupied and owned by public authorities have a stipulated deadline for 31 December 2018 (Article 9.1(b).161 The transition to nZEB is meant for Member States to realize the potential for energy savings in their building stocks (Annunziata, Frey, & Rizzi, 2013). The EPBD defines the concept of nZEB as a "building that has very high energy performance", and that "the nearly zero or very low amount of energy required should be covered to a very significant extent by energy from renewable sources produced on-site or nearby" (Recast, 2010). Energy demands should be reduced as far as possible before the remaining energy needs are supplied by renewables. nZEB combines high efficiency technologies with renewable energy production and represents a new holistic approach to energy efficiency in EU building stocks. The energy performance of a building is the energy demand associated with the typical use of the building, which includes energy used for heating, cooling, hot-water production, mechanical ventilation and lighting (Paleari et al., 2016). The EPBD does not give a numerical definition of nearly zero-energy building or desirable levels of energy consumption. It rather focuses the attention from minimizing the energy needs of buildings to harnessing renewable energy sources as a way of reducing GHG emissions. This creates a conflict between reducing energy needs and upscale renewable energy usage. A study by (Paleari et al., 2016) shows that the EU regulations do not give specifications on energy balance calculation and as a consequence, “many designers take care to install a large number of devices for energy production and for consumption control, rather than to reduce the energy requirements.” In this regard the net zero balance of the buildings is promoted by installing more renewable energy sources rather than promoting the efficiency of buildings. In this case, the balance between the two actions is closely dependent on the economic issue, sometimes considered in a life cycle perspective, rather than on the environmental matter (Paleari et al., 2016).

Member States are required to draw up National Plans for increasing the number of nZEBs, with targets that may be differentiated for different building categories. According to paragraph 3 of Article 9, these plans shall include a nZEBs definition reflecting national, regional or local conditions, and a numerical indicator of primary energy use. What is still missing is a formal, comprehensive and reliable framework that considers all the relevant aspects characterizing nZEBs and allow each country to define a consistent definition in compliance with the country’s policy targets and specific conditions. Therefore, a common agreed definition can be seen as a first step towards the nZEB target laid down in the EPBD recast.

Furthermore, paragraph 2 of Article 9 asks Member States to show a leading example by developing particular policies and measures for refurbishing public buildings towards nearly zero-energy levels and to inform the EC about National Plans. Articles 6 and 7 of the EPBD recast, and Article 13 (4) of RED, state that Member States have to give information on policies, financial or other measures adopted for the promotion of nZEBs, including details on the use of RES in new buildings and existing buildings undergoing major renovation.

Tab. 2.1 summarizes the main EPBD requirements that can be related to different nZEBs arguments to be defined, such as building category, balance type, physical boundary, system boundary demand and generation, balance period, normalization, metric, time dependent weighting, and renewables.

Tab. 2.1 - Summary of the EPBD requirements related to different nZEBs arguments (D'Agostino, Zangheri, Cuniberti, Paci, & Bertoldi, 2016; Recast, 2010).

EPBD requirements	**EPBD reference**	**nZEBs arguments**
Member States shall ensure that by 31 December 2020, all new buildings are nZEBs and after 31 December 2018, new buildings occupied and owned by public authorities are nZEBs.	Article 9.1a/b	Private/public
New, and existing buildings that are subject to major renovation, should meet minimum energy performance requirements adapted to local climate.	Preamble recital 15	New/retrofit
Member States shall […] stimulate the transformation of refurbished buildings into nZEBs.	Article 9.2	
[…] buildings should be adequately classified into […] categories.	Annex I	Category
[…] energy performance of a building means the calculated or measured amount of energy needed to meet the energy demand […]	Article 2.4	Balance type
The Directive lays down requirements as regards the common general framework for […] buildings and building units.	Article 1.2a	Physical boundary
[…] building′ means a roofed construction having walls, for which energy is used to condition the indoor climate.	Article 2.1	
[…] energy performance of a building means the calculated or measured amount of energy needed to meet the energy demand associated with a typical use of the building, which includes, inter alia, energy used for heating, cooling, ventilation, hot water and lighting.	Article 2.4	System boundary demand
[…] energy from renewable sources means energy from renewable non-fossil sources, namely wind, solar, aerothermal, geothermal, hydrothermal and ocean energy, hydropower, biomass, landfill gas, sewage treatment plant gas and biogases.	Article 2.6	System boundary generation
[…] minimum levels of energy from renewable sources […] to be fulfilled through district heating and cooling […].	Article 13.4	
[…] The methodology for calculating energy performance should be based not only on the season in which heating is required, but should cover the annual energy performance […]	Preamble recital 9	Balance period
[…] including a numerical indicator of primary energy use expressed in kWh/m²/y.	Article 9.3a	Normalization
The energy performance of a building shall be expressed in a transparent manner and include an energy performance indicator and a numeric indicator of primary energy use, based on primary energy factors per energy carrier, which may be based on national or regional annual weighted averages or a specific value for on- site production.	Annex 1 9.3a	Primary metric
[…] primary energy means energy from renewable and non- renewable sources which has not undergone any conversion or transformation process […]	Article 2.5	
Primary energy factors […] may be based on national or regional yearly average values and may take into account […] European standards.	Article 9.3a	Time weighting

EPBD requirements	EPBD reference	nZEBs arguments
Member States shall introduce […] appropriate measures […] to increase the share of all kinds of energy from renewable sources in the building sector […], require the use of minimum levels of energy from renewable sources in new buildings and in existing buildings […] The nearly zero or very low amount of energy required should be covered to a very significant extent by energy from renewable sources […]	Article 2.2 (RED Article 13.4)	Fraction of renewables
nZEB means a building that has a very high energy performance […].	Annex 1	Energy performance
The energy performance […] shall […] include an energy performance indicator and a numeric indicator of primary energy use [….]		
The methodology shall […] take into consideration: thermal characteristics […], heating installation, hot water supply, air-conditioning, natural, mechanical ventilation, built-in lighting, the design, positioning and orientation of the building, outdoor climate, passive solar systems and solar protection, […] internal loads.		
This Directive […] takes into account […] indoor climate requirements […]	Article 1.1	Comfort and IAQ
The methodology shall […] take into consideration […] indoor climatic conditions […] that includes […] indoor air-quality, adequate natural light [ ]	Annex 1 Preamble recital 9	
[…] energy performance of a building means the calculated or measured amount of energy needed […]	Article 2.4	Monitoring
Member States shall encourage the introduction of intelligent metering systems […], the installation of automation, control and monitoring systems […]	Article 8.2	

2.3.4 EPBD implementation status in Europe

The progress made by EU Member States towards the establishment of nZEBs Plans has been assessed through the analysis of two reporting templates developed by the Commission and filled in by Member States and submitted to the Commission in the form of a questionnaire and a table in the period between April and October 2014 as well as the additional information and national plans received since (Action, 2011).

The EU Member States that have submitted the consolidated information on the basis of non-binding template are: Austria (AT), Belgium (BE) (Brussels Capital region, Flemish region, Walloon region), Bulgaria (BG), Croatia (HR), Cyprus (CY), Czech Republic (CZ), Denmark (DK), Estonia (EE), Finland (FI), France (FR), Germany (DE), Hungary (HU), Ireland (IE), Italy (IT), Latvia (LV), Lithuania (LT), Luxembourg (LU), Malta

(MT), Netherlands (NL), Poland (PL), Portugal (PT), Slovakia (SK), Sweden (SE), and the United Kingdom (UK). Slovenia (SI) submitted the Action Plan for Nearly Zero Energy Buildings Up to 2020 in April 2015. Greece (EL), Romania (RO), and Spain (ES) have not yet finalized their templates, but ES and RO have established nZEBs national plan. However, the ENER templates allow to structure and make the information assessable. Many national plans have missing or vague information, which prevents a consistent and detailed evaluation and comparison across EU Member States (D'Agostino et al., 2016)

General information provided by EU Member States on Regulations, Directives, or Certification schemes are summarized in Tab. 2.2.

Tab. 2.2 - General information on EU Member States regulations, Directive, or Certification scheme (D'Agostino et al., 2016).

Member States	**Regulation/ Directive/Certification scheme**	**Editor**	**Year of introduction**
AT	OIB-Dokument zur Definition des Niedrigstenergiegebäudes und, on the definition of nearly zero-energy building and setting of intermediate objectives (National Plan, the basic document for OIB Guideline 6, Energy economy and heat retention).	OIB/Länder	2012
BE	Brussels Capital: The Brussels Air, Climate and Energy Code (COBRACE), Flemish region: Flemish Action Plan nZEB – Energy Decree, Energy Law, Walloon region: Co-ZEB study – Regional Policy Statement, execution order adopted on 28th of January 2016 settings nZEB definition.	Flemish Energy Agency in Flemish region	2013
BG	National Plan for Nearly zero-energy buildings	Ministry of Investment	2014
CY	Nearly Zero-Energy Buildings Action Plan - Decree 366	Ministry of Energy, Commerce, Industry and Tourism	2012-2014
CZ	The Energy Management Act n. 406/2000 Coll.	Ministry of Industry and Trade	2012
DE	EnEG, EnEV, EEWärmeG	Government	EnEG 2013, EEWärmeG 2011
DK	Building Regulation (BR10)	Ministry of Economic and Business	2010
EE	Minimum requirements for energy performance- VV n. 68: 2012	Ministry of Economic Affairs and Communications	2012

Member States	Regulation/ Directive/Certification scheme	Editor	Year of introduction
FI	National Building Code of Finland	Ministry of the Environment	2012
FR	Réglementation Thermique 2012 (RT 2012)	Government	2013
HU	7/2006 (V. 24.) TNM degree	Ministry of Interior	2012
IE	Building regulation Part L amendement-Buildings other than Dwellings SI	DECLG	2008
IT	Decree of June 26th, 2015 concerning new minimum requirements and methodology for calculating energy performance of buildings	Ministry of Economic Development	2015
LT	Building technical regulation STR 2.01.09:2012. Law on Renewable Energy, on Construction, Construction Technical Regulation STR 2.01.09:2012 "Energy Performance of Buildings. Certification of Energy Performance", STR 2.05.01:2003 "Design of Energy Performance of Buildings"	Government	2012
LU	1) RGD 2007: Règlement grand-ducal modifié du 30 novembre 2007 concernant la performance énergétique des bâtiments d'habitation2) RGD 2010: Règlement grand-ducal modifié du 31 août 2010 concernant la performance énergétique des bâtiments fonctionnels 3) Nationaler Plan Luxemburgs zur Erhöhung der Zahl der Niedrigstenergiegebäude	Ministry of Economy	2007-2010-2013
LV	Cabinet Regulation n.383 from 09.07.2013 "Regulations regarding Energy certifications of Buildings" and amendments adopted on November 10th 2015, entered into force on November 21st, 2015.	Government	2013
MT	LN 376/2012, transposing Directive 2010/31	Ministry for Transport and Infrastructure	2012
NL	EPG 2012 - National Plan to promote nearly zero-energy buildings Bouwbesluit	Government	2011

Member States	Regulation/ Directive/Certification scheme	Editor	Year of introduction
PL	Resolution No. 91/2015 of the Council of Ministers of 22 June 2015 On the adoption of the National Plan aimed at increasing the number of buildings with low energy consumption (MP pos. 614)	Government	2015
PT	Decreee-Law 118/2013, August 20th	Government	2013
RO	National Plan for Nearly zero-energy buildings – included in the 3rd NEEAP, approved by Governmental Decision no.122/2015	Ministry of Regional Development and Public Administration	2014
SI	Action Plan for Nearly Zero-Energy Buildings Up to 2020 (AN sNES)	Government	2015
SE	Building regulations BBR 2012	The Swedish Board of Housing, Building and Planning	2013
SK	Act No. 555/2005 Coll. as amended by the act No. 300/2012 Coll.	Ministry of Transport, Construction and Regional Development	2013
UK	Building Regulations Energy Efficiency Requirements: England (Part L); Wales (Part L); Scotland (Section 6); Northern Ireland (Technical Booklet F)	HM Government; Welsh Government; Scottish Government; Northern Ireland Assembly	2013

2.3.5 EPBD implementation in Italy

The Italian Ministerial Decree 26/06/2015 on the "Application of the energy performance calculation methods and establishment of prescriptions and minimum requirements of buildings" (MD) entered into force in October 2015. It implements the national law no. 90/2013 which transposes the Directive 2010/31/EU (EPBD recast) in Italy, by modifying and integrating the legislative decree no. 192/2005. The MD sets the methodology for calculating the energy performance of buildings and establishes the minimum energy performance requirements of buildings and building units. It introduces new prescriptions, both for new buildings and for the energy refurbishment and renovation of existing buildings. It also specifies the requirements of nZEBs that will be applied to new buildings and major renovations from 1st January 2019 for the public buildings and from 1st January 2021 for all the other buildings.

In compliance with the decree, during the design phase many parameters must be checked, ranging from the features of single components to energy performance (EP) indicators regarding the whole building. In the latter case, the building energy performance requirements are based on the comparison between the building and a reference building, which has the same location, function, size, but with parameters replaced by reference values.

The MD requires for new buildings to verify the following parameters concerning the building envelope:

- the mean overall heat transfer coefficient by thermal transmission (H'_T), calculated as:

- **eq. 2.1**

$$H_T^{'} = \frac{H_{tr,adj}}{\sum_k A_k}$$

where, $H_{tr,adj}$ is the overall heat transfer coefficient by thermal transmission of the building envelope calculated in accordance with EN ISO 13789 (ISO, 2005), and A_k is the area of the opaque or transparent envelope component k.

The maximum allowable value of H'_T is fixed by the MD 26/06/2015 in function of the climatic zone and of the compactness ratio of the building (A_{env}/V_g), as shown in Tab. 2.3.

Tab. 2.3 - Maximum allowable value of the mean overall heat transfer coefficient by thermal transmission (H'_T) [W $m^{-2}K^{-1}$].

Compactness ratio (A_{env}/V_g) [m^{-1}]	**Italian climatic zone**				
	Zone A - B (900 ≤ HDD)	**Zone C** (900 < HDD ≤1400)	**Zone D** (1400 < HDD ≤2100)	**Zone E** (2100 < HDD ≤3000)	**Zone F** (HDD ≥ 3000)
$A_{env}/V_g < 0.4$	0.80	0.80	0.80	0.75	0.70
$0.4 \leq A_{env}/V_g < 0.7$	0.63	0.60	0.58	0.55	0.53
$A_{env}/V_g \geq 0.7$	0.58	0.55	0.53	0.50	0.48

- the summer solar effective collecting area of the building ($A_{sol,sum}$), calculated as:

eq. 2.2
$$A_{Sol.sum} = \sum_k F_{sh,ob,k} \cdot g_{gl,sh,k} \cdot (1 - F_F)_k \cdot A_{w,p,k} \cdot F_{sol,sum,k}$$

where, for each transparent envelope component k: $F_{sh,ob,k}$ is the shading reduction factor for external obstacles, $g_{gl+sh,k}$ is the total solar energy transmittance of the transparent part of the element in presence of a shading device, $F_{F,k}$ is the frame area fraction, $A_{w,p,k}$ is the overall projected area of the glazed element, and $F_{sol,sum,k}$ is the correction factor for the incident solar radiation, which is determined as the ratio between the solar irradiation of July, in the same site and orientation, and the mean annual solar irradiation in Rome on a horizontal plane.

According to the decree, the maximum allowable value of the summer solar effective collecting area related to the building conditioned net floor area ($A_{sol,sum}/A_f$) is 0.03 for the residential use and 0.04 for all the other uses.

The decree requires that opaque vertical external walls, except walls at North, North-West and North-East, must have surface mass not lower than 230 kg·m^{-2} or periodic thermal transmittance (Y_{ie}) not higher than 0.10 W·$m^{-2}K^{-1}$. In addition, Y_{ie} of horizontal or tilted external walls must be not higher than 0.18 W·$m^{-2}K^{-1}$.

The performance parameters concerning the whole building and its systems are the energy performance (EP) and the mean global seasonal efficiency of the thermal systems (η). In particular, the following variables must be determined for the building under design:

- $EP_{H,nd}$ and $EP_{C,nd}$ are the annual energy needs of the building for space heating and space cooling, respectively, divided by the building conditioned net floor area,

- $EP_{gl,tot}$ is the global total annual primary energy of the building divided the conditioned net floor area, where "global" means all the building services, "total" includes both renewable and non-renewable energy sources,
- η_H, η_C, η_W are the mean global seasonal efficiencies of the heating system, of the cooling system and of the domestic hot water system, respectively.

The limit values of the above listed parameters are not established a priori by the MD, but they are determined for a notional building, named reference building. The reference building has the same location, building function, size of the building under analysis, but with parameters of the thermal envelope and of the technical systems replaced by reference values. The reference parameters are provided by the MD and consist of:

- thermal transmittance of the envelope components and of components between units or attached buildings as shown in Tab. 2.4;

Tab. 2.4 - Reference building envelope U_{values} [W $m^{-2}K^{-1}$].

Uvalues [W/m²K¹]	**Floor**		**Roof**		**External Walls**		**Windows**	
	2015	**2019/2021**	**2015**	**2019/2021**	**2015**	**2019/2021**	**2015**	**2019/2021**
Climate zone A and B	0.46	0.44	0.38	0.35	0.45	0.43	3.20	3.00
Climate zone C	0.4	0.38	0.36	0.33	0.38	0.34	2.40	2.2
Climate zone D	0.32	0.29	0.3	0.26	0.34	0.29	2.00	1.80
Climate zone E	0.3	0.26	0.25	0.22	0.3	0.26	1.80	1.40
Climate zone F	0.28	0.24	0.23	0.2	0.28	0.24	1.50	1.10

- total solar energy transmittance of windows in presence of a shading device (0.35 for all climate zones);
- heat utilization and heat generation subsystems efficiencies of space heating, space cooling and DHW systems;
- specific electricity need for mechanical ventilation in function of the air flow.

The past rating system with 8 classes (A+ / A / B / C / D / E / F / G), established on the basis of a fixed range of EP index (kWh/m^2), is replaced by a new rating system based on 10 adaptable classes (A4 / A3 / A2 / A1 / B / C / D / E / F / G), based on a range proportional to the EP of the reference building. The energy performance class is obtained by positioning the $EP_{gl,nonren}$ index, (primary energy global non renewable primary energy needs of the building) in a predefined scale of classes, each one representing a performance level, as shown in Tab. 2.5.

Tab. 2.5 - The energy performance classes.

$EP_{gl,nren}$ (2019/21)	Class	$EP_{gl,nren}$ (2019/21)
	A4	≤0.40
0.40<	A3	≤0.60
0.60<	A2	≤0.80
0.80<	A1	≤1.00
1.00<	B	≤1.20
1.20<	C	≤1.50
1.50<	D	≤2.00
2.00<	E	≤2.60
2.60<	F	≤3.50
	G	>3.50

Finally, according to the legislative decree no. 28/2011 on the renewable energy sources (RES), 50% of energy demand for DHW and 50% of the sum of energy demands for DHW, space heating and space cooling must be covered by RES (from 1st January 2017). In addition, the minimum electrical power of a system fed by RES calculated in function of the building footprint area on ground, is prescribed.

2.3.6 EPBD challenges and opportunities

An overview of the main barriers and challenges in relation to nZEBs appear common among the countries (Lindkvist, Karlsson, Sørnes, & Wyckmans, 2014). They are primarily political, but also technical, financial, and related to a lack of information and awareness of key actors and stakeholders. Energy efficiency policies can generate other barriers such as some invisible extra costs such as maintenance and transport.

The EPBD does not take into account energy inefficiency or any verification about the environmental impacts generated by building construction, maintenance and disposal (Paleari et al., 2016). This has resulted in considerable energy efficiency during the buildings' operational phase while undermining the environmental impacts and energy inefficiencies of buildings that result from the buildings construction, maintenance and disposal.

A disconnection can be identified between developing innovative technologies from the building industry and the lack of uptake due to budget constraints. Awareness of how users consume energy in residential buildings should be increased. Furthermore, it is widely recognized that energy targets are challenging for cultural and historic buildings. In relation to nZEBs renovation, existing building structures set limits to what extent the existing technical solutions can be implemented. This limitation is more relevant where the architectural value of the building needs to be conserved, making the retrofit processes more challenging. Furthermore, existing technical solutions are perceived as expensive adding to the main financial challenge of having high investment in renovation projects. A return of the investment appears often as difficult apart from considering savings through the life cycle of the building; in this case the initial investment costs are lower than those of the overall operational costs. The payback period for renovation may take between 15 and 30 years, and often residents do not benefit from this period. Moreover, a landlord cannot, or does not want to raise rents and becoming uncompetitive in the market as the difference between non-efficient and efficient buildings is not considered by the tenants.

It is also common that a lack of knowledge regarding efficiency is spread among professionals and residents. Communication of best practices is important to increase knowledge among professionals and general public on energy-efficient renovation and technical solutions. A follow-up is important to ensure that residents use buildings properly.

Communicating with end users has been identified as necessary. End user behavior after a completed renovation is also a challenge in the retrofit process. In relation to financial barriers, public authorities have a leading role in setting up financing schemes for national or local contexts. The level of ambition of financial programs rises in order to have greater impact and unlock further private investment for energy efficiency. Legislation and financial incentives also have a strong influence in developing nZEBs projects.

The cooperation between institutions and individuals is essential for the implementation of energy efficiency policies. Communication and information between involved actors and organizations of the renovation project, as well as with the residents, are among the factors that can provide a successful efficiency renovation. Involving the media in energy and environmental issues can raise customers' awareness.

To overcome financial barriers, market-based regulatory instruments like Energy Performance Contracting (EPC) can reduce transaction costs as well as researching financial support establishing partnerships with international bodies and institutions.

Spreading local energy audit programs in public buildings can also help remove barriers as well as a global diffusion of new technologies using renewable resources. This is also important to fill the technological gap and ensure the effectiveness of energy efficiency measures.

2.4 OTHER DIRECTIVES

The EU has other regulatory instruments to decrease energy consumption, promote energy efficiency, reduce GHGs emissions and mitigate climate change from buildings. The Union also relies on the Renewable Energy Directive (RED) and the Eco-Design Directive to achieve an EU-wide goal of improving energy efficiency by 27% by 2030 among other instruments. The EU deploys a mix of legal instruments to target different parts of the problem of escalating energy demand to ensure that the Climate change and energy package broad objectives and goals are achieved.

2.4.1 Renewable Energy Directive (RED)

The EU's climate and energy policy goals are both served by the expansion of the renewable energy sector as incorporated into the RED (Oberthur & Oberthür, 2010). The new RED amended and repeals Directives 2001/77/EC and 2003/30/EC) and aims to promote the use of energy from renewable sources by establishing a common framework for the use of energy from renewable sources in order to limit GHG emissions.

The Directive specifies national renewable energy targets for each country, taking into account their overall potential for renewable production. This aspect is crucial in nZEBs as these buildings must combine high efficiency technologies with renewable production.

The co-existence of the RED framework measures and the energy efficiency may lead to overlaps, synergies and conflicts between them (Del Río, 2010). RED enables the full potential to reach energy efficiency in buildings to be realized through potentially increasing building renovation. Renewable energy and energy efficiency are the twin pillars that must be developed aggressively together to reduce emissions in buildings (Prindle, Eldridge, Eckhardt, & Frederick, 2007). Slowing the demand of energy usage should be met by the increased adoption of clean energy to effectively reduce emissions from buildings.

RED promotes green buildings and energy efficiency of buildings by ensuring that the Member States adopt policies and targets that enhance the uptake of renewable energy sources particularly in heating and cooling of existing and new buildings. RED obliges Member States to adopt a requirement for a minimum level of energy from renewable sources in new and renovated buildings into their building codes (Sajn, 2016). It also defines technology-specific restrictions of heat pumps and bioliquids in new and existing buildings that are subject to major renovations thereby promoting buildings energy efficiency (Parejo-Navajas, 2015). The EU has advocated for public buildings to be exemplary and in this regard, the directive provides a supportive legal framework that obliges Member States to enhance the deployment and use of RES in new public buildings and those that are subject to major renovation (Parejo-Navajas, 2015). The directive aims to provide the strongest basis for consistent growth of renewable energy production towards significant GHG emission reductions, energy supply diversification and technological innovation (Oberthur & Oberthür, 2010).

2.4.2 Eco-Design Directive

The Eco-Design directive was initially introduced in 2005 and updated in 2009 introducing measures for Member States to become more efficient in energy consumption by addressing issues pertaining to energy using products and energy related products in buildings. It is a fundamental directive that has a wider mandate in addressing the environmental performance of products during the product life cycle. The directive has a large potential towards EU objectives on energy efficiency and GHGs emissions reduction (Dalhammar, 2014).

It establishes “a framework for the setting of eco-design requirements for energy-related products” in buildings focusing on energy and environmental performance standards (Parejo-Navajas, 2015). In its entirety it stipulates minimum efficiency standards for technologies used in the building sector such as boilers, hot water generators, pumps, ventilation, fridges, lamps, windows, insulation materials etc. (Economidou et al., 2011) that meets the qualification criteria in Art 15 (2). The directive applies to products that have more than 200,000 sales units per year in the EU, significant environmental impact and there should be a great potential of environmental improvement (Dalhammar, 2014).

The Eco-Design directive recognizes that energy savings can be achieved through improved design of products that use, generate, transfer, or measure energy usage. In Finland alone it has resulted in energy savings of 1,278 GWh/a in 2016 and a projected 4,259 GWh/a by 2020 while the EU has a yearly projected savings of 39 TWh on domestic lighting, 135 TWh on electric motors (boilers and pumps and circulators), 8 TWh on domestic refrigeration and 34 TWh on fans yearly by 2020 (Dalhammar, 2014). The directive ensures the achievement of energy efficiency in buildings by ensuring that the most inefficient and poorest performing products are eliminated from the market, thus not finding their way in buildings. It is important to market transformation and behavioral changes in the equipment selection and operation of new and existing building stocks (De Almeida, Fonseca, Schlomann, & Feilberg, 2011).

2.5 THE EPBD UPDATE

EU decision makers are focusing on legislation and measures to maximize energy efficiency and minimize the environmental impact of energy generation and use. In this context, On Tuesday 17 April 2018 the Commission has approved an update to the EPBD focusing on what works and what could be improved to enhance the implementation and include targeted amendments for strengthening core articles.

The revised Energy Performance of Buildings Directive (EU) 2018/844, published in the EU Official Journal (L156) on the 19 June 2018 and entered into force as of 9 July 2018, aims to support the ambitious commitments of the Energy and Climate Policy Framework for 2030 (Union, 2014) without restricting “Member States from setting more ambitious energy performance requirements” at national level in compatible with Union law. The 2030 commitments aim to improve energy security, competitiveness and a sustainable decarbonized energy system by ensuring a 40% GHG emissions reduction, increase renewable energy uptake by 27% and improve energy efficiency by 30% The update aims to promote the role of Information and Communications Technologies and smart technology in buildings, increase renovation rates of buildings, streamline the existing obligations and to help deliver the EU 2030 energy and climate goals within a broader Clean Energy Package. This is a clear indication that further action in buildings is still needed towards, modernization of national regulations in the building sector, opening wider markets for innovative products and enabling cost reduction. The EU realized that the next generation smart energy technologies should be harnessed to effectively address and resolve the societal difficulties associated with the current energy mix to combat climate change impacts with a vision that looks at the 2030 (mid-term) and 2050 (long-term) perspectives and objectives.

The drive for an update is a further testimony that the existing energy efficiency and performance of buildings laws within the EU are insufficient to achieve climate change mitigation and energy security objectives within the necessary timeframe although the evaluation reveals relatively limited regulatory failures. The revision of the EPBD is expected to drive energy savings between 60 – 80 Mtoe/year by 2020 with a 160 to 210 Mt/year of CO_2 savings by 2020. That will translate into a reduction of 5-6% final energy consumption in 2020 and 4-5% CO_2 emissions in 2020. The update clearly shows the ambitious nature of the EU in establishing long term goals reaching 2030 to accelerate the decarbonization of the building stocks. The update is also in line with international obligations and commitments. The strengthened language of the Paris Climate Agreement of holding the increase in the global average temperature to well below 2°C above pre-industrial levels, and to pursue efforts to limit the temperature increase to 1.5°C above preindustrial levels translates into a need for even stronger and more immediate mitigation action than previously assessed (Stocker D. Qin, G., K. Plattner, M. Tignor, S.K. Allen, J. Boschung, A. Nauels, Y. Xia, V. Bex and P.M. Midgley (eds.), 2013). The EU has further indicated its willingness to take a prominent global leader position in climate change mitigation policies by putting its energy and climate goals in line with the Paris Climate Agreement.

Although the ex-post evaluations show that the recast EPBD is effective and is delivering on its general and specific objectives, the update clearly indicates that the EU is still seeking an adequate and stable regulatory approach to address the impacts of climate change particularly from buildings. The ever-changing EU laws show that finding the optimal regulatory approach is proving to be an enormous challenge to the EU. The EU is thriving for stronger legislation to limit greenhouse gas emissions and promote consistent policies that are relevant to modern challenges. The EU has also shown that making regulations more effective should include rigorous updating of standards to promote the development and use of new and efficient technology that promote green buildings (Parejo-Navajas, 2015). The EU has focused on developing consistent mandatory regulation with increasing, rigorous compliance and effective penalties for those who do not comply with the transposition of directives, to help the energy efficiency goals and targets.

Besides broad goals of the amendments discussed above, there are proposed targeted updates of core Articles as briefly discussed below. The revised EPBD amend Article 2(b) to address the EU energy poverty through building renovation which enhances energy savings and efficiency improvements of the building stocks.

Article 4 EED (provisions on long-term renovation) is moved to the EPBD where it fits more coherently to ensure the introduction of specific mechanisms by Member States to finance renovation of the building stocks. The update aims to attract more investors to see the light in the energy efficiency market with much hope on the smart finance for smart buildings. Financial conditions will be improved through the reinforcement role of the European Structural and Investment Funds and the European Fund for Strategic Investments. The changes in the EPBD will undoubtedly have significant consequences of enhancing investor confidence in climate-friendly technology.

Electro-mobility infrastructure installation will be promoted through Article 8. The drive for support will cover installations in all new and renovated buildings to further drive the decarbonization of the economy. The updated Article 8 will also reinforce the use of automation and control, improve building electronic monitoring and introduce the ‘smartness indicator rating system. Article 10 is amended to include two new provisions to drive more transparency on the use of EPCs particularly in public buildings and provide actual energy usage data to the public to determine the energy savings before and after renovation. The amendment will ensure that all necessary parameters for calculations, for both certification and minimum energy performance requirements, are set out and applied consistently through an enhanced certification process and compliance checking. Transparency and consistency in energy performance are enhanced by the update of Annex 1 also. The update will also ensure that heating and air-conditioning systems are regularly inspected as further strengthened in Article 14 and 15. This aims to ensure improved indoor environments and maintain building performances to maximize energy efficiency potential. The amendment will strengthen the monitoring ability of the Commission to ensure that the revised objectives are met since the Member States’ reporting and planning obligations will be connected to the Commission’s monitoring obligations.

3 LITERATURE REVIEW

3.1 INTRODUCTION

This chapter focuses on review of related literature on the subject with a view to putting the work in the context of previous studies. In detail, the first part of the chapter shows the concept of net-zero energy buildings in more detail: it presents the review of different definitions, related technologies and measures to reach NZEB target. Moreover, since the energy performance and environmental effects of traditional buildings have been previously studied in detail, while a limited number of works about prefabricated construction is available, in the second part of the chapter, literature studies on the energy and environmental of prefabricated buildings are discussed.

3.2 NET ZERO ENERGY BUILDING - NZEB

The concept of a Net Zero Energy Building (NZEB) entails one which produces as much energy as its users can consume within a given time period .i.e. monthly, annually etc. (Hernandez & Kenny, 2010; W. T. O'Brien, Athienitis, & Kesik, 2011; Sartori, Napolitano, & Voss, 2012). A summary of the evolution of the ZEB definition can be found in Marszal et al. (A J Marszal et al., 2011). Throughout the past two decades, this approach has witnessed a dramatic evolution leading from research to reality (Panagiotidou & Fuller, 2013). In addition, recent advances in construction technologies, renewable energy systems and rigorous academic research have also prompted the concept of a zero energy building to be increasingly feasible (Noguchi, Athienitis, Delisle, Ayoub, & Berneche, 2008; Parker, 2009; Vale & Vale, 2006; K Voss et al., 1996). Consequently, the number of buildings which meet this criterion of zero energy continues to increase (Musall et al., 2010; Karsten Voss & Musall, 2013). Governments and policy makers in Europe and in North America have championed the enquiry on how the development of buildings that meet this criterion could potentially benefit the entire society (Carlisle, Van Geet, & Pless, 2009; Musall et al., 2010). The increasing awareness of their technical feasibility calls into question their applicability in the wider built environment today.

Zero energy building principles can be applied to a wide range of construction project types including residential and commercial buildings in both existing and new construction scenarios (Musall et al., 2010). The application of zero energy building concepts to modern building practices has become possible not only through the progress made in new construction technologies and techniques, but it has also been significantly improved by academic research on conventional and experimental buildings which collected precise energy performance data across various market sectors and climate zones (Musall et al., 2010; Karsten Voss & Musall, 2013).

The analysis of the literature in the field has shown the lack of common understanding of the concept and, as a result, a number of approaches to define a net-zero energy building. An early application to the NZEB concept was proposed by Vale and Vale as an autonomous building with no connection to any offsite sources (Vale & Vale, 1975). However, the authors' conclusion when they built the Autonomous House in 1993 was that connecting domestic renewable systems to the electricity grid and achieving a "net zero energy" building can have the same or even much better life-cycle performance than a free-standing autonomous house (Vale & Vale, 2000). This was due to the fact that the use of electricity storage systems was being avoided and that some flexibility in the use of appliances was being gained in the process. Ultimately, the title "net zero energy " makes the notion to specifically refer to the grid connected buildings only, by demonstrating that a form of energy balance is taking place with energy being both taken from and delivered to an existing energy grid. Nonetheless, stating the precise chronology of how the applications evolved from inception is difficult because such evolution probably happened in many forms.

The most cited publication gives the following NZEB definition: "*A net zero-energy building is a residential or commercial building with greatly reduced energy needs through efficiency gains such that the balance of energy needs can be supplied with renewable technologies"*. However, the authors state that a net-zero energy building *"can be defined in several ways, depending on the boundary and the metric*" (P. Torcellini, Pless, Deru, & Crawley, 2006).

The paper presents "four commonly used definitions" for NZEBs (P. Torcellini et al., 2006):

- **Net Zero Site Energy**: A site ZEB produces at least as much energy as it uses in a year, when accounted for at the site.
- **Net Zero Source Energy**: A source ZEB produces at least as much energy as it uses in a year, when accounted for at the source. Source energy refers to the primary energy used to generate and deliver the energy to the site. To calculate a building's total source energy, imported and exported energy is multiplied by the appropriate site-to-source conversion multipliers;
- **Net Zero Energy Costs**: In a cost ZEB, the amount of money the utility pays the building owner for the energy the building exports to the grid is at least equal to the amount the owner pays the utility for the energy services and energy used over the year;
- **Net Zero Energy Emissions**: A net-zero emissions building produces at least as much emissions-free renewable energy as it uses from emissions-producing energy sources.

From these four definitions it can be concluded that in order to define a NZEB it is necessary, first, to understand the aim of such a definition and target audience (e.g. reduce energy consumption of a household, promote a policy instrument, create the incentives for corporate actors, etc.) and, second, set the system boundaries (e.g. consider only the energy consumed and produced in the building or take into account also the energy supplied through the grid).

Crawley et.al. point out that "*agreeing to a common definition of NZEB boundaries and metrics is essential to developing design goals and strategies*" (D. Crawley, Pless, & Torcellini, 2009). In this regard the authors further developed the classification of NZEB definitions provided by Torcellini, Pless, and Deru (P. Torcellini et al., 2006) on the basis of renewable energy sources (RES) applicable for buildings, and presented in a more comprehensive way. An updated classification includes four types of NZEBs ranging from NZEB A to NZEB D depending on the type of RES and its/their location in respect of the building.

Giving such a complex classification the authors, however, state that "*there is no "best" definition or energy-use accounting method; each has merits and drawbacks, and the approach for each project should be selected to align with the owner's goals*" (D. Crawley et al., 2009). The authors also emphasize one common design rule applicable to all NZEB types and definitions: "*tackle demand first, then supply*" (D. Crawley et al., 2009). It means that in order to achieve net zero energy balance in a building it is necessary, first, to reduce its energy consumption and energy losses by means of energy efficiency measures (such as daylighting, insulation, passive solar heating, high-efficiency equipment, natural ventilation, evaporative cooling, etc.) and only then establish energy supply through renewable energy sources.

Mertz, Raffio, and Kissock considers only two definitions of ZEB: a net- zero energy building and a CO_2 neutral building. A net-zero energy building is "*a home, that over the course of year, generates the same amount of energy as it consumes. A net-zero energy home could generate energy through photovoltaic panels, a wind turbine, or a biogas generator (however, the last two options are more applicable in rural rather than in urban areas). The net- zero energy home considered in this paper uses photovoltaic panels (PV) to offset electricity purchased from the grid*" (G. A. Mertz, Raffio, & Kissock, 2007).

A CO_2 neutral building is a building whose operation does not add carbon dioxide to the atmosphere. "*This could be accomplished by purchasing tradable renewable certificates generated by solar, wind, or biogas. It could also be accomplished by purchasing CO_2 credits on a carbon trading market. In addition, the home could generate all of its energy on-site like a net- zero energy home*" (G. A. Mertz et al., 2007). Therefore, according to Mertz, Raffio, and Kissock, a CO_2 neutral building is at the same time a net-zero energy building, but a net-zero energy building is not necessarily CO_2 neutral.

Laustsen (Laustsen, 2008) also provides two main definitions in relation to NZEB discussion, which are similar to the one given in Mertz, Raffio, and Kissock (G. A. Mertz et al., 2007). The first one considers zero net energy buildings as "*buildings that over a year are neutral, meaning that they deliver as much energy to the supply grids* *as they use from the grids*". Therefore, the author allows the opportunity for a net-zero energy building to consume energy from the grid. He emphasizes that in the absence of a determined definition of NZEB (which, in his opinion, "*do not use fossil fuels but only get all their required energy from solar energy and other renewable energy sources*"), "*a traditional building, which is supplied with very large solar collector and solar photo voltage systems*" can also become a zero-energy building if "these systems deliver more energy over a year than the use in the building" (Laustsen, 2008).

The second definition is given for zero carbon buildings, which are "*buildings that over a year do not use energy that entails carbon dioxide emission*". In this regard, the main difference between zero net energy and zero carbon buildings is that the latter can consume energy from some carbon free sources, which, however, are not applicable to zero net energy houses, "*such as large windmills, nuclear power and PV solar systems which are not integrated in the buildings or at the construction site*" (Laustsen, 2008). Therefore, if a building is net zero energy it does not automatically mean that it is zero carbon and vice versa. However, a building can comply with both definitions at the same time.

Lund et al. distinguish four types of ZEBs in reference to energy demand and installed renewable typology (Lund, Marszal, & Heiselberg, 2011). A PV-ZEB is a building with a relatively low electricity demand and a photovoltaic system (PV), while a Wind-ZEB has a relatively low electricity demand and a small on-site wind turbine. A PV-Solar thermal-heat pump ZEB is characterized by a low heat and electricity demand as well as by a PV installation in combination with a solar thermal collector, a heat pump and heat storage. A wind—solar thermal-heat pump ZEB has a low heat and electricity demand and a wind turbine in combination with a solar thermal collector, a heat pump and heat storage (Lund et al., 2011).

A different aspect of the NZEB concept is touched upon in the definition provided by Kilkis (Kilkis, 2007). The author points out the importance of exergy, meaning that energy received by a NZEB from and supplied to the grid should be the same quality. Kilkis states that in practice a NZEB can supply to the district energy the same amount of heat it received but at lower temperature, creating a negative exergy balance which has to be covered by "*additional fuel spending and harmful emissions*" (Kilkis, 2007).

In this regards, Kilkis develops a new definition of a net-zero exergy building as "*a building, which has a total annual sum of zero exergy transfer across the building-district boundary in a district energy system, during all electric and any other transfer that is taking place in a certain period of time*" (Kilkis, 2007). According to Kilkis, the key advantage of such an approach is that it gives the opportunity to estimate an overall building's impact on the environment through quantifying the compound emissions of a building. Therefore, the author argues that the implementation of the net zero energy concept in buildings without including an exergy dimension is insufficient for tackling global climate change challenge (Kilkis, 2007).

There is a number of definitions of NZEBs, which include different aspects depending on the goal of the project, local conditions, balance available for a NZEB project, etc. It is very important to know and take into account these aspects in order to define a NZEB accurately.

In this context, in 2008, the IEA established a joint ZEB research taskforce (Musall et al., 2010; Jaume Salom, Marszal, Widén, Candanedo, & Lindberg, 2014) "Towards Net Zero Energy Solar Buildings" that is made up of 70 participating building scientists and architects across 18 different countries. The main objective was to develop a common ZEB understanding across its member countries (Musall et al., 2010). Much effort has fundamentally been exerted towards formulating clear definitions of buildings which embody the ZEB notion and this has so far provided a certain degree of clarity and theoretical framing (Cole & Fedoruk, 2015; A J Marszal et al., 2011; Sartori et al., 2012).

With this highlighted, however, there is still no consensus regarding a common expression which can be satisfied by all participants in the research field due to the uniqueness of project goals and construction paradigms across different regions in the world (Deng, Wang, & Dai, 2014; Panagiotidou & Fuller, 2013). Nevertheless, the work of Sartori et al. (Sartori et al., 2012) gives rather a more concrete definition framework which contains different elements, such as boundary systems, balancing metrics etc. Some of these aspects are derived from the literature and presented in the following section. In detail, the NZEB features discussed here are:

- System Boundary;
- Balance metric;
- Balance period;

- Type of balance;
- Energy efficiency requirements;
- Renewable energy supply;
- Connection with the energy infrastructure;
- Load matching and grid interaction (LMGI) issues;
- Life Cycle assessment (LCA) and NZEB;
- The cost dimension.

3.2.1 System Boundary

The physical boundary is the point where the comparisons/measurements or calculations of the energy inflows and outflows of the system are carried out in order to identify the energy from renewable sources on-site or offsite. The boundary of a system may include a single building or groups of buildings. In the latter case it is not necessarily required that every building has a zero energy balance, but the combined overall energy balance of these buildings does need to meet this requirement.

Renewable energy integration into a district thermal energy system is typically at neighbourhood or infrastructural level, while a PV system is mostly taken into account at building or building complex level. If there is PV plant in an area close to a building and the boundary is restricted to the building, this PV would be considered off-site, otherwise, it is on-site as long as the PV plant is connected to the same grid as the building.

As explained in (Sartori et al., 2012), the boundary is the result of combining the physical boundary and the balance boundary. The first specifies which renewable sources are considered as on-site and off-site, while the second decides which energy uses are included. These uses could be heating, cooling, ventilation, lighting, domestic hot water, appliance. According to the EPBD, it is not mandatory to consider appliances in the balance, which include the electricity for households and outlets (Recast, 2010). However, most of the studies include them. According to this boundary combination concept, energy flows crossing both boundaries will be incorporated into the balance.

3.2.2 Balance metric

The proposed distinction between different metrics is brought up and further discussed in a number of publications. Definitions of NZEBs, outlined above, proposed by (Kilkis, 2007; A J Marszal et al., 2011; P. A. Torcellini & Crawley, 2006), use different metrics.

If energy use is considered as an indicator the main question to be answered is whether final or primary energy is analyzed. For example, EPBD uses primary energy use as a metric of the balance for "nearly zero-energy buildings" (Recast, 2010). According to the review of calculation methodologies for zero energy buildings presented in (A J Marszal et al., 2011), "the primary energy clearly is the most favoured metric of the net ZEB balance" because this is quite comprehensive, considering different kinds of energy, as well as the transmission losses from the grid. However, it must be noted that there are also some issues related to primary energy balance, in particular, the changing with time primary energy factors as the result of changing characteristic of the energy infrastructure and the underestimation of renewable energy sources: hydro, wind, sun (A J Marszal et al., 2011). (Hernandez & Kenny, 2010) and (Leckner & Zmeureanu, 2011) also use primary energy as the indicator for the annual energy use. Hermandez et.al. point out the advantage of this indicator as "primary energy allows differentiation between electricity and fossil fuel use and includes an indication of the efficiency of delivering heating, hot water, lighting, etc" (Hernandez & Kenny, 2010).

The delivered energy is the easiest unit to implement and as well to understand for most of the people. However, it has two major drawbacks: firstly, conversion and transportation losses are not accounted and secondly the quality of different kinds of energy is fully neglected. The only case for adopting this metric is for the ZEB using only one energy carrier e.g. full-electrical ZEB (A J Marszal et al., 2011).

Finally, the last of the most common metrics is emissions. The main reason could be the fact that globally the discussion on climate change mainly refers to the national and/or international emissions reductions targets and further actions to reduce the GHG emissions (Wilford & Ramos, 2009). On the other hand, in practice in the building community the buildings are more commonly evaluated and certificated based on energy performance rather than on emissions performance.

Other crediting options, depicted in the literature and used in the calculation methodologies, are the energy costs (G. a. Mertz, Raffio, & Kissock, 2007; Stefanović, Bojić, & Gordić, 2014) or exergy (Kilkis, 2007; Kılkış, 2012). If the authors of a study choose costs as a metric for the net balance, there will be also a dependency with the specific energy sources as each of them have a different price. The energy costs could be a very 'catchy' advertisement of the ZEB concept, understandable for wide audience, however, with a major drawback of being very unstable. (Kilkis, 2007) states that the metric of the balance in the ZEB definition should address both the quantity as well as the quality of energy, if we want to assess the complete building's impact on the environment. Therefore, he proposes a new definition for the term ZEB, in particular a net zero exergy building and defines it as 'a building, which has a total annual sum of zero exergy transfer across the building-district boundary in a district energy system, during all electric and any other transfer that is taking place in a certain period of time'. However, although, exergy as metric for calculation allows to evaluate the complete environmental impact of a building (Kilkis, 2007), it is not a well understood outside the academic community and thus difficult for the building industry and policy makers to correctly relate to such thermodynamic concept.

3.2.3 Balance period

The period of balance can have an impact on the achievability of the goal given the seasonal variability of renewable energy resources. In particular, the period of time over which the building calculation is performed can vary very much. It can be an exhaustive full life cycle of a building or the operating time of the building (e.g. 50 years) or very commonly used annual balance or applied in special situations a seasonal or monthly balance. It is obvious that applying different approaches to the same building may give different results. For example, an annual energy balance could show that the building meets net zero energy requirements, while its energy consumption during some months may exceed energy production.

However, in the existing literature on the ZEB concept the annual balance is the most favoured balancing period (Esbensen & Korsgaard, 1977; Iqbal, 2004; Noguchi et al., 2008; Rosta, Hurt, Boehm, & Hale, 2008; P. A. Torcellini & Crawley, 2006) since this takes into account the full meteorological cycle and thus the complete operating energy range of a building. Moreover, a yearly balance period includes both warm and cold seasons and thereby includes the complete range of on-site renewable energy generation potential when using PV or solar thermal collectors (Ayoub, Aelenei, Aelenei, & Scognamiglio, 2017). These findings are generally in keeping with those found by Marszal et al. (A J Marszal et al., 2011).

Even if it is not a very common approach, selection of shorter time spans, such as seasonal or monthly balance (Bojić, Nikolić, Nikolić, Skerlić, & Miletić, 2011; Iqbal, 2004; Miller & Buys, 2010), could be highly demanding from the design point of view, in terms of energy efficiency measures and supply systems, in order to reach the target in critical time, such as winter time (Sartori et al., 2012).

On the other hand, Hernandez and Kenny (Hernandez & Kenny, 2010) acknowledge that the full life cycle of the building could be more appropriate period for the energy balance. By applying this balance it is possible to include not only the operating energy use, but also the energy embodied in the building materials, construction and demolition and/or technical installations and thus evaluate true environmental impact of the building.

Sartori et al. (Sartori et al., 2012) argued that a yearly balance covering all seasonal conditions is most suitable. Longer periods in the order of decades may be selected to account for embodied energy; however it is possible to annualise this contribution to retain a yearly balance period.

3.2.4 Type of balance

The choices of balance boundary and which energy end uses to include in the balance calculation, have a major influence on the Net ZEB balance. Marszal et al. (A J Marszal et al., 2011) argued that for a grid connected NZEB, there are two possible types of balance: energy use/renewable generation, and energy delivered from grid/energy fed into grid. It was stated that energy use/renewable energy generated is more applicable for the design phase of a building while the delivered/exported balance should be used in operational monitoring. Sartori et al. (Sartori et al., 2012) concurs with the study by Marszal et al. (A J Marszal et al., 2011).

Publications by Gilijamse (Gilijamse, 1995), Torcellini et al (P. Torcellini et al., 2006), Noguchi et al (Noguchi et al., 2008), and Rosta (Rosta et al., 2008) illustrate that reaching balance between energy use and production of renewable energy is most favoured. On the other hand, energy balance concept refers to the energy transfer between building and energy supply systems in publications Laustsen (Laustsen, 2008) and Mertz et al (G. A. Mertz et al., 2007).

To manage the seasonal mismatch between load and generation some national energy codes already require calculations on a monthly basis and set monthly accounting limitations. The calculation and comparison of monthly on-site generation compared to the monthly load per energy carrier results in a so-called virtual load match. Only monthly residuals, that is, monthly generation surplus or remaining load, are summed to determine annual totals and to compensate other forms of energy that have been imported. Such a balancing method is called monthly net balance (Karsten Voss, 2012; Karsten Voss, Musall, & Lichtmeß, 2011).

3.2.5 Energy efficiency requirements

In a review of NZEB definitions and calculation methodologies, it was suggested that reduction of energy demand should come before renewable energy technology is considered, and that energy reduction should be a pre-requisite to NZEB development (A J Marszal et al., 2011).

Energy efficiency implies that the energy demand for heat and electrical power is reduced, and this reduced demand is met on an annual basis from renewable energy supply (Wang, Gwilliam, & Jones, 2009). When analyzing the existing highly efficient building concepts, it was clear that the high level of insulation, efficient windows, high level of air tightness and installing efficient appliances are the typical elements of energy efficiency (Attia, Evrard, & Gratia, 2012; Szalay & Zöld, 2014).

Energy efficiency does not come at the expenses of thermal comfort or electrical demands' fulfillment, on the contrary, energy efficient buildings are able to provide the users with their needs, but at minimum energy usage. Moreover, cost-effectiveness and environmental aspects are positively affected by the energy decrease methodology. Some of the suitable strategies to improve the energy efficiency of a building are choosing adequate building envelope, installing efficient conditioning systems and enhancing the windows' insulation levels (Rodriguez-Ubinas, Rodriguez, Voss, & Todorovic, 2014).

Instead, Lausten (Laustsen, 2008) opposed this view by highlighting that, in principle; a zero energy building can be a conventional building without extreme efficiency gains which is supplied with very large solar photovoltaic and solar thermal collectors. If these systems deliver more energy over the year than the use in the building then it is a net zero energy building. Similarly, in New Zealand, Vale and Vale (Vale & Vale, 2006) demonstrated that there is no obvious technical barrier to zero energy building retrofit and they further suggested that the use of optimized solar photovoltaic systems combined with non-invasive energy improvements is an alternative to achieving the zero energy balance requirements.

On the other hand, some researches state that energy reduction process in the aim of reaching energy efficiency is even more advantageous towards environmental and financial aspects than installing renewable energy systems. As emphasized by Thomas & Duffy (Thomas & Duffy, 2013), the less energy a building consumes, the smaller a renewable energy system is required to reach net-zero. This is why energy efficiency should come as a first priority in the design strategy of NZEBs and if the designer succeeded in decreasing the energy consumption to a significant degree, then the renewable energy phase would be simplified to a great extent. The necessity of energy efficiency strategies in NZEBs is also emphasized in (Charron & Athienitis, 2006; D. Crawley et al., 2009; Iqbal, 2004; Laustsen, 2008; Pless & Torcellini, 2010; P. Torcellini et al., 2006; Tse & Fung, 2007). Energy efficiency measures usually include those applied in the passive houses. Examples of these strategies are shown in the following techniques:

- Thermal mass: The use of a thermal mass like concrete in the external envelope can lessen temperature swings through the envelope (Alonso & Mathisen, 2017; Hootman, 2012; Reilly & Kinnane, 2017; Verbeke & Audenaert, 2018).
- Insulation: The use of thermal insulation through a lower U-factor and reduction of thermal bridging can reduce the effect of the external climate on the internal environment (Aditya et al., 2017; Bojić, Miletić, & Bojić, 2014; Hootman, 2012; Simona, Spiru, & Ion, 2017).
- Airtightness: Airtightness achieved by using a low-permeability air barrier can reduce the effect of the external climate on the internal environment (Feist, Peper, Kah, & von Oesen, 2005; Hootman, 2012).
- Shading: Providing shading in the glazing system can aid in reducing the cooling loads in high temperatures (Hootman, 2012; Kamal, 2010; Weston, 2010).
- Natural ventilation: The use of operable windows can provide a cooling effect to decrease the internal temperature (Alonso & Mathisen, 2017; Gil-Baez, Barrios-Padura, Molina-Huelva, & Chacartegui, 2017; Hootman, 2012; Schulze, Gürlich, & Eicker, 2018).

- Daylighting: Incorporating daylight into the building through top and side lighting and by using control systems to change the internal lights in response to daylight can save energy (Carletti, Cellai, Pierangioli, Sciurpi, & Secchi, 2017; Hootman, 2012; Wong, 2017).

3.2.6 Renewable energy supply

Once energy efficiency measures have been put in place, the remaining energy requirements can be met using renewable energy systems (RES). Common on-site energy generation from RES include: solar photovoltaics, solar water heating, wind turbines and others such as biomass (A J Marszal et al., 2011; Sartori et al., 2012). As has been shown earlier, in respect of energy supply in the NZEBs Torcellini, Pless, and Deru, (P. Torcellini et al., 2006) distinguish between on-site and off-site buildings. Summing up, on-site energy supply is usually provided by photovoltaic, solar collectors for hot water and/or space heating and/or cooling, on-site wind or mini hydroelectric installations - mostly in rural areas. Some studies also consider the installation of heat pumps to supply additional energy for NZEBs (Biaou & Bernier, 2008; Bojić et al., 2011; Deng, Dalibard, et al., 2011; Deng, Dai, Wang, Matsuura, & Yasui, 2011). Off-site energy supply options include any energy sources which can be transported to the building to generate energy on-site, such as biomass, wood pellets, ethanol, biodiesel or any purchases of renewable energy produced outside the building's site.

The most applicable and widely used energy supply options are those utilizing solar energy on the building's site, i.e. solar collectors and photovoltaic. The Task 40/Annex 52 examined NZEBs (J.-H. Kim, Kim, & Kim, 2015) testing 'advanced building design technologies' with the aim to provide guidelines for construction of demonstration projects as well as international collaborative projects. This exercise resulted in the formulation of a ZEB database that includes, 30 case studies of zero energy buildings categorized by country, climate, building use and renewable energy applications. Analysis of these 30 case studies revealed that renewable energy systems were applied in virtually all cases. Solar photovoltaic systems were the most applied and they accounted for 97% (29 cases). The solar thermal systems accounted for 63% (19 cases) while the geothermal systems accounted for 33 % (10 cases). The wind and biomass were the least applied and they accounted for less than 20%.

The dominance of solar PV systems on zero energy buildings can also be observed in numerous housing projects that were not included in the case study database (see for example (Attia, 2010; Doub, 2009; Noguchi et al., 2008;

Panagiotidou & Fuller, 2013; Parker, 2009; Vale & Vale, 2006). On the other hand, examples of studies considering wind as an energy supply option for NZEBs include: (Dalton, Lockington, & Baldock, 2008; Hamada, Nakamura, Ochifuji, Nagano, & Yokoyama, 2001; Iqbal, 2004; Wang et al., 2009). Bagci (Bağcı, 2009) also considers tidal, wave, energy crops and municipal solid waste as potential renewable energy supply options for NZEBs. In this context, the large scale adoption of zero energy buildings could entails large scale penetration of solar PV systems. This further could leads to a number of issues concerning the implications of increased solar penetration within existing grids today. On the other hand, the domination of PVs as an application on zero energy buildings is very likely to continue reigning supreme due to their lower cost. Along this thread, a paper by Bourrelle (Bourrelle, 2014) claims that the large scale adoption of zero energy buildings can be a potential weapon against the so-called "rebound effects" (Sorrell, 2009), and also a potential tool to reduce global non-renewable energy demand. Bourrelle (Bourrelle, 2014) argues that by diverting cost savings from energy efficiency improvements into capital investment in RES, zero energy buildings could effectively help to dampen rebound effects where money saved from energy efficiency is spent on other energy consuming products or activities. However, the environmental impact associated with RES such as PV systems is often overlooked in most studies that evaluate zero energy buildings today (Maurizio Cellura, Guarino, Longo, & Mistretta, 2014; Lützkendorf, Foliente, Balouktsi, & Wiberg, 2015; Paleari, Lavagna, & Campioli, 2013; Rovers, 2014).

3.2.7 Connection with the energy infrastructure

There are two possible types of NZEBs: those that are connected to the energy infrastructure and those that are not connected. Energy infrastructure in the literature is usually devoted to the electricity grid, district heating and cooling systems, gas pipe network, biomass and biofuels distribution networks (A J Marszal et al., 2011). In this regards, these two types of NZEBs are often called on-grid (or grid-connected, or grid-integrated) and off-grid (or energy autonomous, energy self-sufficient or stand alone) buildings.

The literature provides a number of examples for both grid-connected (Bojić et al., 2011; Deng, Dalibard, et al., 2011; Gilijamse, 1995; Hamada, Ochifuji, Nagano, & Nakamura, 2000; Iqbal, 2004; A J Marszal et al., 2011; Merrigan, 2001; Noguchi et al., 2008; Pietila, Beausoleil-Morrison, & Newsham, 2012; Tse & Fung, 2007; Zhu, Hurt, Correa, & Boehm, 2009) and energy self-sufficient NZEBs (Abegg, 2011; Chen, Chu, Cheng, & Lin, 2009;

Dalton et al., 2008; Miller & Buys, 2010; Mrkonjic, 2006). The main difference between these two types of NZEBs is that the first has the opportunity to take energy from and give energy to the grid, while the second has to produce and consume all the energy by itself on the building's site. However, in both cases the energy consumption should be covered by renewable energy supply for a certain time scale. Connection to the grid allows a building to exchange energy with it when it is needed: for example, when a building needs more energy than it can produce, it can get the required energy from the grid. The opposite situation is also possible: when a building produces more energy than it needs, it can supply the surplus to the grid. In both situations the building can be net zero energy on an annual basis. Therefore, the electricity grid may be considered as a means of energy storage. In off-grid buildings there is no such an opportunity, thus, other (usually more expensive and space-consuming) means of energy storage should be applied (e.g. water tanks or thermal mass). Another drawback of energy autonomous houses is that the lack of energy storage may lead to oversizing of renewable energy systems in order to meet a peak energy demand (Iqbal, 2004; P. Torcellini et al., 2006).

3.2.8 Load matching and grid interaction (LMGI) issues

As NZEB buildings are typically grid connected buildings there might be a need to measure grid interactions as a part of NZEB performance with additional indicators. Different terms are used for the topic of energy match characteristics. Transient characteristics (Karsten Voss, 2012) or mismatch factors (Dokka, Sartori, Thyholt, Lien, & Lindberg, 2013) are two. But they all describe the same issues regarding NZEBs interaction with the grid. Ensuring that on-site generation matches up with on-site consumption and that energy exported to the grid is done so at a time that does not create grid stability issues due to oversupply, are factors to be considered if the NZEB concept is to be widely adopted (Butera, 2013). Matching on-site generation with on-site demand is known as load matching (LM), whilst grid interaction (GI) concerns the matching of grid export, and grid quality & stability requirements (Jaume Salom et al., 2014; Sartori et al., 2012; Karsten Voss et al., 2010).

The temporal match between load and generation for an energy carrier gives a first insight on a building's ability to work in synergy with the grid. When there is a poor correlation between load and generation, e.g. load mainly in winter and generation mainly in summer, the building will more heavily rely on the grid. If load and generation are more correlated, the building will most likely have higher chances for fine tuning self-consumption, storage and export of energy in response to signals from the grid. Load matching can be addressed in design by separate calculations or simulations on load and generation, without need to know or estimate self-consumption. For this reason indicators of load matching fit well for being used in combination with a load/generation balance (Sartori et al., 2012).

Measures to improve the load match are strategies of Demand Side Management (DSM) as well as careful design of generation capacity. By moving the time of some energy intensive activities to time of the day where generation output is at its peak, a better match between load and generation is possible. Introducing on-site storage will greatly improve the flexibility of the building to load-match, while reducing reliance on the grid in times of low generation (Karsten Voss et al., 2010). In addition to battery storage, the placement and orientation of solar panels can also have effects on load matching. Salom et al. (Jaume Salom et al., 2014) recommends that for a net-metered residence, solar panels should be oriented east-west instead of north-south in order to take advantage of morning and afternoon sun since this coincides with times of peak demand. An office building on the other hand would orient panels north-south to catch peak midday generation potential. It is recommended that for a gross metered system, array orientation should always be so that maximum production can be achieved at all times.

Grid interaction refers to the variability of energy exchanged between the building and the grid. A method of indicating this is the grid interaction index. It is a measure of energy exchange variability within a year, normalised on the highest absolute value (Jaume Salom et al., 2014; Sartori et al., 2012). The grid interaction can be addressed based on metering or simulation data of delivered and exported quantities. Therefore, indicators of grid interaction fit well for being used in combination with an import/export balance.

Several indicators have been proposed to analyses the interaction between buildings and grids, with a viewpoint from either the building, the grid interaction index, or the grid perspective, grid interaction flexibility (Jaume Salom et al., 2014). The main differences found are due to the following factors:

- Objectives, i.e. possible goals and targeted markets for grid support,
- Supply concepts in buildings, i.e. different technologies used for heat and cold generation and storage, which make it necessary to adjust energy balances and to interpret numerical results in different ways,

- Constraints, i.e. technical and operational limitations that need to be considered, such as maximum powers, storage capacities, user requirements and hydraulic configurations,
- Data, i.e. the data used to calculate the metrics,
- System boundaries, i.e. physical scopes under evaluation, which may be limited to single components (e.g. battery, heat pump) or may comprise entire buildings or districts,
- Time scales to be considered, ranging from seconds to operating years.

Salom et al. (J Salom et al., 2011) classified the Load Matching and Grid Interaction (LMGI) indicators in to four categories. Metrics in the first category analyze the coincidence of local electric load and local electricity generation of building energy systems. Metrics in the second category analyze the electrical power exchanged between a building and the grid. The analyses serve two purposes: first, reduce investment cost by using smaller cables in new buildings and second, minimize grid stress as a result of variability in the net electricity load of the building. Metrics in the third category account for the time of use of electricity consumption. An external grid signal (e.g. energy price, carbon intensity, etc.) is used as a weighting factor to consider a time-variable cost or value of electricity. Metrics in the fourth category analyze the interaction of buildings with surrounding districts, markets, or grids. Tab. 3.1 provides an overview of indicators related load matching and grid interaction, together with their formal mathematical definition.

Tab. 3.1 - Overview of indicators related load matching and grid interaction.

LMGI indicator	Mathematical definition	Reference
Load cover factor	$\gamma_{load} = \frac{\int_0^T \min[g(t) - S(t) - \zeta(t), l(t)]dt}{\int_0^T l(t)dt}$	(R Baetens, de Coninck, Helsen, & Saelens, 2010; De Coninck & Helsen, 2016; Jaume Salom et al., 2014)
Supply cover factor	$\gamma_{\text{supply}} = \frac{\int_0^T \min[g(t) - S(t) - \zeta(t), l(t)]dt}{\int_0^T [g(t) - S(t) - \zeta(t)]dt}$	

LMGI indicator	Mathematical definition	Reference
Loss of load probability	$LOLP = \frac{\int_0^T dt_{l(t)>g(t)-S(t)-\zeta(t)}}{T}$	(Jaume Salom et al., 2014)
No grid interaction probability	$P_{e\approx 0} = \frac{\int_0^T dt_{\lvert ne(t)\rvert<0.001}}{T}$	
Peak power generation	$\overline{G} = \frac{\max[g(t)]}{E_{des}}$	
Peak power load	$\overline{L} = \frac{\max[l(t)]}{E_{des}}$	
Dimensioning rate	$DR = \frac{\max[\lvert ne(t)\rvert]}{E_{des}}$	(J Salom et al., 2011; Jaume Salom et al., 2014; Sartori et al., 2012; Karsten Voss et al., 2010)
Capacity factor	$CF = \frac{\int_0^T \lvert ne(t)\rvert dt}{E_{des}\cdot T}$	
Generation multiple	$GM = \frac{G_{des}}{L_{des}}$	
Connection capacity credit	$E_c = 1 - \frac{DR}{DR_{ref}}$	(Jaume Salom et al., 2014; Verbruggen et al., 2011; Karsten Voss et al., 2010)
Grid interaction index	$f_{grid} = STD\left(\frac{ne(t)}{\max(\lvert ne(t)\rvert)}\right)$	
Equivalent hours of storage	$N_{h\_S} = \frac{S_{des}}{L_{des}}$	
Flexibility (optimum cost)	$\Phi_{pos} = l(t)_{\max} - l(t)_{ref} \geq 0$ $\Phi_{neg} = l(t)_{\min} - l(t)_{ref} \leq 0$ $\Gamma_{\max} = J_{c,\max} - J_{c,ref} \geq 0$ $\Gamma_{\min} = J_{c,\min} - J_{c,ref} \geq 0$	(De Coninck & Helsen, 2016)
Flexibility factor (cost)	$FF_{PC} = \frac{PC_{\max} - PC}{PC_{\max} - PC_{\min}}$	(Dar, Sartori, Georges, & Novakovic, 2014; Masy, Georges, Verhelst,

LMGI indicator	Mathematical definition	Reference
		Lemort, & André, 2015)
Flexibility factor (volume)	$FF_{shift} = \frac{FF_{PC} - FF_{PC,ref}}{FF_{PC,ref}}$	(Masy et al., 2015)
Flexibility factor	$FF = \frac{\int_{LPT} l_{heating} dt - \int_{HPT} l_{heating} dt}{\int_{LPT} l_{heating} dt + \int_{HPT} l_{heating} dt}$	(Le Dreau & Heiselberg, 2016)
Power Shifting capability	$l_{shift} = l_{ADR} - l_{ref}$	(Reynders, Diriken, & Saelens, 2015)
Mismatch compensation factor	$f_{MMC} = \frac{C_{\cos t-balance}}{C_{energy-balance}}$	(Lund et al., 2011)
Load shift for CO_2	$V = \int_0^T C_{Co_2}(t) \cdot l(t) dt$	(Favre & Peuportier, 2014)
Grid Support Coefficient	$GSC_{abs}(G) = \frac{\sum_i W_{el}^i \cdot G^i}{W_{el}^i \cdot \overline{G}}$. $GSC_{rel}(G) = 200 \cdot \frac{GSC_{abs}(lowerPB) - GSC_{abs}(achieved)}{GSC_{abs}(lowerPB) - GSC_{abs}(upperPB)}$	(Klein, Herkel, Henning, & Felsmann, 2017; Klein, Langner, Kalz, Herkel, & Henning, 2016)

The supply cover factor γ_s (also called self-consumption) and load cover factor γ_l (also referred to as autonomy or autarchy) are frequently used in the analysis of net-zero energy buildings in order to analyze the matching of local load and local generation. γ_s is the fraction of local generation that is used on-site, whereas γ_l is the fraction of the load that is covered by the on-site generation (Jaume Salom et al., 2014). Other derivatives of the supply and load cover factors for different building typology have been proposed as part of individual studies (Ruben Baetens et al., 2012; S. Cao, Hasan, & Sirén, 2013; Castillo Cagigal et al., 2010).

The loss of load probability LOLP indicates the time share during which the local generation is insufficient to supply the local load (Jaume Salom et al., 2014). The no grid interaction probability ($P_{e\approx 0}$) shows the probability that the building is acting autonomously of the grid. In that case, the entire load is covered by the direct use of renewable energy or by the stored energy (Jaume Salom et al., 2014).

The peak power generation $\overline{G}$ is calculated as the peak on-site generation capacity divided by the design capacity of the grid connection. Correspondingly, the peak power load $\overline{L}$ is calculated as the peak electricity load divided by the design capacity of the grid connection. Both metrics provide an indication of the safety factor in the sizing of the grid connection in case local load and generation do not coincide (Jaume Salom et al., 2014).

The dimensioning rate DR is similar to the Peak power load, but analyzes the highest net electricity load (i.e. load minus local generation) in relation to the capacity of the grid connection. The capacity factor CF is the integral of the instantaneous dimensioning rate over time and indicates the average utilization of the grid connection. It is calculated as the total energy exchange with the grid divided by the maximum transferrable energy considering the nominal connection capacity. The generation multiple GM is the relation of the installed local generation capacity and the design electricity load of the system. It can be either applied to the local generation and local load, or the import and export of electricity of a building (J Salom et al., 2011; Jaume Salom et al., 2014; Sartori et al., 2012; Karsten Voss et al., 2010).

The connection capacity credit E_c indicates the percentage of grid connection capacity that could be saved over a reference case if a particular optimization strategy was implemented. The grid interaction index f_{grid} is the standard deviation of the utilization factor of the grid connection (i.e. the net load divided by the connection capacity), indicating average grid stress due to the variability in net load (Jaume Salom et al., 2014; Verbruggen et al., 2011; Karsten Voss et al., 2010). If the index is positive, it describes a net positive energy building, while a negative index signifies a net negative energy building. It is a measure of the fluctuation of energy exchange between building and grid and has nothing to do with the amount of grid electricity required by the building (Jaume Salom et al., 2014; Karsten Voss et al., 2010).

The equivalent hours of storage N_{h_S} corresponds to the storage capacity expressed in hours. The physical capacity is the number of hours of storage multiplied by the power design load. This index should be explored as potential indicator of flexibility in buildings with storage system (Jaume Salom et al., 2014; Verbruggen et al., 2011; Karsten Voss et al., 2010).

Energy flexibility indicators (e.g. equations 12-18) are often price-based and show whether energy/electricity is consumed during high- or low-price periods. Their generic nature allows their application to various building types, climates and energy systems (Dar et al., 2014; De Coninck & Helsen, 2016; Le Dreau & Heiselberg, 2016; Masy et al., 2015). The flexibility factor proposed by Masy et al. (Masy et al., 2015) indicates the possible energy cost savings if all energy were consumed at the lowest price of each operating day, assuming a realtime-pricing model. De Coninck et al. (De Coninck & Helsen, 2016) proposed the concept of Cost Curves which provide a relation between the load increase/decrease at specific time and the associated additional incremental operating cost compared to a cost-optimal reference case, i.e. the incremental cost of flexibility provision. Le Dréau and Heiselberg (Le Dreau & Heiselberg, 2016) defined the flexibility factor, which analyzes the electricity consumption during low-price times and high-price times assuming a three-step electricity tariff derived statistically from day-ahead prices at the Nord Pool electricity market.

The Mismatch Compensating Factor f_{MMC} proposed by Lund et al. (Lund et al., 2011) gives the relation of the installed capacities of the local generation system under two conditions: a) a net zero electric energy balance and b) a net-zero cost balance assuming real time pricing for electricity consumption and feed-in. Values larger than unity indicate that electricity consumption from the grid occurs on average during time periods with relatively high stock electricity prices, whereas feed-in of excessive local generation occurs during time periods with lower stock electricity prices (Lund et al., 2011).

GSC_{abs} proposed by Klein et al.(Klein et al., 2017, 2016) weights a time-resolved electricity consumption profile with a time-resolved grid signal, such as the stock electricity price or the fraction of wind and PV in the electricity mix the residual load. Since GSC_{abs} does not reveal whether the current operation scheduling is close to the optimum, or whether there is significant room for improvement from the building operation perspective, the authors introduced the additional metric GSC_{rel} has been introduced, which relates the achieved value of GSC_{abs} to the worst and best possible values on a scale of −100 to +100. The potential boundaries are determined by re-scheduling the electricity consumption of each day to the most favorable (best case, upper potential boundary) and least favorable (worst case, lower potential boundary) periods in terms of the grid signal, respectively, under consideration of the maximum power of the variable load or generator and assuming that the amount of electricity

\does not change due to the load shifting. This procedure is repeated for each day within the evaluation period and GSC is calculated for both cases (Klein et al., 2017, 2016).

3.2.9 Life Cycle Assessment (LCA) and NZEB

Buildings demand energy in their life cycle right from its construction to demolition. The overall environmental impacts of buildings extend beyond the use phase, as they also encompass the embodied energy and environmental burdens related to resource extraction and manufacturing, construction activities, as well as dismantling and construction waste disposal at end of life. Moreover, life cycle impacts are highly inter-dependent, as one phase can influence one or more of the others. For instance, the selection of building materials can reduce heat requirement, but might also increase embodied energy and transport-related impacts or affect the service duration of the whole building, and could even influence the generation of recyclable (or disposable) demolition waste (Sesana & Salvalai, 2013).

In this context, as buildings move towards to zero energy target, the impacts of product embodied energy becomes much more important to the building's life cycle, as evident by many published work (Luisa F Cabeza, Rincón, Vilariño, Pérez, & Castell, 2014; M Cellura, Guarino, Longo, & Mistretta, 2015; Hernandez & Kenny, 2010; Paleari et al., 2013; Ramesh, Prakash, & Shukla, 2010; Sartori & Hestnes, 2007; Sharma, Saxena, Sethi, Shree, & Varun, 2011; P. Torcellini et al., 2006)

Paleari et al. (Paleari et al., 2013) stated that the excessive attention paid to the operational energy consumption and the concomitant lack of control on the other stages of the lifecycle involves the reduction to almost zero of the environmental burden of this phase but it does not guarantee in any way that the overall balance will be improved compared to the actual conditions already in place. In particular, depending on the design and the manufacturing choices, it is possible to obtain an improvement in the environmental profile of the building without cancelling the use phase but through the reduction of the impacts during the production stage or increasing the useful life of the components with a consequent decrease of the impacts linked to the maintenance activities.

A review study by Sartori and Hestnes (Sartori & Hestnes, 2007) that examined 60 case study buildings, both conventional and low-energy, found that as operational energy was reduced the relative importance of the embodied energy was increased. Conventional buildings had an embodied energy of between 2% and 38% of total life cycle energy whilst the embodied energy of low energy buildings was between 9% and 46%. Of particular interest in this review is a zero-energy solar house which has such a high embodied energy from the use of photovoltaic panels that it exceeds the total life cycle energy of some low-energy buildings. As such when operational energy levels are reduced to very low levels and employ significant amounts of renewable technologies a focus is required on the embodied energy and carbon of the systems employed in order to ensure there is a net benefit in terms of life cycle energy and carbon.

A similar review work on the life cycle energy analyses is presented by Ramesh et al. The amount of cases in this reference increases to 73 across 13 countries (Ramesh et al., 2010). The case analysis showed that life cycle energy use of buildings depends on the operation (80 ~ 90%) and embodied (10 ~ 20%) energy. It also pointed out that low energy buildings perform better than zero operating energy buildings in the life cycle context, based on the existed data. It proved that if the evaluation is updated from energy balance analysis to life cycle analysis, some existing NZEB cases may not show a satisfied performance in the aspect of sustainable development.

The review performed by Chastas et al. (Panagiotis Chastas, Theodosiou, & Bikas, 2016) brings out other cases wherein the embodied energy nearly matches or exceeds the operating one. For instance: a low-energy family house built in Northern Italy (Blengini & Di Carlo, 2010); two attached houses built according to the passive standard in the French region of Picardy (Thiers & Peuportier, 2012); a nZEB (nearly Zero Energy Building) residential complex located in a suburb of Milan, Italy (Paleari et al., 2013); several Minergie-A buildings reported by Berggren et al. (Berggren, Hall, & Wall, 2013); a multi-family building located in the Marches region, Central Italy, redesigned to meet the nZEB standard (Copiello, 2017). Furthermore, life-cycle based studies raise the same question (Crawford, Bartak, Stephan, & Jensen, 2016; Stephan & Stephan, 2014).

Hernandez and Kenny (Hernandez & Kenny, 2010) proposed an appropriate methodology called LC-ZEB defined as a building whose primary energy use in operation plus the energy embedded in materials and systems over the life of the building is equal or less than the energy produced by renewable energy systems within the building. They chose primary energy as the indicator for annual energy use in operation and for embodied energy because it allows differentiation between electricity and fossil fuel use and it includes an indication of the efficiency of delivering heating, hot water, lighting, etc. The main advantage of this methodology is that it allows building designers to carry out comparative analysis of the life cycle relevance of design decisions related to building envelope design, materials, HVAC and renewable energy systems. All such components can be included in the analysis through their annualized embodied energy and annual energy use.

One of the methods that takes into account all environmental impacts associated with all the stages of a product's lifetime is the Life-cycle Assessment (LCA). LCA is a research method used for the quantitative assessment of material used, energy flows and environmental impacts of products. It has been widely applied in the building industry, because it cannot only provide more comprehensive and reasonable analysis on the energy and environment impact of product for the whole life cycle, but also be used to determine top design priorities and quantitatively inform sustainable design decision-making for various buildings (Faludi, Lepech, & Loisos, 2012). For a building, LCA evaluation process, which is defined by (ISO, 2006a, 2006b) and by the standard UNI EN 15978:2011 (EN, 2011)generally consists of four stages: goal and scope definition, life cycle inventory, impact assessment and interpretation (Luisa F Cabeza et al., 2014; Sharma et al., 2011).

This comprehensive methodology has been widely applied to buildings; however, due to the complexity and variability associated with these systems, significant challenges should be addressed in future research, including how to model unpredictable data, such as: the systems adopted, the end-users behavior (systems operation), the maintenance and service life and the building dismantling and end-of-life.

Cabeza et al. (L F Cabeza, Castell, & Pérez, 2014) reviewed the studies available within the bibliography that addressed the life-cycle assessment of buildings. The authors found that the case studies previously found within the literature were difficult to compare, due to the specific properties of each case study, such as climate, comfort requirements, local regulations etc. Considering the scopes of the studies, while some studies focused solely on the material use for the building construction, other studies also considered the inputs required for building operation. Moreover, functional unit selected was not clearly mentioned in all studies, especially in the cases where the life-cycle impacts over the whole building lifetime were evaluated. Since there is currently no agreement on the functional unit to be used, the comparison between different studies was even more difficult. As for the lengths of building lifetime considered, most of the authors assumed a 50-year lifetime (50 % of the papers within the existing bibliography), while other lifetime lengths were more sparingly used (19 % assumed 40 years and 9 % considered 80 or 100 years). It was also noted that the studies that considered the whole building (rather than just elements) accounted for three life-cycle phases: construction, operation (use) and demolition. It was also found that almost all studies clearly presented type and location of the building studied, since in most studies, existing buildings were considered. Finally, it was pointed out that most of case studies selected were located in the United States or Western Europe. Thus, further case studies should be preferably located in other regions, in order to broaden the insights of building environmental impacts in different regions.

3.2.10 The cost dimension

The current technologies related to energy savings, energy efficiency and renewable energies are sufficient to reach, in combination, the NZEB target. However, one of the primary barriers to the adoption of NZEBs and to energy efficient buildings is linked to economic issues.

In this context, the Energy Performance of Buildings Directive (Recast, 2010), obliges Member States to ensure that minimum energy performance requirements for buildings are set with a view to achieve cost-optimal levels. All the countries shall also take the necessary measures to ensure that minimum energy performance requirements are set for building elements that form part of the building envelope and that have a significant impact on the energy performance of the building envelope when they are replaced or retrofitted, with a view to achieve cost-optimal levels. The cost-optimal level is defined as the energy performance level which leads to the lowest cost during the estimated economic lifecycle from two different perspectives: financial (looking at the investment itself at the building level) and macro-economic (looking at the costs and benefits of energy efficiency for society as a whole).

Before the EBPD cost optimal approach, studies were mostly focused on the energy saving accomplishments, investigating also the assessment of life cost analysis (Azari, 2014; Gustavsson & Joelsson, 2010) or the total net present value in a defined building life cycle; moreover, generally in economic calculation, only the upfront investment cost was considered (Dolmans, 2011), whilst according to the EPBD Guidelines (Commission, 2012) initial investment cost, running costs, replacement costs and disposal costs must be included over the building lifecycle. Since the launch of the EPBD recast, several researches focused on the cost optimal approach, together with the study of zero energy solutions for new and existing buildings. Two exemplar reports on the cost optimal methodology by BPIE identified strengths and weakness of the cost optimal approach (Optimality, 2010) and provided results from case studies in three different countries (Austria, Germany and Poland) (Atanasiu et al., 2013). The first report (Optimality, 2010) analyzed the current energy policy and provided guidance and support to the methodology addressing mainly to policy makers. In particular different gaps for each country (Atanasiu et al., 2013) were investigated in the cost-optimal energy performance levels, due to different national requirements (e.g. prescribed building envelope U-values).

In literature, it is available an extensive number of studies on the cost optimization of specific building element calculation, e.g., the optimal insulation thickness for the various building elements and in various climatic conditions, as summarized by Fokaides and Papadopoulos (Fokaides & Papadopoulos, 2014).

Pylsy and Kalema (Pylsy & Kalema, 2008) made a life-cycle cost sensitivity analysis, addressing four building insulation levels, four building tightness levels, three ventilation-heat recovery types, and nine heating systems to find cost-effective concepts for low-energy houses. The analysis found that the improvement of the thermal insulation of the building envelope is the most effective way to reduce the space-heating energy need. However, the lowest building insulation level is selected as a cost-optimal solution when ground-source heat pump (GSHP) is selected for heating. Hasan et al. (Hasan, Vuolle, & Sirén, 2008) combined simulation and optimization to minimize the life-cycle cost (LCC) of a single-family detached house. The study investigated a wide range of wall, roof, and floor insulation levels, two types of windows, and two types of ventilation-heat recovery units. However, no heating alternatives were addressed. Alanne et al. (Alanne, Salo, Saari, & Gustafsson, 2007) considered the selection of a residential energy-supply system as a multi-criteria decision-making problem involving both financial and environmental issues. The study analyzed the competitiveness of micro-CHP as 1 of 10 alternative heating systems for a Finnish single-family house. The analysis showed that the micro-CHP is a reasonable alternative to traditional systems, particularly from the environmental point of view. Pardo and Thiel (Pardo & Thiel, 2012) identified environmental and economic results of several measures on single family houses and also relationship between energy consumption, CO_2 emission, investment and operational costs. Saari et al. (Saari et al., 2012) studied eight different energy-saving design concepts and three heating modes for a typical new Finnish detached house. The study showed that the payback time of the heating system depends on the real interest rate and the building construction.

However, these studies were conducted exploring a limited number of evaluated design options, therefore the presented optimal solutions may be far from the absolute optimal configuration at building level. On the other hand, rarer is the published applications of cost optimization procedures on the whole building-plant.

Barthelmes et al. (Barthelmes, Becchio, Bottero, & Corgnati, 2014) and Becchio et al. (C Becchio, Bottero, Corgnati, & Ghiglione, 2015; Cristina Becchio, Dabbene, Fabrizio, Monetti, & Filippi, 2015) highlighted the use of cost-optimal methodology as a decision-making tool for supporting architects in the energy design of some nearly-zero energy residential buildings. Similar analyses were proposed by Bonoli and Fabbri (Bonoli & Fabbri, 2013) that tried to apply the methodology both on new and existing buildings needed to be refurbished. Ascione et al. (Ascione, Cheche, Masi, Minichiello, & Vanoli, 2015) investigated the use of cost-optimal methodology for the assessment of the refurbishment of a XV century historic building in Naples (Italy). Zacà et al. (Zacà, D'Agostino, Congedo, & Baglivo, 2015) exploited the cost-optimal method to evaluate high performing technical solutions for residential buildings located in the Mediterranean area.

Hamdy et al. (Hamdy, Hasan, & Siren, 2013) introduced an efficient and time-saving simulation-based optimization method to find the cost-optimal and nZEB energy performance levels for a single-family house in Finland. They proposed a multi-stage optimization: in the first stage they selected the optimal passive strategies in terms of heating demand and total investment costs; followed by the second stage where the active systems were evaluated from the primary energy consumption and Life Cycle Cost point of view; to finalize with the renewable energy design in order to improve the results obtained in the second stage. Moreover, they used two different optimization technics in the different stages of the study (genetic and deterministic algorithms). Ferrara et al. (Ferrara, Fabrizio, Virgone, & Filippi, 2014) utilized a similar simulation-based optimization method for cost-optimal analysis applied to residential nZEBs.

Kurnitski et al. presented a systematic and robust scientific procedure to determine cost optimal and nZEB energy performance levels, by means of building simulation, of an Estonian residential reference building (Kurnitski et al., 2011) and of an office building (Pikas, Thalfeldt, & Kurnitski, 2014). In the case of office buildings (Pikas et al., 2014), they concluded that a construction concept with a specific heat loss of 0.33 W/(K m^2) and district heating at around 140 kWh/(m^2 a) is the cost optimal solution. This specific heat loss coefficient, which includes transmission and infiltration losses through the building envelope per heated net floor area, shows a reasonably good insulation level of the envelope. The authors included labor costs, material costs, overheads and value added tax in the energy performance related construction costs. They did not, however, take into account maintenance, replacement and disposal costs, as these had a minimal impact on net present value, and this also allowed them to keep the calculations transparent.

Stocker et al. (Stocker, Tschurtschenthaler, & Schrott, 2015) reported a study of cost-optimal building renovation arrangements regarding the heating energy performance of eight primary schools, located in the Alps and characterized by different ages and construction techniques. The objective of the study was to reduce the heating energy consumption and they implemented measures to improve the envelope performance as well as, the efficiency of the heating system. Additionally, they developed a sensitivity analysis in order to evaluate the impact of some parameters used for the calculation. They obtained that the variation on the energy price, the measure cost and the interest rate are the most influential in the results.

Similar results were obtained in ECOFYS study (Schimschar et al., 2013), where analyzed the link and consistency between the nearly zero energy buildings definition and the cost-optimal levels of the minimum energy requirements. One of the aspects that they evaluated was the gap in the global cost calculation, mainly related to the variability of some parameters over the period calculation: technology costs, energy costs and primary energy factors for electricity or district heating. They performed some scenarios to quantify the impact of this variability into the cost-optimal analysis, obtaining significant changes in the optimum levels (from 25% to 50% of variability, depending on the scenario).

Brandão et al. (Brandão de Vasconcelos, Pinheiro, Manso, & Cabaço, 2016) developed the cost-optimal evaluation for a residential building of Portugal. They studied around 35,000 combinations of passive measures to evaluate which was the most suitable strategy for the envelope renovation. They used EnergyPlus for the primary energy calculation. The work concluded that the rehabilitation of the roof produces the greatest variation in terms of primary energy consumption and the combination of thermal envelope measures creates synergy effects that lead to better results than single measures.

Aelenei et al. (Aelenei et al., 2015) implemented the methodology for the refurbishment of public buildings toward nearly Zero Energy Buildings (nZEB). The analysis was applied to a reference building of an existing office building in five different countries: Italy, Portugal, Romania, Spain and Greece. The evaluation tool used a new cost optimization procedure based on a sequential search optimization technique considering discrete options (Corrado, Ballarini, & Paduos, 2014), which was implemented before in a cost-optimal study in residential buildings in Italy. The results were presented in terms of optimal "package of measures", primary energy consumption and global costs, as well as a cross-country comparison.

Asadi et al. (Asadi, da Silva, Antunes, & Dias, 2012) wanted to demonstrate the potentiality of the cost-effective evaluation to provide decision support. For that, an optimization methodology was developed based on combining TRNSYS, GenOpt and a multi-objective optimization algorithm in MatLab. The optimization approach was applied to a case study to evaluate all available combinations of alternative retrofit actions. Ganiç et al. (Ganiç & Yılmaz, 2014) implemented the cost optimal methodology in Turkey and investigated the validity of the procedure under national market conditions.

Finally, it is clear that there is a wide range of possibilities to develop this type of studies, from the point of view of the criteria and parameters and, from the point of view of the tools. In that sense, Tadeu et al. (Tadeu et al., 2016) compared the cost-optimal evaluation with the return of investment. The results from the real options perspective enabled to conclude that the global cost is not enough for the investors and must be complemented with additional information (as the value of operational flexibility and other strategic factors), and the return of investment must be evaluated in a long-term rather than in the short-term perspective. Other point of view of the same discussion is described by Becchio et al. (C Becchio, Corgnati, Orlietti, & Spigliantini, 2015). They introduced the need to incorporate some additional benefits to the global cost calculation, in order to achieve more interesting results for all the actors involved, including investors and final users. They proposed a method for quantify qualitative benefits in monetary terms, as the increase of the real estate market value, the enhancement of the indoor comfort, the reduction of CO_2 emissions.

3.3 PREFABRICATED BUILDINGS

Conventionally, a building's construction begins and ends on the same construction site. It is a linear process, and when one benchmark has been completed, the project moves to the next. This process is known as on-site, stick-built, conventional, site-built, or traditional construction, and can be incredibly inefficient—one delay along the line can push the project weeks or months behind schedule (Kamali & Hewage, 2016).

On the other hand, prefabrication refers to a building that is (fully or partially) manufactured in a factory, delivered, and assembled on site. Based on the degree of work off the construction site, off-site construction is categorized into the following levels (Kamali & Hewage, 2016):

- Component subassembly: small scale elements are constructed in the factory (e.g. windows or doors);
- Non-volumetric preassembly, elements are assembled in a factory to create non-volumetric building components before installation at the construction site;
- Volumetric Preassembly, similar to the previous, but components actually create fully-furnished, spatial units that are then shipped to the site and fit to site-built components;
- Modular, all building components, aside from foundation and sitework, are preassembled into modules which together, when assembled, make a building.

Modular systems refer to prefabrication of volumetric building units. Modules are three-dimensional independent units, which could be produced fully or partially in sections. Fully modular houses represent the most complete form of prefabrication, where the entire housing spaces such as kitchen, bedrooms, and living rooms are included in a module. Fully modular units require only installation on the site, and they can be immediately used after electricity and water facilitates are connected. Due to design, production or transportation limits, a modular system can comprise multiple modules, which can be combined in different ways In this way, modules are repeated by stacking or joining, side by side (Beim, Nielsen, & Vibæk, 2010; Knaack, Chung-Klatte, & Hasselbach, 2012). Modular units may be purchased and assembled on-site by different manufacturers, and assembly is performed by connecting the elements to each other via identical interfaces (Beim et al., 2010; Kamali & Hewage, 2016).

Modular prefabricated houses are the most cumbersome and technically challenging systems. The design and production of modular systems (full or partial) are tightly dependent on the size and weight of modules, transportation, and installation costs. The weight of modules is limited by capacity of trucks and lifters, while the size of the module should be limited by road width and shipping standards, where exceeding the maximum width requires special permission. The installation of modules on site may also require special skills.

In component systems, building elements are individually manufactured in the factory and brought to the site, where they can be assembled in a variety of ways. Component systems can be categorized as a “kit-of-parts,” which are panelized and pre-cut (Huang, 2008). The kit-of-parts refers to a collection of discrete building elements, which are prefabricated, efficiently packed, and delivered to the site, where they can be assembled. Panelized systems have been widely applied in the design and construction of non-residential building with complex geometries. In the pre-cut systems, the building is designed in a more structured way, where building components are joined like puzzles that fit together in a unique order (Sass, 2007). It has been argued that due to the large number of components, pre-cut systems have cost-saving potentials when implemented with digital fabrication, and also reduce labor expense (Sass, 2007).

3.3.1 Advantages and disadvantages of modular building

The various benefits of the use of prefabrication comparing with traditional cast in-situ construction technologies have been identified by many researchers, including shorten construction period, cost reductions, better safety environment for workers on site and environmental benefits (Kamali & Hewage, 2016).

One of the most important benefits of prefabricated construction is fast turnaround between “ground breaking” and occupancy. In other words, building construction and site preparation activities take place simultaneously (Kawecki, 2010). In addition, the risk of delays due to weather extremes, vandalism, and site theft are minimal in prefabricated construction (L. C. Jaillon, 2009; Lu, 2007). Prefabrication may be a key option for cases where construction deadlines are often inflexible, such as for the education sector, or for projects on active sites (e.g., an extension of a hospital complex constructing a new building) (Kamali & Hewage, 2016).

Prefabricated construction can save around 40% of construction time compared with traditional construction (R M Lawson & Ogden, 2010; Smith, 2010). Some literature stated that when the number of stories increases in a prefabricated project (e.g., multi-family vs. single-family buildings), the time savings decreases considerably because the project becomes more complicated and subsequently extra engineering and communication as well as more work in the jobsite are required (Ramaji & Memari, 2015). However, the completion time of prefabricated buildings is still less than that of conventional ones even though the project is a high-rise building (Cartz & Crosby, 2007).

Off-site methods could yield a lower overall project cost due to many related factors (Kozlovská, Kaleja, & Struková, 2014; R. Mark Lawson et al., 2012). Manufacturing numerous building components simultaneously can save costs because materials can be ordered in bulk and labor and machinery transportation can be reduced (Quale et al., 2012). In addition, prefabricated construction decreases the number of laborers on site, which results in less labor congestion, leading to higher craft productivity (Lu, 2007). Moreover, cost reductions could be achieved by other factors, such as on-site overhead reduction, avoidance of weather extremes, standardization of design, high level of energy efficiency, and higher efficiency in installation (Kamali & Hewage, 2016). However, some literature emphasized that the impact of using off-site construction on project costs is not very clear due to a variety of contributing variables (Chiang, Hon-Wan Chan, & Ka-Leung Lok, 2006; R.M. Lawson & Ogden, 2008; Pan, Wong, & Hui, 2011). For example, the lack of access to confidential financial information of projects and the use of modern equipment are among the unknown variables (Lu, 2007).

Workplace accidents, working at height, congestion, severe weather, dangerous activities, and neighboring construction operations can be reduced by transferring the main construction work to factories with easier and highly repetitive site operations (Cartz & Crosby, 2007; Kamali & Hewage, 2016; R. Mark Lawson et al., 2012; Lu, 2007). According to Lawson et al. (2012), when prefabricated construction is used, on-site reportable accidents can be reduced by 80% compared to on-site construction (R. Mark Lawson et al., 2012).

Several environmental benefits are offered in modular construction. Less waste is one of the most important benefits of more precise purchasing, planning, and cutting of materials and appropriate recycling opportunities (L. C. Jaillon, 2009; R. Mark Lawson et al., 2012; Lu, 2007, 2009; Moon, 2014). At the end of the modular buildings' life cycle, modules can be disassembled, relocated or refurbished to be used in other projects instead of disposal (Li & Li, 2013). On-site reduction of greenhouse gas (GHG) emissions is another benefit of modular systems

(Amiri et al., 2013; Lu & Korman, 2010). Reduced construction time leads to less energy consumption, fewer workers' trips, fewer trips by suppliers and subcontractors to the construction sites (due to material delivery in bulk to the factory plants) (Kamali & Hewage, 2016).

Finally, higher quality can be achieved with the use of prefabricated construction due to the controlled manufacturing facilities in which the components are built. Repetitive processes and operations, as well as automated machinery, can result in a higher level of product quality (Ambler, 2013; Cartz & Crosby, 2007).

On the other hand, the reviewed literature pointed to some disadvantages for using prefabricated buildings. Among the most notable difficulties are project planning, transportation difficulties, negative perceptions, site constraints, difficulty in coordination, and upfront costs (Kamali & Hewage, 2016).

Among these difficulties, the greatest difficulty with modular construction is the far greater requirement for planning and coordination of all aspects of the project. Prefabrication design is significantly different from conventional design. Complex construction need more engineering design because of the subsequent design complexity. A clear scope is needed in advance as it is hard to make any changes later during the construction phase (L. Jaillon & Poon, 2010; Lu, 2009).

Transportation logistics are also a key consideration for prefabricated construction. Before taking any design step, the project team should investigate the limitations of transportation in the area. In addition to studying the general transportation regulations, special traffic control allowance requirements for heavily populated areas should be checked (O'Connor, O'Brien, & Choi, 2015). Generally, it is not possible to transport manufactured houses or completed modules to distant locations because it is costly and requires complex arrangements (Boyd, Khalfan, & Maqsood, 2013; Lu, 2009; Martinez, Jardon, Navarro, & Gonzalez, 2008; O'Connor et al., 2015). The dimensional constraint is another transportation barrier which can be dictated by the transportation regulations of each country (Kamali & Hewage, 2016).

Much literature noted the public's negative perception of off-site construction methods. It is a considerable factor that hinders the fast development of off-site construction techniques all around the world. As an example, modular and prefabricated homes are usually believed to be similar to temporary buildings in the Unites States; however, they are completely different cc (Boyd et al., 2013; Rahman, 2013). The end users 'lack of awareness on the benefits and different options offered by off-site construction techniques can influence the market demand and subsequently the development of these techniques (Mao, Shen, Pan, & Ye, 2013).

A considerable amount of initial capital is needed to set up appropriate machinery to run a manufacturing plant (Chiang et al., 2006; R. Mark Lawson et al., 2012; Rahman, 2013). In addition, local economy is a determining factor to initiate modular construction services in an area. In those areas, where the labor is cheap, new methods of construction may not be possible. Likewise, the lack of availability of knowledgeable and experienced experts, such as engineers and designers who have enough experience for prefabricated systems is a limitation (L. Jaillon & Poon, 2010).

Finally, there is a need for an increased and more detailed and effective coordination in all stages of a prefabricated building, including pre-project planning, procurement, supply chain scheduling, installation and construction, and delivery (Lu, 2007; O'Connor et al., 2015; Rahman, 2013).

3.3.2 State of the art: energy and environmental performance of prefabricated buildings

The energy performance and environmental effects of traditional buildings have been previously studied in detail, while a limited number of works about prefabricated construction is available. In the following paragraphs, some literature studies on the energy and environmental of prefabricated buildings are discussed: most of them do not take in consideration the entire life cycle of the building, and if they do, the approach is usually simplified or there is no reference to a detailed building performance simulation analysis.

Cao et al. (X. Cao, Li, Zhu, & Zhang, 2015) compared the environmental impacts of a residential prefabricated building with a traditional building through the application of LCA. Both buildings are located in the Fangshan District of Beijing, China. The prefabricated building is made of the assembly of precast concrete wall systems. The prefabricated elements account for approximately 38% of the total volume of the prefabricated building. Traditional building has reinforced-concrete wall structure and it relies on the traditional cast-in-situ construction method. The system boundaries for both buildings included materials extraction, off site component manufacturing, transportation, construction and on site - assembling. The results showed that the prefabricated building construction is less energy intensive: it has a total final energy consumption of less than 20.5% compared to the traditional building. Moreover, the use of prefabrication showed lower environmental impacts, including

35.8% reduction in resource depletion, 6.6% in health damage and 3.5% in ecosystem damage (X. Cao et al., 2015).

Atmaca (Atmaca, 2017) addressed the primary life cycle energy consumption and the CO_2 emissions of the construction, use and end-of-life stages of two temporary houses (a prefabricated house and a container). The buildings life cycles were assumed 15 and 25 years for the container and the prefabricated building, respectively. The prefabricated building had a gross area of 70 m^2 with one story, two rooms, one kitchen and a sitting room. The container was a small building with a gross area of 21 m^2, with two rooms, a toilet and a kitchen inside the room. Life cycle primary energy consumption of the prefabricated and container housings were calculated to be 29.1 GJ/m^2 and 32.6 GJ/m^2, respectively, while the CO_2 emissions were respectively 255 kg $CO_{2eq}/(m^2$ year) and 491 $CO_{2eq}/(m^2$ year). The use stage was dominant over the life cycle of the housings, accounting for 85.9% and for 90.3% of total primary energy use of the prefabricated and container respectively and for 94.6% and 95.7% of total CO2 emissions. Finally, the results showed that the prefabricated housings compared to the container allowed to save the 12% of primary energy use and the 93% of the CO_2 emissions.

Faludi et al. (Faludi et al., 2012) performed a LCA, from the material acquisition to the end-of-life, of a prefabricated modular commercial building (465 m^2) in San Francisco. The building has a structural steel frame with light-gauge steel wall panels and aluminum curtain walls. Three different energy consumption scenarios for the operation stage were analyzed: 1) standard building with average Northern California energy use; 2) 30% of the energy supplied by rooftop photovoltaic and the rest by the grid; 3) a NZEB (photovoltaic supply 100% of energy). The lifetime of the building was estimated to be 80 years. Energy consumption in the use stage was estimated through a non-steady state simulation. The result showed that the standard building was the worst scenario (during the entire life cycle about 3,000 tons of CO_{2eq} emissions and around 180,000 EcoIndicator 99 points) while the NZEB building was the best scenario (around 500 tons of CO_{2eq} emissions and approximately 40,000 EcoIndicator 99 points). Results also showed that energy consumption in the operation stage caused the highest impacts (83% of CO_2 emissions) in the standard building. In the third scenario the most impactful stage was the material production (55% of CO_2 emissions) (Faludi et al., 2012).

Similar to the study done by Faludi et al. (Faludi et al., 2012), in Paya-Marin et al. (Paya-Marin, Lim, & Sengupta, 2013), the life cycle performance of two modular schools were assessed to identify the energy consumption and environmental impacts. Two 120 m2 school buildings with different materials and energy consumption system were investigated. The first one was a typical modular school called "Standard building" built in Northern Ireland, UK. The other one was called "Eco Modular Solutions building" (Eco building), which was modeled with a different HVAC System, lighting system and materials as well as a photovoltaic installation that can produce a portion of the school′s energy by itself. IES Virtual Environment software was used to quantify the energy consumption during 50 years lifetime. The results of the LCA stated that the embodied carbon in the case of the standard building was 60% more than that of the Eco building. Likewise, the Eco building emitted 48% less GHG emissions annually, compared to the standard school building. It can be understood from this study that using energy efficient technologies, such as low-emissivity windows, thermal insulation, efficient HVAC systems, and daylighting controls, will lead to less energy consumption, hence less environmental impacts (Paya-Marin et al., 2013).

Monahan and Powell (Monahan & Powell, 2011) performed a "from cradle to construction site" LCA of a low energy modular building based on timber frame wall modules, which was constructed in 2008 in Norfolk, United Kingdom. In addition to the case study (base scenario), two further scenarios (scenarios 2 and 3) were modelled. Scenario 2 used a panelized modular timber frame with steel cladding, while the third scenario was a traditional masonry building. For the base scenario, the total embodied energy was estimated to be 5.7 GJ/m^2 while the embodied carbon was approximately 405 kg CO_{2eq}/m^2. The 82% of the total embodied carbon was due to materials. In scenario 2, the embodied energy and carbon were quantified as 7.7 GJ/m^2 and 535 kg CO_{2eq}/m^2, respectively. This means that 35% more embodied energy was consumed and 32% more embodied carbon was produced compared to the base scenario. Scenario 3 was the worst scenario (8.2 GJ/m^2 and 612 kg CO_{2eq}/m^2). Compared to the base scenario, the embodied energy is higher by 35% and the embodied carbon by 51% (Monahan & Powell, 2011).

Mao et al. (Mao, Shen, Shen, & Tang, 2013) performed a LCA of two types of buildings in Shenzhen, China: a prefabricated building and a traditional one. System boundaries included building materials production and transports, transports of soil, transports of prefabricated components and buildings construction. The aim of the study was the determination of the extent of the reduction of Greenhouse Gas (GHG) emissions that can be achieved by prefabrication in comparison to conventional construction. A reduction of 1.1 tons of CO_{2eq} per 100 m^2 was found in the prefabrication building, approximately 3.2% less than that emitted in the project with conventional construction. The main contributor to GHG emissions reduction was the embodied emissions of building materials, accounting for 86.5% (Mao, Shen, Shen, et al., 2013).

Similarly to Mao et al. (Mao, Shen, Shen, et al., 2013), Park et al. (Park & Kim, 2014) compared the life cycle carbon emissions of a modular house and of a concrete apartment building; both buildings were analyzed with the use of recycled materials and without. The results show that the modular house with reusable materials has lower impacts than other buildings.

Kawecki (Kawecki, 2010) quantified the carbon footprint of factory production output, as measured by home, module, and square foot of fabrication, based on his observations and data collection during one month in a modular home fabrication company in Pennsylvania, US. All energy consumed for the manufacturing process in the fabrication plant as well as the delivery and installation of the modules were taken into account. However, the embodied energy, associated with materials and material delivery to the factory, and the construction waste were considered outside of the study scope. Furthermore, only CO_2 emissions were measured and the other greenhouse gases were excluded. The carbon emissions for a 130 m^2, two-module home were estimated to be 3051 kg of CO_{2eq}. In addition, the researcher compared a three-module residential home with a similar stick-built home and suggested that the modular home produces 30% less carbon than the conventional home. In terms of CO_2 emission sources during the manufacturing period, electricity was found to be the predominant energy source (Kawecki, 2010).

Zea Escamilla and Habert (Escamilla & Habert, 2015) identified twenty prefabricated emergency shelters over 11 different locations worldwide and assessed their environmental, economic, and mechanical/technical performances. The environmental assessments was based on LCA approach choosing as functional unit a single module. System boundaries included building materials production and transports to the construction sites. Four impact categories were considered (human health, ecosystem quality, CO_2 emissions and primary energy use) and subsequently were normalized and presented as a single score. The shelters were clustered into 4 groups in function of the main construction materials used: bamboo, wood, steel and concrete/brick. The environmental impact assessment results showed that the bamboo-based shelters have the lowest impact per functional unit. Moreover, the authors concluded that the systems construction using local materials can provide the best compromise between environmental impacts and costs (Escamilla & Habert, 2015).

In the same way, Song et al. (Song, Mithraratne, & Zhang, 2016), performed a life-cycle performance analysis of temporary housing in China, looking at embodied, operating and end-of-life energy. It was found that energy consumed in the construction process contributes to 65% of the life-cycle energy resulting in the life-cycle energy of post-disaster temporary housing being much higher than that of low-energy buildings. Based on this they suggested reducing the life-cycle energy of post-disaster shelters by using recycled and less energy-intensive materials.

Kim performed an LCA on a one-story single-family modular house and a traditional stick-built house in Michigan, US, to investigate the environmental impact through the use of different construction techniques over the lifetime of 50 years (D. Kim, 2008). The functional unit was considered to be the usable area (135 m^2). The modular home was modeled based on real data provided by the modular manufacturer. Since it is difficult to find a conventional home with an identical size and comparable conditions, the industry average data for the same volume and floor area was used to analyze the conventional home. The author used a life cycle approach to compare the total energy consumption (including embodied and operational energies), resource use, GHG emissions, and waste generation between the modular and conventional homes. For the modular home, four phases of its life cycle, including material acquisition, module fabrication, site assembly, and occupancy, were taken into account. Similarly, for the conventional home, the material acquisition, construction, and occupancy phases were within the assessment boundary. For both case studies, the end of life (demolition) phase, as well as maintenance/renovation related tasks were considered to be outside of the boundary. SimaPro and BEES databases were used for the LCA of material and energy consumption before the occupancy phase. Energy consumption during the occupancy phase was simulated by eQuest. Kim's study confirmed that the use phase for both modular and conventional homes is the dominant phase in terms of energy consumption and accounts for 94.8% and 93.2% of the total energy used during the life cycle, respectively. However, the energy consumption of the modular home was 4.6% less than its counterpart. In terms of GHG, the use phase alone emitted more than 95% of the total life cycle emissions in both cases, but still the modular case was in better condition. The global warming potential for the stick-built home was calculated to be 5% higher than the modular home. Moreover, it was estimated that the on-site construction process generates solid waste up to 2.5 times more than the modular construction process (D. Kim, 2008).

Al-Hussein et al. focused on the construction phase of modular and conventional buildings and compared their CO_2 equivalent emissions. They analyzed a 42-suite multi-family four-story residential modular building located in Alberta, Canada. All the construction activities needed for this building, and a similar conventional building, such as material delivery transportation, workforce trips, equipment usage and winter heating, were identified separately. Therefore, CO_2 emissions from each of these activities were quantified. However, the CO_2 quantification, related to the embodied energy of the building materials, was not taken into account. The authors' analyses showed that modular processes led to a 43% reduction in CO_2 emissions compared to on-site processes (Al-Hussein, Manrique, & Mah, 2009).

Islam et al. (Islam, Zhang, Setunge, & Bhuiyan, 2016) evaluated the environmental impacts of a container building (121.6 m^2) located in Melbourne (Australia). The LCA approach uses six impacts categories: cumulative energy demand, water use, solid waste, global warming potential, acidification potential and eutrophication potential. The functional unit is a building over its 60 year lifetime including construction, operation (only heating and cooling energy requirement), maintenance and disposal. The operational heating and cooling requirements were evaluated by the AccuRate software (Delsante, 2004). Life cycle primary energy consumption and CO_2 emissions were calculated to be 1737.7 GJ and 103.6 tons of CO_{2eq} emissions, respectively. Results also show that the operation stage has the most dominating impact for all the indicators (cumulative energy demand: 67.5%, global warming potential: 69.1%, acidification potential: 65.7% and eutrophication potential: 77%), while water use was the most dominant impact indicator for the construction stage (about 60.5%) and solid waste was for the disposal stage (about 80.9%).

Aye et al. quantified and compared the embodied and operational energy of three residential buildings including a prefabricated steel-framed modular, a prefabricated timber-framed modular and a conventional concrete building (Aye, Ngo, Crawford, Gammampila, & Mendis, 2012). The buildings were assumed to be located in Melbourne, Australia. The resulting GHG emissions and also the potential areas to manage the generated waste were investigated as well. Each building was an eight-story multi-family with the gross floor area of 3943 m^2 and 63 apartments. The researchers used the LCA technique over the full life cycle of the buildings. The occupancy phase for all the scenarios was assumed to be 50 years. The embodied energy, because of potential material replacement over the life time, was excluded in this study. SimaPro database was used for the embodied energy quantifications. Also, energy use during the operation phase was simulated using TRNSYS. The total embodied energy for the steel modular case study was reported around 50% more than the conventional concrete case, while the total mass of the latter was much more than the former building (4 times). The total embodied energy for the modular steel, wood, and conventional case studies was calculated for 14.4, 10.5, and 9.6 GJ/m^2 of floor area, respectively. According to the authors, this was due to higher energy-intensive steel manufacturing processes compared to concrete. For all the construction techniques, the greatest material volume happened in external walls (followed by the floor panels), accounting for the total material volume of 39%, 47% and 49% for, conventional building, modular timber, and steel buildings, respectively. It means these areas have the potential for waste reduction through the use of more durable materials as well as implementing a better construction waste management strategies such as reuse and recycling. The study showed that there is only a minor variance in energy use during the occupancy period among different construction methods. The estimated life cycle energy, in the case of the modular steel building, was 36 GJ/m^2, which was greater than that of the concrete building (30 GJ/m^2). The embodied energy represented at least 32% of the total life cycle energy for the case study buildings, which shows the importance of suitable strategies to reduce the embodied energy in the design, material use, and end of life stages. When it comes to greenhouse emissions, the study indicated that the modular steel building emited 13% more over the life cycle compared to the conventional building. The percentage of GHG emissions associated with the embodied energy contributed between 21% and 27% of the total emissions for all the case studies. If the embodied emissions, resulting from the replacement of potential materials and components over the use phase, are taken into account, the percentage will be even higher. According to the researchers, despite the fact that in their study the conventional scenario consumes less energy than the other two modular ones; however, new construction methods, such as modular technique, are capable to provide better environmental impacts through the use of less embodied energy-intensive materials and including reuse strategy in the initial building designs. Therefore, less embodied energy requirements and subsequent GHG emissions will be achievable (Aye et al., 2012).

Hong et al. (Hong, Shen, Mao, Li, & Li, 2016) analyzed the life cycle energy consumption of six typical prefabricated components (pre-stressed concrete structures, precast form, slab, balcony, staircase and panel) in China. The system boundaries for the energy quantification cover the whole life cycle of the prefabricated components, including prefabrication manufacturing, transportation, on-site assembling, and recycling in the demolition phase. Results showed that the life-cycle energy use of prefabricated components range from 7.33 GJ/m^3 for precast staircase to 13.34 GJ/m^3 for precast form. Prefabrication manufacturing consumes over 90% of the total embodied energy consumption. The embodied energy use in the transportation and on-site construction processes are negligibly small compared with those in other processes, while the recycling process could achieve 16% – 24% energy reduction (Hong et al., 2016).

Pons and Wadel (Pons & Wadel, 2011) addressed the CO_2 emissions of a school building located near Barcelona (Spain). A LCA is carried out for the same building, by comparing three different prefabricated envelopes and a non-prefabricated one. In detail, the prefabricated approaches were classified in three groups according to their structure material: concrete, steel and timber. The analysis was repeated four times for the same building using different solutions. It took into account the following stages: materials productions, transport, building construction, use (taking into account 50 years of useful life), maintenance and demolition. Life cycle total CO_2 emissions for these four scenarios showed similar results despite the different emissions generated during each life cycle phase. (Non-prefabricated: 1359 kg CO_{2eq}/m^2, Concrete: 1229 kg CO_{2eq}/m^2, Timber: 1106 kg kg CO_{2eq}/m^2 and Steel: 1461 kg kg CO_{2eq}/m^2). Steel structures were responsible for the highest CO_2 emissions in the material production stage (about 700 kg CO_{2eq}/m^2), while timber structures were cause of the lowest emissions (about 300 kg CO_{2eq}/m^2). For the use stage, the steel technology and the non-prefabricated building had the highest emissions values (about 600 kg CO_{2eq}/m^2), while the concrete technology had the lowest emissions values (about 530 kg CO_{2eq}/m^2) (Pons & Wadel, 2011).

Quale et al. in 2012 (Quale et al., 2012) focused on the construction phase of modular and traditional buildings and quantified the energy consumption from cradle to end of construction, and compared the consequent environmental impacts between the two construction methods. The case study buildings included three residential modular buildings and five conventional buildings; all were two-story wood frame homes with the floor area of 186 m^2. Data such as utility bills, worker transportation, materials and waste information, employee and construction schedules, etc., was taken from three residential modular companies in the eastern US based on their completed projects. Finding two versions of a building constructed with two different techniques is impossible. Thus, after compiling the specifications for the modular building, on-site professional homebuilders were asked by the researchers to provide the data if they were going to build on-site buildings in the same region using the same specifications. The embodied energy for modular case studies was estimated in different categories including: material quantities, material and labor transportation as well as energy consumed in the factory, when transporting modules, and assembling them on the jobsite. In the case of conventional buildings, again, material quantities, material and labor transportation were considered in addition to energy consumption on-site. Finally, waste generated during construction was quantified for both case study buildings. It should be noted that as the authors wanted to compare the two construction methods, only those building materials that differed between two methods were taken into account. Again, regarding construction waste the net difference waste amount between two methods was considered. In addition, it was assumed that all the generated waste is sent to landfills. SimaPro database was used for energy quantification. The results of LCA analyses for GHG emissions for the modular and conventional case studied showed that, on average, modular buildings have lower negative environmental impacts compared to their counterparts. Average GHG emissions for modular buildings was estimated to be nearly 6 t of $CO_{2\text{-eq}}$ less than that of traditional buildings per 186 m^2 home. Furthermore, energy consumption on-site and labor transportation significantly contributed to GHG emissions in conventional construction which reveals the potential areas to reduce the environmental impacts. In addition to the carbon footprint, other impacts were moderately higher in case of conventional buildings (20–70%).

Schiavoni et al. (Schiavoni, Sambuco, Rotili, D’Alessandro, & Fantauzzi, 2017) focused on the design of innovative nearly Zero Energy Buildings realized using end of life shipping containers named Housing Pull & Push (HPP). The paper reports the outcomes of studies performed to evaluate the energy, lighting and environmental performance of some case studies characterized by different floor areas, i.e. 14 m^2 (S type), 7 m^2

(XS type) and 5.6 m^2 (XXS type), and external coverings (Corian, Corten and wood). Moreover, each HPPs were equipped with PV modules and a rainwater recovering system.

Energy demand of HPPs was simulated in unsteady regime taking into account thermal insulation of the envelope and HVAC system characteristics using EnergyPlus. The simulations were performed using the weather data of Perugia (central Italy) and maintaining thermal control setpoints at 20 °C from 15th October to 15th April and at 26 °C from 15th April to 15th October. Concerning the design of the photovoltaic panels, all the available roof area was used. Lighting systems were designed to guarantee adequate indoor illuminance values considering different furniture configurations and the effect of natural and artificial light. Environmental performance was evaluated following the Life Cycle Assessment (LCA) methodology assessing impacts in terms of primary energy consumption and greenhouse gas emissions. In detail, a cradle to grave LCA was performed and the whole cycle of HPP was subdivided in four stages: the product stage, the construction stage, the use stage and the end of life stage. The life span of HPP is assumed to be 10 years. Even if materials could have different service life, it was assumed that materials would not be substituted during 10 years of usage and, consequently, maintenance operations were excluded from the boundaries.

The results showed that the total consumption increases with the volume of the case study while specific energy consumptions decreases; the behaviour of the latter parameter is influenced by the S/V ratio. The best energy performance was obtained with the wood covering panel; in these cases the total energy consumption for S, XS and XXS HPP were respectively 759.30, 438.41 and 391.01 kWh. Energy demand is covered completely by the energy produced from the photovoltaic panels placed on the roofs. Concerning the specific energy consumption, for the same cases values equal to 54.24, 62.63 and 69.82 kWh/m^2 were calculated.

The results of LCA analysis, by varying the material of exterior cladding, showed that the configuration with wooden coating has the best environmental performance: primary energy consumption and greenhouse gas emissions were estimated equal to 9878 MJ_{eq} and 621 kg $CO_{2\text{-}eq}$ per year, respectively. Although the impacts of HPP with wooden cladding in values were the lowest, the importance of selecting recoverable materials emerged from the analysis. In fact, the HPP module with Corten coating allows to avoid more impacts at the end of life with respect to the other two configurations. Steel recycling allows to avoid 17 694 MJ_{eq} of primary energy and 1161 kg $CO_{2\text{-}eq}$ of greenhouse gas emissions per year after the end of life of HPP module.

Finally, the combination of the above-mentioned methodologies allowed to demonstrate that the designed HPPs are nZEB characterized by comfortable conditions and by interesting environmental performance. Moreover, the HPP modules can be a sustainable and feasible way to reusing old containers (Schiavoni et al., 2017).

The reuse of shipping containers in architecture was also analyzed by Ulloa et al (Ulloa, Arce, Rey, Míguez, & Hernández, 2017) and by Elrayies (Elrayies, 2017). In (Ulloa et al., 2017) three typologies of modules have been analyzed. A thermal analysis of the design proposals has been carried out in TRNSYS environment, analyzing the energetic demands in 5 dissimilar places among them (Port-au-Prince, Haiti; Yibuti, Yibuti; Colonia, Uruguay; Yakutsk, Russia; Puerto Williams, Chile). Instead, Elrayies assessed the thermal performance of shipping containers in Port Said, Egypt (Elrayies, 2017). In detail, the author presented a comparative analysis of six simulation models, including a conventional building as a base model, an uninsulated container, and four externally insulated container with four different thermal insulation materials: rock wool, wool, polyurethane foam and straw. The results asserted that the need for thermal insulation in shipping containers is indispensable for habitation. The most compatible thermal insulation in the hot and humid climate of Port Said is the polyurethane foam, which has the lowest total discomfort hours.

Dong et al. (Dong, Wang, Li, Jiang, & Al-Hussein, 2018) performed a LCA of lightweight prefabricated building (30 m^2) equipped with renewable energy systems in Nanjing (China). The case study was designed for use as a temporary residence and has a service life of 20 years. Additionally, solar photovoltaic and solar thermal systems are deployed to supply daily operating energy in order to guarantee independence from the energy grid for at least one month. The life cycle of the building was divided into six stages: construction materials preparation, building elements prefabrication, logistics, on-site assembly, building operations and building disposal. The LCA results indicated a carbon emissions of 35.7 kg/m^2 per year. Furthermore, with the aim of reducing the environmental impacts, life cycle carbon reduction measures were proposed for each stage of temporary housing. For example some passive energy-saving strategies, such as natural ventilation, sun-shade design, and optimization of thermal performance of building envelope, allowed a reduction of the operational emissions of 91.5%.

3.4 CHAPTER CONCLUSIONS

Despite the ZEB concept is intuitively clear, both theoretical and methodological aspects of this and related concepts are under-investigation. Several studies faced the challenge (A J Marszal et al., 2011; Panagiotidou & Fuller, 2013; J Salom et al., 2011; Sartori et al., 2012; P. Torcellini et al., 2006), giving birth to a structured framework and identifying criteria detailing the general ZEB concept. In this context and in order to comprehensively understand the key aspects relating to this study's goals, the first part of the chapter reviews literature to holistically understand the concept of NZEB and the key factors to achieve this target.

The boundary is one of the most discussed arguments as it is linked to RES inputs that can be included or not in the balance. The boundary of a system may include a single building or groups of buildings, in this last case it is not important that every building is nearly zero, but the overall sum of the buildings has to be. The renewable integration into district heating system is at neighborhood or infrastructural level, while a PV system is mostly taken into account at building or building complex level. If there is a PV plant in an area close to a building and the boundary is restricted to the building, this source is considered off-site, otherwise it is on-site.

Another main point of discussion is the metric of balance. More than one unit can be used in the definition or in the calculation methodology. The most frequently applied unit is primary energy while the easiest unit to implement is final or delivered energy. Among other options there are: end use energy, CO_2 equivalent emissions, exergy, delivered/site energy, and cost of energy.

The period of the balance over which the calculation is performed can vary very much. It can be hourly, daily, monthly, seasonal or annual, or the full life cycle of a building or its operating time.

With regard to the type of balance, the energy use has to be offset by RES generation in off-grid ZEBs, while two possible options are possible in grid-connected ZEBs. The first is preferred during the design phase of a building and it balances energy demand with RES generation. The second is applicable during the monitoring phase as it balances energy delivered with energy feed into the grid.

The RES supply can be on-site, nearby, or off-site depending on the availability on site (sun, wind) or to be transported to the site (biomass). A ranking of preferred application of different renewable supply side options is proposed in (P. Torcellini et al., 2006). As a starting point there is a reduction of site energy use through low-energy technologies (daylighting, high-efficiency HVAC—heating, ventilation, air conditioning, natural ventilation, evaporative cooling). On-site supply options use RES available within the building footprint (such as PV, solar hot water, wind, heat pumps), or within the building site (such as PV, solar hot water, low impact hydro, wind). Off-site supply options use RES available off-site to generate energy on-site (such as biomass, wood pellets, ethanol, biodiesel that can be imported, or wasted streams used on-site to generate electricity and heat), or purchase off-site RES (such as utility-based wind, PV, emissions credits, or other "green" purchasing options and hydroelectric). The different RES options and the fraction of RES production to be included have to be also defined.

Another argument is the possible connection to the energy infrastructure. Most nZEBs definitions implicitly assume connection to one or more utility grids. These can be electricity grid, district heating and cooling systems, gas pipe network, or biomass and biofuels distribution network. Therefore, buildings have the opportunity to both import and export energy from these grids and thus avoid on-site electricity storage. While on-grid nZEBs are connected to one or more energy infrastructures using the grid both as a source and a sink of electricity, off-grid nZEBs require an electricity storage system in peak load periods or when RES are not available.

Moreover, ensuring that on-site generation matches up with on-site consumption and that energy exported to the grid is done so at a time that does not create grid stability issues due to oversupply, are factors to be considered if the NZEB concept is to be widely adopted. Matching on-site generation with on-site demand is known as load matching (LM), whilst grid interaction (GI) concerns the matching of grid export, and grid quality & stability requirements.

In general, the literature review demonstrates that the main idea of NZEBs is that they consume not more energy than they produce renewable energy. The review has demonstrated that the achievement of the NZEB status depends on the choice of the definition for a NZEB. Different types of such definitions have been discussed. They include different aspects depending on the building's functions, target audience, local conditions, design preferences, etc. Therefore, the same building can be NZE, according to one definition, and not to be, according to another.

Although there is a variety of approaches to define NZEBs with different features and peculiarities, they have a common requirement for achieving NZE goal: first of all, energy demand of the building needs to be reduced through energy efficiency improvement and, secondly, the remaining energy consumption should be covered by renewable energy.

Different energy efficiency measures could be considered, which can be applied in NZEBs, starting with building orientation and design and finishing with utilization of energy efficient lighting and appliances. The main conclusion is that the complex of these measures can dramatically reduce energy demand.

Different renewable supply options are also discussed in order to provide the understanding of how renewable energy can be produced in different types of building under different conditions. The analyzed literature shows that the wide utilization of renewable energy technologies in buildings is usually aggravated by their dependency on climatic and weather conditions and, consequently, unstable performance.

In general, the subject of NZEBs is becoming more and more acute nowadays, having both supporters and opponents, which makes it complex, challenging and very interesting for the research.

In the second part of the chapter, since the case study is a prefabricated building, a review of the previous research and papers about the energy and environmental performances of prefabricated buildings are discussed. In detail, some final considerations can be formulated to sum up the literature analysis:

- compared to traditional buildings, few studies have been conducted to evaluate the environmental impacts of the prefabricated buildings. One of the reasons behind having fewer studies could be the fact that this construction method is relatively new compared to conventional methods. Therefore, there is limited information and data based on real projects supported by prefabricated building manufacturers/developers to perform various analyses.

- whilst the international literature provides substantial coverage of site-built net zero energy buildings, that research is not easily transposable to prefabricated buildings. Moreover, the critical examination of the literature exploring energy use in prefabricated buildings, and the strategies to reduce those energy use impacts, found there is scant evidence on the way in which these type of buildings can reach a net zero energy performances.

- some studies limit the boundaries of the analysis to some life cycle stages, for example, some studies focused only on the construction stage. Thus, the results cannot be generalized to the whole life cycle.

- most of the existing studies were developed using a single indicator, e.g. the use of primary energy or the GHG emissions. However, since environmental impacts produced by any process have variable effects, it is difficult to investigate the buildings environmental and energy performances through the use of a single indicator but different environmental impacts should be considered.

- similar to previously performed studies for conventional buildings, energy consumption in the use phase of prefabricated buildings dominates the other life cycle phases. This phase alone accounts for more than 70% and up to 98% of energy consumption and consequent impacts over the life cycle of buildings, while the contribution of the construction phase is relatively small. This reveals that the top priority for improving the environmental performance is reducing energy consumption during the building operation phase.

- only limited efforts are performed towards the building performance modeling to analyze the effects of the design to the whole life cycle of the construction.

4 THE CASE STUDY

4.1 INTRODUCTION

In this chapter the case study building will be shown, starting from the design phase and explaining the main features of the building: the IDEA (Integrating Domotics, Energy and Architecture) building, Fig. 4.1, a prefabricated building module built in context of the research project "CNR for Southern Italy - Advanced technologies for energy efficiency and zero impact mobility". This building is an application of new concepts of the architectural design: comfort, sustainability, energy and economy. It was also built as a laboratory where new sustainable technologies are studied and further developed. In particular, the case study is a prototype of a housing module integrating renewable sources energy production systems (PV system) and innovative materials (fiber reinforced polymers materials (FRP)).

In the following paragraphs the main features of the case study will be presented.

Fig. 4.1 - The IDEA building.

4.2 THE CLIMATE

The case study is located in Messina, Fig. 4.2 (latitude 38.15°, longitude 15.53°, altitude 132 m), at the "National Research Council of Italy– Institute for Advanced Energy Technologies" (CNR-ITAE).

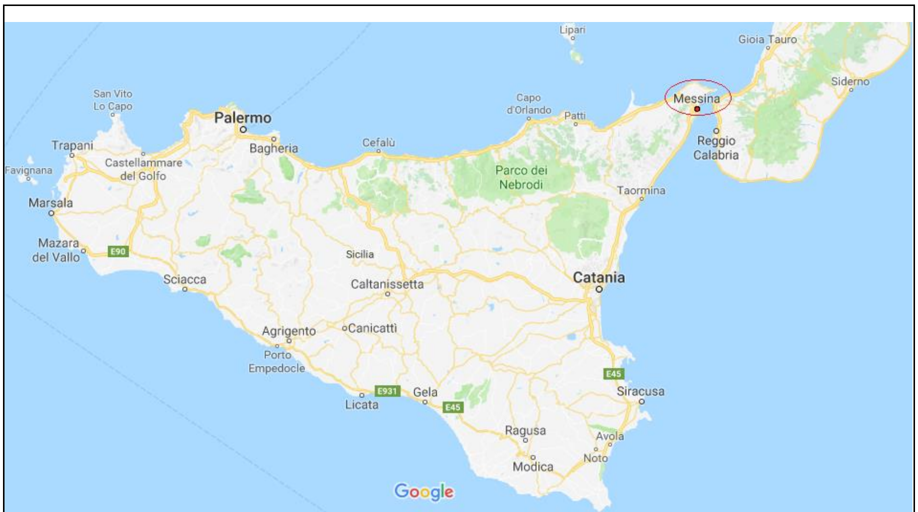

Latitude [°]:	38.15	Altitude [m]:	132
Longitude [°]:	15.53	Time Zone:	+1

Fig. 4.2- The National Research Council of Italy – Institute for Advanced Energy Technologies" (CNR-ITAE).

Climate encompasses the statistics of temperature, humidity, atmospheric pressure, wind, precipitation, atmospheric particle count and other meteorological elemental measurements in a given region over long periods.

Climate can be contrasted to weather, which is the present condition of these elements and their variations over shorter periods. The climate of a location is affected by its latitude, terrain, and altitude, as well as nearby water bodies and their currents. Climates can be classified according to the average and the typical ranges of different variables, most commonly temperature and precipitation. The most commonly used classification scheme was originally developed by Wladimir Köppen (Kottek, Grieser, Beck, Rudolf, & Rubel, 2006). The Köppen classification depends on average monthly values of temperature and precipitation. The most commonly used form of the Köppen classification has five primary types labeled A through E (Fig. 4.3). These primary types are:

- tropical;
- dry;
- mild mid-latitude;
- cold mid-latitude;
- polar.

The five primary classifications can be further divided into secondary classifications such as rain forest, monsoon, tropical savanna, humid subtropical, humid continental, oceanic climate, Mediterranean climate, steppe, subarctic climate, tundra, polar ice cap, and desert.

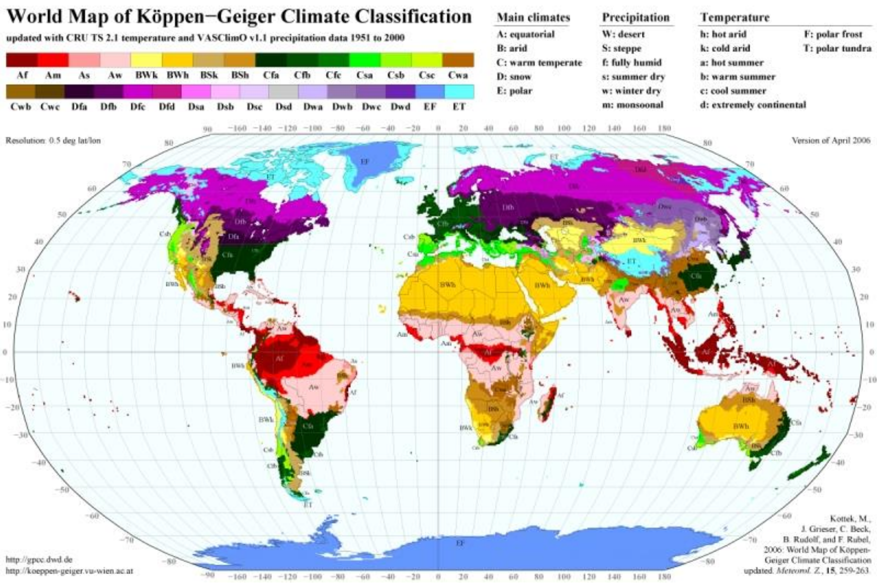

Fig. 4.3 - Koppen climate classification (Kottek et al., 2006).

Messina, located near the northeast corner of Sicily, is characterized by a comfortable climate, with mild winters and hot summers, in detail:

- minimum annual temperature is 7 °C;
- maximum annual temperature is 32.2 °C;
- mean annual humidity is 72%;
- mean annual horizontal solar radiation is 363 W/m^2.

The horizontal solar radiation monthly mean varies during the year between 179 W/m^2 (in December) and 501 W/m^2 (in July), while Fig. 4.4 shows the mean daily values for global horizontal, direct normal and diffuse solar radiation.

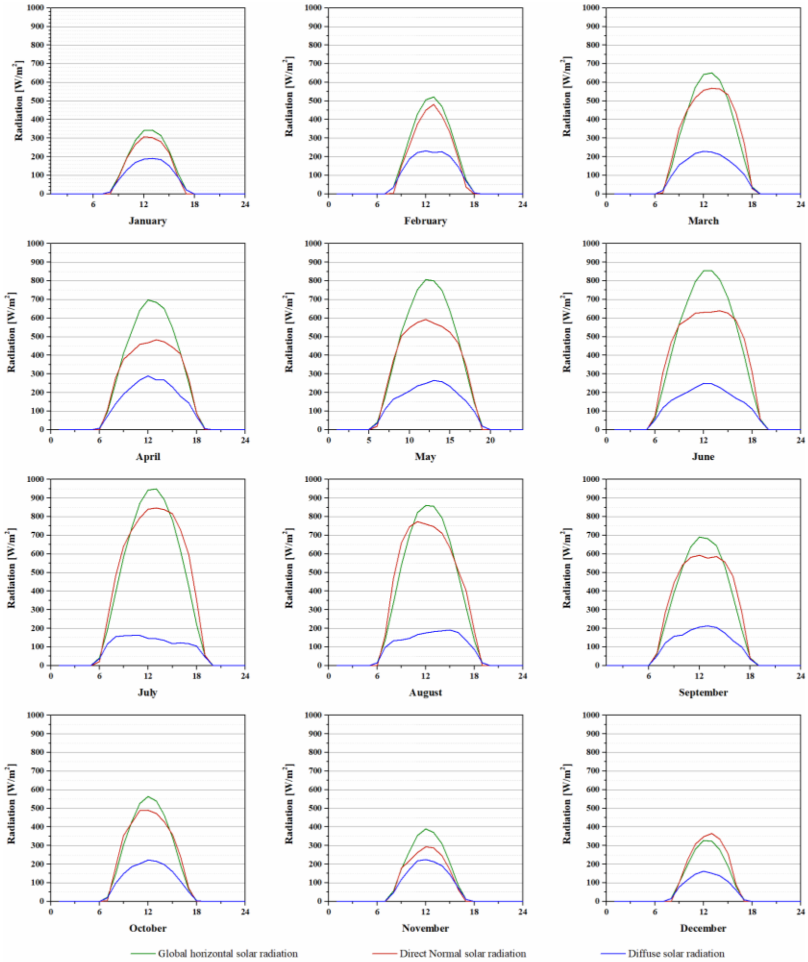

Fig. 4.4 - Average monthly solar radiation for Messina, Italy (Thevenard & Brunger, 2002).

As shown in Fig. 4.5, the outdoor dry-bulb temperature can easily reach 30 °C during summer, the minimum value is around 7 °C during winter, while the annual mean temperature is about 18.9 °C.

February is characterized by the mean temperature closest to zero (12 °C) and the minimum and maximum values are 7 °C and 15.6 °C, respectively. For 75% of the data analysed, the temperature is below 13.7 °C, for 50% it is below 12.5 °C, while for 25% of the data it is below 10.4 °C.

August is characterized by the highest monthly mean temperature (27.4 °C) and for 75% of the data analysed the temperature is below 29 °C, for 50% it is below 27 °C, while for 25% of the data it is below 26 °C.

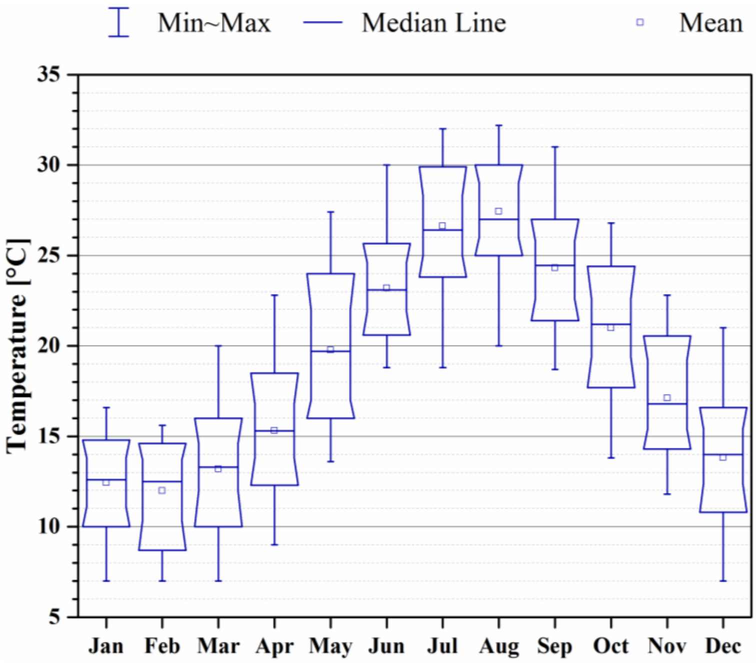

Fig. 4.5 - Outdoor air temperature for Messina, Italy (Thevenard & Brunger, 2002).

Tab. 4.1 shows the monthly mean value of relative humidity and wind speed for Messina. The relative humidity varies from 62.9 % in April to 80.9 % in November, while the annual mean value is about 71.7 %. The year average wind speed wind is about 2.7 m/s., while it varies between 1.2 m/s (July) and 4.1 m/s (April).

Tab. 4.1 - Monthly mean value of relative humidity and wind speed for Messina, Italy (Thevenard & Brunger, 2002).

Month	Relative humidity [%]	Wind speed [m/s]
January	72.96	1.50
February	67.56	2.89
March	71.94	3.09
April	62.91	4.10
May	76.46	3.03
June	66.03	3.04
July	65.73	1.24
August	68.08	2.58
September	75.50	2.94
October	71.56	1.81
November	80.85	3.13
December	78.56	3.23
Year	71.67	2.68

The data used to elaborate the charts above belongs to the same weather files used in the simulations of this study. In detail, the file is the ASHRAE International Weather for Energy Calculations (IWEC) data for Messina (Thevenard & Brunger, 2002).

4.3 THE CASE STUDY

The module develops on a single level of about 45 m^2, including 2 rooms (Fig. 4.6 shows floor plan while a brief summary of the building properties can be found in Tab. 4.2).

Tab. 4.2 – Building main properties.

Floor area	45 m^2
Total window area	24 m^2
Azimuth of the southern façade	117°
Window to wall area ratio of the south-east façade	90 %
Window to wall ratio of the north-west façade	65 %
Internal height of the rooms	3.2 m

The technical room has an area of about 9 m^2 and contains technical equipment while the main room has a gross surface of 36 m^2 and is used as office. During the working days the building is occupied by three people from 8:00 a.m. until 5:00 p.m., with a break for lunch from 2:00 p.m. to 3:00 p.m.

Total thermal internal loads are caused by lighting (22.2 W/m^2) and office equipment (about 200 W). The lighting system is controlled by an illuminance dimmering with a setpoint of 500 Lux activated by the presence of people inside the building.

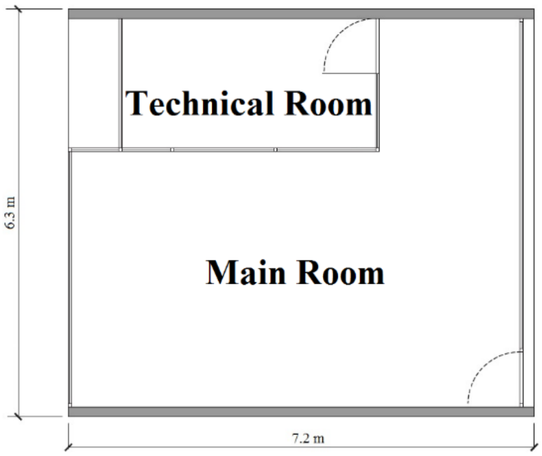

Fig. 4.6 - Floor plan of the building.

The entire structure of the housing module is made of pultruded fiber reinforced material (FRP). The external (total surface dimension equals to 61 m^2) and internal (20 m^2) walls have a thickness of 25 cm (Fig. 4.7a). The floor and the roof (Fig. 4.7b) have the same thickness and the same composition of the vertical walls.

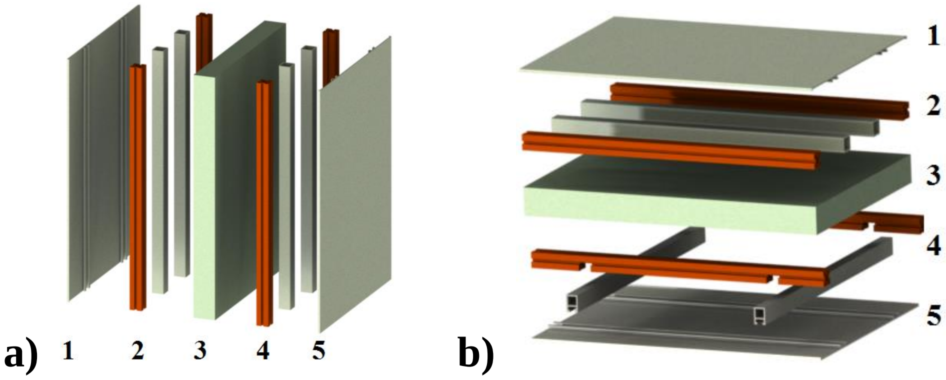

Fig. 4.7 - Section of the wall (a) and the roof/floor (b) (1- 5: FRP panels, 2 - 4: FRP profiles, 3: Thermal insulation material).

Tab. 4.3 shows the information regarding wall layers' physical properties. The envelope of the building was properly insulated by 0.09 m of polyester insulation panel (thermal resistance equal to 2.67 m^2K/W). Particular attention is paid to the thermal insulation of the thermal bridges.

Tab. 4.3 - Wall layers' physical properties.

	Thermal conductivity [W/(m K)]	Thermal capacity [J/(kg K)]	Density [kg/m3]
Roofingreen panel	0.0569	5088.3	124.6
FRP panel	0.3000	1350	1800
Polyester insulation panel	0.0337	1450	43
Barrisol sheet	0.0001	1	1800

The building is south-east oriented (117° east from north). The window-to-wall area ratio (WWR) of the south-east façade is about 90%, with nearly 15 m^2 of glazed area (20% openable). The window to wall ratio of the north-west is 65%. The windows are made of double low-emissivity insulated glazing with 0.005 m external glass, 0.016 m gap filled with argon and 0.004 m internal glass; the glass U value is 1.10 $W/(m^2K)$ while the window frame U value is 1.4 $W/(m^2K)$.

The case study envelope is compliant to the instructions of the Italian Ministerial Decree 26/06/2015 that defines the limits for the thermal transmittance of the walls and of the glazing components for all new buildings built from 2021 onwards (Ministero dello Sviluppo Economico, 2015). Tab. 4.4 shows the comparison between the global transmittance limit (U values) imposed by the law and the calculated transmittance value for the building envelope.

Tab. 4.4 - Comparison between the U value limits imposed by the Italian Ministerial Decree 26/06/2015 and the calculated U value of the structures (Ministero dello Sviluppo Economico, 2015).

Unit		Description	Case study	Law limits
$U_{ext,wall}$	$[W/(m^2K)]$	External wall thermal transmittance	0.3	0.40
U_{roof}	$[W/(m^2K)]$	Roof thermal transmittance	0.3	0.32
U_{floor}	$[W/(m^2K)]$	Floor thermal transmittance	0.3	0.42
U_{window}	$[W/(m^2K)]$	Window thermal transmittance	1.1	3

The building reaches the nZEB target according to the Italian Ministerial Decree 26/06/2015 (Ministero dello Sviluppo Economico, 2015) on the "Application of the energy performance calculation methods and establishment of prescriptions and minimum requirements of buildings" entered into force in October 2015 (Tab. 4.5 shows the comparison between nZEB limit values and those calculated for the case study). In detail, it implements the national law no. 90/2013 (Presidente della Repubblica, 2013) which transposes the Directive 2010/31/EU (EPBD recast) in Italy (Recast, 2010). The Italian Ministerial Decree sets the methodology for calculating the energy performance of buildings and establishes the minimum energy performance requirements of buildings. It introduces new prescriptions, both for new buildings and for the energy refurbishment and renovation of existing buildings. It also specifies the requirements of nearly zero-energy buildings (nZEBs) that will be applied to new buildings and major renovations from 1st January 2019 for the public buildings and from 1st January 2021 for all the other buildings. The nZEB limit values are not established a priori by the Italian Ministerial Decree 26/06/2015, but they are determined for a notional building, named reference building. The reference building has the same location, building function, size of the building under analysis, but with parameters of the thermal envelope and of the technical systems replaced by reference values (Ministero dello Sviluppo Economico, 2015).

Tab. 4.5 - Comparison between nZEB limit values imposed by the Italian Ministerial Decree 26/06/2015 and those calculated for the case study (Ministero dello Sviluppo Economico, 2015).

	Unit	**Description**	**Case study**	**nZEB limit**
H'T	[W/(m²k)]	Mean overall heat transfer coefficient by thermal transmission	0.45	0.58
$A_{sol'}$	-	Summer solar effective collecting area of the building	0.03	0.04
$EP_{H,nd}$	[kWh/(m²year)]	Annual energy needs of the building for space heating	18.40	29.95
$EP_{C,nd}$	[kWh/(m²year)]	Annual energy needs of the building for space cooling	172.48	235.64
$EP_{gl,tot}$	[kWh/(m²year)]	Global total annual primary energy of the building	117.62	255.42
η_{Gh}	-	Mean global seasonal efficiencies of the heating system	0.63	0.62
η_{Gc}	-	Mean global seasonal efficiencies of the heating system	2.87	1.35

4.4 CONSTRUCTION STEPS

The supporting structure is realized through a beam / pillar system, which provides for the presence of a regular mesh of pillars and beams arranged in the two directions on which the floors rest (Fig. 4.8). The construction site has not undergone any processing and following the future dismantling of the prefabricated will be restored to the original conditions. The ground connection of the structure takes place through a point system, made with adjustable supports, to overcome the small differences in level of the ground.

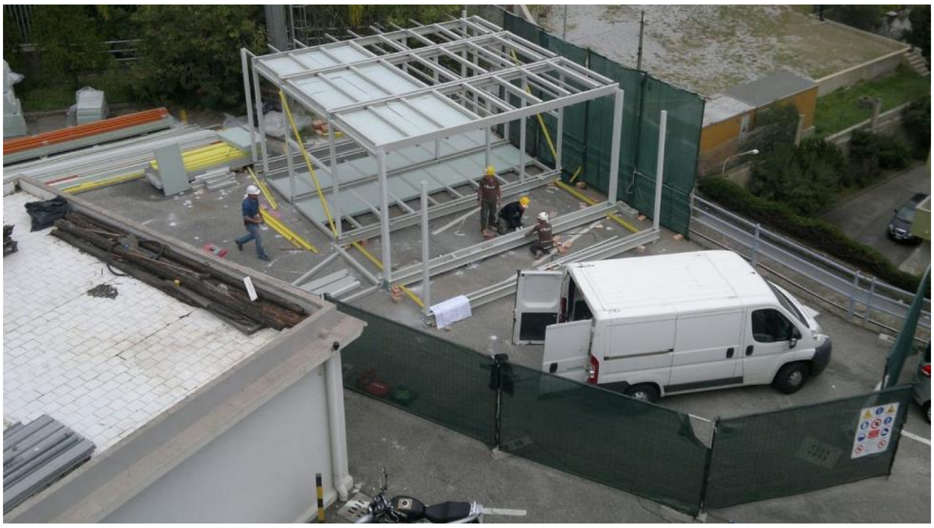

Fig. 4.8 - The case study during the construction stage.

The construction of the building consists of the following phases:

- assembly of the supporting structure;
- assembly of the floor and roof;
- assembly of the perimeter walls;
- assembly of the internal dividing walls;
- installation of windows and doors;
- assembly of internal and external finishes;
- installation of the technical systems.

Fig. 4.9 shows the construction process through a 3D visualization.

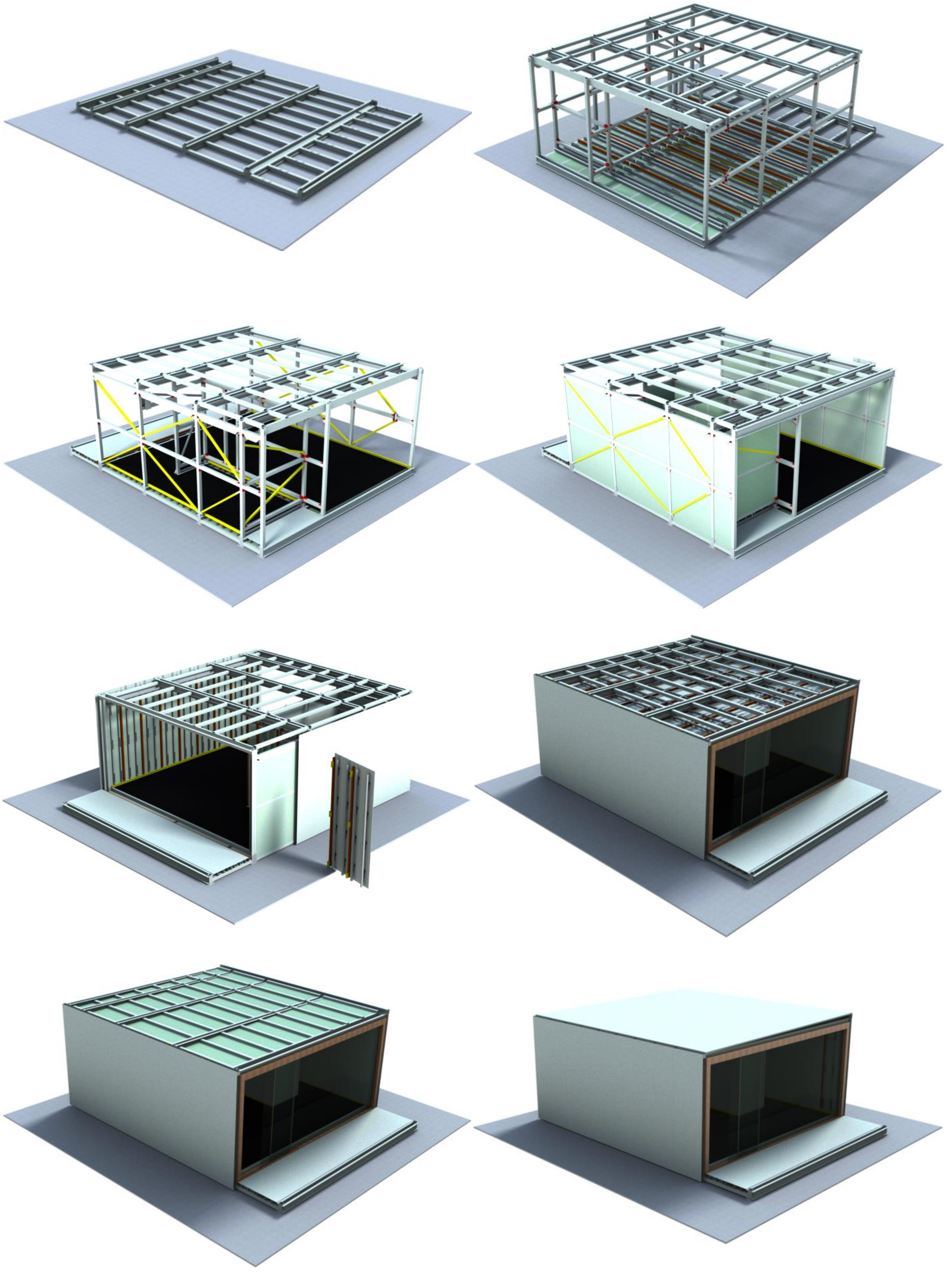

Fig. 4.9 - The case study construction process.

4.5 EQUIPMENT AND ENERGY SYSTEMS

The building is powered by a rooftop building integrated photovoltaic system, a heat-pump-air conditioning system, and finally it is connected to the electricity grid, which therefore constitutes the third electricity supplier.

Moreover, in order to optimize the energy flows and the power exchange with the grid an Energy Management System (Fig. 4.10) set-up in the technical room equipped with a 3KVA multi-source.

Fig. 4.10 - Energy Management System.

4.5.1 The PV System

The building is equipped with a grid-connected photovoltaic system (PV) for the production of electricity. The photovoltaic system has a peak power of 5.76 kW_p, made up of 24 modules of 240 W_p (Tab. 4.6 shows the technical data). Each PV module has an area of 1.7 m^2, for a total area of about 41 m^2.

Tab. 4.6 - Technical data of the photovoltaic module (merimp, 2019).

Number of cells in series	[-]	72
Active Area	[m^2]	1.75
Semiconductor bandgap	[eV]	1.12
Short circuit current	[A]	8.1
Open circuit voltage	[A]	48.5
Reference temperature	[°C]	25
Reference insolation	[W/ m^2]	1000
Module current at maximum power	[A]	7.33
Module voltage at maximum power	[V]	39.5
Temperature coefficient of short circuit current	[A/°C]	0.002
Temperature coefficient of open circuit voltage	[V/°C]	-0.162

In Fig. 4.11 are shown the overall performances of the PV modules, according to the temperature variation and at a standard value of the incident radiation (merimp, 2019).

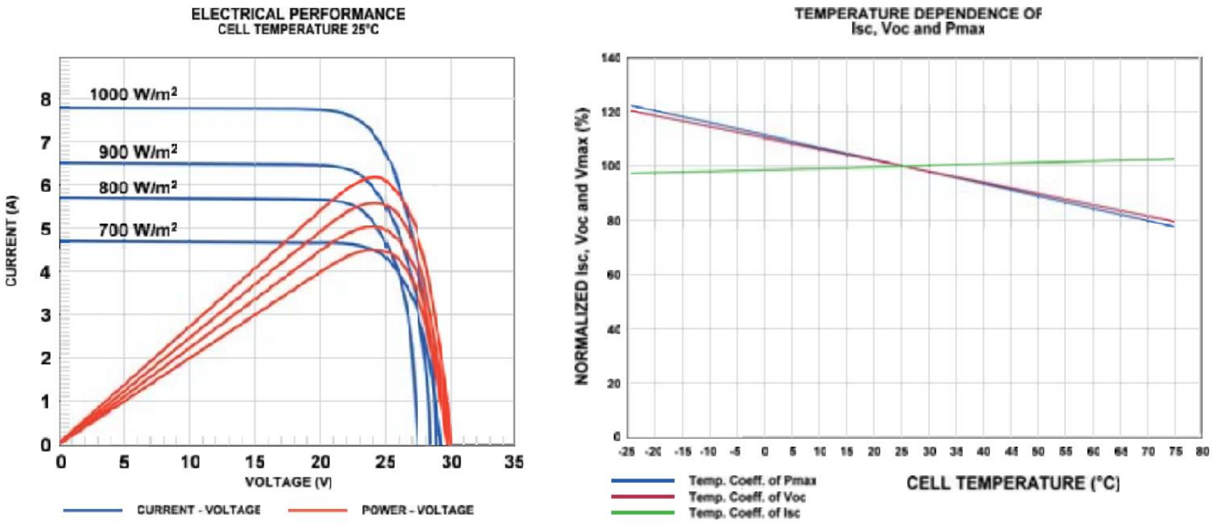

Fig. 4.11 - Overall performances of the PV modules (merimp, 2019).

4.5.2 The thermal plant

The building is equipped with a heat-pump air conditioning system. The heat pump is an air-to-air interface heat pump (heating nominal capacity = 8.2 kW, cooling nominal capacity= 7.1 kW), with the external condensing unit distincted from the inner part which contains the hydronic circuit and compressor (Maxa, 2018). Tab. 4.7 shows the technical data of the heat pump, while Fig. 4.12 shows the operating range in both cooling and heating mode.

Tab. 4.7 – Air-to-air heat pump technical data (Maxa, 2018).

Nominal cooling capacity	[kW]	7.1
Minimum cooling capacity	[kW]	2.3
Maximum cooling capacity	[kW]	8.5
SEER	[-]	4.9
EER	[-]	3.0
Nominal heating capacity	[kW]	8.2
Minimum heating capacity	[kW]	2.3
Maximum heating capacity	[kW]	10.2
SCOP	[-]	3.5
COP	[-]	3.2
Compressor power input	[kW]	1.9
Power consumption fans	[W]	66

The refrigerant fluid is R-410A, the compressor is the type Rotary Twin-Scroll with permanent magnet synchronous motors and variable speed. The machine is equipped with hydronic pumps and variable speed fans, and brazed plate heat exchangers and has a built-in defrost.

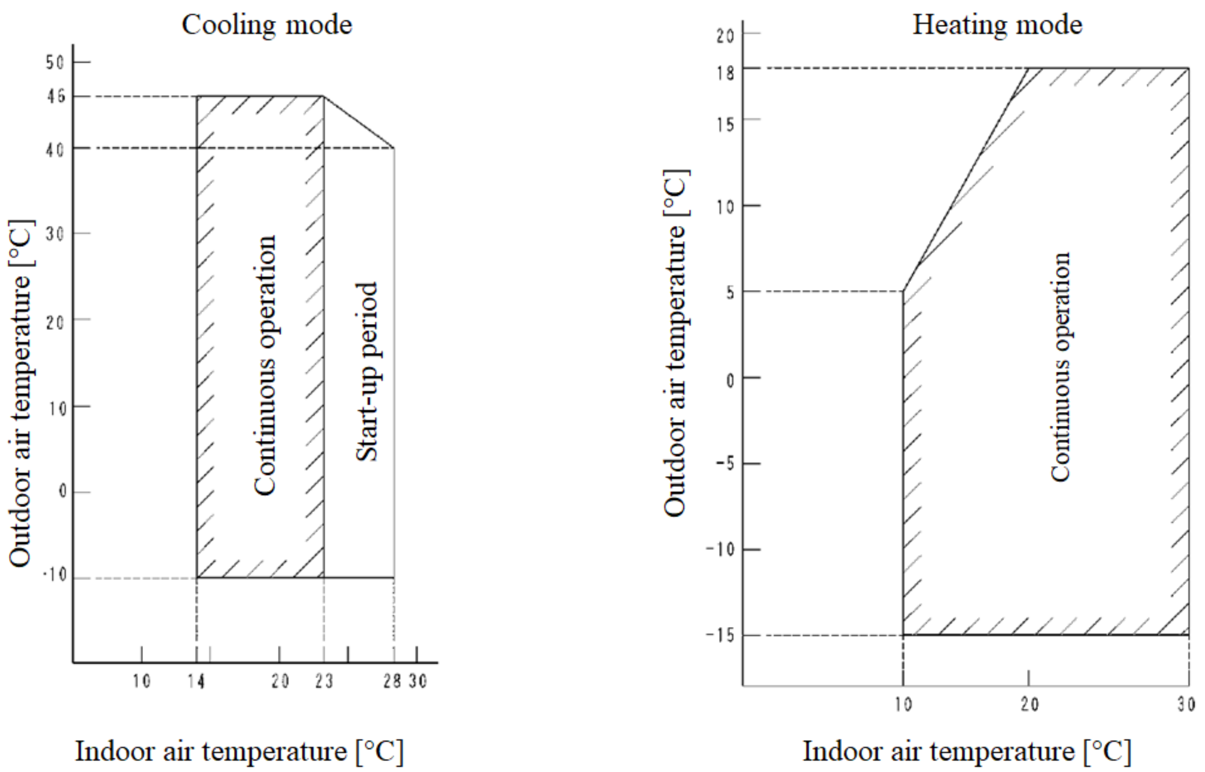

Fig. 4.12 – Heat pump operating range in cooling and heating mode (Maxa, 2018).

Finally, Tab. 4.8 and Tab. 4.9 show the cooling/heating capacities due to both internal and external air temperature changes. In particular, in heating mode the COP varies between 2.11 (indoor dry-bulb air temperature = 27 ° C, outdoor dry-bulb air temperature = -10 ° C) and 3.57 (indoor dry-bulb air temperature = 15 ° C, outdoor dry-bulb air temperature = 10 ° C). In particular, the COP varies between 2.11 (indoor dry-bulb air temperature = 27 ° C, outdoor dry-bulb air temperature = -10 ° C) and 3.57 (indoor dry-bulb air temperature = 15 ° C, outdoor dry-bulb air temperature = 10 ° C). On the other hand, the EER varies between 2.38 (indoor dry-bulb air temperature = 20 ° C, outdoor dry-bulb air temperature = 40 ° C) and 4.82 (indoor dry-bulb air temperature = 32 ° C, outdoor dry-bulb air temperature = 20 ° C).

Tab. 4.8 - Heating capacity due to both internal and external air temperature changes (Maxa, 2018).

	Outdoor dry-bulb temperature [°C]									
IDT	**-10**		**-5**		**0**		**6**		**10**	
	HC	**IP**	**HC**	**IP**	**HC**	**IP**	**HC**	**IP**	**HC**	**IP**
15	5.52	2.16	6.45	2.26	7.37	2.37	8.48	2.49	9.22	2.58
20	5.24	2.21	6.16	2.32	7.09	2.49	8.2	2.55	8.94	2.63
22	5.12	2.24	6.05	2.34	6.98	2.45	8.09	2.57	8.83	2.66
24	5.01	2.26	5.94	2.36	6.86	2.47	7.97	2.6	8.71	2.68
25	4.95	2.27	5.88	2.38	6.81	2.48	7.92	2.61	8.47	2.68
27	4.84	2.29	5.77	2.4	6.69	2.5	7.8	2.63	7.92	2.68

HC= Heating Capacity [kW] – IP = Input Power [kW] - IDT = Indoor dry-bulb air temperature [°C]

Tab. 4.9 - Cooling capacity due to both internal and external air temperature changes (Maxa, 2018).

		Outdoor dry-bulb air temperature [°C]																	
IWT	**IDT**	**20**			**25**			**30**			**32**			**35**			**40**		
		CC	**SCC**	**IP**	**CC**	**SCC**	**IP**	**CC**	**SCC**	**IP**	**CC**	**SCC**	**IP**	**CC**	**SCC**	**IP**	**CC**	**SCC**	**IP**
14	**20**	7.03	4.95	1.78	6.94	4.90	1.98	6.61	4.73	2.15	6.48	4.66	2.22	6.28	4.56	2.32	5.95	4.39	2.5
16	**22**	7.60	4.99	1.81	7.27	4.83	1.99	6.94	4.66	2.16	6.81	4.60	2.23	6.61	4.50	2.33	6.28	4.34	2.51
18	**25**	7.93	5.17	1.82	7.60	5.02	2.00	7.27	4.87	2.17	7.13	4.80	2.24	6.94	4.71	2.34	6.61	4.57	2.52
19	**27**	8.09	5.41	1.83	7.76	5.26	2.00	7.43	5.11	2.18	7.30	5.05	2.25	7.10	4.96	2.35	6.77	4.82	2.52
22	**30**	8.58	5.2	1.84	8.25	5.06	2.02	7.92	4.93	2.19	7.79	4.88	2.26	7.59	4.80	2.37	7.26	4.67	2.54
24	**32**	8.91	5.04	1.85	8.58	4.92	2.03	8.25	4.80	2.20	8.12	475	2.27	7.92	4.68	2.38	7.59	4.56	2.55

CC= Total cooling capacity [kW] – SCC = Sensible cooling capacity [k] - IP = Input power [kW] – IDT = Indoor dry-bulb air temperature [°C] - IWT = Indoor dry-bulb air temperature [°C]

5 RESEARCH METHOD

5.1 INTRODUCTION

The aim of this chapter is to define the research method used in order to answer the research questions presented at the end of chapter 1 and to show the framework used for the integrated life cycle energy and environmental assessment of the building case study. In detail, the energy performance and the environmental impacts of the building case study were investigated, combining both the analysis of the use stage through dynamic simulation, and of the life cycle assessment of the building, in order to avoid the shifting of environmental and energy burdens from one stage to others or from one impact assessment indicator to another and analyze the hotspots of the building during its life cycle. All life cycle stages were included in the study: materials and component production, construction process, use and end-of-life. A thermo-physical model of the building is implemented in EnergyPlus environment (D. B. Crawley et al., 2000), which was calibrated using data collected during on-site monitoring. A LCA approach is used to assess the life cycle impacts of the prefabricated module.

The overall methodology of the current study is illustrated in Fig. 5.1. The first part of the chapter provides a detailed insight of the modelling and simulation steps followed. In section 5.2.1 a description of the building energy model is presented. In section 5.2.2 the monitoring studies performed are described. Lastly, section 5.2.3 shows the model calibration and the validation process.

The second part of the chapter describes the life cycle model developed to assess environmental impacts caused by the building. In section 5.3.1 the goal and scope is presented along with the system boundaries and the functional unit. In section 5.3.2 the Life Cycle Inventory (LCI) is described identifying the LCI approach and the LCI framework implemented for the case study. In section 5.3.3 the life cycle impact assessment (LCIA) methods and the environmental categories included are presented. Finally, in section 5.3.5 energy and environmental payback times (PBT), calculated for each impact category analysed in the LCIA stage, are shown

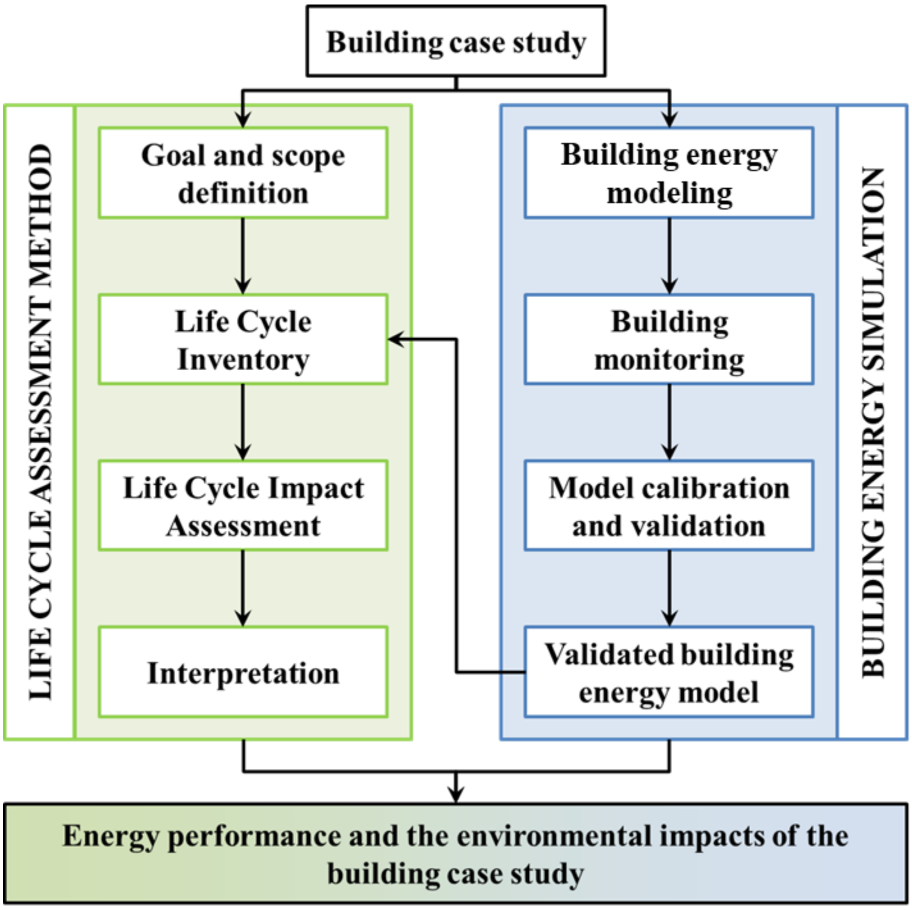

Fig. 5.1 - Framework for an integrated life cycle energy and environmental assessment of the building case study.

5.2 BUILDING ENERGY SIMULATION

The tool chosen for the building modeling was EnergyPlus, a state of the art validated software, whose validation has been evaluated through several standards, e.g., ASHRAE Standard 140-2011 and IEA BESTEST (D. B. Crawley, Hand, Kummert, & Griffith, 2008; D. B. Crawley et al., 2000; Henninger & Witte, 2004). In detail, EnergyPlus is a thermal load and energy analysis calculation program which uses hourly or sub hourly time intervals to calculate building energy demand and advanced building physics aspects. This takes into account the interplay between building occupancy and aspects such as HVAC systems, lighting and other appliances. Fig. 5.2 below shows the overall program structure, links to various other programs and capability to add future modules. EnergyPlus has three basic requirements – a simulation manager, a heat and mass balance module, and a building systems simulation module. The simulation manager controls the entire simulation process. The heat balance calculations are based on IBLAST – a research version of BLAST with integrated HVAC systems and building loads simulation. More details regarding the capabilities of EnergyPlus are given in (D. B. Crawley et al., 2008, 2000).

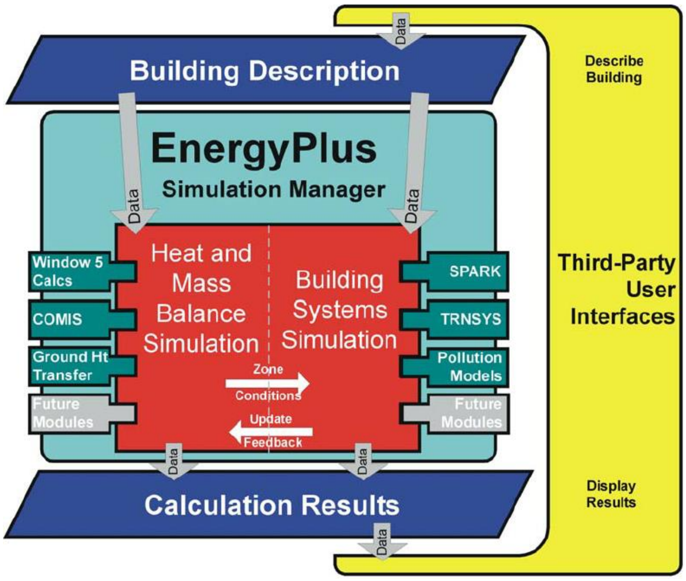

Fig. 5.2 - Overall EnergyPlus Structure.

This section provides a detailed view of the modelling and simulation methodology. Fig. 5.3 schematically shows different steps of the methodology which ultimately leads to a calibrated and validated model:

- Analysis of the system and survey of operational variables. This step consists of the description of the building's equipment or sub-systems in their interaction with the building, including their schedule of operation and related parameters The operational requirements must be evaluated, including the analysis of the variables with the largest influence;
- Creation of a dynamic model of the building;
- Evaluation of the accuracy of the predicted building model, by means of validation and calibration of the model variables. The process focused on the model parameters uncertainties by manual tuning the unknown variables according to the metered data. Since model calibration is the iterative process of comparing the model to the real system, adjusting the input of each variable to see the effect on the output, while other variables are kept unchanged, the model calibration was repeated until the difference between the simulated and monitored data was acceptable (recalibration).
- Assessment of the performances of the building through the development of simulation studies and parametric analyses on the calibrated model.

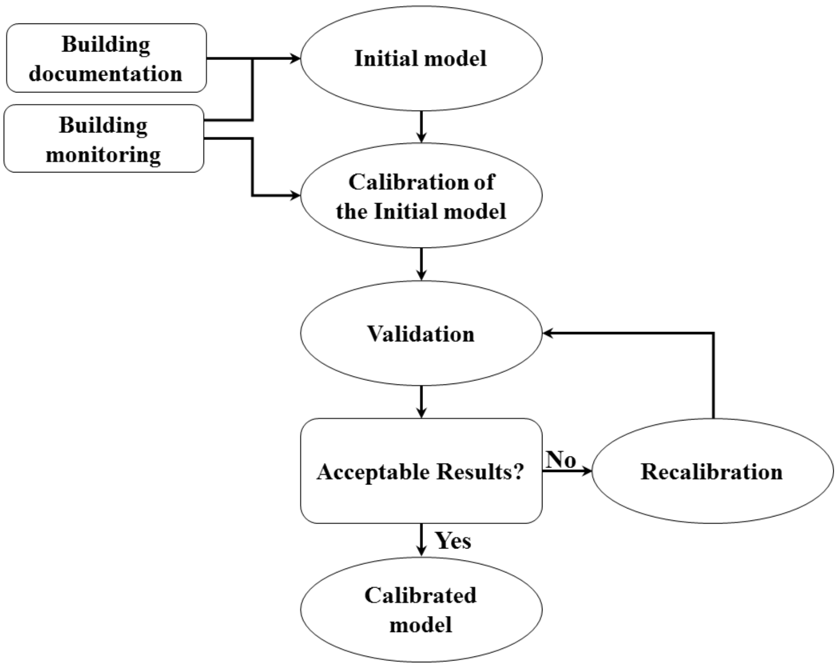

Fig. 5.3 - Different steps of the methodology which ultimately leads to a calibrated model.

5.2.1 Building energy modelling

A typical building simulation process starts with the definition of the initial building model. Detailed dynamic energy modeling usually requires extensive input data to accurately model the energy use and performance of the buildings (D. B. Crawley et al., 2000). The input data used in the current work can be summarized in two main categories:

- firstly, the physical input data, such as building geometry, building elements' constructions, thermal properties of the materials;
- secondly, the dynamic input data, such as the monitored data, like the data points from occupants' behaviors, output of heating terminals, state of the devices such as luminaires, window, etc.

In the next paragraphs a brief description of the required input variables, shown in Fig. 5.4, in order to create the building model has been presented.

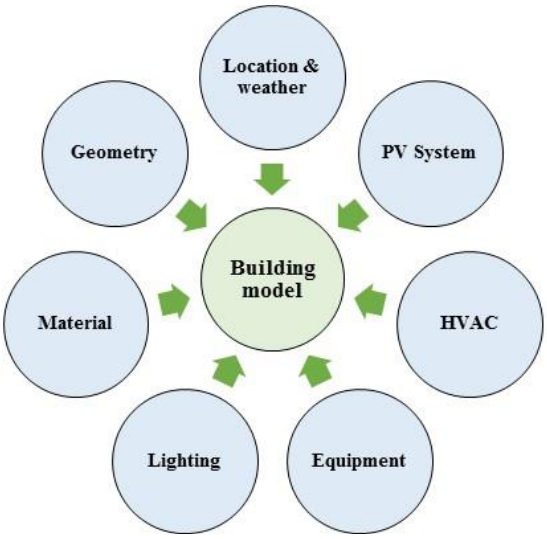

Fig. 5.4 - Input assumptions of the building model.

5.2.1.1 Geometry and thermal zoning

By means of the existing plans, measurements and observations at the building site the required information for the geometry modeling was collected. The geometric modeling of the building was performed, dividing it into thermal zones that are based on the building's shape and partitions. This stage was developed with the SketchUp tool and with Euclid plug-in (Murdock, 2009). Fig. 5.5 illustrates the geometry model.

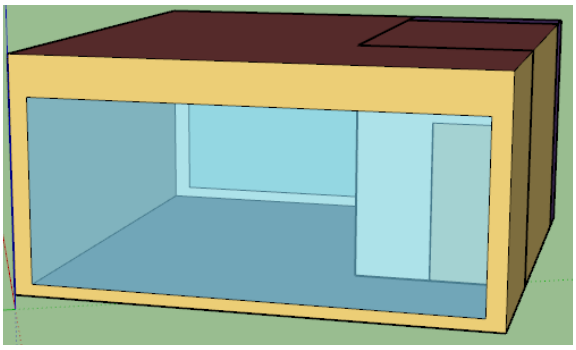

Fig. 5.5 – The building case study model in Sketchup environment.

The case study is shaded by some surrounding buildings, therefore these were included in the model, taking into account the actual height of the surrounding buildings and the distance between these and the building case study. In detail, Fig. 5.6 shows the comparison between the overall model created in Sketchup environment and a real photo of the building site (Clarke, Ailshire, Melendez, Bader, & Morenoff, 2010).

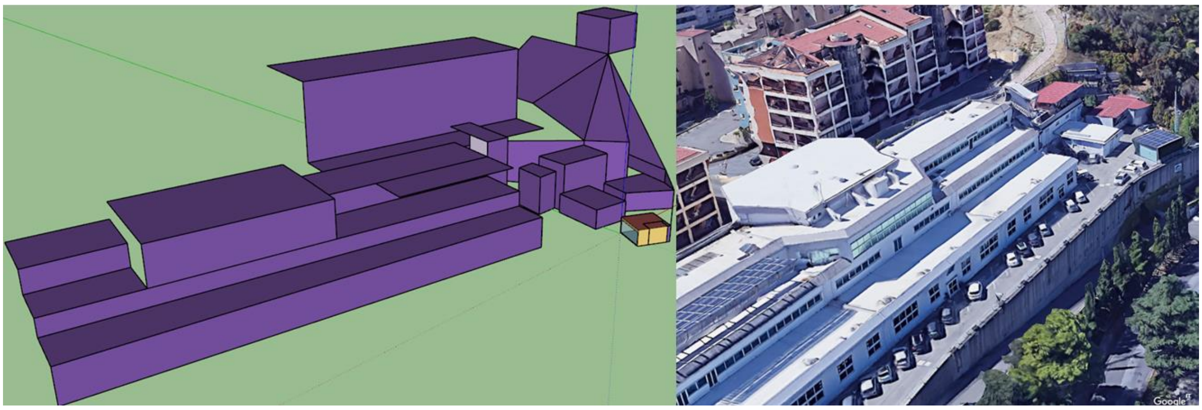

Fig. 5.6 – The overall model in Sketchup environment (Clarke et al., 2010).

The module develops on a single level of about 45 m^2, including 2 rooms, the main room and the technical room. The technical room has an area of about 9 m^2 and contains technical equipment while the main room has a gross surface of 36 m^2 and it is used as office. Moreover, the building is equipped with a heat pump air conditioning system serving main room, while the technical room is not served by any air conditioning system. For these reasons and based on the definitions of (Butcher & Craig, 2015; Nielsen et al., 2005), that refer to a thermal zone as a room or group of rooms with similar thermal loads, with the same HVAC (Heating, Ventilation and Air Conditioning) system or the same thermostat set-points can be considered as a zone, the case study was divided in two thermal zones. Tab. 5.1 shows the main geometric features of the two thermal zones.

Tab. 5.1 – Building model thermal zone.

	Surface [m²]	**Ceiling height [m]**	**Volume [m³]**
Zone 1	36	3.2	115.2
Zone 2	9	3.2	28.8

5.2.1.2 Thermal properties of the constructions

In the current work, definition of the properties of the materials and constructions was firstly based on available building plans. Secondly, product labels in cases such as façade and glazing were useful to find the constructions and thermal properties from the catalogues provided by the factories (Fibrenet, 2018; Freudenberg Politex, 2015; Ripamonti, 2018). Tab. 5.2 shows the information regarding envelope materials thermal features. The entire structure of the housing module is made of pultruded fiber reinforced material (FRP) (Fibrenet, 2018). Moreover, the envelope of the building is insulated by 0.09 m of polyester insulation panel.

Tab. 5.2 - Envelope materials thermal features (Fibrenet, 2018; Freudenberg Politex, 2015).

	Layers (outside to inside)	**Thickness [m]**	**Conductivity [W m⁻¹K⁻¹]**	**Density [kg m⁻³]**	**Specific Heat [J kg⁻¹ K⁻¹]**
Exterior wall Type 1	FRP	0.05	0.3	1800	1350
	Air Gap	0.1	-	-	-
	Insulation	0.09	0.034	40	1200
	Air Gap	0.1	-	-	-
	FRP	0.05	0.3	1800	1350
Exterior wall Type 2	Roof Green				
	FRP	0.05	0.3	1800	1350
	Air Gap	0.1	-	-	-
	Insulation	0.09	0.034	40	1200
	Air Gap	0.1	-	-	-
	FRP	0.05	0.3	1800	1350
Interior wall	FRP	0.05	0.3	1800	1350
	Air Gap	0.1	-	-	-
	Insulation	0.09	0.034	40	1200
	Air Gap	0.1	-	-	-
	FRP	0.05	0.3	1800	1350
Floor	FRP	0.05	0.3	1800	1350
	Insulation	0.09	0.034	40	1200
	FRP	0.05	0.3	1800	1350
Roof	FRP	0.05	0.3	1800	1350
	Air Gap	0.1	-	-	-
	Insulation	0.09	0.034	40	1200
	Air Gap	0.1	-	-	-
	FRP	0.05	0.3	1800	1350

As shown in Tab. 5.3, the windows are made of double low-emissivity insulated glazing with 0.005 m external glass (lowE 5 mm), 0.016 m gap filled with argon and 0.004 m internal glass (lowE 4 mm); the glass U value is 1.10 W/(m^{2}K) while the window frame U value is 1.4 W/(m^{2}K).

Tab. 5.3 - Properties of the window components (Ripamonti, 2018).

	Layers	Thickness [m]	Conductivity [W m^{-1}K^{-1}]	Solar transmittance at normal incidence	Visible transmittance at normal incidence
Glazing	LowE 5 mm	0.005	0.9	0.36	0.63
	LowE 4 mm	0.004	0.9	0.36	0.63
Gas	Argon	0.016	-	-	-

5.2.1.3 Occupant behavior and schedule modeling

Occupants' heat loads were based on CIBSE Guide A and are presented in Tab. 5.4 (Butcher & Craig, 2015). The case study was modelled with three occupants and this was also the case during the actual monitoring period.

Tab. 5.4 - Heat loads from occupants.

Degree of activity	Total rate of heat emission [W]	Total rate of sensible heat emission [W]	Total rate of Latent heat emission [W]
Seated, very light work	115	70	45

Occupancy schedules presented in Tab. 5.5 were based on the real occupancy levels of the case study. Zone 1 was used as office, during working days it was occupied by three people from 8:00 a.m. until 5:00 p.m., with a break for lunch from 2:00 p.m. to 3:00 p.m. Zone 2 was a technical room, so it was only seldom occupied.

Tab. 5.5 - Occupancy schedules.

Hours	0:00 - 8:00	8:00 – 14:00	14:00 - 17:00	17:00 - 24:00
Zone 1	0	1	0	1
Zone 2	0	0	0	0

The lighting and equipment loads used for each thermal zone are presented in Tab. 5.6. Lighting loads were calculated from the actual wattage of lights in the space. Total lighting power installed was 34.46 W/m^2, controlled by an illuminance dimmering system with a setpoint of 500 lux activated by the presence of people inside the building. The equipment loads were based on the equipment power and expected usage.

Tab. 5.6 - Lighting and equipment loads from each thermal zone.

Thermal zone	Lighting load (W/m^2)	Equipment load (W/m^2)
Zone 1	27.78	146.4
Zone 2	6.68	36.6

5.2.1.4 HVAC system

The HVAC system used in the building model was a heat pump manufactured by Maxa (Maxa, 2018). The heat pump was an air-to-air interface heat pump (heating nominal capacity = 8.2 kW, cooling nominal capacity= 7.1 kW). As shown in Fig. 5.7, the heat pump modeled used the following three elements:

1. Direct Expansion (DX) Cooling coil element;
2. Direct Expansion (DX) Heating coil element;
3. Fan (draw through fan).

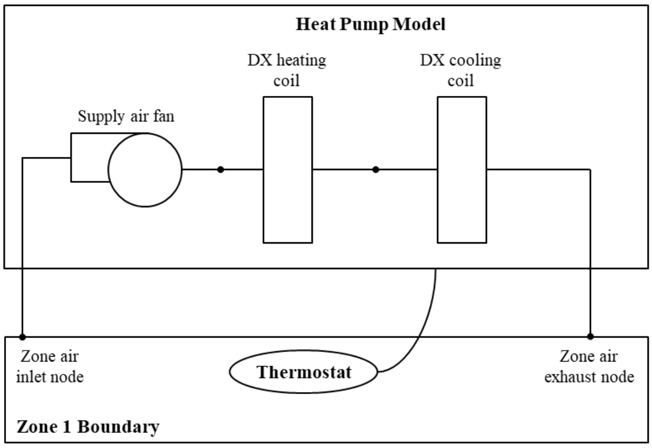

Fig. 5.7 – Schematic of heat pump model.

The thermostat input used was dual set point thermostat as it can provided heating or cooling at any time during the day depending on the requirements. The thermostat settings are shown in Tab. 5.7.

Tab. 5.7 – Thermostat settings.

Time [h]		Heating setpoint [°C]	Cooling setpoint [°C]
From	To		
00:00	08:00	-	-
08:00	17:00	20	26
17:00	00:00	-	-

DX Cooling Coil

The building heat pump used a single speed DX cooling coil. Tab. 5.8 shows the technical data of the DX cooling coil.

Tab. 5.8 – DX cooling coil technical data.

Field	Unit	Value
Rated total cooling capacity	W	7100
Rated sensible heat ratio		07
Rated COP		3.02
Rated air flow rate	m^3/s	0.29
Rated evaporator fan power per volume flow rate	$W/(m^3/s)$	473.3

The model used performance information at rated conditions along with curve fits for variation in total capacity, energy input ratio and part-load fraction to determine performance at part-load conditions. In detail, the performance curve are:

- Total Cooling Capacity Function of Temperature Curve

  It is a biquadratic performance curve that models the variation of the total cooling capacity as a function of the wet-bulb temperature and the dry-bulb temperature. The total cooling capacity at particular operating point is obtained by multiplying the output of this curve with the rated total cooling capacity.

- Total Cooling Capacity Function of Flow Fraction Curve

  This performance curve is quadratic or cubic in nature. It parameterizes the variation of total cooling capacity as a function of the ratio of actual air flow rate across the cooling coil to the rated air flow rate (at full load conditions). The total cooling capacity at specific operating conditions is a product of the curves output, rated total cooling capacity and total cooling capacity modifier curve.

- Energy Input Ratio Function of Temperature Curve

  This is a biquadratic performance curve that represents the energy input ratio (EIR) as a function of the wet-bulb and the dry-bulb temperature. The EIR at specific operating conditions is obtained by multiplying the output of the curve with the rated EIR (inverse of rated COP).

- Energy Input Ratio Function of Flow Fraction Curve

  This is a quadratic or cubic curve that characterizes energy input ratio (EIR) as dependent on the ratio of actual air flow rate across the cooling coil to the rated air flow rate (at full load conditions). The EIR is the inverse of the COP. The output of this curve is multiplied by the rated EIR and the EIR modifier curve (function of temperature) to give the EIR at the specific conditions.

- Part Load Fraction Correlation Curve

  This curve which is in form of quadratic or cubic equation models the electrical power input variation to the DX unit as a function of the part load ratio (PLR). The effective EIR at a particular simulation time step is obtained by dividing the product of the rated EIR and EIR modifier curves is by the output of the curve. The part load fraction (PLF) signifies losses in efficiency due to cyclic compressor operation.

DX Heating Coil

The building heat pump used a single speed DX heating coil. Tab. 5.9 shows the technical data of the DX heating coil.

Tab. 5.9 – DX Heating coil technical data.

Field	**Unit**	**Value**
Rated heating capacity	W	8200
Rated COP	-	3.22
Rated air flow rate	m^3/s	0.3303
Rated evaporator fan power per volume flow rate	$W/(m^3/s)$	473.3

Similarly to the cooling coil, the heating DX coil model used performance information at rated conditions along with curve fits for variations in total capacity, energy input ratio and part load fraction to determine performance at part-load conditions. In detail, the performance curves of the heating coil are:

- Total Heating Capacity Function of Temperature Curve

  This bi-quadratic, quadratic or cubic performance curve models the total heating capacity as a function of the both the indoor and outdoor air dry-bulb temperature or just the outdoor air dry-bulb temperature. The product of the curves output and rated total heating capacity gives the total heating capacity at specific operating conditions.

- Total Heating Capacity Function of Flow Fraction Curve

  This curve is in form of a quadratic or cubic equation. It characterizes the total heating capacity which depends on the ratio of actual air flow rate across the heating coil to the rated air flow rate (i.e., at full load conditions). The total heating capacity at particular operating conditions is obtained as product of the curves output, rated total heating capacity and the total heating capacity modifier curve (function of temperature).

- Energy Input Ratio Function of Temperature Curve

  This curve illustrates energy input ratio (EIR) as a dependent variable of either the indoor and outdoor air dry-bulb temperature or just the outdoor air dry-bulb temperature. The result of this curve is multiplied by the rated EIR (inverse of rated COP) to give the EIR at specific temperature operating conditions This performance curve can be of bi-quadratic, quadratic or cubic form.

- Energy Input Ratio Function of Flow Fraction Curve

  This performance curve (quadratic or cubic) parameterizes the variation of the energy input ratio (EIR) as a function of the ratio of actual air flow rate across the heating coil to the rated air flow rate. The output of this curve is multiplied by the rated EIR and the EIR modifier curve (function of temperature) to give the EIR at the specific operating conditions.

- Part Load Fraction Correlation Curve

This curve which is in form of quadratic or cubic equation models the electrical power input variation to the DX unit as a function of the part load ratio (PLR). The effective EIR at a particular simulation time step is obtained by dividing the product of the rated EIR and EIR modifier curves is by the output of the curve. The part load fraction (PLF) represents efficiency losses due to compressor cycling.

Fan

The heat pump used a constant volume fan that cycles on and off along with the compressor operation. Tab. 5.10 shows the technical data of the fan. The motor in airstream fraction defines the fraction of motor heat added to the air stream. It varies from 0 to 1.

Tab. 5.10 – Fan technical data.

Field	Unit	Value
Fan total efficiency	-	0.7
Pressure rise	Pa	400
Maximum flow rate	m^3/s	0.3283
Motor efficiency	$W/(m^3/s)$	0.9

5.2.1.5 Infiltration and ventilation

Infiltration and ventilation were modeled using the Airflow Network (AFN) model in EnergyPlus (DoE, 2010; Gu, 2007). Since no natural ventilation specific strategy is followed in the actual building, only the contribution due to outdoor air infiltration was modeled. AFN models are based on the concept of representing buildings as a grid of pressure nodes. These nodes represent individual thermal zones and exterior environments, which are interconnected by airflow paths representing infiltration routes or other intended openings. Thermal zones are assumed as characterized by well-mixed air and uniform temperature.

The AFN model is integrated into the building energy simulation to utilize both the coupled thermal and Airflow Network model approaches, thus providing the ability to simulate the performance of air distribution, thermal conduction and air leakage losses.

The process of AFN model calculation is described in the following sequential steps:

- Pressure and airflow calculations

- Node temperature and humidity calculations
- Sensible and latent load calculations

Pressure and airflow calculations determine the pressure at each node and the airflow through each linkage. Based on what is calculated for each, the AFN model determines node temperatures and humidity ratios per a given zone's air temperatures and humidity ratios. Using these, the sensible and latent loads can be calculated and summed up with all possible leakage for each zone's total, which can then be used to predict the final zone's air temperatures and humidity ratios.

Pressure and airflow calculations

To initialize the calculation node air pressures are estimated using Newton's method. A linear approximation relating airflow to pressure drop is used to determine the initial pressure:

eq. 5.1

$$\dot{m}_i = C_i \rho \left(\frac{\Delta P_i}{\mu} \right)$$

where:

m_i = Air mass flow rate at the i^{th} linkage (kg/s);

C_i = Air mass flow coefficient (m^3);

ρ= Air density (kg/m^3);

ΔP_i = Pressure difference across the i^{th} linkage (Pa);

μ= Air viscosity (Pa s).

A linkage model connects two nodes, an inlet and an outlet. This could be a window, an air vent, a crack etc. It is the linkage component which gives the relationship between airflow and pressure. Bernouli's equation is used to calculate the pressure difference:

eq. 5.2

$$\Delta P = \left(P_n + \frac{\rho V_n^2}{2} \right) - \left(P_m + \frac{\rho V_m^2}{2} \right) + \rho g \left(z_n - z_m \right)$$

where:

ΔP = Total pressure difference between nodes n and m (Pa);

P_n; P_m = Entry and exit static pressures (Pa);

V_n; V_m = Entry and exit air flow velocities (m/s);

g = Acceleration due to gravity (m/s^2);

z_n; z_m = Entry and exit elevations (m);

By including the effect of wind pressure and simplifying this can be rewritten as:

eq. 5.3

$$\Delta P = P_n - P_m + P_S + P_W$$

where;

P_n; P_m = Total pressures at nodes n and m (Pa);

P_S = Pressure difference due to density and height differences (Pa);

P_W = Pressure difference due to the wind (Pa).

Node temperature and humidity calculations

The following equation is used to calculate the temperature distribution across a flow element for a given air flow rate:

eq. 5.4

$$\dot{m} C_p \frac{dT}{dx} = U\ P\left(T_\infty - T\right)$$

where:

C_p = Specific heat of air flow (J/(kg K));

P = Perimeter of a duct element (m);

T = Temperature as a field variable (°C);

T_∞ = Temperature of air surrounding the duct element (°C);

U = Overall heat transfer coeffcient (W/(m^2 K)).

The humidity calculations follow a similar form to the node temperature calculations:

eq. 5.5 $$\dot{m}\frac{dW}{dx} = U_m P\left(W_\infty - W\right)$$

where:

W = Humidity ratio (kg/kg);

W_∞ = Humidity ratio of air surrounding the duct element (kg/kg);

U_m = Overall moisture transfer coefficient (kg/(m^2 s)).

Sensible and latent load calculations

The sensible loads for the multizone calculation can be written as:

eq. 5.6 $$MCP_{airflow} = \dot{m}_{\inf} C_p + \sum(\dot{m}_{mix} C_p)$$

eq. 5.7 $$MC\dot{P}T_{airflow} = \dot{m}_{\inf} C_p T_{amb} + \sum(\dot{m}_{mix} C_p T_{zone})$$

where:

$MCP_{airflow}$ = Sum of air mass flow rate multiplied by specific heat for infiltration and mixing (W/K);

$MCPT_{airflow}$ = Sum of air mass flow rate multiplied by specific heat and temperature for infiltration and mixing (W);

m_{inf} = Incoming air mass flow rate from outdoors (kg/s);

m_{mix} = Incoming air mass flow rate from adjacent zones (kg/s);

T_{amb} = Outdoor air dry-bulb temperature (°C);

T_{zone} = Adjacent zone air temperature (°C).

The latent loads can be written as:

eq. 5.8 $$M_{airflow} = \dot{m}_{\inf} + \sum \dot{m}_{mix}$$

eq. 5.9 $$MW_{airflow} = \dot{m}_{\inf}\, W_{amb} + \sum (\dot{m}_{mix}\, W_{zone})$$

where:

$M_{airflow}$ = Sum of air mass flow rate for infiltration and mixing (kg/s)

$MW_{airflow}$ = Sum of air mass flow rate multiplied by humidity ratio for infiltration and mixing (kg/s)

W_{amb} = Outdoor air humidity ratio (kg/kg)

W_{zone} = Adjacent zone air humidity ratio (kg/kg)

The loads calculated in the AirflowNetwork are then integrated into the heat balance equation.

Airflow network modeling

The AFN was modeled using the following EnergyPlus objects (DoE, 2010; Gu, 2007):

- Airflow network: simulation control. The building was considered as multizone with distribution system. Surface average pressure coefficient (C_p) were adopted in simulation according to the literature (DoE, 2010; Gu, 2007). Default value were attributed for parameters related with initialization calculation type, convergence tolerance and convergence acceleration limit.
- Airflow network: multizone: zone. Since no natural ventilation strategy is implemented in the actual building, only the contribution due to outdoor air infiltration was evaluated in the initial model.
- Airflow network: multizone: surface. The surface object enables an individual characterization of all leakage surfaces, associated whit heat transfer surfaces as walls, roofs, or subsurfaces as doors, windows, through which the air flow.
- Airflow network: multizone: reference crak condition. This object specifies the reference conditions for temperature, humidity, and pressure which correspond to the AirflowNetwork: MultiZone: Surface: Crack object.

- Airflow network: multizone: surface: crack. This object specifies the properties of air flow through a crack and the associated measurement conditions. The following power law form is used that gives air flow through the crack as a function of the pressure difference across the crack:

eq. 5.10 $$Q = (CrackFactor)\ C_T\ C_Q\ (\Delta P)^n$$

Where:

Q = air mass flow (kg/s);

C_Q = air mass flow coefficient (kg/s-Pan @ 1 Pa), determined by calibrating the model;

C_T = reference condition temperature correction factor;

ΔP = pressure difference across crack (Pa);

n = air flow exponent, determined by calibrating the model.

- Airflow network: multizone: component: detailed opening. As shown in Tab. 5.11, this object specifies the openings characteristics as well as the particularities of the air that flows through them. Table shows the input for this object used to model the outdoor glass door. Air mass flow coefficient and air mass flow exponent when the window is closed were assumed equal to 3.33 10^{-5} kg/(m s) and 0.65, respectively, as suggested in (ASHRAE, 2017; Orme & Leksmono, 2002) for a new window.

Tab. 5.11 - Airflow network: multizone: component: detailed opening (DoE, 2010; Gu, 2007).

Air mass flow coefficient when opening is closed	3.33 10^{-5}
Air mass flow exponent when opening is closed	0.6
Type of rectangular large vertical opening	NonPivoted
Number of sets of opening factor data	2
Opening factor 1	0
Discharge coefficient for opening factor 1	0.001
Opening factor 2	1
Discharge coefficient for opening factor 2	0.6

- Airflow network: distribution: node. This object was used to represent air distribution system nodes for the AirflowNetwork model.

- Airflow network: distribution: component: leakage: ratio. It was used to define supply and return leaks with respect to a constant fan flow.
- Airflow network: distribution: duct.
- Airflow network: distribution: fan.
- Airflow network: distribution: coil.
- Airflow network: distribution: linkage. This object specifies a connection between two AirflowNetwork:Distribution:Node objects and an AirflowNetwork component defined above.

5.2.1.6 PV System

The PV system was modelled using the model "Equivalent One-Diode" (DoE, 2010) based on real-time performance data. It is a four-parameter empirical model to predict the electrical performance of crystalline (both mono and poly) PV modules. In detail, the model simulates a PV module with an equivalent circuit consisting of a direct-current source, diode, and one resistor (Fig. 5.8).

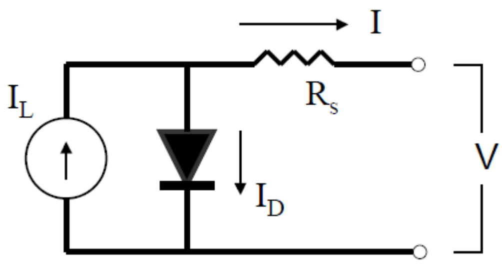

Fig. 5.8 – Equivalent circuit in the Equivalent One-Diode model.

The model assumes that the slope of the IV curve is zero at the short-circuit condition:

eq. 5.11 $$\left(\frac{dI}{dV}\right)_{v=0} = 0$$

The current-voltage equation of circuit shown in the previous figure is as follows:

eq. 5.12 $$I = I_L - I_0 \cdot \left[\exp\left(\frac{q}{\gamma \cdot k \cdot T_c} \cdot \left(V + I \cdot R_s\right)\right) - 1\right]$$

where, I is the PV module output current, I_L is the module photocurrent, I_0 is the saturation current, q is the electron charge constant, γ is PV curve fitting parameter, k is the Boltzmann constant, T_C is the module temperature, V is the PV module voltage, and R_S is the module resistance.

The module photocurrent is dependent on incident solar radiation as in eq. 5.13.

eq. 5.13
$$I_L = I_{L,ref} \cdot \frac{G_T}{G_{T,ref}}$$

where, $I_{L,ref}$ is the module photocurrent at reference conditions, G_T is the total radiation incident on PV array and $G_{T,ref}$ is the incident radiation at reference conditions.

The diode reverse saturation current I_0 is a temperature dependent quantity:

eq. 5.14
$$I_0 = I_{0,ref} \cdot \left(\frac{T_C}{T_{C,ref}} \right)^3$$

where, $I_{0,ref}$ is diode reverse saturation current at reference conditions and $T_{C,ref}$ is the module temperature at reference conditions.

Once I_0 and I_L are found from eq. 5.13 and eq. 5.14, Newton's method is employed to calculate the PV current. Moreover, an iterative search routine finds the current (I_{mp}) and voltage (V_{mp}) at the point of maximum power along the IV curve.

The performance of an array of identical modules was assumed to be linear with the number of modules in series and parallel. Moreover, since the "four parameters" are empirical values that cannot be determined directly through physical measurement, the model automatically calculates parameter values from manufacturers' PV module catalogs data, such as short-circuit current, open-circuit voltage, current at maximum power, etc. The manufactures' values are used to determine the equivalent circuit characteristics I_{Lref}, $I_{0,ref}$ and R_S. These characteristics define an equivalent circuit that is employed to find the PV performance at each timestep, as described previously. The major parameters used in PV panel model are summarized in Tab. 5.12.

Tab. 5.12 - PV panel model parameter (DoE, 2010).

Parameter	Value	Unit
Module active area	1.46	m^2
Number of cells in series per module	60	-
Open circuit voltage	37.42	V
Short circuit current	8.38	A
Reference temperature	25	°C
Reference Insolation	1000	W/m^2
Module current at maximum power	7.55	A
Module voltage at maximum power	39.7	V
Temperature coefficients of short circuit current	2.47	mA/K
Temperature coefficients of open circuit voltage	-163	mV/K

5.2.1.7 Weather data

Once validation has been achieved using monitored weather data, typical meteorological year data were used to carry out the overall intended objectives of the building model. The weather file used for simulation was an IWEC (International Weather for Energy Calculations) weather file for Messina (Thevenard & Brunger, 2002). This weather file was produced by ASHRAE in 2000 from the actual average weather data and therefore does not account for any extreme or unusual weather conditions that may occur.

5.2.2 Building monitoring

In order to calibrate and validate the building energy model, by comparing the monitored data to that of the model on the same day using recorded weather data as a model input, it was necessary to conduct a monitoring campaign of the building. In detail, monitoring was performed for around 60 days during May – July 2018 (24 May – 27 July 2018). The case study was equipped with a weather station installed near the building, registering global horizontal radiation, dry bulb temperature, wind speed and direction, air relative humidity and atmospheric pressure. Tab. 5.13 shows the observed climate variables.

Tab. 5.13 - Monitored weather varaibles for creating the weather file.

Data point	Unit
Global horizontal radiation	Wm^{-2}
Outdoor dry bulb temperature	°C
Outdoor air relative humidity	%
Wind speed	ms^{-1}
Wind direction	degree
Atmospheric pressure	Pa

Tab. 5.14 and Fig. 5.9 shows the main features of the used weather station.

Fig. 5.9 – The weather station used during the monitoring period.

Tab. 5.14 - The weather station used during the monitoring period.

	Type	Range	Uncertainty	Resolution
Temperature	thermocouple Pt100	-40÷60 °C	±0.1%	0.1°C
Relative humidity	Capacitive	0÷100%	±1.5%	0.1%
Pressure		600÷1100 hPa	±0.5 hPa	0.1 hPa
Global radiation	Thermopile	0÷2000 W/m2	<± 1 %	
Wind Direction	Ultrasonic	0÷360°	±2°	0.1°
Wind Speed	Ultrasonic	0÷60 m/s	±2%	0.01 m/s

Since the model for solar radiation calculations uses also direct normal and diffuse horizontal radiation, while it was possible to measure only the global horizontal radiation, the Perez split mathematical model (Richard Perez, Seals, Ineichen, Stewart, & Menicucci, 1987; RSRACSR Perez, Stewart, Arbogast, Seals, & Scott, 1986) was used to separate the measured global horizontal radiation into direct normal and diffuse horizontal radiation values.

Moreover, the case study was equipped with an indoor monitoring system that measure:

- air temperatures;
- surface temperatures.

Fig. 5.10 shows the position of all sensors used during the monitoring.

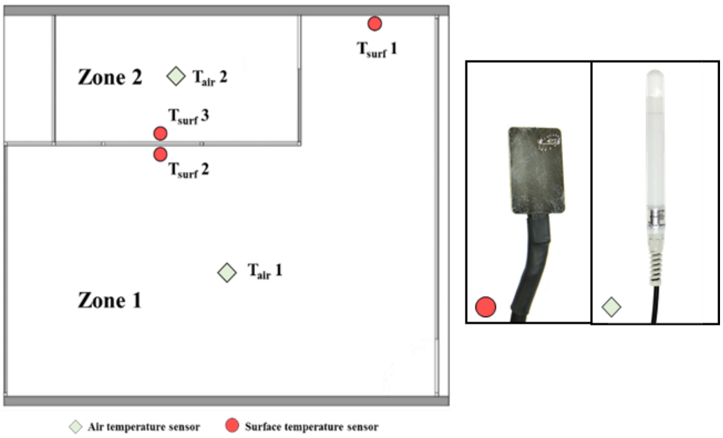

Fig. 5.10 – Sensors position during the building monitoring.

Tab. 5.15 shows the main features of the instruments used during the monitoring. Moreover, during the monitoring period, the occupant behavior was also registered. In particular, through questionnaires, the building occupancy, the opening of the window was recorded.

Tab. 5.15 - Main features of the sensors used.

Zone	Available Sensor	Type	Range [°C]	Uncertainty [%]	Resolution [°C]
Zone 1	Air temperature	thermocouple Pt100	-50÷70	±0.10	0.01
	Surface Temperature	thermocouple Pt100	-50÷70	±0.15	0.01
Zone 2	Air temperature	thermocouple Pt100	-50÷70	±0.10	0.01
	Surface Temperature	thermocouple Pt100	-50÷70	±0.15	0.01

Fig. 5.11 shows the installed sensors in the rooms.

Fig. 5.11 – The instrumentation used during on-site monitoring.

Finally, the photovoltaic generation has been studied on a sub-hourly base comparing the simulated and monitored power production in kW of a single photovoltaic module. However, since the building was not in use during the monitoring period, it was not possible to analyze and validate the building energy consumption.

5.2.3 Calibration and validation

A common problem encountered in building performance simulation is that of a gap between simulated performance and measured real performance. There can be many contributing factors to this ‘performance gap’ but most commonly, the source of error stems from inaccuracies associated with assumptions used in place of hard-to-measure building inputs. Therefore, for a building model to be useful and provide a meaningful contribution, it must be calibrated and validated to best represent the real operation of the building. Once calibrated and validated, a model can be used to investigate a wide variety of aspects regarding the building.

By calibration of the initial model, the objective was to maintain fidelity in the simulation model through a systematic process. Calibration is an expression which has been used here to express the process of finding optimal values for a set of uncertain-input parameters to obtain the maximum accuracy in a simulation model. By the method applied in the current work, calibration is an iterative process starting with the base case model, over the successive steps, to obtain a model which faithfully represents the thermal performance of the building.

During the calibration process, it is quite common to use a “trial and error” method, given the large number of parameters involved. Before starting the entire calibration assessment, a decision regarding the possible most significant input parameter elements must be made. As shown Tab. 5.16, in Heo et al. (Heo, Choudhary, & Augenbroe, 2012) identified within the building physics domain the four main categories, to be the sources of uncertainties in building models, when carrying out building energy evaluations. Their identification has a great impact on the model reliability.

Tab. 5.16 - Source of uncertainty in building energy models (Heo et al., 2012).

Category	Factors
Scenario uncertainty	Outdoor weather conditions Building usage/occupancy schedule
Building physical/operational uncertainty	Building envelope properties Internal gains HVAC systems Operation and control settings
Model inadequacy	Modelling assumptions Simplification in the model algorithm Ignored phenomena in the algorithm
Observation error	Metered data accuracy

The first category, scenario uncertainty, concerns the external environment and the building use. Generally, the use of a real weather file to be employed in a building simulation can address this question. The second and third categories refer to uncertainties in the building model and assumptions/simplifications that may arise from model approximation as a physical representation of a real building. The last category mentions the problem of data quality in the measured data.

Firstly, the large number of candidate model parameters was reduced to a certain extent via literature review based considerations (Heo et al., 2012). Consequently, the input parameter values optimization concentrated on assumptions made during the design of the building model.

Subsequently, the optimized values derived from the calibration process, were required to be validated. In fact, validations are necessary to ensure how accurate the calibrated model represents the actual model under different conditions. Therefore, in this work, the results from each calibration have been examined in the validation periods.

To validate the results produced from the building model statistical techniques were employed as a method to assess the accuracy of outputs and the consistency of the same. In detail, error quantification was completed using the following metrics:

- mean bias error (MBE);
- normalised Mean Bias Error (NMBE);
- root mean square error (RMSE);
- coefficient of variation of the root mean square error (CV(RMSE)).

- coefficient of determination (R^2);

These metrics were selected for this work due to the following reasons:

- they are the most commonly statistical indices used to evaluate the error between measured and simulated data of the building energy models (Coakley, Raftery, & Keane, 2014; Ruiz & Bandera, 2017);
- they express the model uncertainty in different ways and do not always correspond (Carstens, Xia, & Yadavalli, 2017). For example the NMBE is useful to evaluate the overall positive or negative bias of a model, while CV(RMSE) measures the variance of the model (Vogt, Remmen, Lauster, Fuchs, & Müller, 2018).

MBE is the average of the errors of a sample space and is reported in eq.5.15. Generally, it is a good indicator of the overall behavior of the simulated data with regards to the regression line of the sample. In eq. 5.15, m_i is the measured value, s_i is the simulated one and n the number of measured data points. Positive values mean that the model under-predicts measured data, and a negative one means over-prediction. However, the main problem with this index is that it is subject to cancellation errors where the sum of positive and negative values could reduce the value of MBE.

eq. 5.15
$$MBE = \frac{\sum_{i=1}^{n}(m_i - s_i)}{n}$$

NMBE (eq. 5.16) is a normalization of the MBE index that is used to scale the results of MBE, making them comparable. It quantifies the MBE index by dividing it by the mean of measured values ($\overline{m}$), giving the global difference between the real values and the predicted ones. As in the case of MBE, positive and negative values mean the under- or over-prediction of this normalization.

eq. 5.16
$$NMBE = \frac{1}{\overline{m}} \cdot \frac{\sum_{i=1}^{n}(m_i - s_i)}{n} \cdot 100$$

The RMSE (eq. 5.17) is a measure of the variability of the data. For every hour, the error, or difference in paired data points is calculated and squared.

eq. 5.17

$$RMSE = \sqrt{\frac{1}{n} \cdot \sum_{i=1}^{n} \left(m_i - s_i \right)^2}$$

CV(RMSE) measures the variability of the errors between measured and simulated values (eq. 5.18). It gives an indication of the model's ability to predict the overall load shape that is reflected in the data. It is not subject to cancellation errors, and hence, AHSRAE Guidelines (ASHRAE, 2014, 2002), FEMP (FEMP, 2008) and IPMVP (Committee, 2001; Webster et al., 2015) use it with NMBE to verify the accuracy of the models.

eq. 5.18

$$CV(RMSE) = \frac{1}{\overline{m}} \cdot \sqrt{\frac{1}{n} \cdot \sum_{i=1}^{n} \left(m_i - s_i \right)^2} \cdot 100$$

Finally, R^2 (eq. 5.19) indicates how close simulated values are to the regression line of the measured values. It is another statistical index commonly used to measure the uncertainty of the models. It is limited to between 0.00 and 1.00 where the upper value means that the simulated values match the measured ones perfectly and the lower ones do not.

eq. 5.19

$$R^2 = \left(\frac{n \cdot \sum_{i=1}^{n} m_i \cdot s_i - \sum_{i=1}^{n} m_i \cdot \sum_{i=1}^{n} s_i}{\sqrt{\left(n \cdot \sum_{i=1}^{n} m_i^2 - \left(\sum_{i=1}^{n} m_i \right)^2 \right) - \left(n \cdot \sum_{i=1}^{n} s_i^2 - \left(\sum_{i=1}^{n} s_i \right)^2 \right)}} \right)^2$$

5.2.4 Performance Indicators and Evaluation Criteria

The energy performances of the case study were investigated with a sub-hourly detail (3 minutes time-step) from two main performance aspects in this study:

- monthly and yearly energy consumption;
- load-matching levels and grid interaction.

In detail, the 3 time step was used since the conduction finite difference (CondFD) algorithm was selected in EnergyPlus from the different conduction heat transfer algorithms. Consequently, the selection of time step with CondFD was limited up to 3 min, avoiding any problems with time-step dependence as shown in previous studies (DoE, 2010; Tabares-Velasco, Christensen, & Bianchi, 2012)

Firstly, to study the answer of the dynamic model, the temperature trends in some critical days in terms of insulation and temperature were analyzed. In detail, free-floating conditions, HVAC plant considered as not operating, were assumed in order to investigate the natural indoor thermal performance of the spaces. Then, in order to investigate also the energy consumption for heating and cooling, the HVAC system modeled was activated with temperature set points in summer and winter. Finally, two different energy balances were calculated: LG Balance and Weighted Balance.

Secondly, in order to quantify the load-matching levels and the grid Interaction for the case study, quantitative indices, presented in the next paragraph, were used. In detail, load cover factor (γ_{load}), representing the percentage of the electrical demand covered by on-site electricity generation, the supply cover factor (γ_{supply}), defined as the percentage of the on-site generation that is used by the building, and the net exported energy were analysed using 3 minute time step resolution. Finally, the loss of load probability (LOLP), the no grid interaction probability ($P_{e\approx0}$) and the grid interaction index (f_{grid}) were also investigated to evaluate the system reliability.

5.2.4.1 Monthly and yearly energy balances

The energy balances treat separately the energy need from the demand or the generation from the load, so that the balance equation is expressed in terms of energy generation (G) and energy load (L):

eq. 5.20
$$Energy\ Balance = G \cdot w_g - L \cdot w_l$$

where:

- G is generated energy;
- w_g is a generation weighting factor;
- L is the load;

- w_l the weighting factor for the energy consumed.

The terms G and L were calculated as the sum of the whole final energy generated and consumed. W_g and w_l represent the ratio between final and primary energy: they are calculated keeping into account all the energy required to achieve 1 kWh of final energy, from the raw material acquisition until the final and usable energy carrier. These factors are heavily influenced by the processes that occur in the supply chain and by the features of the local power generation.

In detail, two different energy balances were calculated: LG Balance and Weighted Balance. The weighing factors used for both balances are shown in Tab. 5.17. The LG Balance was calculated as “load generation” balances, where no weighting factors are used (w_g and w_l equal to 1) and the result was simply calculated as the difference between generation and load. Instead, the Weighted Balance, focused on primary energy consumption, allows to take into account all inefficiencies occurring in the final energy generation process. In detail for the Weighted Balance, according to (European Committee for Standardization, 2008), w_g and w_l were set equal to 1 and 2.5, respectively.

Tab. 5.17 - Weighing factors used to calculate balances.

	w_g	w_l
LG Balance	1	1
Weighted balance	1	2.5

5.2.4.2 Load match and grid interaction analysis

In order to investigate the load-matching levels and the grid interaction for the case study the following indicators were calculated:

- load cover factor (γ_{load});
- load supply factor ($\gamma_{lsupply}$);
- loss of load probability (LOLP);
- net exported electricity(ne);

- no grid interaction probability ($P_{e\approx0}$)

These indicators were selected for this work because they investigate in different ways and from different points of view the issues related to the building load matching and the grid interaction.

In detail, the γ_{load}, defined in (eq. 5.21), represents the percentage of the electrical demand covered by on-site electricity generation (Sartori et al., 2012).

eq. 5.21

$$\gamma_{load} = \frac{\int_{\tau_1}^{\tau_2} \min\left[\overline{g(t)} - \overline{S(t)} - \overline{\zeta(t)}, \overline{l(t)}\right] dt}{\int_{\tau_1}^{\tau_2} \overline{l(t)} dt}$$

where $\overline{g(t)}$ is the on-site generation (kW), $\overline{S(t)}$ is the storage balance (kW), $\overline{\zeta(t)}$ are losses (kW), $\overline{l(t)}$ is the building load (kW), *t* is the time, τ_1 and τ_2 are the start and the end of the evaluation period, respectively.

The $\gamma_{lsupply}$ (eq. 5.22), the index complementary to the γ_{load}, is the fraction of local generation that is used on-site (Sartori et al., 2012).

eq. 5.22

$$\gamma_{supply} = \frac{\int_{\tau_1}^{\tau_2} \min\left[\overline{g(t)} - \overline{S(t)} - \overline{\zeta(t)}, \overline{l(t)}\right] dt}{\int_{\tau_1}^{\tau_2} \left[\overline{g(t)} - \overline{S(t)} - \overline{\zeta(t)}\right] dt}$$

When γ_{load} index is 1, it means that the system produces more energy than the real needs of the system, while γ_{load} equal to zero indicates periods with no on-site generation. On the other hand, γ_{supply} equal to 1 means that the on site produced energy is lower than the building energy requirements, while γ_{supply} equal to zero indicates with no building energy demand. These two indicators would have the same numerical value when the balance for the energy carrier is exactly zero in the observed period, while it would differ for nearly zero or plus balances.

The LOLP (calculated as in eq. 5.23) indicates the time share during which the local generation is insufficient to supply the local load (Jaume Salom et al., 2014). LOLP is an important parameter to use, because it shows how often during a given period the on-site supply does not cover the on-site load, and thus how often energy must be supplied by the grid However, this index does not provide any information about the amount of delivered electricity.

eq. 5.23
$$LOLP = \frac{\int_{\tau_1}^{\tau_2} dt_{\overline{l(t)} > \overline{g(t)} - \overline{S(t)} - \overline{\zeta(t)}}}{\tau_2 - \tau_1}$$

To quantify the energy exchange between the building and the power grid to which it is connected, the net exported electricity (kWh) was calculated as in (eq. 5.24):

eq. 5.24
$$ne = \int_{\tau_1}^{\tau_2} \overline{e_i(t)}\ dt - \int_{\tau_1}^{\tau_2} \overline{d_i(t)}\ dt$$

where $\overline{e_i(t)}$ and $\overline{d_i(t)}$ are the mean exported power (kW) and mean imported power (kW).

Finally, the no grid interaction probability (eq. 5.25) shows the probability that the building is acting autonomously of the grid. In that case, the entire load is covered by the direct use of renewable energy or by the stored energy (Jaume Salom et al., 2014).

eq. 5.25
$$P_{e \approx 0} = \frac{\int_{\tau_1}^{\tau_2} dt_{\left|\overline{ne(t)}\right| < 0.001}}{\tau_2 - \tau_1}$$

5.3 LIFE CYCLE ASSESSMENT METHOD

In this thesis, LCA methodology was applied to the case study according to the international standards of series ISO 14040 (ISO, 2006a, 2006b) and to the UNI EN 15978 (UNI, 2011b). In the following paragraphs the different methodology steps will be defined in detail. Moreover, in order to compare the environmental impacts due to the entire building life cycle to the environmental impacts potentially avoided thanks to the renewable energy produced during the use stage, environmental payback times were calculated for each impact category analysed.

The standards of the ISO 14040 series (ISO, 2006a, 2006b) define a calculation method that allows for evaluating the environmental behaviour of any product and also establish how to communicate the results of this evaluation. The general LCA methodology consists on four phases (Fig. 5.12), which will be described in detail in the following sections.

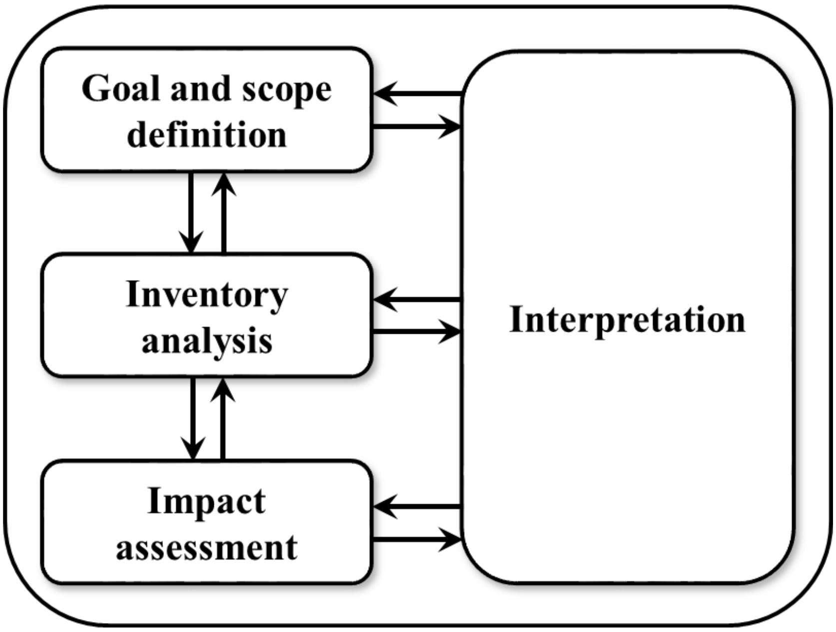

Fig. 5.12 - Stages of LCA methodology (ISO, 2006a).

In particular, LCA approach adapted to the building is defined in EN 15978 (UNI, 2011b) that represents a methodological guide for the quantification of the environmental impacts on buildings. The standard is applicable to new and existing buildings and refurbishment projects. In detail, EN 15978 (UNI, 2011b) is organized according to the "modularity principle" of building life cycle: the building's life cycle is divided into different information modules (A, B, C, D) which represent the product stage, construction stage, use stage, end-of-life and benefits and loads beyond the building lifecycle. According to the "modularity principle" all processes influencing the environmental performance of the building in its useful life must be assigned to the module of the life cycle in which they occur. These stage and modules are shown in Fig. 5.13 and cover from A1 to C4 "impacts and environmental aspects" developed within the system boundary, while D module covers benefits and loads that go beyond the system boundary.

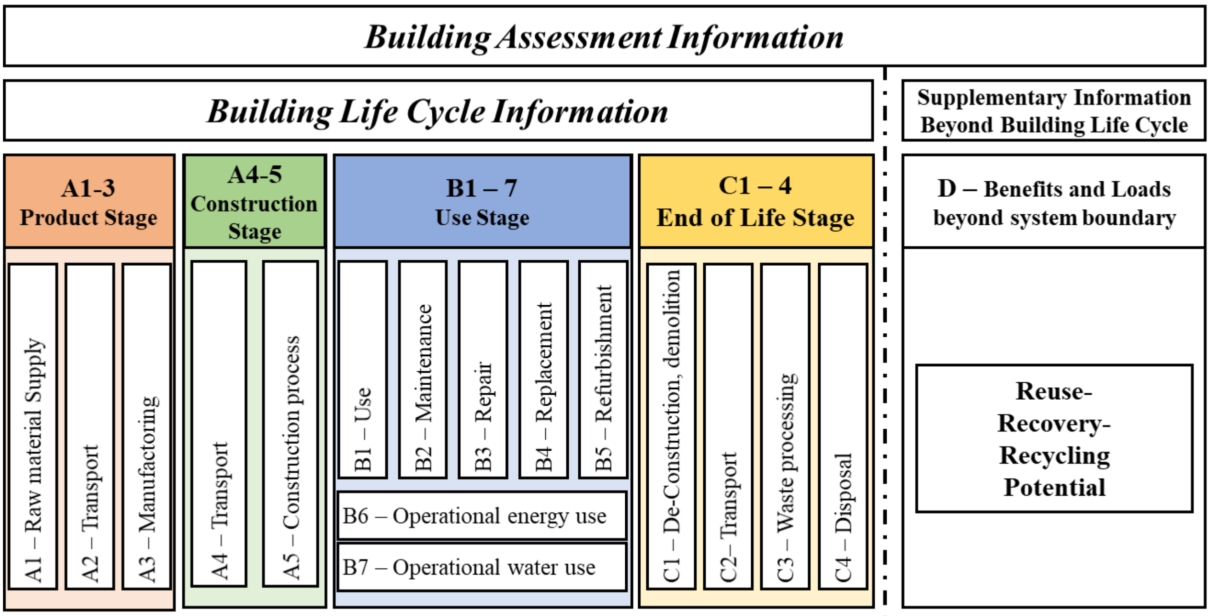

Fig. 5.13 - Modular information for the different stages of the building assessment (UNI, 2011b).

5.3.1 Goal and scope definition

The whole LCA process is guided by the direction set in the Goal and Scope Definition phase (ISO, 2006a, 2006b). This phase will help to maintain consistency of the LCA.

According to the standard ISO 14040 (ISO, 2006a), this point include a definition of the product or system that is going to be studied (see chapter 4), the functional unit, the system boundaries, allocation procedures and data quality.

5.3.1.1 LCA goals

The main goals of this thesis section can be briefly summarized as follows:

- investigate the primary energy and the environmental impacts associated with the case study;
- assess the contribution to environmental impacts and primary energy use of each stage of the life cycle of the prefabricated building when compared to the entire life cycle of the building;
- identify the hot-spots for each stage of the life cycle;
- evaluate if the environmental impacts potentially avoided thanks to the renewable energy produced during the use stage compensate the environmental impacts due to the entire building life cycle. To this aim, payback indices were added to the set of life-cycle impact indicators.

The life cycle impacts of the system were determined by an attributional LCA including an inventory process-analysis (described in the next section), which allowed not only identifying the most significant processes but also to evaluate their influence in the total life cycle results.

5.3.1.2 Specification of the object of assessment

The object of assessment is the entire building, including its foundations and external works within the curtilage of the building’s site, over its life cycle. According to the international standards of series ISO 14040 (ISO, 2006a, 2006b) and to the UNI EN 15978 (UNI, 2011b), the main characteristics of the system were described in the chapter 4.

5.3.1.3 Functional unit

According to the standard ISO 14040 (ISO, 2006a), the functional unit is defined as the quantified performance of a product system for use as a reference unit. Defining an adequate functional unit (FU) is essential when one of the main goals of the study is to allow future comparisons.

According to the most commonly functional unit used in buildings LCA studies (Adalberth, Almgren, & Petersen, 2001; Luisa F Cabeza et al., 2014; Sharma et al., 2011), the FU is 1 m^2 of building useful floor area with reference to 1 year.

5.3.1.4 Reference study period

According to the building design team, the case study was assumed to have a required service life (ReqSL) of 25 years. According standard to EN 15978 (UNI, 2011b), assessment was carried out on the basis of a chosen reference study period. The default value for the reference study period shall be the required service life of the building. However, the reference study period may differ from the required service life given for the object of assessment (Fig. 5.14) depending on the intended use of the assessment:

- Case 1: the reference study period (RSP) and ReqSL are the same, RSP/ReqSL = 1;
- Case 2: the RSP is shorter than the ReqSL, the quantified values of impacts and aspects for the use stage (modules B1 - B7) and benefits and loads presented in module D that come from modules B1-B7, must be adjusted by a factor RSP/ReqSL;
- Case 3: the RSP is longer than the ReqSL, scenarios for refurbishment, or demolition and construction of an equivalent new building shall be developed. The values for impacts and aspects for modules in the use stage (modules B1 - B7) and for the loads and benefits reported in module D must be multiplied by the ratio of the reference study period to the required service life (RSP/ReqSL).

In this work, since the reference study period was set equal to the required service life of the building (Case 1 of Fig. 5.14), no type of adjustment is envisaged for impacts and aspects for the use stage (modules B1 - B7) and for the loads and benefits reported in module D.

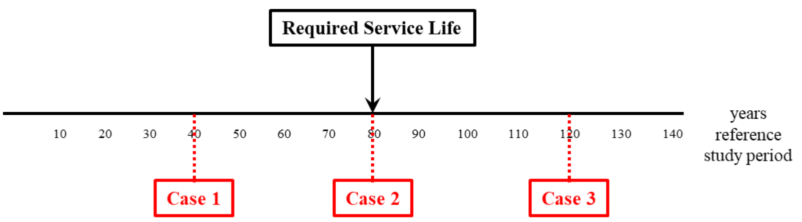

Fig. 5.14 - Reference study period versus required service life of the assessed object (UNI, 2011b).

5.3.1.5 System boundaries

The system boundaries determine the processes that are taken into account for the object of assessment. In this thesis, the object of assessment was the building and its site. This includes all the upstream and downstream processes needed to establish and maintain the functions of the building, from the acquisition of raw materials to their disposal or to the point where materials exit the system boundary either during or at the end of the building life cycle.

According to the EN 15978 (UNI, 2011b), Fig. 5.15 illustrates the organization of the different modules used for the assessment of the building case study. The setting of the system boundaries follows the "modularity principle": Where processes influence the building's environmental performance during its life cycle, they are assigned to the module in the life cycle where they occur.

Modules A1 to C4 cover environmental impacts and aspects that are directly linked to processes and operations taking place within the system boundary of the building, while module D provides the net benefits relating to exported energy and secondary materials or secondary products resulting from reuse, recycling and energy recovery that take place beyond the system boundary.

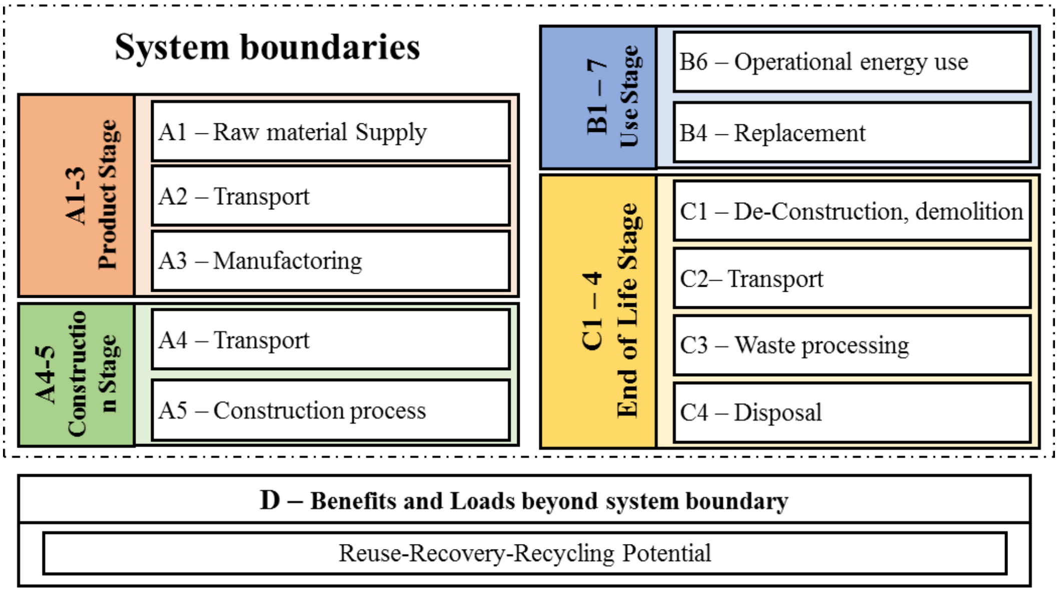

Fig. 5.15 - The system boundary (UNI, 2011b).

In detail the system boundaries considered in the study include:

- **The Product Stage (Modules A1 to A3).** These Modules covers the 'cradle to gate' processes for the materials and services used in the construction; the rules for determining their impacts and aspects are defined in EN 15804 (UNI, 2014).
- **Transport to the building site (Module A4).** The boundary for this module include the transport of materials, products, services and equipment from the factory gate to the building site.
- **The Construction Process Stage (Module A5).** The boundary for this module include:
    - building construction process;
    - on site production and transformation of a product;
    - waste management processes of other wastes generated on the construction site.
- **The use stage (Modules B4 – B6).** This stage covers the period from the practical completion of the construction work to the point of time when the building is deconstructed/demolished. In particular, this stage includes replacement (Module B4) of some building components and the operational energy use (Module B6).

  Module B1 (installed products in use) that encompasses the impacts and aspects arising from the normal conditions of use of components of the building were neglected. Moreover, maintenance (Module B2), repair (Module B3) and refurbishment (Module B5) were neglected, because the required service life for the building is the same as the estimated one for the plants and it guarantees a use of the building without any particular refurbishment or maintenance. Finally, since the building is not equipped with a water and sanitary supply system, the energy and materials data input due to the consumption of water during the use stage (Module B7) were also neglected.
- **The end-of-life stage (Modules C1-C4).** The end-of-life stage of a building starts when the building is decommissioned and is not intended to have any further use. At this point, the building's demolition/deconstruction is considered as a multi-output process that provides a source of materials,

products and building elements that are to be discarded, recovered, recycled or reused. The scenarios for these end-of-life options for the products and materials determine the system boundary.

- **The benefits and loads beyond the system boundary (Module D).** Components for reuse and materials for recycling and energy recovery are considered as potential resources for future use. Module D quantifies the net environmental benefits or loads resulting from reuse, recycling and energy recovery resulting from the net flows of materials and exported energy exiting the system boundary.

According to the EN 15978 (UNI, 2011b), as shown in Fig. 5.16, all impacts and aspects of the specified imported energy were assigned in module B6. On the other hand, the net environmental benefits and/or loads of the energy exported beyond the building system boundary were reported in Module D by calculating the substituted impacts and aspects from the most likely corresponding energy supply, based on current average technology and practice.

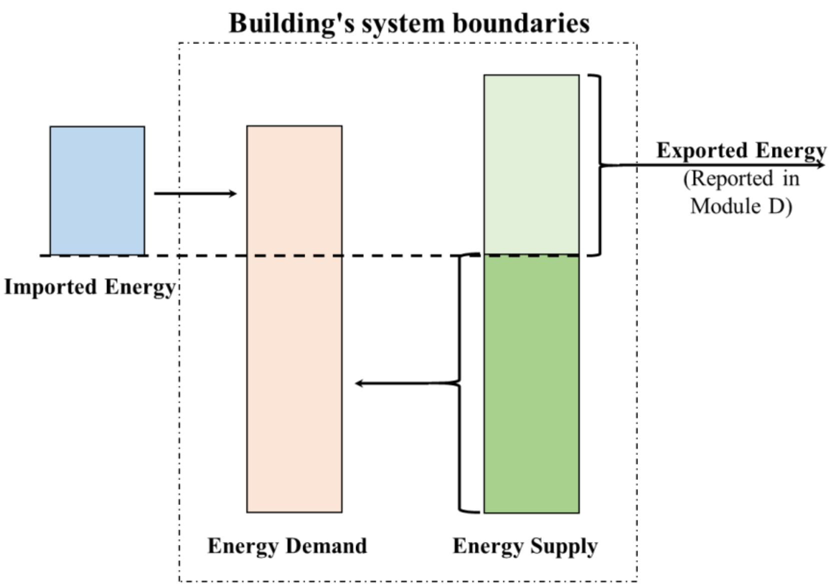

Fig. 5.16 – Allocation of imported and exported energy (UNI, 2011b).

5.3.1.6 Data quality

The data quality has a major influence on results, and proper evaluation of data quality is therefore an important step in every LCA (Guinée, 2002; ISO, 2006a). The data used for the case study are representative of this particular study. For all the life cycle stages of the building, both primary and secondary data were used. In particular, the quality of the data were reported taking into account justification of the choices of data sources selected in relation to the goal of the study.

For the materials production stage, both primary and secondary data were used. The eco-profiles of each material of the building envelope and systems are from the Ecoinvent database (Frischknecht et al., 2005). Tab. 5.18 shows major details for the main materials used.

Tab. 5.18 - Sources of data relating to the materials constituting the building envelope.

Material	Description	Database
Steel	Steel, low-alloyed, at plant/RER U	Ecoinvent
HDPE plastic	Polyethylene, HDPE, at plant/RER U	Ecoinvent
Window Wood Frame	Window frame, U=1,5 W/m^{2}K, at plant/RER U	Ecoinvent
Glass	Flat glass, uncoated, at plant/RER U	Ecoinvent
Polyester fiber	Polyester resin, unsatured, at plant/RER U	Ecoinvent
PVC Plastic	Polyvinylclorite, at regional storage, at plant/RER U	Ecoinvent
Paints	Alkid plant, white, 60% in H2O, at plant/RER U	Ecoinvent
Cooper	Copper concentrate, at beneficiation/RER U	Ecoinvent
PV module	Photovoltaic panel, multi-Si, at plant/RER/I U	Ecoinvent
Inverter	Inverter, 2500 W, at plant/RER/I U	Ecoinvent

For the building construction and the transport stages, energy consumption, types of transport (Tab. 5.19) and scraps production due to the building process were estimated.

Tab. 5.19 - Sources of data relating to the types of transport.

Type of transport	Description	Database
Transport by road	Transport, lorry >16 t	Ecoinvent unit process
Transport by road	Transport, van 16t/RER U	Ecoinvent unit process
Transport by sea	Transport Barge/RER U	Ecoinvent unit process

The use phase encompasses all activities related to the use of the building, over the 25 year life span. These activities include all operating energy consumed for heating, cooling, lighting and appliances. The assessment of the use stage was carried out using EnergyPlus simulations. Finally, to assess the environmental impacts of the end-of-life stage, secondary data from the Ecoinvent database (Frischknecht et al., 2005) have been used (Tab. 5.20 shows the **s**ources of data relating to the end-of-life of some material).

Tab. 5.20 - Sources of data relating to the end-of-life of some material.

Material	Description	Database
Steel	Recycling ECCS steel B250	Ecoinvent database
PVC Plastic	Recycling PVC B250	Ecoinvent database
Recycling	Recycling glass B250	Ecoinvent database
Cooper	Copper, secondary, from cable treatment, at plant/GLO S	Ecoinvent database

5.3.1.7 Technological, geographical and time data representativeness

The data used in the study represent the current European average technology. The only exceptions is the energy imported from the electricity grid that represent the Italian average electricity mix.

5.3.1.8 Other information

No allocation procedures were performed. All the energy and environmental loads were attributed to the case study. Moreover, there was no cut-off (i.e. specification of the amount of material or energy flow or the level of environmental significance associated with unit processes or product system to be excluded from a study) in the impact assessment of the study, meaning that every inventoried process is included in the impact assessment and the results.

5.3.2 Life Cycle Inventory

After defining the objective and scope of the building case study, the next step was to perform the Life Cycle Inventory (LCI) analysis of all input and output associated with each building life cycle stages. To carry out the analysis the building has been divided into two classes of technological units:

- building envelope;
- building systems.

These two macrosystems have in turn been divided into increasing levels of detail. The building envelope has been divided into:

- external platform;
- floor;
- foundation;
- rainwater system;
- roof;
- wall;
- windows.

On the other hand, the building systems includes:

- electrical system;
- thermal system;
- photovoltaic system.

The first stage of the LCI was focused on the estimation of masses and volumes of each type of material used during the material production stage (Modules A1 - A3), through project analysis and investigations of the construction site. Then, the data related to the transport of the materials from the production site to the building site (Module A4) were estimated in terms of tkm. For the construction stage (Module A5) the energy consumption and the amount of waste and site scraps produced during this life cycle stage were assessed. For the Modules B4 and B6 (use stage) the energy consumption and production were estimated. Moreover, replacement assumptions (amount and frequency of replacement activities) were defined for some building components. Finally since the building is currently standing and no information is still available on its end-of-life, for the Modules C1 - C4, some assumptions were made. Detailed data for each life cycle stage are described in the followings sub-sections.

5.3.2.1 Material production stage (Modules A1 – A3)

For this stage, construction materials were estimated. Masses and volumes for each materials were obtained through project analysis and investigations of the construction site. The Life Cycle Inventory of building materials, according to “from cradle to gate” approach, includes also the manufacturing to processes to make them ready for the use in the construction process. The eco-profiles of each material of the building envelope and systems are from the Ecoinvent database (Frischknecht et al., 2005).The only exception is FRP. For this material, the eco-profile was modelled using both primary data, provided by the manufacturer, and secondary data from literature (Bakis et al., 2002; Basbagill, Lepech, & Ali, 2012; Uddin, 2013). In detail, all mass and energy inputs for manufacturing of FRP were obtained from the manufacturer through production site investigations and questionnaires, while the eco-profiles of materials and energy sources were modelled using the Ecoinvent database (Frischknecht et al., 2005). Tab. 5.21 shows the quantities of raw materials used to produce 1 kg of FRP material.

Tab. 5.21 - Quantities of raw materials used to produce 1 kg of FRP material.

	Raw material	**Weight (kg / 1 kg))**
Fibers	Glass Fiber	0.7000
Thermosetting matrix	Styrene	0.0925
	Isophthalic acid	0.0315
	Propylene glycol	0.0473
	Maleic anhydride	0.0440
	Dietilenglicole	0.0284
	Diethylene glycol	0.0063
Catalysts	Percarbonate	0.0125
	Perbenzoate	0.0125
Paints	Inorganic polyester paint	0.0250

Fig. 5.17 shows the production process modelled for the FRP material. The transport of the raw materials up to the production plants of the components (fibers, matrices, additives) was not included in the analysis, while that of the components from the production plants to that of FRP material production was considered.

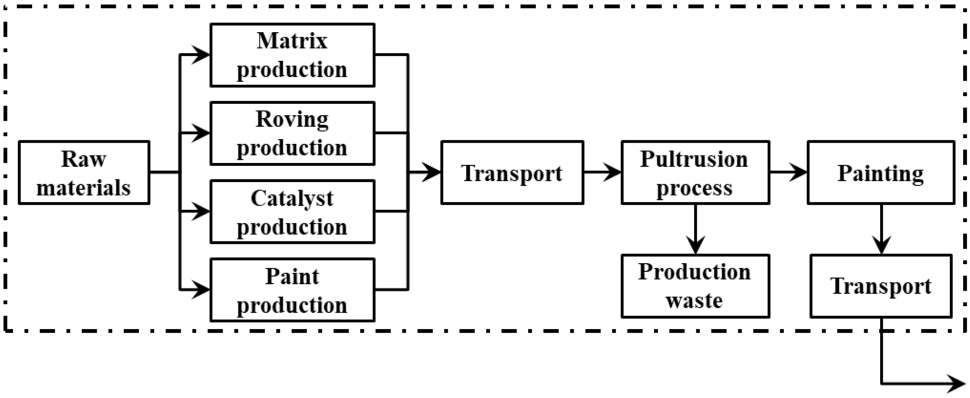

Fig. 5.17 - Production process of the FRP material.

Tab. 5.22 shows the inventory data of all materials used to build the envelope.

Tab. 5.22 - Inventory data of all materials used to build the envelope.

	FRP [kg]	**Glass [kg]**	**HDPE Plastic [kg]**	**Polyester fiber [kg]**	**PVC Plastic [kg]**	**Steel [kg]**	**Wood [kg]**
External platform	419.6	-	-	-	-	1.2	-
Floor	1856.4	-	1.5	118.8	-	5.5	17.9
Foundation	-	-	-	-	-	90.2	-
Rainwater system	1.2	-	-	-	7.9	0.4	-
Roof	1959.7	-	14.2	118.7	-	5.5	-
Wall	2328.4	-	46.7	343.0	-	4.3	-
Windows	-	569.5	6.1	-			622.4
Total	6565.3	569.5	68.5	580.5	7.9	107.0	640.3

The building is mainly made of FRP; as shown in Fig. 5.18 this material constitutes 77% of the mass of the building envelope.

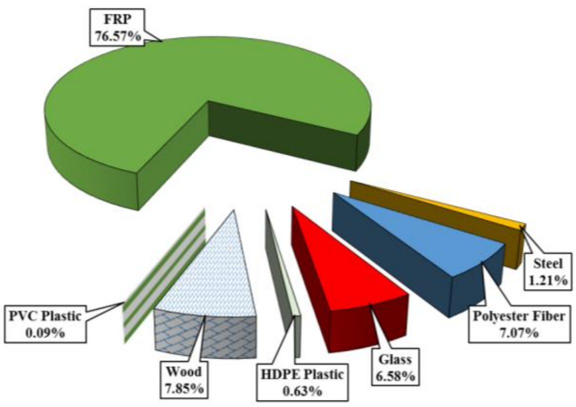

Fig. 5.18 - Mass share of the materials constituting the building envelope.

5.3.2.2 Transport stage (Module A4)

Details on the transport of materials by manufactures to the construction site are given in Tab. 5.23. In particular, the building envelope materials are from production sites more than 1000 km far, while the plants materials are from much closer production sites.

Tab. 5.23 - Transport of materials during the construction stage.

Type of material	Production site	Distance [km] By road	Distance [km] By road
Steel	Bernareggio (MI, Italy)	846	320
FRP	Bernareggio (MI, Italy)	846	320
Polyester fiber	Novedrate (CO, Italy)	904	320
Windows	Treviolo (BG, Italy)	1209	–
Drainage system of rainwater	Messina (ME, Italy)	15	–
Electrical system	Messina (ME, Italy)	15	–
Photovoltaic system	Belpasso (CT, Italy)	102	–
Thermal system	Catania (CT, Italy)	89	–

The data related to the transport of the materials constituting both the building envelope (Tab. 5.24) and the plants (Tab. 5.25) refer to the tkm units.

Tab. 5.24 - Inventory data due to the transport of the building envelope materials.

	FRP		Glass	Polyester fiber		PVC Plastic	Steel		Wood
	By road [tkm]	By sea [t km]	By road [tkm]	By road [tkm]	By sea [tkm]	By road [tkm]	By road [tkm]	By sea [tkm]	By road [tkm]
External Platform	410.6	155.3	-	-	-	-	1.0	0.4	-
Floor	1,570.6	594.1	-	107.4	38.0	-	4.9	1.8	-
Foundation	-	-	-	-	-	-	76.3	28.9	-
Rainwater drainage	1.0	0.4	-	-	-	0.1	-	-	-
Roof	1,652.1	624.9	-	136.0	48.1	-	2.4	0.9	-
Wall	1,157.2	249.6	-	46.4	16.1	-	2.2	0.5	-
Windows	-	-	688.6	-	-	-	-	-	763.4
Total	4,791.3	1,624.2	688.6	289.8	102.3	0.1	86.8	32.5	763.4

Tab. 5.25 - Inventory data due to the transport of the building plants materials.

	Electric Plant	PV system	Thermal Plant	Total
Transport by road [tkm]	1.1	107.7	26.5	135.3

5.3.2.3 Construction stage (Module A5)

Fig. 5.19 shows the module during the construction stage. The energy consumption during this stage is mostly due to the electricity needed to power machinery and tools. In particular, for the on-site construction of the entire module it was recorded an energy consumption of 150 MJ.

Fig. 5.19 - Construction stage of the module.

Furthermore, the amount of waste and site scraps produced during this life cycle stage were assessed. Due to the type of building, the amount of waste and scraps produced during the building construction is lower than that produced during the construction of the traditional buildings. In detail, Tab. 5.26 shows the quantity of scraps produced during the construction stage.

Tab. 5.26 - Building scraps produced during the construction stage.

Type of material	Building scraps [%]	Building scraps [kg]
FRP	2	320
Polyester fiber	5	30

5.3.2.4 Use stage (Modules B4 and B6)

For this stage, the energy consumption during the building use stage (Module B6) was estimated. The building is simulated with a sub-hourly detail (3 minutes time-step) in EnergyPlus environment. According to (Frischknecht, Heath, Raugei, Sinha, & de Wild-Scholten, 2016; Fthenakis et al., 2011), the degradation of the modules reducing efficiency over the life time has been taken into consideration. In detail, a linear degradation of 0.7% per year was considered (Frischknecht et al., 2016; Fthenakis et al., 2011).

This stage also includes replacement (Module B4) of some building components. Replacement assumptions (amount and frequency of replacement activities) were defined for some building components. In particular, it was planned to replace the inverters of the photovoltaic system and the heat pump because a 15 year useful life was estimated for these components. The replacement materials background data were taken from Ecoinvent database (Frischknecht et al., 2005). In detail, the boundary for replacement products included:

- the production of the material;
- their transportation;
- the waste management for the replaced products;
- the end-of-life stage of the replaced building component.

Since the estimated useful life for the building (25 years) is the same as the estimated one for the plants and it guarantees a use of the building without any particular refurbishment or maintenance, the energy and materials data input due to the installed products in use (Module B1), maintenance (Module B2), repair (Module B3) and refurbishment (Module B5) were neglected. Furthermore, since the building is not equipped with a water and sanitary supply system, the energy and materials data input due to the consumption of water during the use stage (Module B7) were also neglected.

5.3.2.5 End-of-life stage (Modules C1 - C4) and benefits/loads beyond the system boundaries (Module D)

The end-of-life stage includes the following steps:

- de-construction/demolition of the building (Module C1);
- transport of materials (Module C2);
- recycling or landfilling of waste (Modules C3 – C4).

Since the building is currently standing and no information is still available on its end-of-life, for the de-construction/demolition stage it was assumed that the same operations performed for the assembly of the housing module will occur, thus the energy consumption for the demolition was assumed equal to the construction stage (150 MJ). For the transport of waste to the site of recycling or disposal details are shown in Tab. 5.27.

Tab. 5.27 - Transport of materials during the end-of-life stage.

Type of material	End-of-life -	Quantity [t]	Distance [km]
FRP	Landfilled	6.62	60
Glass	Recycled	0.57	350
HDPE Plastic	Recycled	0.02	198
Polyester fiber	Recycled	0.61	198
PVC Plastic	Recycled	0.01	198
Steel	Recycled	0.1	350
Wood	Recycled	0.63	198

FRP waste is assumed to be landfilled while the polyester fiber material and other plastic wastes are supposed to be recycled. Iron and steel are supposed to undergo a recycling process used for the production of reinforcing rods. The glass withdrawn from fixtures is entirely recycled through a re-melting process.

According to (UNI, 2011b), the environmental benefits and loads resulting from the recycling of materials were allocated in the benefits and loads beyond the system boundaries (Module D).

5.3.3 Life Cycle Impact Assessment

In this phase, from the LCI were evaluated the potential environmental impacts (ISO, 2006a). Indicators used represent the quantified environmental impacts and aspects caused by the object of assessment during its whole life cycle. In Tab. 5.28 are shown the categories of environmental impact used for the assessment, chosen according to the European Standard UNI EN 15978 (UNI, 2011b) prepared by Technical Committee CEN/TC 350. In detail, the following environmental indicators have been chosen on the basis that there are agreed calculation methods for the indicators referred to in this European Standard. According to the UNI EN 15978 (UNI, 2011b), other indicators, for which there is no scientifically agreed calculation method within the context of LCA - e.g. human toxicity, eco-toxicity, biodiversity, land use - are not included. However, the UNI EN 15978 (UNI, 2011b) does not present any methodology for the aggregation of the individual indicators. For this reason, the environmental impact categories were calculated in agreement with the CML - IA Baseline impact assessment method (Van Oers, 2015) while the energy impact categories were calculated by means of the Cumulative Energy Demand method (Frischknecht et al., 2007).

Tab. 5.28 - Categories of environmental impact.

Indicator	**Acronym**	**Unit**
Global Warming Potential	GWP	kg CO_{2eq}
Ozone Depletion Potential	ODP	kg CFC 11_{eq}
Acidification Potential	AP	kg SO_{2eq}
Eutrophication Potential	EP	kg $PO_4^{3-}{}_{eq}$
Photochemical Ozone Creation Potential	POCP	kg C_2H_{4eq}
Abiotic resource Depletion Potential for elements	ADP_e	kg Sb_{eq}
Abiotic resource Depletion Potential for fossil fuels	ADP_{ff}	MJ
Global Energy Requirement	GER	MJ
No renewable Global Energy Requirement	GER_{no-ren}	MJ
Renewable Global Energy Requirement	GER_{ren}	MJ

The modelling of the stages of the life cycle of building elements, materials and equipment for the quantification of environmental indicators was performed using the SimaPro v8.5 software(PRè Consultant, 2010).

The environmental impact categories were chosen in agreement with the CML - IA Baseline impact assessment method (Van Oers, 2015) while the energy impact categories were calculated by means of the Cumulative Energy Demand method (Frischknecht et al., 2007).

Global Warming Potential (GWP) [kg $CO_{2\ eq}$]

Climate change may result in adverse effects to human health, to ecosystem preservation and to performance of materials. This category is related to the emission of greenhouse gases into the atmosphere and is expressed as Global Warming Potential, for a time horizon of 100 years (GWP100), in equivalent kilograms of carbon dioxide (CO_2) per kg of emissions released to the atmosphere. This indicator has repercussions on a global scale and is related not only to the radioactive properties of emissions, but also with the time scale that characterizes and depletion of the substance in the atmosphere.

Ozone Depletion Potential (ODP) [kg CFC 11_{eq}]

Stratospheric ozone depletion is the thinning of the stratospheric ozone layer as a result of anthropogenic emissions, such as CFCs and halons (Guinée, 2002). This causes a greater fraction of solar UV-B radiation to reach the Earth’s surface, with a potential damage to human health, ecosystems, biochemical cycles and materials. The natural seasonal Antarctic 'ozone hole' has been growing since the early 1980s. On a global scale, the decline of ozone in the stratosphere has recently slowed. The depletion is mainly caused by CFCs which are used in aerosols, air conditioning, and refrigerators. Halon, which is a fire retardant, is one of the key ozone-depleting gases. However, the use of this substance has been reduced significantly and will soon be phased out completely due to the successful implementation of the Montreal Protocol. It is therefore important to state in the impact assessment how much of the Ozone Depletion Potential (ODP) is due to halon. ODP is the ratio between the amount of ozone destroyed by a unit of a substance “x” and a reference substance, normally taken as CFC-11. The unit of the ODP is therefore kg CFC-11 equivalent.

Acidification Potential (AP) [kg $SO_{2\ eq}$]

Acidification is the process where emissions to air (primarily ammonia (NH_3), sulphur dioxide (SO_2) and nitrogen oxide (NO_x)) are converted to acid substances. The sulphur dioxide is formed by the burning of fossil fuels such as coal, which contain high quantities of sulphur; the nitrogen oxide is produced by various industrial activities and is present in emissions from the transport sector. This indicator is expressed in equivalent kilograms of SO_2 for each kilogram of emissions to the atmosphere. Acidifying compounds released into the atmosphere are transported by wind and deposited as acid particles or acid rain to hundreds or thousands of km away from the source. Acid rain is considered an important example of cross boarder pollution (international). Acidification occurs when the capacity of soil organisms or of water to resist or neutralize the atmospheric deposition of acidifiers starts to decrease. The acid substances can attack natural and artificial materials, and cause damage to capital, to human health and to natural values. Materials such as cement, lime and concrete are sensitive to acid, as this can react with its contents and disintegrate the material structure. The acids can also cause considerable corrosion of metal surfaces. The geographic scope of this indicator can be both local and continental.

Eutrophication Potential (EP) [kg $(PO_4)^{3-}{}_{eq}$]

Eutrophication, also known as nitrification, includes all impacts due to excessive levels of macro-nutrients in the environment caused by nutrient emissions to air, to water and to soil. Nutrients are normally added to the soil through fertilization to stimulate the growth of plants and agricultural products. When these nutrients end in natural waterways or sensitive soils, this unintentional fertilization may result in excess of plants or algae which, in turn, can lead to lack of oxygen and consequently to death of species. This environmental problem is usually associated to the emissions of nitrogen (N) and phosphorus (P). The potential of eutrophication is expressed in equivalent kilograms of phosphate (PO_4) per kilogram of emission. The duration of this environmental impact is infinite and it has local and continental repercussions.

Photochemical Ozone Creation Potential (POCP) [kg $C_2H_{4\ eq}$]

The photochemical oxidation corresponds to the formation of reactive chemical compounds (mostly ozone) by the action of ultraviolet radiation (UV). This problem is also known as "summer smog". Currently, tropospheric ozone is one of the most serious air pollutants in Europe. High levels of ozone cause severe health problems, premature death, reduced productivity of agricultural crops, changes in biodiversity and damage to property. The chemical compounds related to this problem, such as nitrogen oxides (NO_x), carbon monoxide (CO) and volatile organic compounds (VOCs) are emitted into the atmosphere from many natural and anthropogenic processes. In the lower part of the Earth's atmosphere, the troposphere, and under the influence of UV radiation photo-oxidants are formed by photochemical oxidation of VOCs and CO in the presence of NO_x. These reactions lead to the formation of ozone (O_3), peroxyacetyl nitrate (PAN), peroxybenzoyl nitrate (PBN) and a number of other substances. In human beings, low concentrations of photochemical smog may cause reduced functionality of the lungs, chest tightness, eyes, and nose and throat irritation. At higher concentrations can cause coughing and decreased ability to concentrate. Regarding to materials, ozone attack natural rubber, cellulose, synthetic polymers, etc., and reduces the lifetime of many materials (textiles, car tires, etc.). This indicator is expressed in equivalent kilograms of ethylene (C_2H_4) per kilogram of emission. These emissions have an effect that is maintained for 5 days and this mechanism has local and continental repercussions.

Abiotic resource Depletion Potential (ADP_e) [kg Sb_{eq}] / (ADP_{ff}) [MJ]

Abiotic resources are natural resources (including energy resources), such as iron ore and crude oil, which are regarded as non-living. Several optional methods for the assessment of abiotic resource depletion are used. The Abiotic Depletion Potential is derived from each extraction of elements and is a relative measure with the depletion of the reference element. The category ADP aims to assess the environmental problem associated with the decreasing availability of natural resources. It is understood by natural resources minerals and materials found on the land, sea or atmosphere, including fossil fuels. Its value is related to the amount of each material and fossil fuel extracted and is based on available reserves and decrease rate thereof. ADP is distinguished in ADPelements (ADP_e) and ADPfossil fuels (ADP_{ff}). The characterization takes the total availability of the resource into account in relation to the availability of the resource antimony. In the case of fossil fuels (ADP_{ff}) a general characterization factor for fossil fuels is multiplied by the heating value of the fuel.

Global Energy Requirement (GER) [MJ].

The assessment of the environmental impacts related to a product or process is based on one parameter: the total energy demand for production, use and disposal expressed in primary energy. Every direct and indirect (e.g.

construction of infrastructure) energy input is taken into account, obtained from process or input-output analysis (Frischknecht et al., 2007). It is also divided between non-renewable (GER_{no-ren}) and renewable primary energy use (GER_{ren}).

5.3.4 Interpretation

The last step in LCA according to ISO was Interpretation. The results were interpreted according to the goal and scope of the study.

5.3.5 Energy and environmental payback times

In order to compare the primary energy use and environmental impacts due to the entire building life cycle to the primary energy use and environmental impacts potentially avoided thanks renewable energy produced during the use stage, energy and environmental payback times (PBT) were calculated for each impact category (Tab. 5.29) analysed in the LCIA stage.

Tab. 5.29 - Energy and the environmental payback times.

Indicator	**Acronym [Unit]**	**PBT acronym**
Global Warming Potential	GWP [kg CO_{2eq}]	PBT_{GWP}
Ozone Depletion Potential	ODP [kg CFC 11_{eq}]	PBT_{ODP}
Acidification Potential	AP [kg SO_{2eq}]	PBT_{AP}
Eutrophication Potential	EP [kg $PO_4{}^{3-}{}_{eq}$]	PBT_{EP}
Photochemical Ozone Creation Potential	POCP [kg C_2H_{4eq}]	PBT_{POCP}
Abiotic resource Depletion Potential for elements	ADP_e [kg Sb_{eq}	PBT_{ADPe}
Abiotic resource Depletion Potential for fossil fuels	ADP_{ff} [MJ]	PBT_{ADPff}
Global Energy Requirement	GER [MJ]	PBT_{GER}

According to the literature (Maurizio Cellura, Guarino, Longo, & Mistretta, 2017), the environmental payback times are defined as the times taken to compensate the potential impacts due to the entire building life cycle with the reduction in impact due to the annual renewable energy produced by the building systems. The payback time indices can be calculated applying eq. 5.26.

eq. 5.26

$$PBT_j = \frac{I_{0,j}}{I_{1,j}}$$

Where $I_{0,j}$ is the potential impact for the impact category j due to the entire building life cycle and $I_{1,j}$ is the impact avoided due to the renewable energy production of the photovoltaic system, equivalent to the impact emitted by a traditional energy system (in this thesis the Italian national energy mix was considered) to produce the same amount of electricity.

However, the environmental payback time calculated using eq. 5.26 does not take in to account the yearly mean degradation (r) of the PV system reducing efficiency over the life time. For this reason, eq. 5.26 was modified to consider an yearly mean degradation of a 0.7% per year for the energy generated (Frischknecht et al., 2016; Fthenakis et al., 2011). In detail, payback period represents the point at which eq. 5.27 is satisfied.

eq. 5.27

$$I_{0,j} = \sum_{t=1}^{T} \frac{I_{1,j}}{(1+r)^t}$$

Where t is the time period expressed in years while T is the building required service life (25 years). Solving for t eq. 5.27 allows to obtain the payback period, as shown in eq. 5.28.

eq. 5.28

$$PBT_j = \frac{\log\left(\left[1 - \frac{I_{0,j}}{I_{1,j}} r\right]^{-1}\right)}{\log(1+r)}$$

In detail, $I_{1,j}$ was calculated using the characterization factors showed in Tab. 5.30, that reflect the impacts avoided by the production of 1 kWh of renewable energy, equivalents to the impacts produced by 1 kWh of electricity produced by the national energy mix.

Tab. 5.30 - Energy and the environmental conversion factors used to calculate the payback times.

Indicator	**Unit**	**Conversion factor**
GWP	kg CO_{2eq}/kWh_e	6.45E-01
ODP	kg CFC $11_{eq}/kWh_e$	5.62E-08
AP	kg SO_{2eq}/kWh_e	3.19E-03
EP	kg $PO_4^{3-}{}_{eq}/kWh_e$	7.71E-04
POCP	kg C_2H_{4eq}	1.31E-04
ADP_e	kg Sb_{eq}/kWh_e	9.01E-07
ADP_{ff}	ADP_{ff} MJ/kWh_e	8.01E+00
GER	GER MJ/kWh_e	1.07E+01

6 MONITORING AND VALIDATION RESULTS

6.2 INTRODUCTION

This chapter, regarding the previously defined concepts and applied methods, focuses on modelling and simulation of energy consumption related to the building case study introduced in chapter 4. Verification of the case study building model is an essential step towards having confidence in the results of the simulations performed in the next chapter.

Therefore, to ensure that the building model is an accurate representation of reality and that their data outputs are reliable, it is critical that it is properly validated and verified so that they can be relied on to give useful conclusions about the building. By comparing the data generated by the model with analogous data measured from the real building, errors in the model can be identified and tuned to a point where the building model can be said to be a satisfactory representation of the real building. The desired result is a model that can represent the building over any given year with reasonable accuracy.

Validation is usually achieved through the calibration of the model, mentioned in the previous chapter, as an iterative process of comparing the model to the numerical data using the discrepancies between the two, and the insights gained, to improve the model. This process is repeated until model accuracy is considered to be acceptable (ASHRAE, 2014).

6.3 BUILDING MODEL VALIDATION RESULTS

Monitoring was performed for around 60 days during May – July 2018, including indoor air temperature of both building room and surfaces temperatures (Fig. 6.1 shows the position of all sensors used during the monitoring).

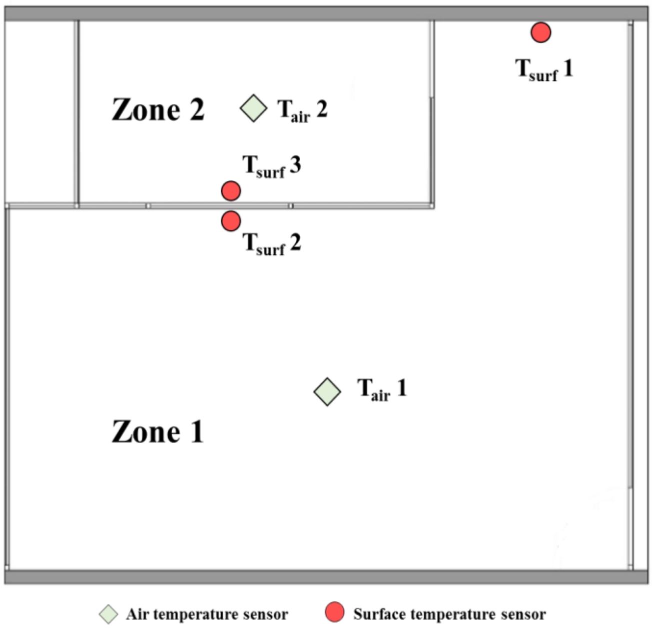

Fig. 6.1 – Sensors position during the building monitoring.

Fig. 6.2 shows a sample of the outdoor monitored weather data, global horizontal radiation (W/m^2) and dry bulb temperature (°C), for 10 days (07 - 16 June 2018) of the monitoring period (24 May – 27 July 2018). During this period, even if it is not summer period, the temperature can easily reach 30 °C and hardly falls below 20 °C.

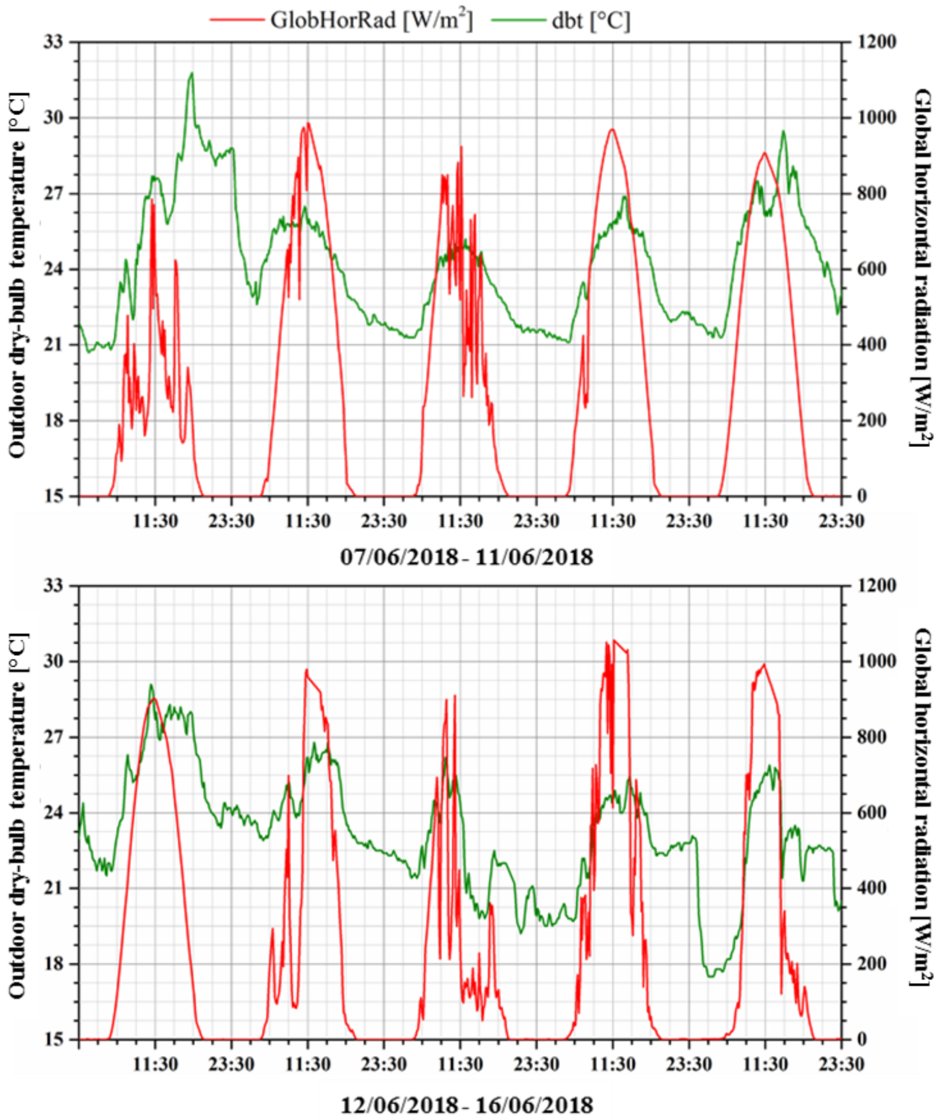

Fig. 6.2 – Dry bulb temperature and global horizontal radiation during 10 days of the building monitoring period (07 - 16 June 2018).

Moreover, the photovoltaic generation has been studied on a sub-hourly base (10 minute time-step) comparing the simulated and monitored output power (kW) of a single photovoltaic module.

By comparing the monitored data to that of the model on the same day using recorded weather data as a model input and performing the calibration process described in the previous chapter, it was possible to tune the building model, acting mainly on the building envelope material properties, the internal gains and on the infiltration rate, to best match that of the real building without uncertainty due to weather factors. To validate the results produced from the building model statistical techniques were employed as a method to assess the accuracy of outputs and the consistency of the same. In detail, error quantification was completed using the following metrics:

- mean bias error (MBE);
- normalised mean bias error (NMBE);
- root mean square error (RMSE);
- coefficient of variation of the root mean square error (CV(RMSE));
- R^2.

The following paragraphs show the results obtained at the end of the model calibration for each of the sensors shown in Fig. 6.1.

6.3.1 Zone 1 air temperature

The model shows that the modeled air room temperature for the Zone 1 (the main room) has high accuracy compared to the monitored air temperature. In detail, the average difference between monitored and simulated data is 0.15 °C. In all cases the differences are below 1.42°C. In 90% of the data, the absolute error is below 0.28°C while for 75% of the calibration data it is below 0.15°C (Fig. 6.3).

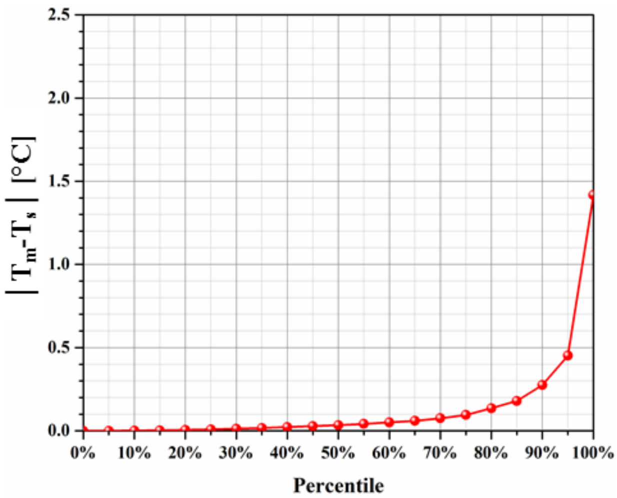

Fig. 6.3 - Validation results for the Zone 1.

The following graphs (Fig. 6.4) represent the outdoor temperature (blue line), the monitored (green line) and the simulated temperature (red line) in the thermal zone of interest for 10 days (07 - 16 June 2018) of the monitoring period (24 May – 27 July 2018). During this period, the temperature difference between the monitored and the simulated temperature is within the range of ±1.05°C.

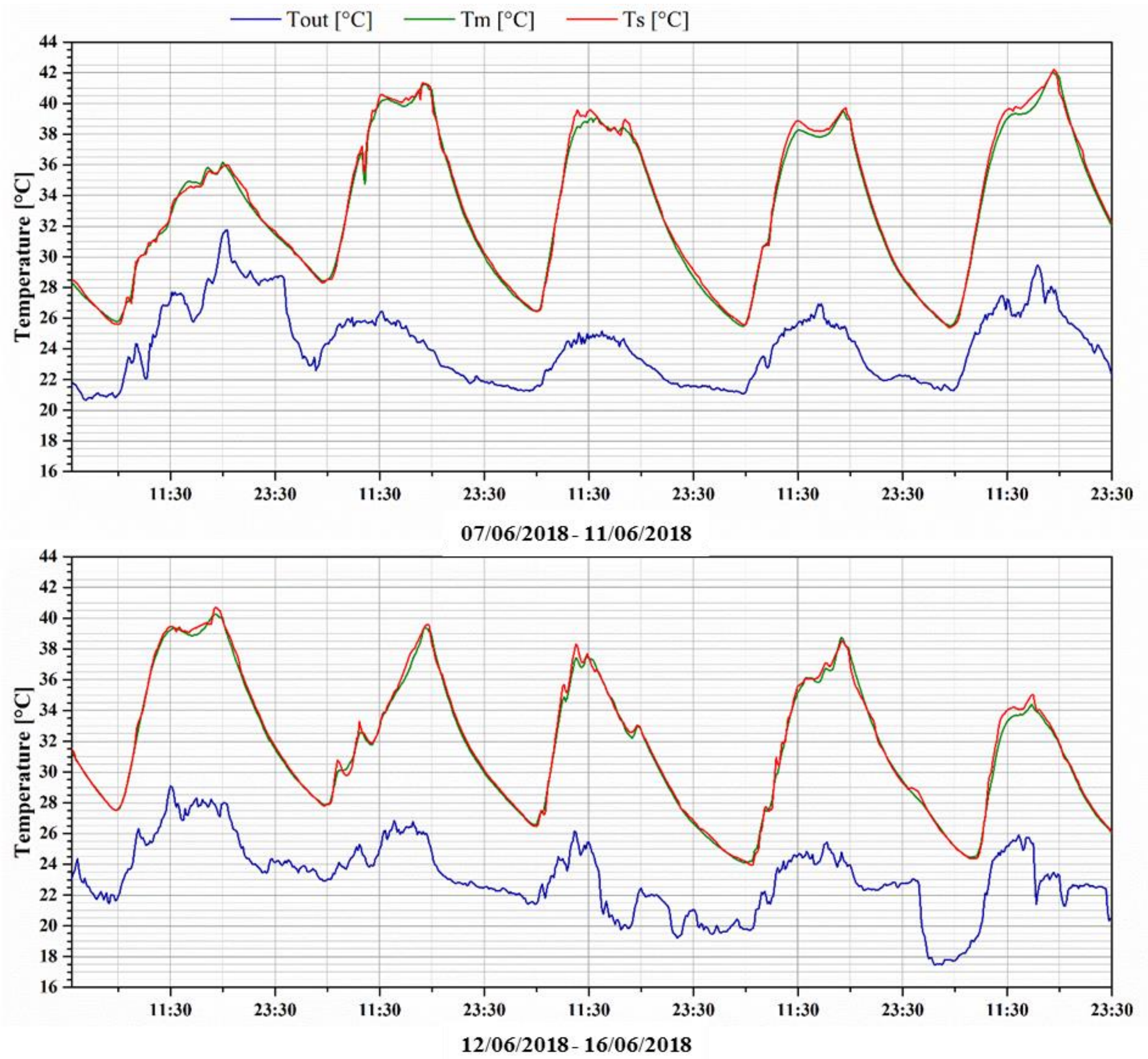

Fig. 6.4 - Comparison of the monitored and simulated air temperature for the Zone 1 (07 - 16 June 2018).

Finally, the Zone 1 air temperature modelled can be considered well calibrated, since the quantification of errors provided the following results:

- MBE: -0.15°C;
- NMBE: -0.45%;

- RMSE: 0.31°C;
- CV(RMSE): 0.96%;
- R^2: 99.68%.

6.3.2 Zone 2 air temperature

Fig. 6.5 shows the validation results for the Zone 2 (the technical room): the differences between monitored and simulated data are below 1.32°C for all data. In 90% of the data, the absolute error is below 0.53°C while for 50% of the calibration data it is below 0.21°C.

In addition, the root mean square error of the simulated indoor temperature (0.32 °C), the coefficient of variation of the root mean square error (1.02%), the mean bias error (-0.02°C), the normalised mean bias error (-0.08%) and R^2 (99.18%) were calculated.

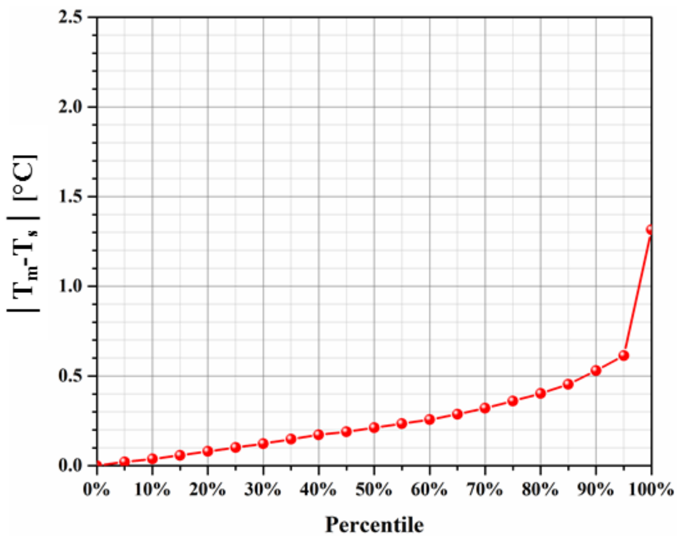

Fig. 6.5 - Validation results for the Zone 2.

The following graphs (Fig. 6.6) shows the external temperature (Tout), the monitored (Tm) and the simulated temperature (Ts) in the thermal zone of interest (the technical room), for the period between 7th - 16th June 2018. The temperatures are in good agreement between the two curves where the max difference between simulated and monitored data is 1.32°C during the all monitoring period.

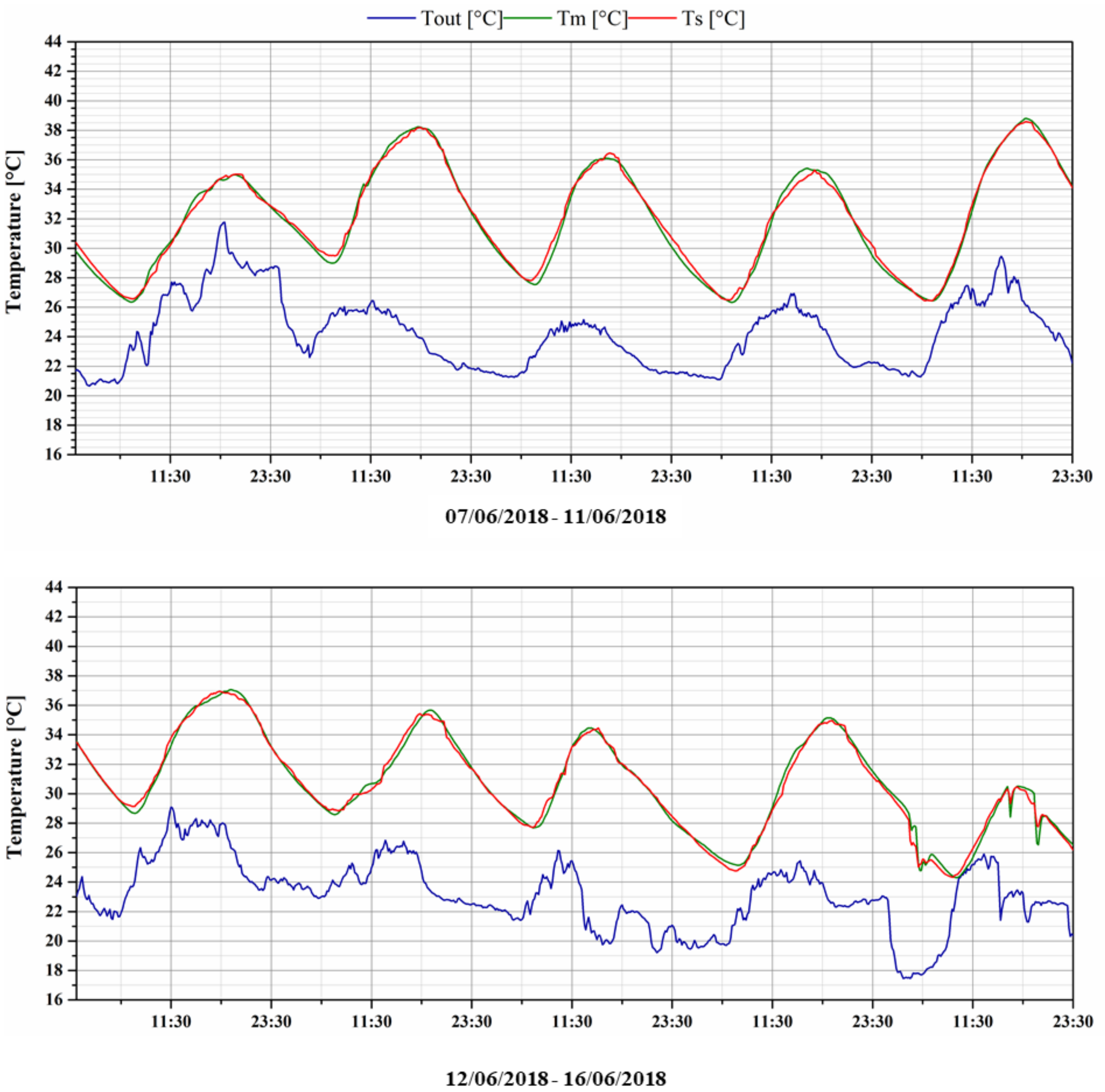

Fig. 6.6 - Comparison of the monitored and simulated air temperature for the Zone 2 (07 - 16 June 2018).

6.3.3 Surface temperatures

The validation results for the surface temperatures are shown for Surface 1, 2 and 3 in Fig. 6.7. From these figure, we can see that there is a good agreement between the simulated and the measured temperatures. In all cases the differences are below 2.38°C. In 90% of the data, the absolute error is below 1.81°C, for 75% it is below 0.90°C, while for 50% of the calibration data it is below 0.66°C.

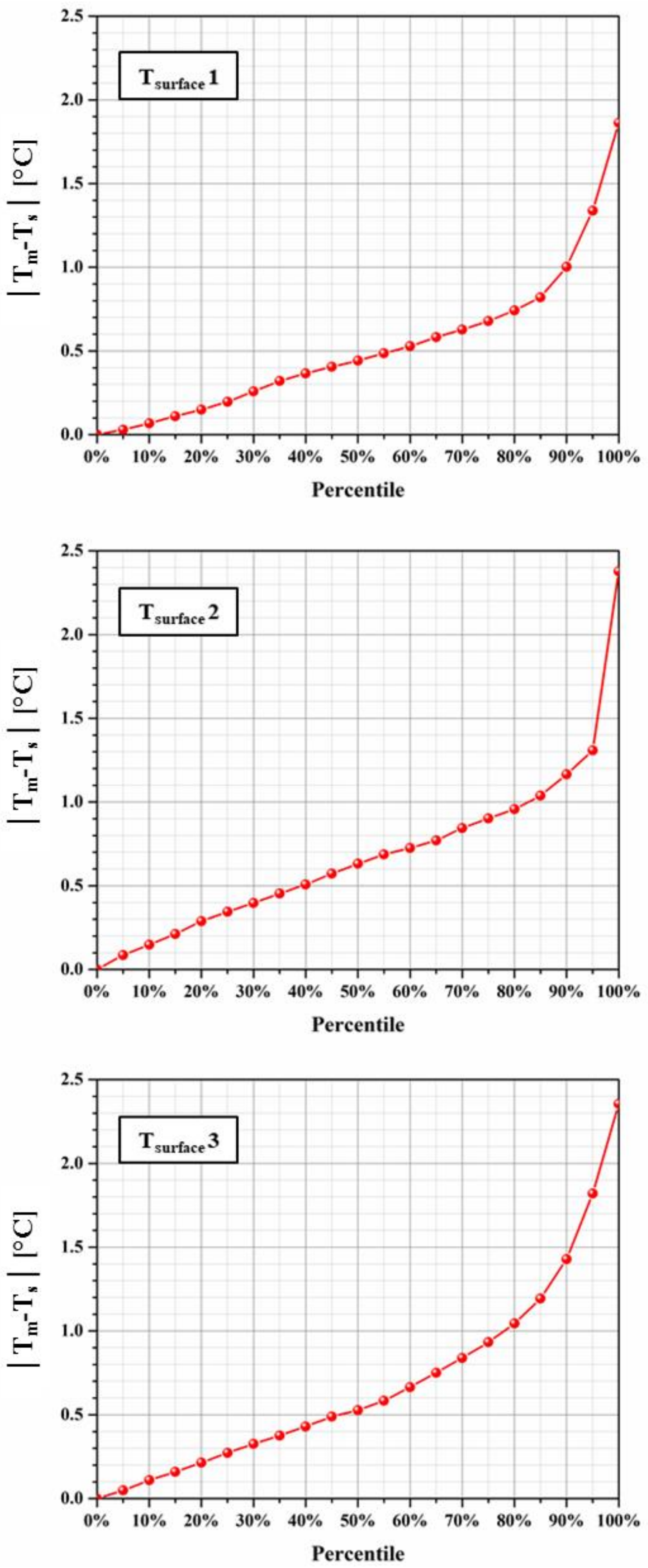

Fig. 6.7 - Validation results for the building surfaces.

The modeled and measured surfaces temperature are shown in Fig. 6.8 - Fig. 6.10. As in the case of the indoor air temperatures, modeled and measured surfaces temperature are similar and both have similar average for each day. However, modeled surface temperature has a larger error amplitude than the indoor air temperature.

Moreover, for the temperature of the surfaces 2 and 3, the peaks are more pronounced in the results of the numerical model at mid-day. The discrepancy between simulation and measurements for these peak hours can reach 2.38°C.

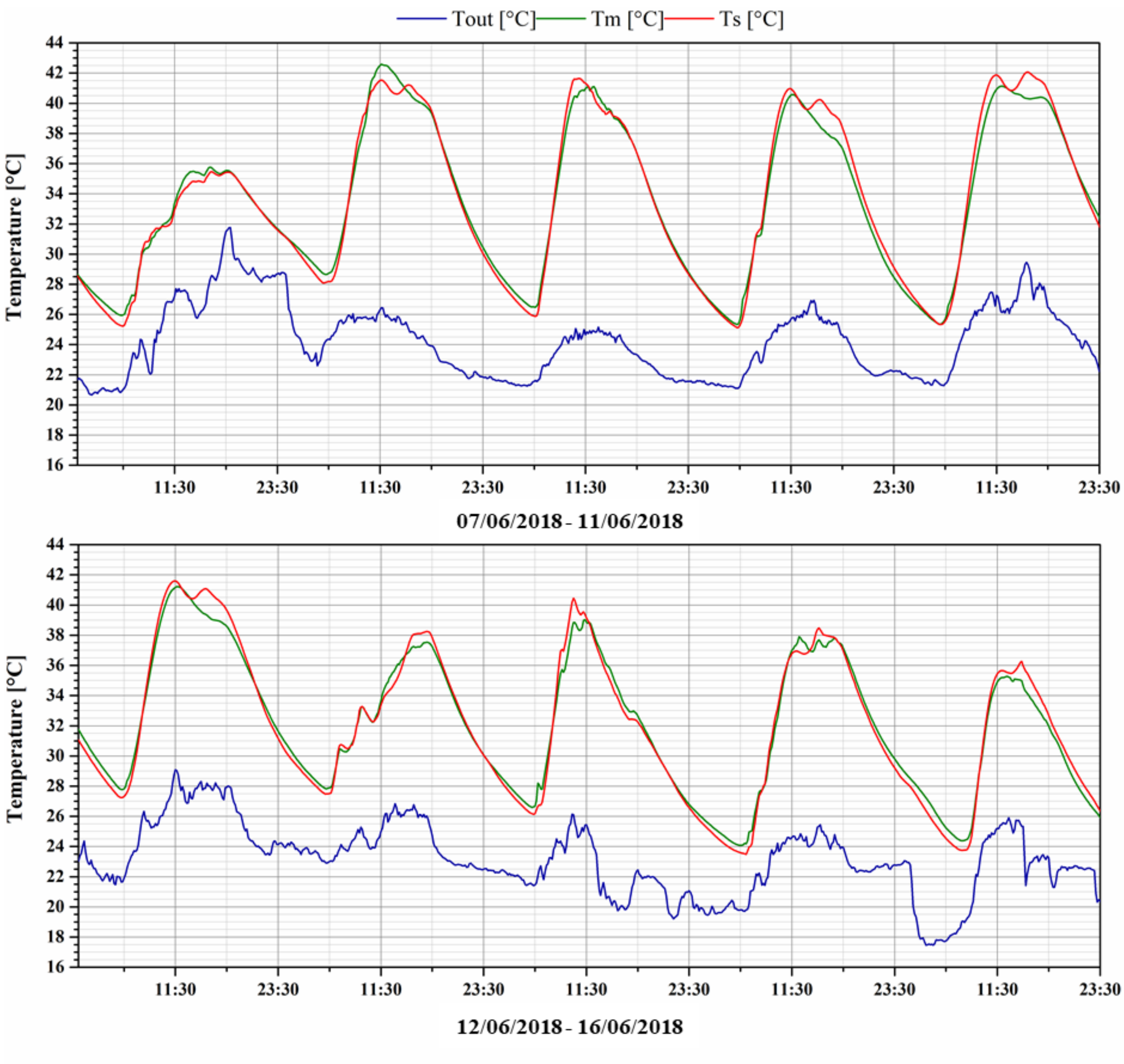

Fig. 6.8 – Comparison of the monitored and simulated air temperature for the Surface 1 (07 - 16 June 2018).

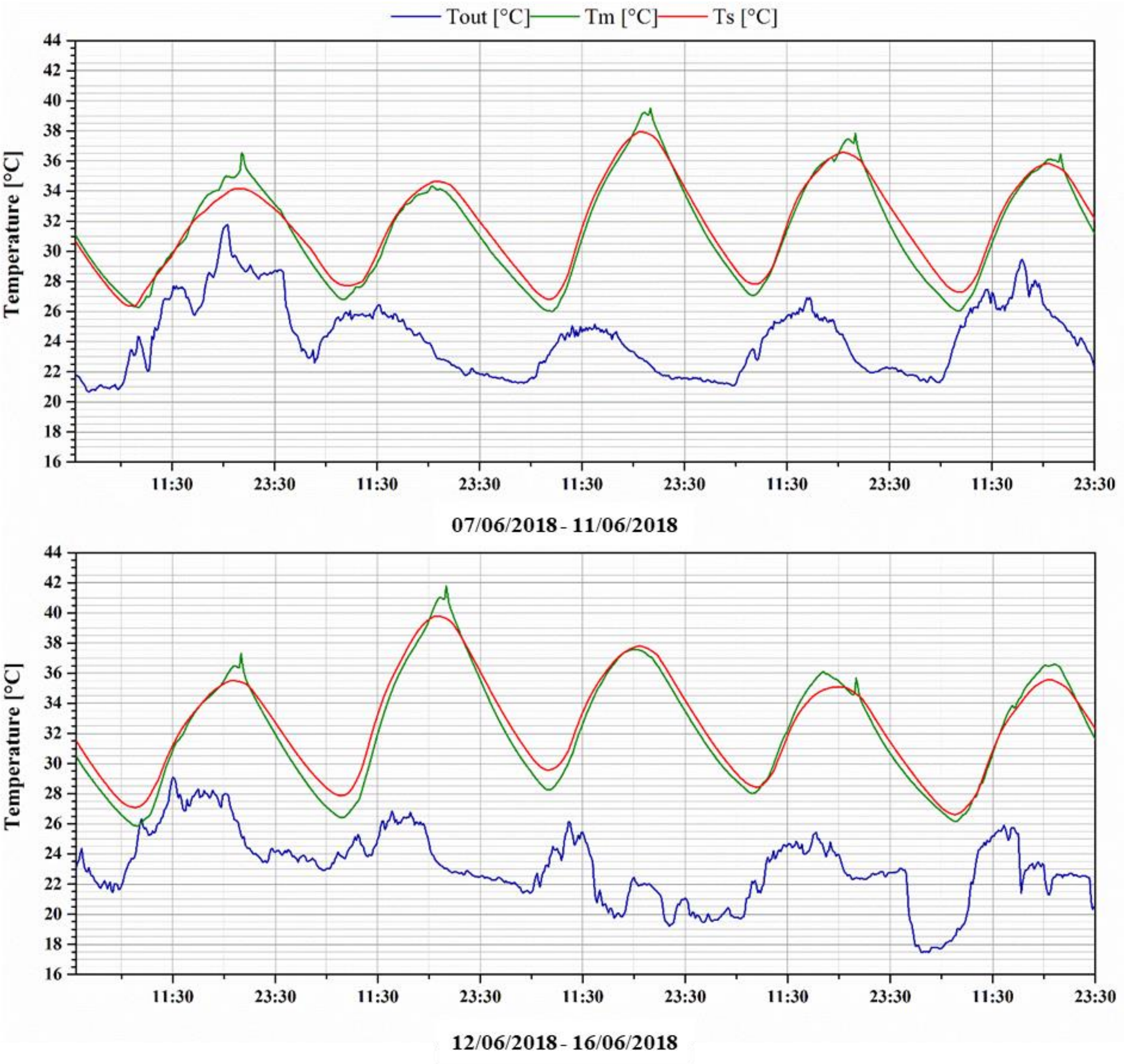

Fig. 6.9 – Comparison of the monitored and simulated air temperature for the Surface 2 (07 - 16 June 2018).

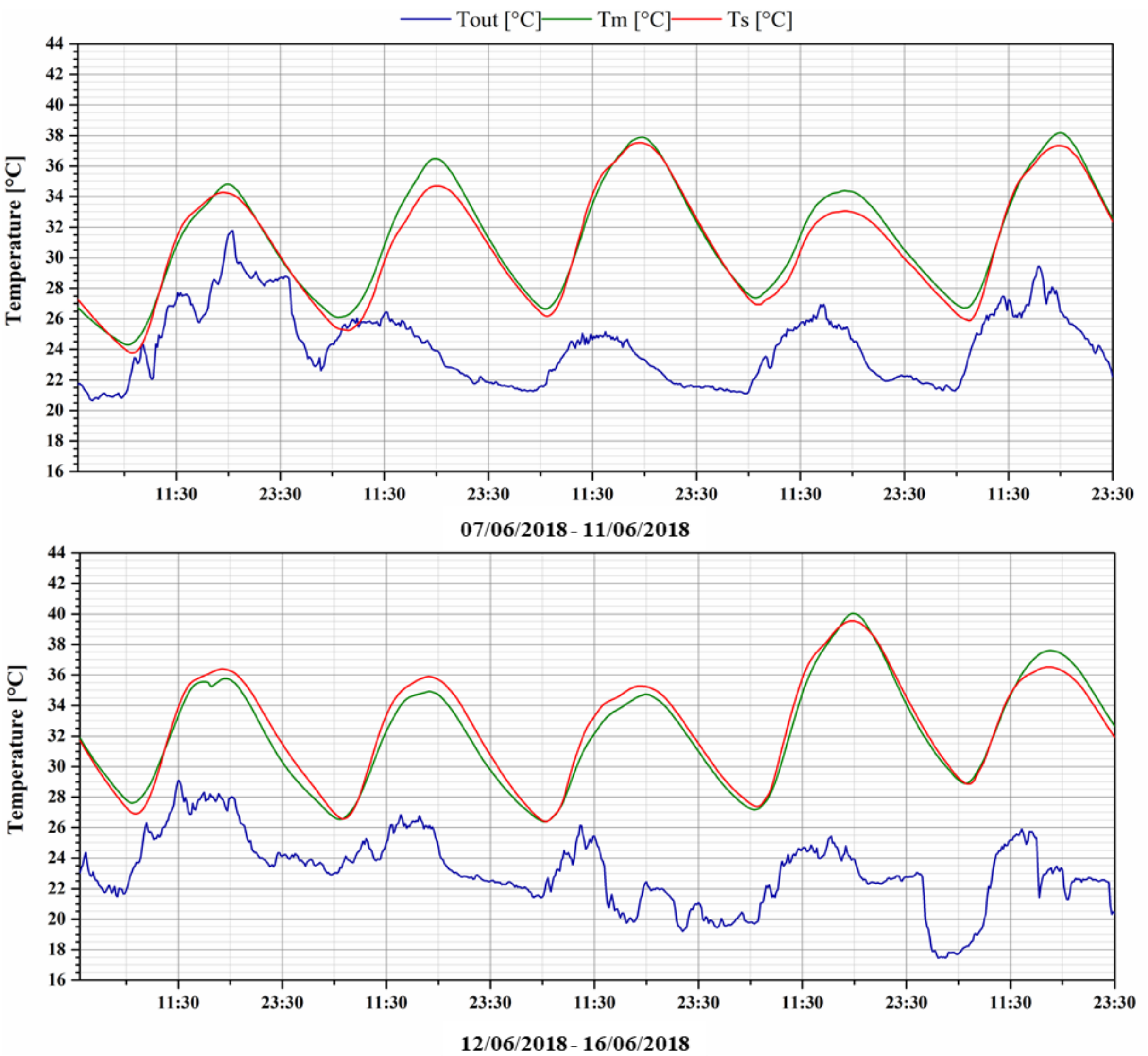

Fig. 6.10 - Comparison of the monitored and simulated air temperature for the Surface 3 (07 - 16 June 2018).

Tab. 6.1 includes the statistical metrics used to assess the modeling error: mean bias error (MBE), the normalised mean bias error (NMBE), root mean square error (RMSE) and the coefficient of variation of the root mean square error (CV(RMSE)).

Surface 1 is characterized by the MBE closest to zero (-0.04°C), while the minimum and maximum MBEs are -0.13°C (Surface 2) and -0.36°C (Surface 3), respectively. Moreover, Surface 1 is characterized by the lower CV(RMSE) (1.93%) and NMBE (-0.11%) compared to the other surfaces.

Tab. 6.1 - Validation results for the building surfaces.

	Surface 1	**Surface 2**	**Surface 3**
MBE	-0.04°C	-0.36°C	-0.13°C
NMBE	-0.11%	-1.13%	-0.41%
RMSE	0.63°C	0.75°C	0.84°C
CV(RMSE)	1.93%	2.15%	2.65%
R^2	98.78%	96.41%	97.31%

6.3.4 PV system

The photovoltaic generation has been studied on a sub-hourly base (10 minute time-step) using the model "Equivalent One-Diode" (DoE, 2010) described in the previous chapter. In the following summarizing graphs and tables both the simulated and monitored power production in W of a single photovoltaic module (240 W peak power) are compared. The model shows that the modeled energy production has high accuracy compared to the monitored one. In detail, the average difference between monitored and simulated data is -1.31 W. In all cases the differences are below 113.65 W, however, this is an error that occurs only once at 12:30 on 6 June, due to a difference between the monitored radiation and the radiation of the created climatic file. On the other hand, in 95% of the data the absolute error is below 18.36 W while for 75% of the calibration data it is below 8.22 W (Fig. 6.11).

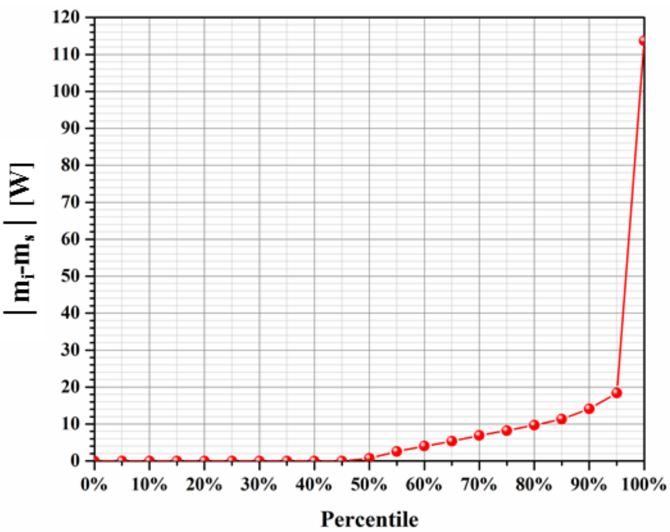

Fig. 6.11 - Validation results for the PV system.

The following graphs (Fig. 6.12) show the monitored power production (green line) and the simulated one (red line) for 20 days (28 May - 16 June 2018) of the monitoring period (24 May – 27 July 2018).

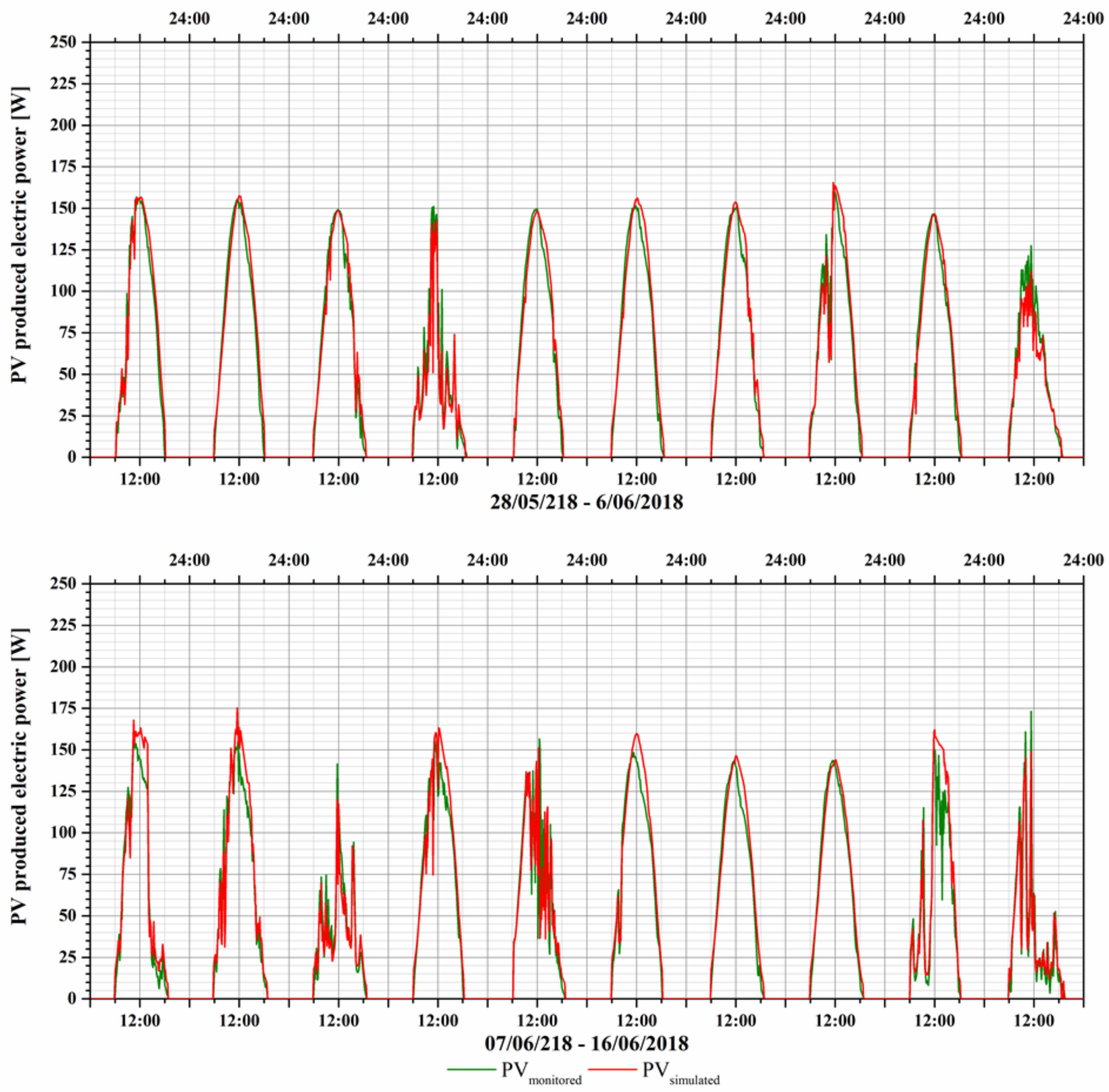

Fig. 6.12 - Comparison of the monitored and simulated energy produced [W] (28 May - 16 June 2018).

Tab. 6.2 shows the MBE, the NMBE, the RMSE and CV(RMSE). In detail, the PV model is characterized by the NMBE equal to -3.22%, while the RMSE is equal to 9.29 W.

Tab. 6.2 – Validation results of the PV system.

MBE	-1.31 W
NMBE	-3.22%
RMSE	9.29 W
CV(RMSE)	22.73%
R^2	97.02%

Although the CV (RMSE) is equal to 22.73%, during the entire monitoring period, as shown in Fig. 6.13, the difference between the monitored energy produced by a photovoltaic module (58.85 kWh) and the simulated one (60.74 kWh) is only 1.89 kWh (percentage variation equal to 3.22%).

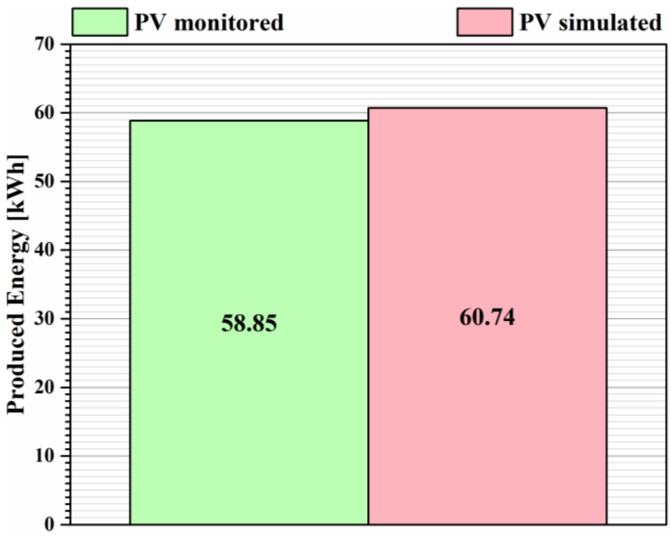

Fig. 6.13 - Comparison of the monitored and simulated energy produced [kWh] during the all building monitoring period.

6.4 CHAPTER CONCLUSIONS

Simulations of the case study building were carried out using real weather data. The data generated from these simulations was compared to that measured from the real building for the same time period and an assessment was made as to whether this building model was sufficiently representative of their real version in order to be able to generate reliable results for the purposes of the research presented here. The assessment of thermal behavior of the building models was performed according to five metrics, including the normalised mean bias error (NMBE) and the coefficient of variation of the root mean square error, CV(RMSE). These results are summarised in Tab. 6.3 and in Fig. 6.14, the root mean square error (RMSE) of the simulated indoor temperature is less of 0.84°C for all the data, while the coefficient of variation of the root mean square error (CV(RMSE)) is less than 2.65%.

Tab. 6.3 – Temperature validation results summary.

	Tair Zone 1	Tair Zone 2	Tsurface1	Tsurface2	Tsurface3
MBE	-0.15°C	-0.02°C	-0.04°C	-0.36°C	-0.13°C
NMBE	-0.45%	-0.08%	-0.11%	-1.13%	-0.41%
RMSE	0.31°C	0.32°C	0.63°C	0.75°C	0.84°C
CV(RMSE)	0.96%	1.02%	1.93%	2.15%	2.65%
R^2	99.68%	99.18%	98.78%	96.41%	97.31%

The summary of the validation results of air temperatures and surface temperatures are presented in Fig. 6.14. For each boxplot, the central mark indicates the mean value of the errors, the edges of each box represent the 25th and 75th percentiles, the segment inside the box shows the 50th percentile and the whiskers are the extreme error values. For all the data, the difference between the monitored and simulated data is between −1.86°C (Surface temperature 1) and 2.38°C (Surface temperature 2).

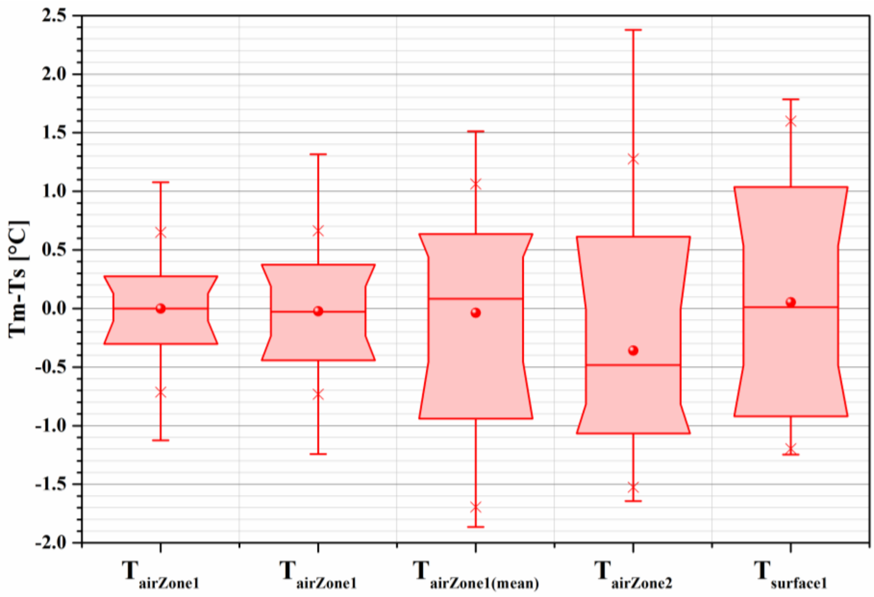

Fig. 6.14 - Temperature validation results summary.

The assessment of the energy production was performed according to the MBE (-1.31W), the NMBE (-3.22%), as well as the RMSE (9.29 W) and the CV(RMSE9 (22.73%) as described in (ASHRAE, 2014). As reported in Fig. 6.15, a good correlation is observed showing an R^2 value of 0.9702 meaning 97.02% of variance is explained by the model.

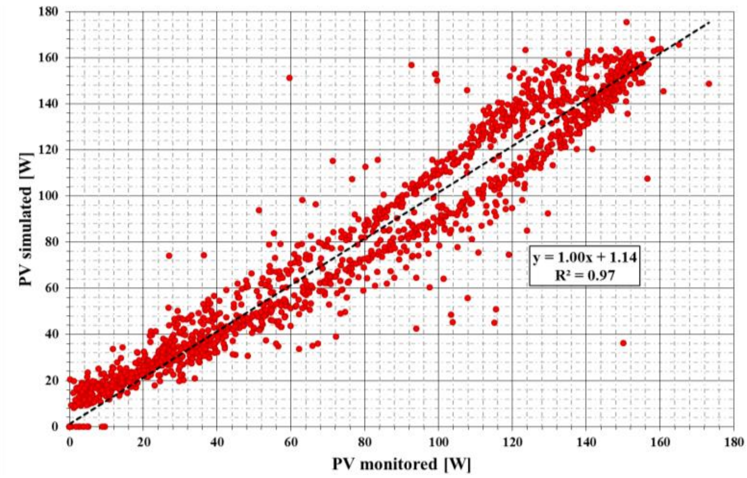

Fig. 6.15 – PV system validation results.

Finally, this chapter presented the results of the calibration process, described in the previous chapter. The case study building model appears to replicate with a good degree of approximation the behavior of the actual building. Therefore, the building model can be said to be valid for the purposes of the research conducted and it is then will be used to analyze the energy performance of the case study.

7 BUILDING ENERGY PERFORMANCES RESULTS

7.2 INTRODUCTION

This chapter investigates energy performance of the existing building case study. In the first part of the chapter, to study the answer of the dynamic model, the temperature trends in some critical days in terms temperature were analyzed. Firstly, free-floating conditions were assumed in order to investigate the natural indoor thermal performance of the spaces. Then, in order to investigate also the energy consumption for heating and cooling, the HVAC system modeled was activated with temperature reference set points in summer and winter.

In the second part, monthly and yearly energy consumption and generation were analyzed. Two different energy balances were calculated: LG Balance and Weighted Balance. The LG Balance is calculated as "load generation" balances, where no weighting factors are used and the result is simply calculated as the difference between generation and load. Instead, the Weighted Balance, focused on primary energy consumption, allows to take into account all inefficiencies occurring in the final energy generation process

Finally, to quantify the load-matching levels and Grid Interaction for the case study, quantitative indices, selected in the chapter 5, were presented. In detail, load cover factor (γ_{load}), representing the percentage of the electrical demand covered by on-site electricity generation, the supply cover factor (γ_{supply}), defined as the percentage of the on-site generation that is used by the building, and the net exported energy were analysed using 3 minute time resolution. Moreover, the loss of load probability (LOLP), the no grid interaction probability ($P_{e\approx 0}$) and the grid interaction index (f_{grid}) were also investigated to evaluate the system reliability.

7.3 SINGLE DAY ANALYSIS

To study the answer of the dynamic model, the temperature trends in some critical days were analyzed. Four day have been chosen with particular characteristics of insulation and temperature: as the literature describes them (Athienitis & O'Brien, 2015; W. O'Brien, Kesik, & Athienitis, 2014), they are:

- Cold cloudy (27 December);
- Cold sunny (2 February);
- Warm sunny (22 August);
- Warm cloudy (14 June).

The choice of the days has been made using the hourly climate data for the city of Messina. Fig. 7.1 shows the outdoor dry-bulb temperature and the global horizontal radiation for the 4 selected days. Moreover, as it is possible to see in Tab. 7.1, the chosen days are significant for the differences or similarities to the average monthly values. The cold cloudy day (27 December) shows an average temperature lower of about 5.7 degrees than the average monthly value while the solar radiation on horizontal value is it is about 40% of the monthly one. The cold sunny day (2 February) shows a mean daily temperature (7.8 °C) lower than the monthly value (12 °C), while the solar radiation on horizontal value (274.9 W/m^2) is only a little higher if compared to the monthly value (270.9 W/m^2). The warm sunny day (22 August) shows a temperature (more than 1 degree higher than the monthly mean and a solar radiation on horizontal value (408.3 W/m^2) comparable to the monthly value (477.1 W/m^2).

Tab. 7.1 - Mean monthly and daily dry-bulb temperature and the global horizontal radiation for the 4 selected days.

	Mean Dbt [°C]	**Mean GlobHorRad** [W/m²]		**Mean Dbt** [°C]	**Mean GlobHorRad** [W/m²]
Dec.	13.8	179.2	27 Dec. (cold cloudy)	8.1	71.7
Feb.	12.0	270.9	2 Feb. (cold sunny)	7.8	274.9
Aug.	27.4	477.1	22 Aug. (warm sunny)	28.5	491.6
Jun.	23.2	450.2	4 Jun. (war cloudy)	23.6	287.2

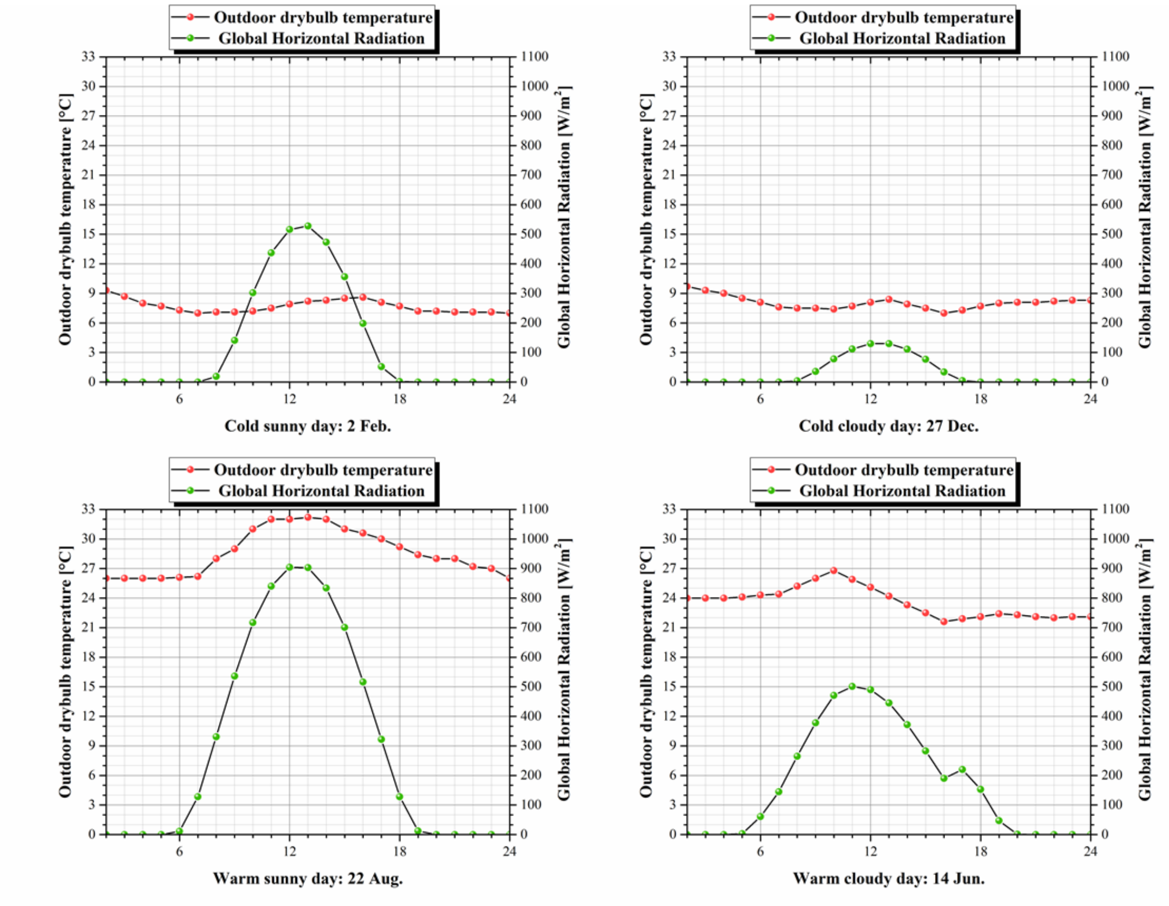

Fig. 7.1 – Dry-bulb temperature and the global horizontal radiation for the 4 selected days.

In order to study the thermal answer of the dynamic model, the Fig. 7.2, Fig. 7.3, Fig. 7.4 and Fig. 7.5 show the results for the free-floating conditions, when the HVAC plant is considered as not operating. Therefore, the simulations are run in free-floating conditions and the temperature trends in particular days were analyzed. In detail, the graphs show that under free-floating conditions, the thermal zones show relevant overheating issues during the warm (Fig. 7.3) and warm cloudy (Fig. 7.4) periods. In particular, the temperature is always higher than 26 °C for the entire period reported in these figures.

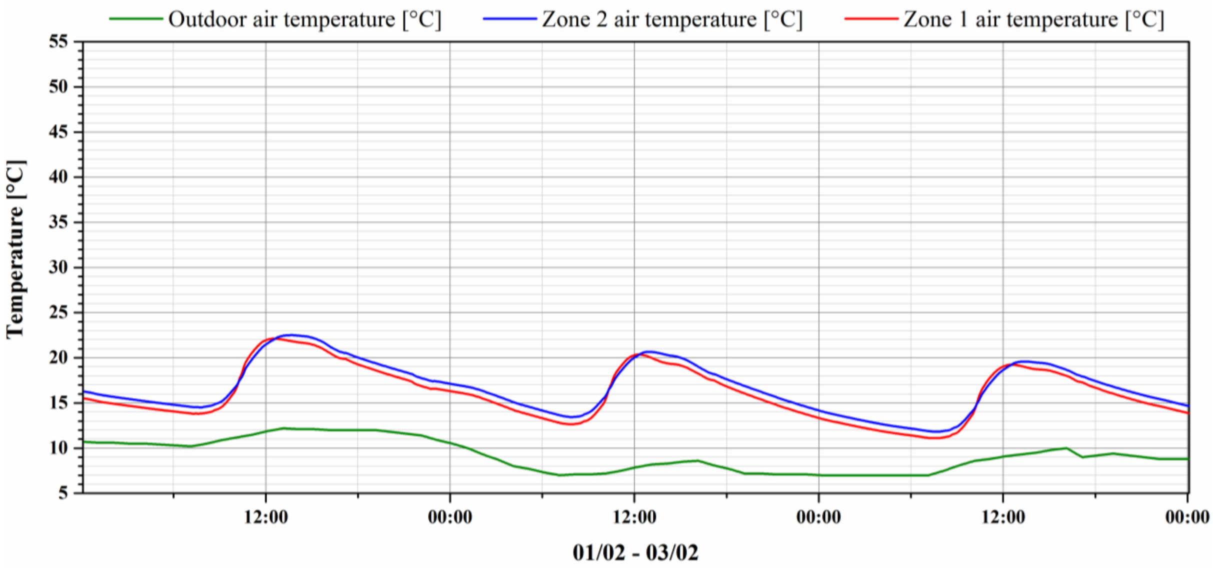

Fig. 7.2 – Free-floating outdoor dry-bulb temperature and zone air temperatures (cold sunny days).

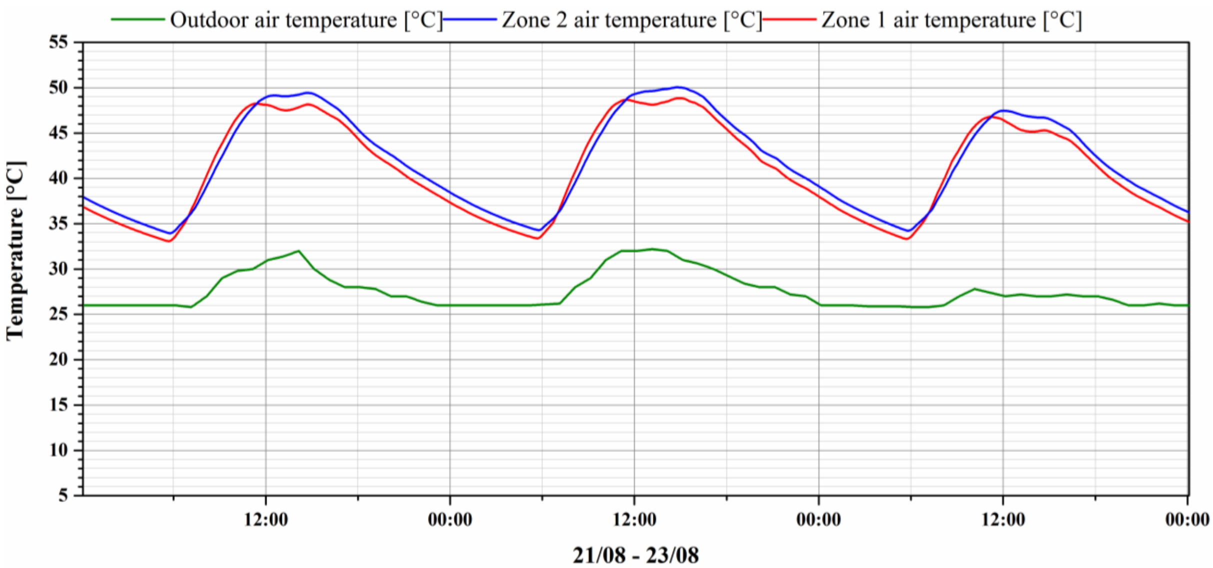

Fig. 7.3 – Free-floating outdoor dry-bulb temperature and zone air temperatures (warm sunny days).

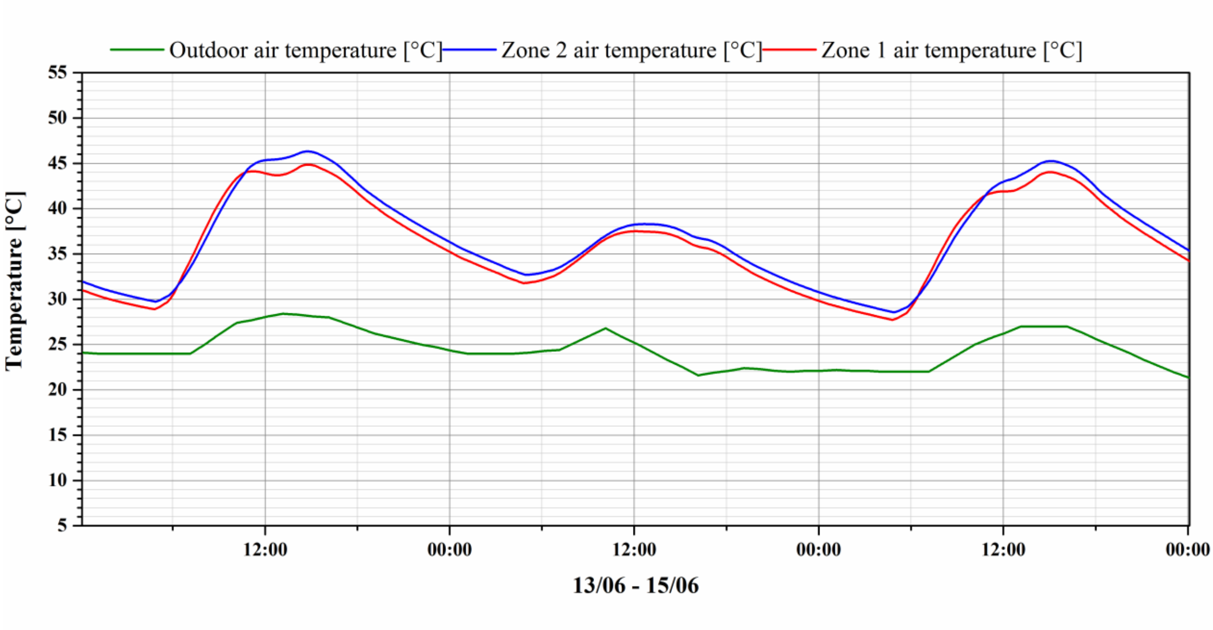

Fig. 7.4 – Free-floating outdoor dry-bulb temperature and zone air temperatures (warm cloudy days).

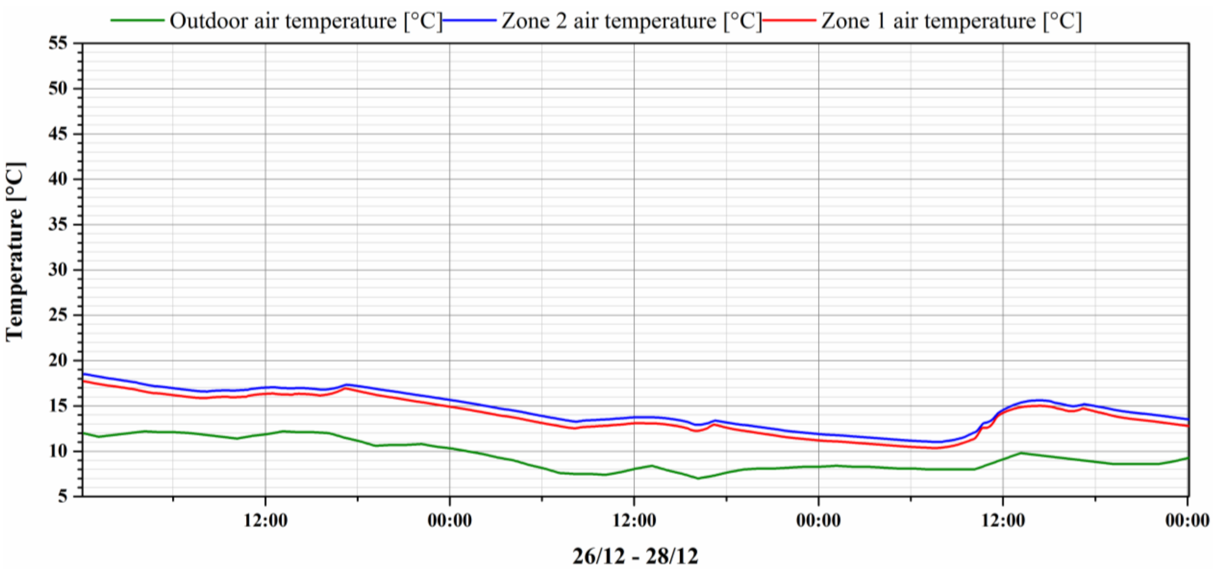

Fig. 7.5 – Free-floating outdoor dry-bulb temperature and zone air temperatures (cloudy cold days).

The following graphs (from Fig. 7.6 to Fig. 7.9) show the heat balance of the building for the selected four periods (cold cloudy (26 - 28 December), cold sunny (1 - 3 February), warm sunny (21 - 23 August) and warm cloudy (3 - 5 October)), which are chosen to represent different seasons, for the case study.

In detail, it can be observed that:

1. During the cold sunny days (from 01/02 to 03/02) the maximum heating energy demand occurs on 03/02 at 9 a.m. and it is equal to 2.95 kWh. Heating energy requirements are low due to a mild climate and large glazed facades. In particular the heating system is switched on sporadically throughout the day in this period, especially during the early hours of building occupancy.

2. During the warm sunny period (from 21/08 to 23/08) maximum cooling energy demand occurs on 21/08 at 9 a.m. and it is equal to 5.66 kWh. Solar radiation through the windows is the main contributor to the thermal load peak. The analysis revealed that the main issue that the building must face, from a thermo-physical point of view, is overheating in summer. In fact, due to the high solar radiation transmitted through the large glass façades and the lightweight envelope, during summer the air temperature can be higher than 35 °C when free-floating.

3. During the warm cloudy period (from 13/06 to 15/06), due to the lower solar radiation, the cooling energy demand is lower than those of the warm sunny period.

4. During the cold cloudy period (from 26/12 to 28/12), in order to maintain a constant zone air temperature of 20 °C, the heating system is switched on during the entire building occupation period, requiring the greatest load especially during the first hours. Finally, the maximum heating energy occurs on 18/12 at 9 a.m. and it is equal to 3.05 kWh (approximately equal to what occurs in the sunny cold period).

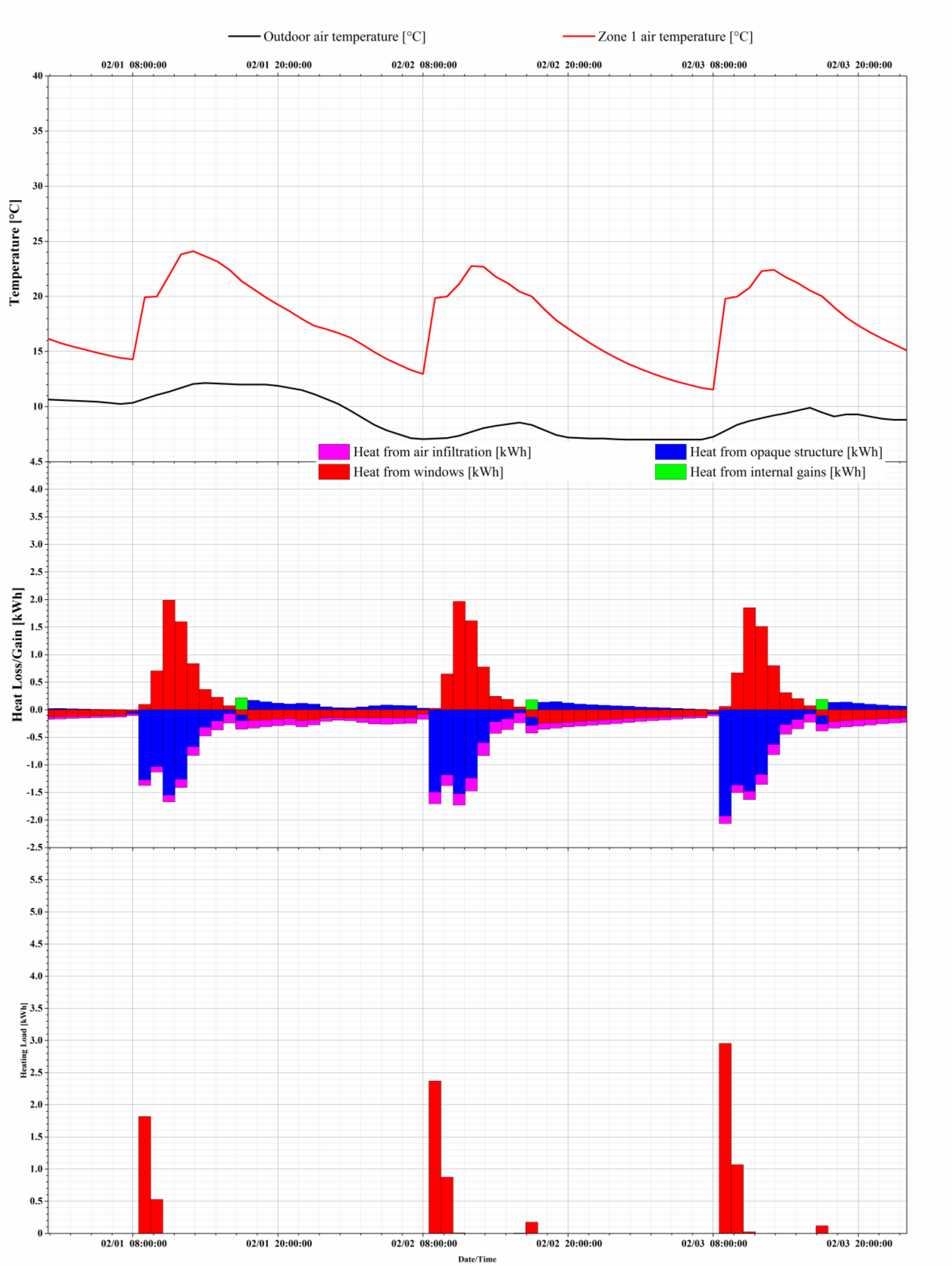

Fig. 7.6 – Heat balance for the cold sunny days (1 – 3 February).

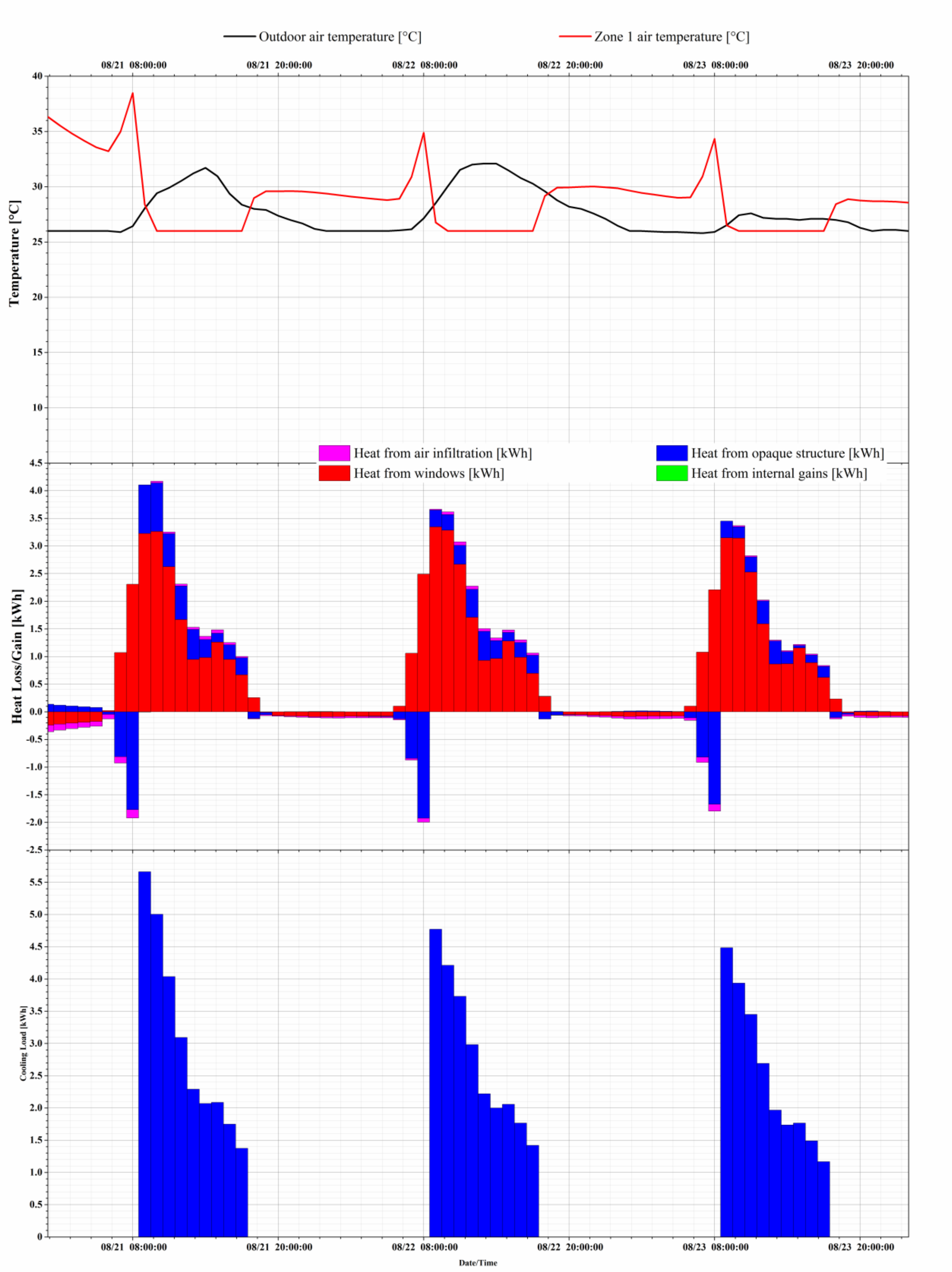

Fig. 7.7 – Heat balance for the warm sunny days (21 – 23 August).

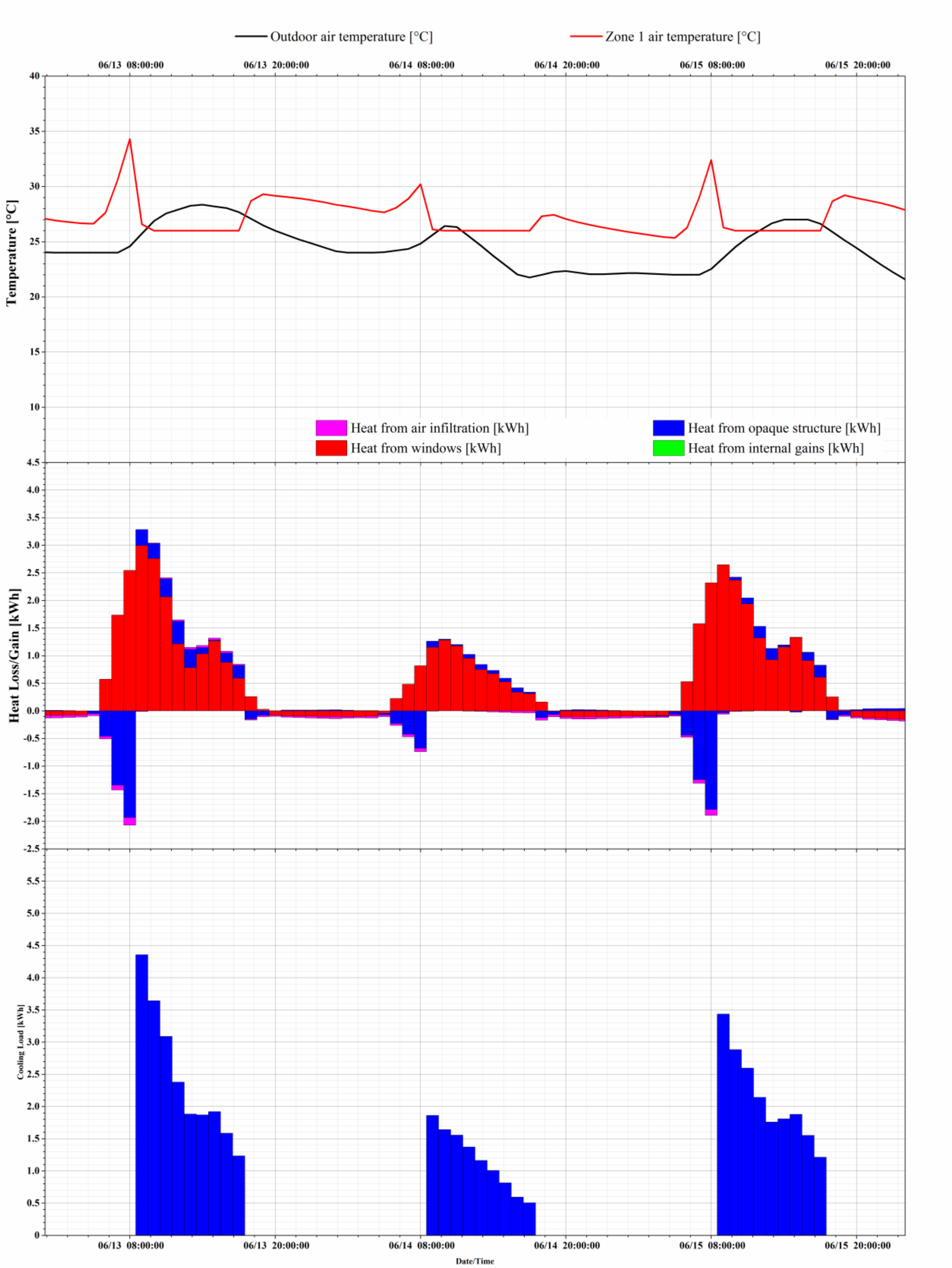

Fig. 7.8 – Heat balance for the warm cloudy days (13 – 15 June).

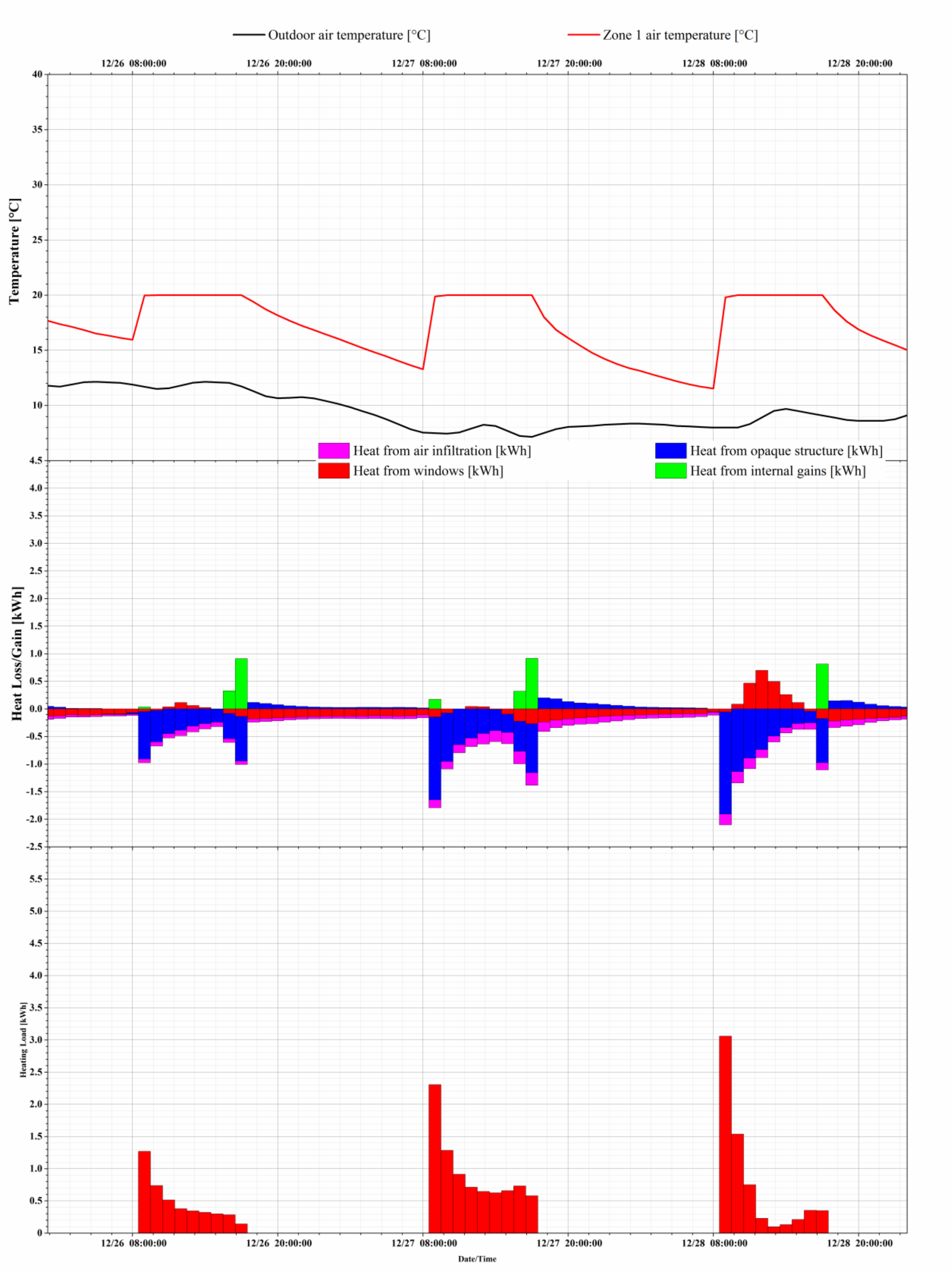

Fig. 7.9 – Heat balance for the cold cloudy days (26 -28 December).

7.4 MONTHLY AND YEARLY ANALYSIS

The results for the case study aggregated on a monthly basis for a year are reported in Fig. 7.10 and in Tab. 7.2. All annual simulations use an IWEC (International Weather for Energy Calculations) weather file for Messina (Thevenard & Brunger, 2002). This weather file was produced by ASHRAE in 2000 from the actual average weather data and therefore does not account for any extreme or unusual weather conditions that may occur. PV generation and overall estimated electricity consumption are included in the figure. The yearly electricity demand is nearly 2,700kWh$_e$ while the PV production is about 8,000 kWh$_e$.

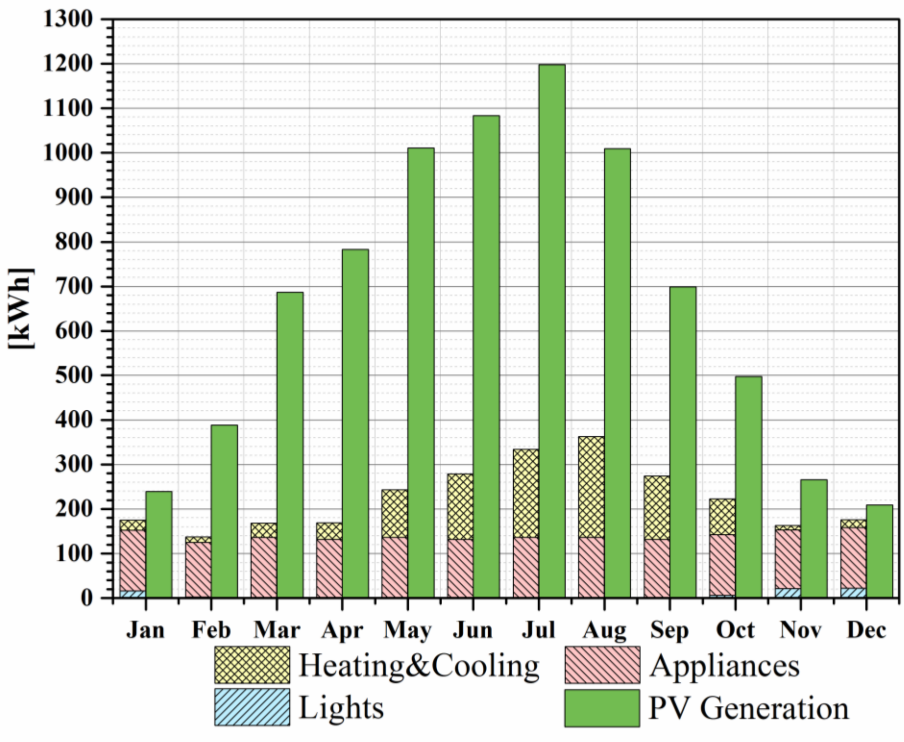

Fig. 7.10 – Electricity generation and use of the case study.

Tab. 7.2 - Electricity generation and use of the case study.

	Light [%]	Equipment [%]	Heating [%]	Cooling [%]	Tot. Load [kWhe]	Generation [kWhe]
Jan	8.84	78.33	12.84	0	173.83	239.42
Feb	1.36	89.78	7.96	0.90	136.98	388.18
Mar	0	80.87	1.17	17.96	168.35	686.99
Apr	0	77.84	0.26	21.91	169.28	782.61
May	0	56.50	0	43.49	240.97	1010.70
Jun	0	47.99	0	52.01	274.53	1083.09
Jul	0	41.34	0	58.66	329.32	1197.23
Aug	0	38.11	0	61.89	357.28	1009.03
Sep	0.04	48.82	0	51.15	269.91	698.83
Oct	2.61	61.79	0	35.58	220.34	497.26
Nov	12.42	81.65	0.81	5.13	161.38	265.75
Dec	11.92	77.77	10.31	0	175.06	208.88
Year	2.39	59.88	2.05	35.68	2677.22	8067.98

Fig. 7.11 shows the monthly energy demand for heating and cooling. The simulated energy demand show that cooling (around 28.85 kWh_e/m^2) is higher than heating demand (about 1.66 kWh_e/m^2). In particular, the months that need more heating are January (0.67 kWh_e/m^2) and December (0.55 kWh_e/m^2), while the months of July and August require the highest cooling demand, respectively 9.95 kWh_e/m^2 and 10.79 kWh_e/m^2.

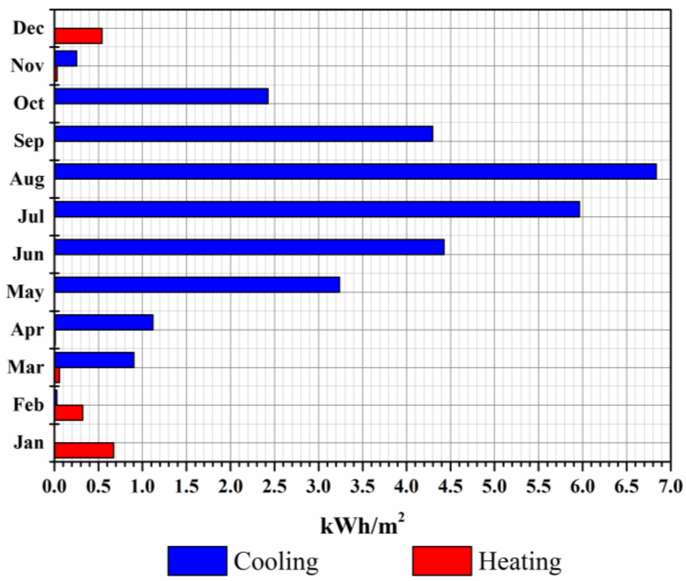

Fig. 7.11 - Monthly heating and cooling electrical energy uses.

As shown in Fig. 7.12, heating and cooling account for around 2.05% and 35.68% of the total electricity consumptions respectively, the rest being caused by lighting (2.39%) and appliances (59.68%).

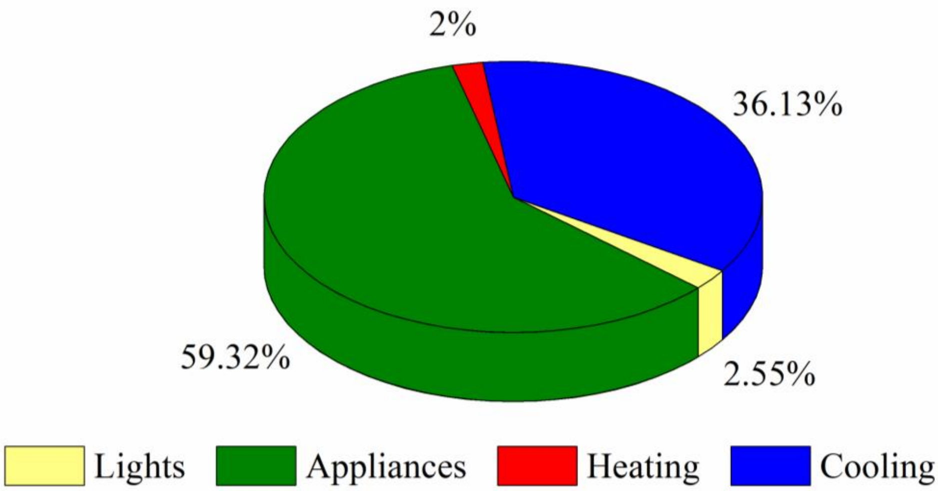

Fig. 7.12 – Yearly electrical energy uses.

Tab. 7.3 shows two different energy balances for the case study; the LG Balance and weighted balance. The LG Balance is calculated as "load generation" balances (Sartori et al., 2012), where no weighting factors are used and the result is simply calculated as the difference between generation and load. The result of the yearly LG balance is + 5390.8 kWhe. Summer months are those for which the LG Balance are highest, in particular these month are July (808.6 kWhe) and August (867.9 kWhe).

The weighted balance focuses on primary energy as in equation (7.1):

$$Weighted\ Balance = G \cdot w_g - L \cdot w_l \tag{7.1}$$

where:

- G is generated energy;
- w_g is a generation weighting factor;
- L is the load;
- w_l the weighting factor for the energy consumed.

This balance can be extended to any energy carrier transformed or generated on site and consider auto-consumption as well. The concept behind using primary energy is the use of a standardized method that is able to take into account all inefficiencies occurring in the final energy generation process.

The terms G and L are usually calculated as the sum of the whole final energy generated and consumed. W_g and W_l represent the ratio between final and primary energy: they are calculated keeping into account all the energy required to achieve 1 kWh of final energy, from the raw material acquisition until the final and usable energy carrier. Such factors are heavily influenced by the processes that occur in the supply chain and by the features of the local power generation.

In the case of conversion into primary energy, electricity from PV usually has, lower primary energy conversion factors than grid electricity (especially in countries with high dependency from conventional resources), since its generation involves only moderate transformations.

If this concepts was introduced in primary energy conversion factors, the hypothesis of using $w_g = 1$ and $w_l = 2.5$ (European Committee for Standardization, 2008) could be performed. In this case the weighting process would cause the results of LG Balance shown in tab to become the weighted balance, thus causing the positive balance to be not achievable in all months with deficits higher than 200 kWh of primary energy.

Tab. 7.3 - Final and primary energy balances for the case study.

	Tot. Load [kWhe]	Generation [kWhe]	LG Balance [kWhe]	Weighted balance [kWh -]
Jan	173.83	239.42	65.59	-181.24
Feb	136.98	388.18	251.20	56.69
Mar	168.35	686.99	518.64	279.58
Apr	169.28	782.61	613.33	372.96
May	240.97	1010.70	769.73	427.56
Jun	274.53	1083.09	808.56	418.72
Jul	329.32	1197.23	867.92	400.28
Aug	357.28	1009.03	651.75	144.42
Sep	269.91	698.83	428.93	45.66
Oct	220.34	497.26	276.92	-35.96
Nov	161.38	265.75	104.37	-124.79
Dec	175.06	208.88	33.82	-214.77
Year	2677.22	8067.98	5390.76	1589.10

7.5 LOAD MATCH AND GRID INTERACTION ANALYSIS

For grid-connected NZEBs, the interaction of electrical energy between the building and the grid is of paramount importance and needs to be considered from the point of view of designing and maintaining grid infrastructure to cope with significant energy flows into the grid network that come with high penetrations of net zero buildings in the future. Energy storage will help to address these issues with their ability to store and discharge energy at convenient and controllable times, however load matching and grid interaction factors must still be understood. For these reasons, to quantify the load-matching levels and Grid Interaction for the case study, the indicators of the IEA Solar Heating and Cooling Task 40 Energy in Buildings and Communities Annex 52 joint program ‘Towards net zero energy solar buildings’ were used (Jaume Salom et al., 2014).

In detail, the following graphs show the electric daily profile for the selected four periods (cold sunny (Fig. 7.13), warm sunny (Fig. 7.14), warm cloudy (Fig. 7.15) and cold cloudy (Fig. 7.16)), chosen to represent different seasons, for the case study. In detail, for all periods the building energy requirements at 8 a.m. show a peak because in that moment the building is activated requiring high energy for air conditioning. Moreover, the building energy requirements in both of the winter period (the cloudy cold period (Fig. 7.16) and the sunny cold period (Fig. 7.13)) show a second peak in in the last hours of the work day, due to the lighting system, controlled by an illuminance dimmering system with a setpoint of 300 Iux activated by the presence of people inside the building. The net exported power ranges from the import of -3.05 kW (cold sunny period, 02/02) to the export of 3.89 kW (warm sunny period, 23/08). Due to the electrical loads that are always active even during the hours when the building is not occupied, the building is never acting autonomously of the grid.

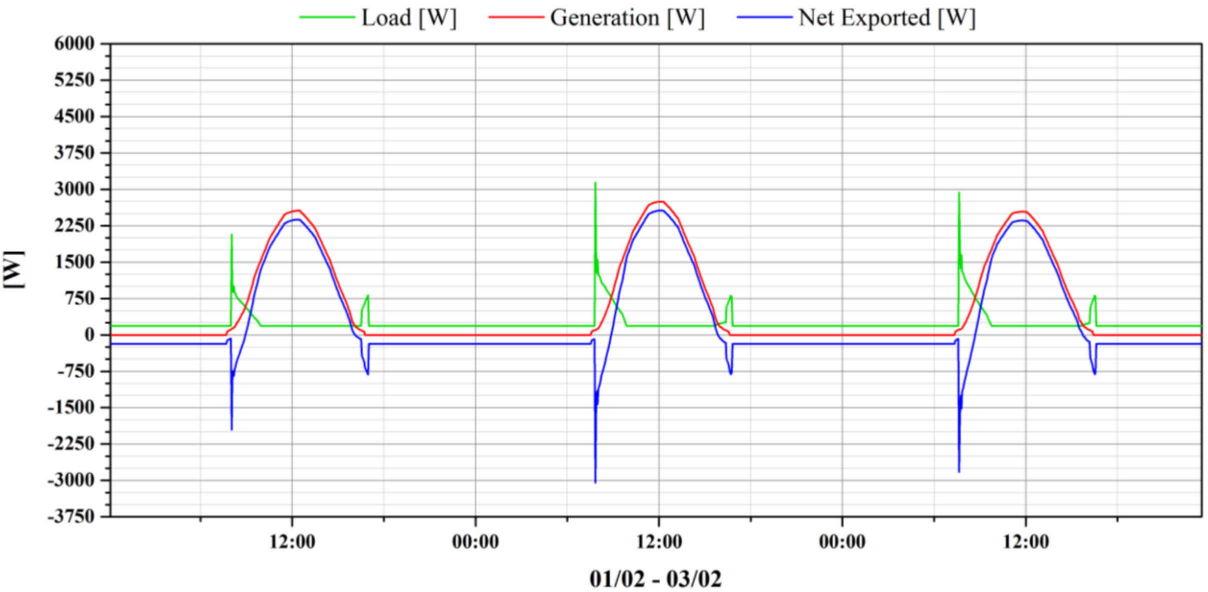

Fig. 7.13 – Electric daily profile of the cold sunny period.

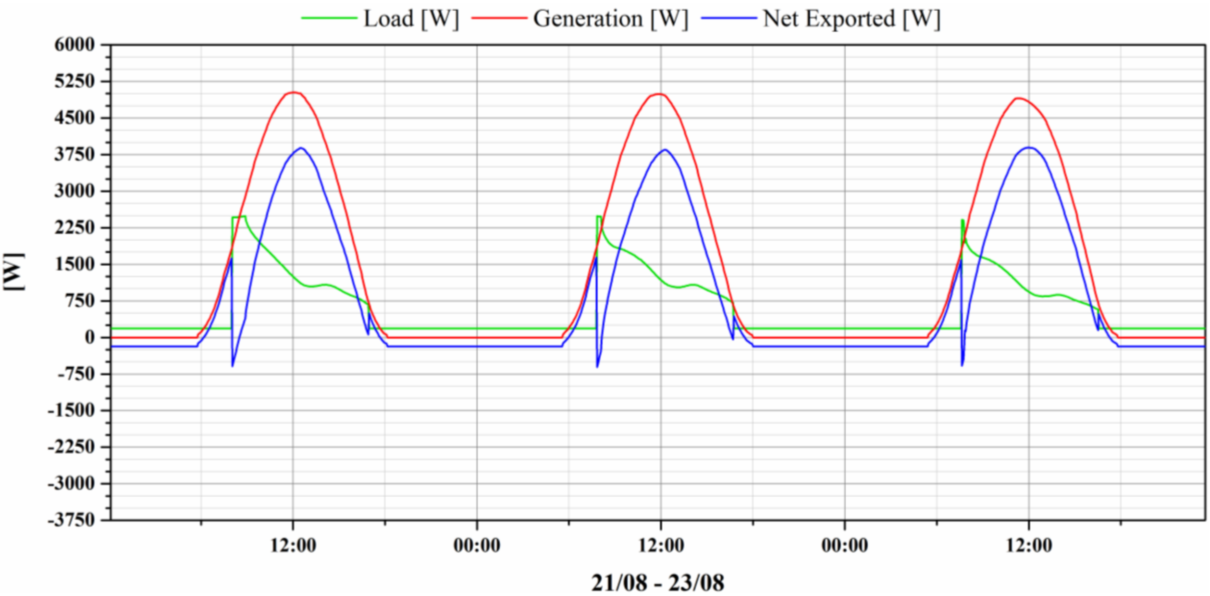

Fig. 7.14 - Electric daily profile of the warm sunny period.

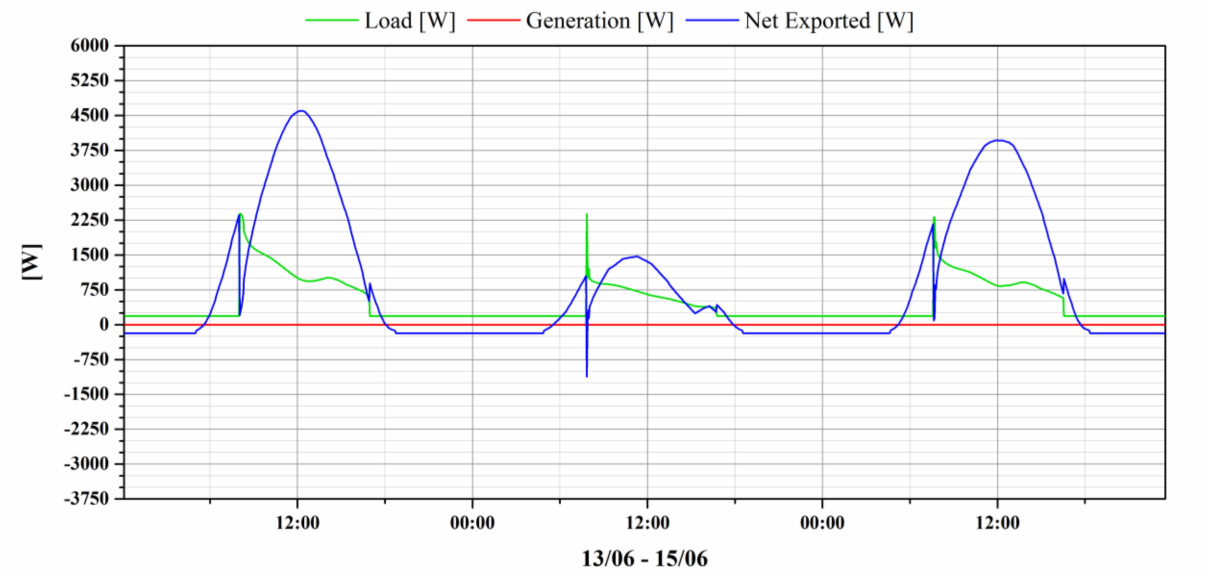

Fig. 7.15 - Electric daily profile of the warm cloudy period.

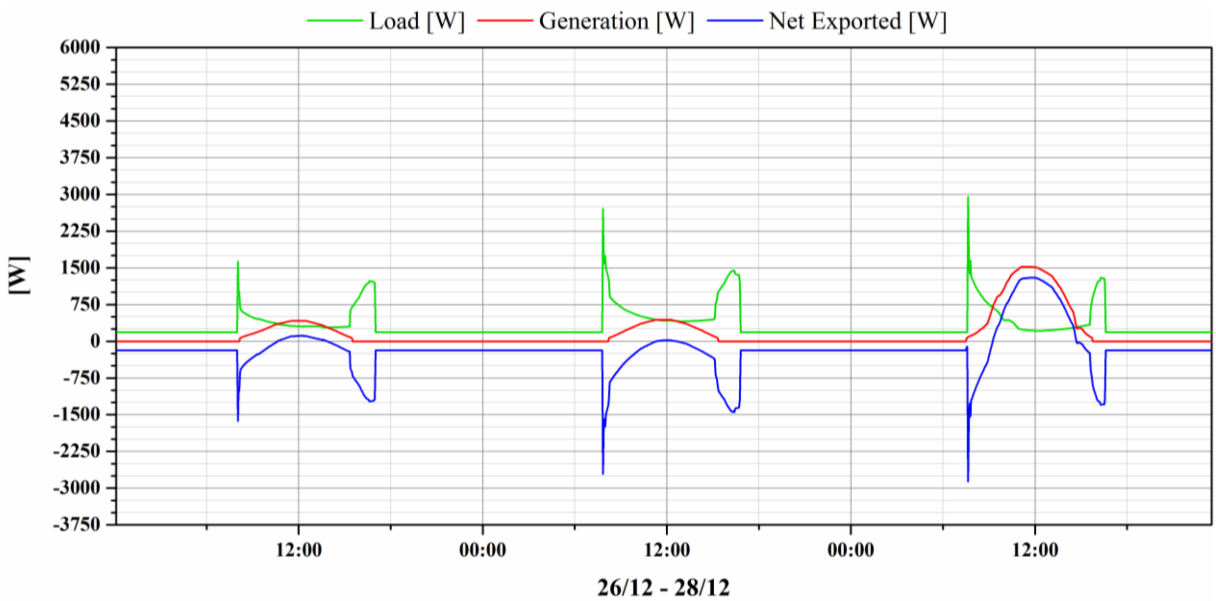

Fig. 7.16 - Electric daily profile of the cold cloudy period.

Tab. 7.4 and Fig. 7.17 show the monthly exported energy and the monthly imported energy for a year as well as the net exported energy. The months with the highest net exported energy are May (769.7 kWhe), June (808.56 kWhe) and July (867.9 kWhe). This is due to the fact that these are also the months with the largest PV production, respectively 1,010.7 kWhe, 1,083.1 kWhe and 1,197.23 kWhe.

Tab. 7.4 – Delivered, exported and net exported energy for the case study.

	Delivered energy [kWhe]	Exported energy [kWhe]	Net exported energy [kWhe]
Jan	120.78	186.37	65.59
Feb	83.41	334.62	251.20
Mar	76.87	595.51	518.64
Apr	67.09	680.43	613.33
May	65.04	834.77	769.73
Jun	59.27	867.83	808.56
Jul	63.49	931.41	867.92
Aug	69.70	721.45	651.75
Sep	74.21	503.13	428.93
Oct	88.48	365.40	276.92
Nov	107.01	211.38	104.37
Dec	126.03	159.85	33.82
Year	1001.38	6392.14	5390.76

However, due to a limited load-matching between generation and load, the energy exported is highest. In particular, in February, March and April the exported energy amounted respectively to 86% of the produced energy.

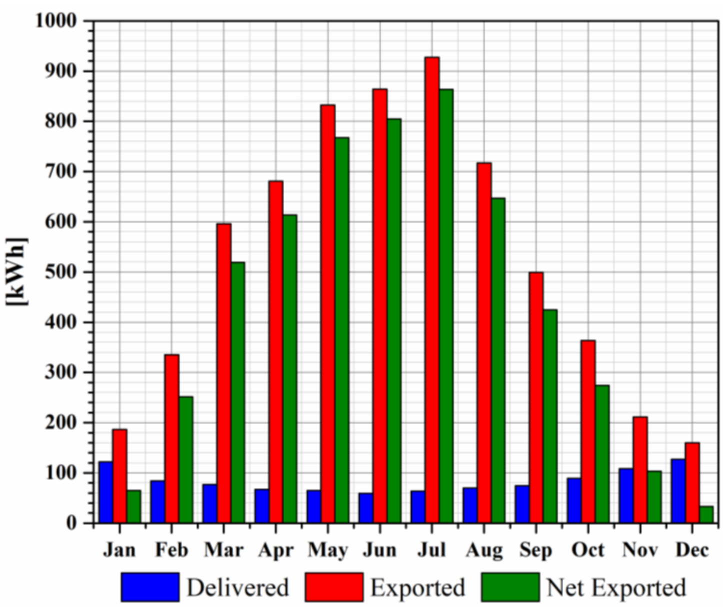

Fig. 7.17 - Delivered, exported and net exported energy for the case study.

Fig. 7.18 shows the yearly instantaneous net exported power. Representation of net exported power in coloured contour graphs gives significant information of when during the whole year the building is exporting or importing energy, depending of the type of building, the generation system and its management system. X-axis in the graph represents the hours of the day (1-24) and the y-axis are the days of the year (1-365). The levels of colours in the graph represent the amount of power imported from the grid (negative values) and exported electricity (positive values).

As shown Fig. 7.18, the case study is a typical case of individual building equipped with PV in a cooling dominated climate, where it clearly can be appreciated that exporting electricity is happening more in summer and midday hours, while import occurs more in winter during the first and last hours of building.

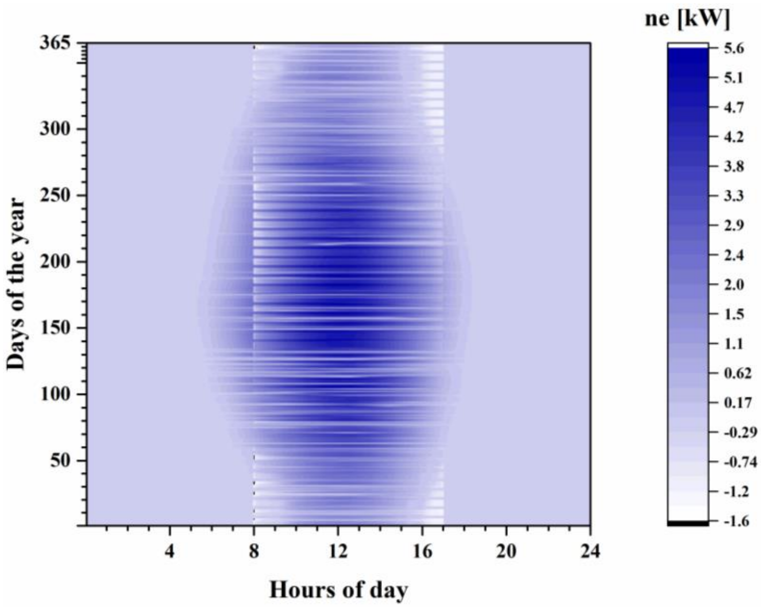

Fig. 7.18 - Instantaneous net exported power for the whole year.

Fig. 7.19 shows the load duration curve for the generation, load and next exported power for the case study. This graphical representation allows to identify the peak values of the net exported energy together with the profile of the grid interaction during the whole year knowing the percentage of time when the building is exporting or importing energy. In detail, during the whole year the delivered and exported power peaks are equal to 3.1 kW and 5.6 kW, respectively. Moreover, for about 40% of the time the building feeds energy to the electricity grid, while for the remaining time it draw energy from the grid, which means that the building is never acting autonomously of the grid.

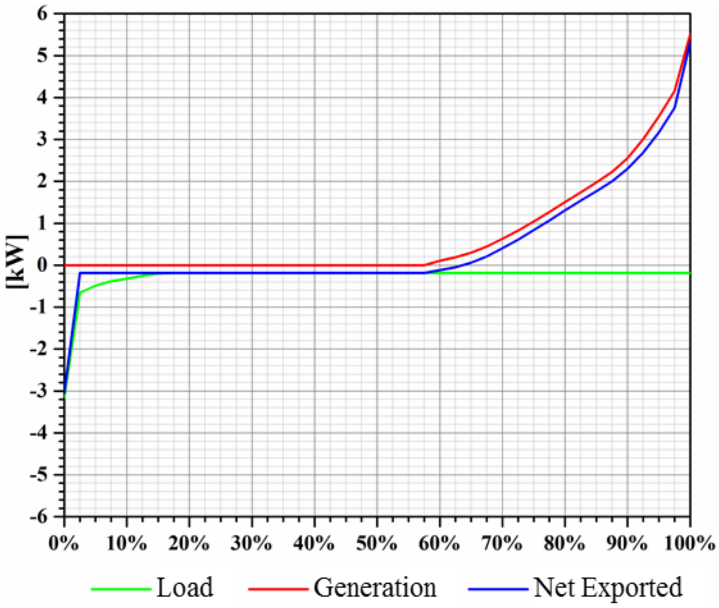

Fig. 7.19 - Duration curve for generation, load and net exported power.

Fig. 7.20 shows the box-plot of monthly net exported power for the case study. For each box, the bottom horizontal line indicates percentile 10%, then the lower quartile, the median (horizontal line), the upper quartile and the upper horizontal line represents the percentile 90%, respectively. Small box inside the each box indicates the mean value. Whiskers extending from the box represent the minimum and maximum values of the distribution.

Fig. 7.20 gives a clear picture of the magnitude of the net exported power and also the seasonal differences between months. The building exports more energy in summer months and the trends of the peak values follows a seasonal trend as the balances. Moreover, the graph help to appreciate the differences between peak values (maximum and minimum) with percentiles. In detail, differences between peak net exported power and percentile 90% is significant and also for negative values (delivered energy). For example, during the months of April and October the differences between peak net exported power and percentile 90% are equal to about 1.9 kW and 2 kW, respectively.

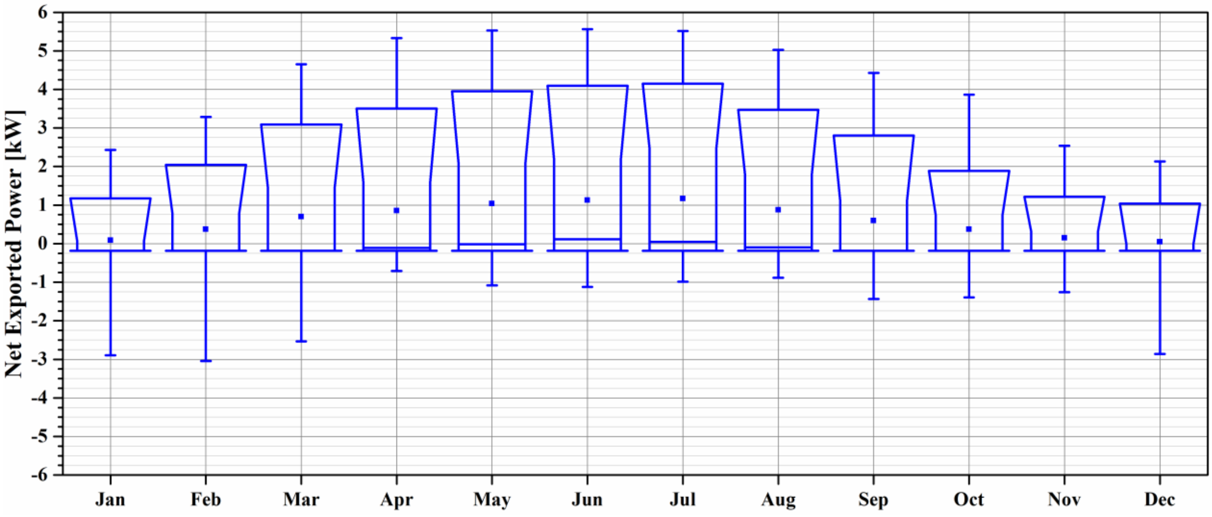

Fig. 7.20 – Box plot of the monthly net exported power.

As presented in chapter 5 the load matching indeces describe the degree of matching of on-site energy generation to local energy demand, and thus they can also indicate the building's expected interaction with the energy infrastructure, i.e. the amount of imported and exported energy. In detail, load cover factor (γ_{load}) represents the percentage of the electrical demand covered by on-site electricity generation while the complementary index, the supply cover factor (γ_{supply}), can be defined as the percentage of the on-site generation that is used by the building.

When γ_{load} index is 1, it means that the system produces more energy than the real needs of the system, while γ_{load} equal to zero indicates periods with no on-site generation. On the other hand, γ_{supply} equal to 1 means that the on site produced energy is lower than the building energy requirements, while γ_{supply} equal to zero indicates with no building energy demand. These two indicators would have the same numerical value when the balance for the energy carrier is exactly zero in the observed period, while it would differ for nearly zero or plus balances.

Mean sub-hourly values of load cover factors and of supply cover factor over 4 months (January, April, July and October), which are chosen to represent different seasons, are shown in Fig. 7.21 and in Fig. 7.22, respectively. There is a significant seasonal variation of γ_{load} and γ_{supply}. It is a result of big azimuth and altitude angle variations during the year. In consequence of it, during summer months the electricity load during the day is almost fully covered by the on-site generation, and still a significant party of the generated electricity is exported to the grid. In particular, during summer period before 8 a.m. γ_{load} equals to 1, this is because the building is not occupied and it requires very low electrical loads, thus significant part of the generated electricity is exported to the grid. Finally, at 8 a.m. γ_{load} shows a significant reduction because in that moment the the occupation of the building begins requiring high energy for air conditioning.

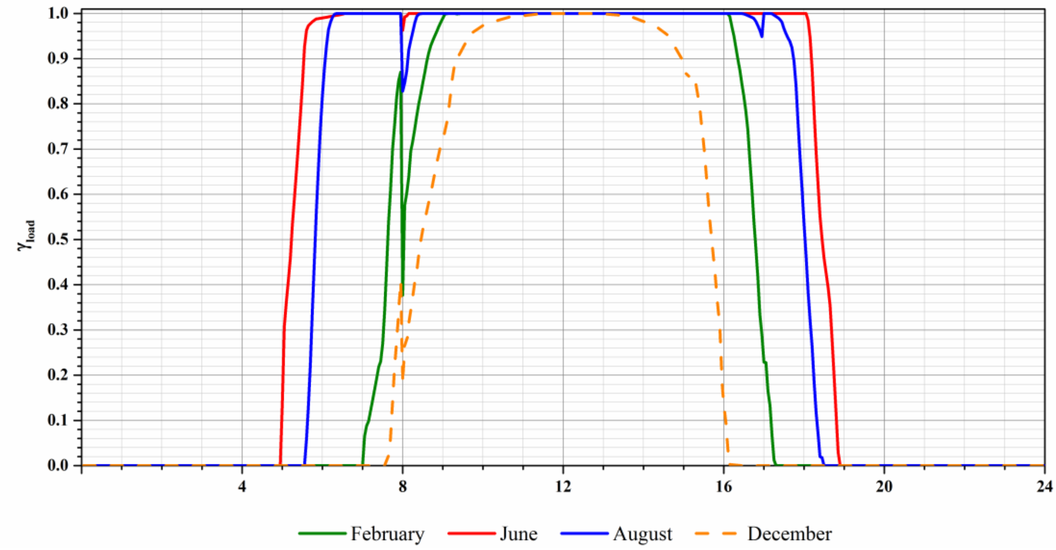

Fig. 7.21 - Daily load cover factor (γ_{load}) for selected four months.

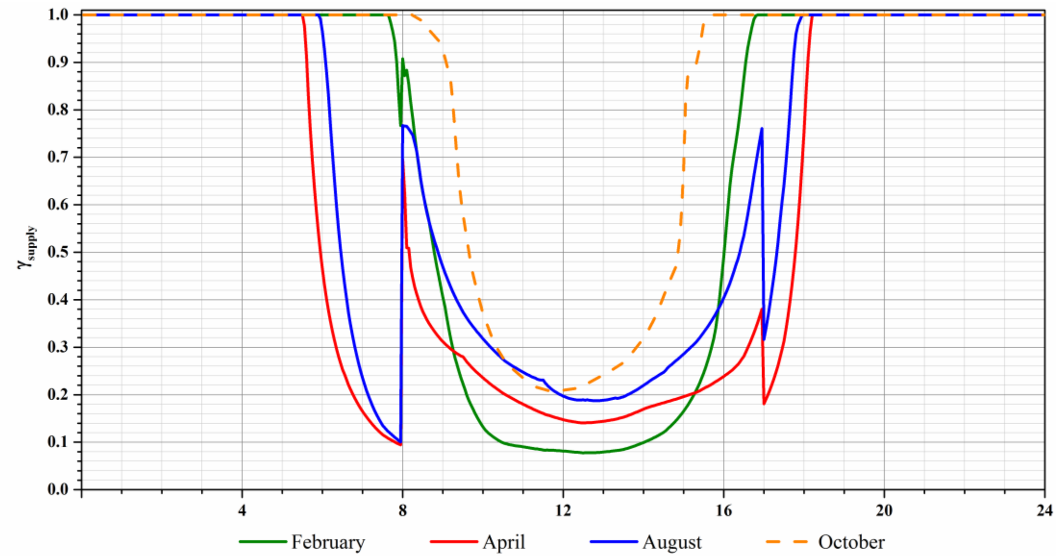

Fig. 7.22 – Daily supply cover factor (γ_{supply}) for selected four months.

The yearly graphical representations of γ_{load} (Fig. 7.23) and γ_{supply} (Fig. 7.24) give a description of the correlation between on-site energy demand and supply. In detail, as shown in Fig. 7.23, the instantaneous γload follows the on-site PV generation. It reaches 1 during the day as generation reaches its peak, decreases during low solar radiation hours while during the night it is equal to zero.

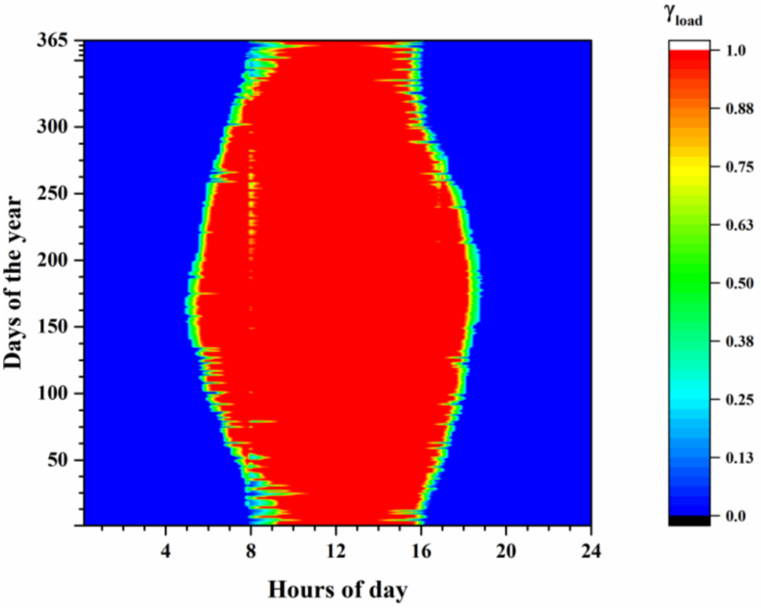

Fig. 7.23 - Instantaneous γ_{load} for the whole year.

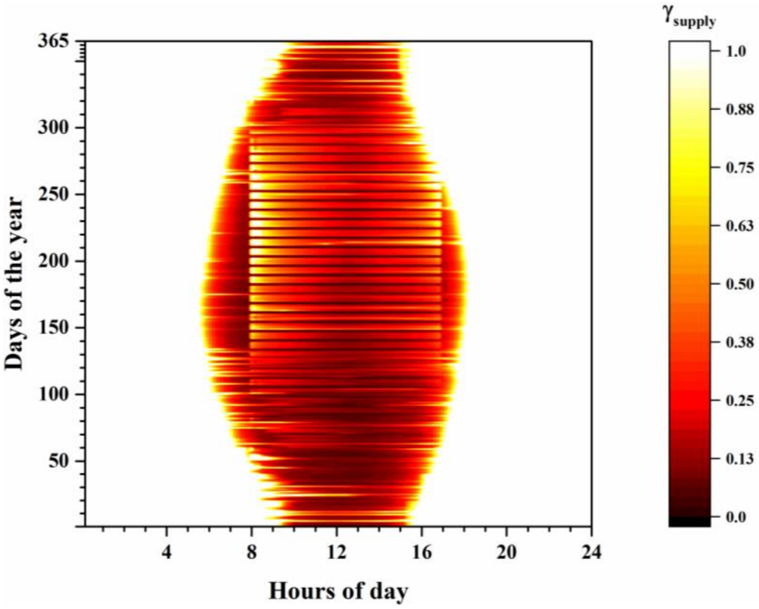

Fig. 7.24 - Instantaneous γ_{supply} for the whole year.

As shown in Tab. 7.5, the yearly mean value of γ_{load} and γ_{supply} are equal to 0.44 and 0.70, respectively. The γ_{load} monthly mean values vary from 0.29 in December to 0.55 in June, while is between 0.61 (June) and 0.83 (December).

Tab. 7.5 - Monthly values of γ_{load} and γ_{supply}.

	γ_{load}	γ_{supply}
Jan	0.31	0.81
Feb	0.37	0.73
Mar	0.44	0.67
Apr	0.49	0.63
May	0.52	0.62
Jun	0.55	0.61
Jul	0.54	0.63
Aug	0.51	0.68
Sep	0.46	0.72
Oct	0.40	0.74
Nov	0.34	0.77
Dec	0.29	0.83
Year	0.44	0.70

Finally, the loss of load probability (LOLP), the no grid interaction probability ($P_{e\approx0}$) and the grid interaction index (f_{grid}) are shown in Tab. 7.6. To quantify the behavior of power generation from PV with respect to the load consumption, LOLP is an important parameter to use, because it shows how often during a given period the on-site supply does not cover the on-site load, and thus how often energy must be supplied by the grid. On the other hand, $PE_{\approx0}$ index means the probability that the building is acting autonomously of the grid. In that case, the entire load is covered by the direct use of renewable energy. Finally, the f_{grid} index indicates the variability of the exchanged energy between the building and the grid within a given period normalized on the maximum absolute value.

As shown in Tab. 7.6 for the LOLP index, even if the yearly PV generation is much greater than the building energy requirements, yearly around 60% of time the load is not covered by on-site generation and thus the electricity must be delivered for the grid. However, this index does not provide any information about the amount of delivered electricity. In particular, during January and December, when energy production is lower than in the summer months, for more than 70% of the time the building must import energy from the grid. As depicted for the $P_{e\approx0}$ index, the yearly probability that the building is acting autonomously of the grid is about 1%, while at monthly level it is between 1.7% (December) and 0.8% (July). However, this index does not provide any information on the type of interaction with the grid (imported or exported energy) and about the amount of electricity exchanged with the grid. Finally, the yearly f_{grid} index is equal to about 23.7%, while at monthly level it is always less than 31.6% (July).

Tab. 7.6 - Monthly values of LOLP, $Pe_{\approx 0}$ and f_{grid}.

	LOLP	$P_{e\approx0}$	f_{grid}
Jan	73.33%	1.08%	21.66%
Feb	65.91%	0.93%	28.28%
Mar	58.31%	0.89%	28.18%
Apr	53.42%	0.99%	28.09%
May	50.27%	0.87%	29.86%
Jun	47.83%	0.87%	30.45%
Jul	49.11%	0.78%	31.60%
Aug	52.80%	1.03%	29.46%
Sep	58.13%	1.02%	26.78%
Oct	62.73%	0.90%	23.64%
Nov	69.06%	1.04%	25.63%
Dec	75.67%	1.73%	20.70%
Year	59.69%	1.01%	23.73%

7.6 CHAPTER CONCLUSIONS

The analysis revealed that the main issue that the building must face, from a thermo-physical point of view, is overheating in summer. In fact, due to the high solar radiation transmitted through the large glass façades and the lightweight envelope, during summer the air temperature can be higher than 35 °C when free-floating.

The yearly electricity demand is about 2,677kWhe. A mild climate, moderate insulation and large glazed facades allow for heating to be low in comparison to cooling that is the main challenge the building must face. In detail, cooling and heating account for around 35.68% and 2.05% of the total electricity consumptions respectively, the rest of the share being caused by lighting (2.39%) and appliances (59.68%).

The result of the yearly LG balance (where no weighting factors are used) is + 5390.8 kWhe. Summer months are those for which the LG Balance are highest, in particular these month are July (808.6 kWhe) and August (867.9 kWhe). On the other hand, in the case the weighted balance the positive balance is not achievable in all months with deficits higher than 200 kWh of primary energy.

The yearly PV production is about 8000 kWhe. However, due to a limited load-matching between generation and load, the energy exported is highest. In detail, during the whole year the delivered and exported power peaks are equal to 3.1 kW and 5.6 kW, respectively. Moreover, for about 40% of the time the building feeds energy to the electricity grid, while for the remaining time it draw energy from the grid, which means that the building is never acting autonomously of the grid.

8 LIFE CYCLE ASSESSMENT RESULTS

8.2 INTRODUCTION

This chapter presents the LCA results. The first section shows the results for the entire building life cycle. Moreover, according to the European Standard UNI EN 15978 (UNI, 2011b) and in order to achieve the goals set in goal and scope definition stage, more details are shown for each life cycle stage. In detail, section 8.4 shows the energy and environmental impacts produced during the materials production stage (Modules A1 - A3). The energy and environmental impacts due to transports of materials and components to the building site (Module A4) and due to building construction are shown in sections 8.5 and 8.6, respectively. Section 8.7 shows the energy and environmental impacts produced during the use stage (Modules B1 - B6). The impacts due to building end-of-life (Modules C1 - C4) and the benefits and loads beyond the system boundaries (Module D) are shown in sections 8.8 and 8.9, respectively. Finally, in order to compare the primary energy use and environmental impacts due to the entire building life cycle to the primary energy use and environmental impacts potentially avoided thanks to the renewable energy produced during the use stage, energy and environmental payback times (PBTs), for each impact category analysed in the LCIA stage, are shown in section 8.10.

8.3 LIFE CYCLE ASSESSMENT RESULTS

All the life cycle impacts investigated were assessed for the life cycle of the case study and aggregated in the different building life cycle stages (Tab. 8.1). All results are expressed in terms of unit/m^2 for one year. These results exclude the environmental benefits and loads due to the exported energy and resulting from the recycling of materials since, according to the regulation UNI EN 15978 (UNI, 2011b), they are allocated outside the system boundaries (Module D).

The total primary energy throughout the building's life cycle is 1.13 GJ/m^2year, of which 0.21 GJ/m^2year (approximately 18%) of renewable energy and 0.92 GJ/m^2year of non-renewable energy. The materials production stage (Modules A1-A3) consumes the highest amount of primary energy (56.7%) followed by the use stage (37%), while the transport (Module A4), the construction (Module A5) and the end-of-life (Modules C1-C4) require the 1.6%, the 0.1% and the 4.6% of total primary energy, respectively.

Tab. 8.1 - Life Cycle environmental impacts of the functional unit.

Indicator	**Unit**	**Material Production (A1 – A3)**	**Transport (A4)**	**Construction (A5)**	**Use (B4 – B6)**	**End-of-life (C1 – C4)**	**Total**
GWP	kg CO_{2eq}/m^2year	3.69E+01	1.08E+00	7.41E-02	1.80E+01	2.84E+00	5.89E+01
ODP	kg CFC 11_{eq}/m^2year	3.37E-05	1.67E-07	1.23E-08	2.99E-05	6.28E-07	6.44E-05
AP	kg SO_{2eq}/m^2year	1.64E-01	5.93E-03	4.61E-04	8.76E-02	1.48E-02	2.73E-01
EP	kg $PO_4{}^{3-}{}_{eq}$/m^2year	6.29E-02	1.59E-03	4.99E-05	2.64E-02	2.33E-03	9.33E-02
POCP	kg C_2H_{4eq}/m^2year	8.42E-03	1.83E-04	1.72E-05	3.80E-03	4.92E-04	1.29E-02
ADPe	kg Sb_{eq}/m^2year	1.04E-03	2.87E-06	4.69E-08	1.63E-04	2.69E-06	1.21E-03
ADP_{ff}	MJ/m^2year	4.67E+02	1.57E+01	8.75E-01	2.11E+02	3.22E+01	7.27E+02
GER	MJ/m^2year	6.38E+02	1.80E+01	1.63E+00	4.16E+02	5.15E+01	1.13E+03
GER_{no-ren}	MJ/m^2year	5.91E+02	1.78E+01	1.52E+00	2.61E+02	4.92E+01	9.21E+02
GER_{ren}	MJ/m^2year	4.67E+01	2.37E-01	1.10E-01	1.55E+02	2.34E+00	2.05E+02

The share of each life cycle impact is shown in Fig. 8.1. Among the different stages of the life cycle, the highest contribution to GHG emissions is due to the production of materials (62.6%) and the use stage (30.6%). Moreover, except for GER_{ren}, materials production stage has a predominant weight in all of the indicators. It has a contribution higher than 50% of the total of all indicators, reaching values above 86% in the case ADP_e. The end-of-life has a contribution to the impacts variable from 0.2% (ADP_e) to 5.4% (AP). A contribution lower than 2.3% is caused by the transport stage.

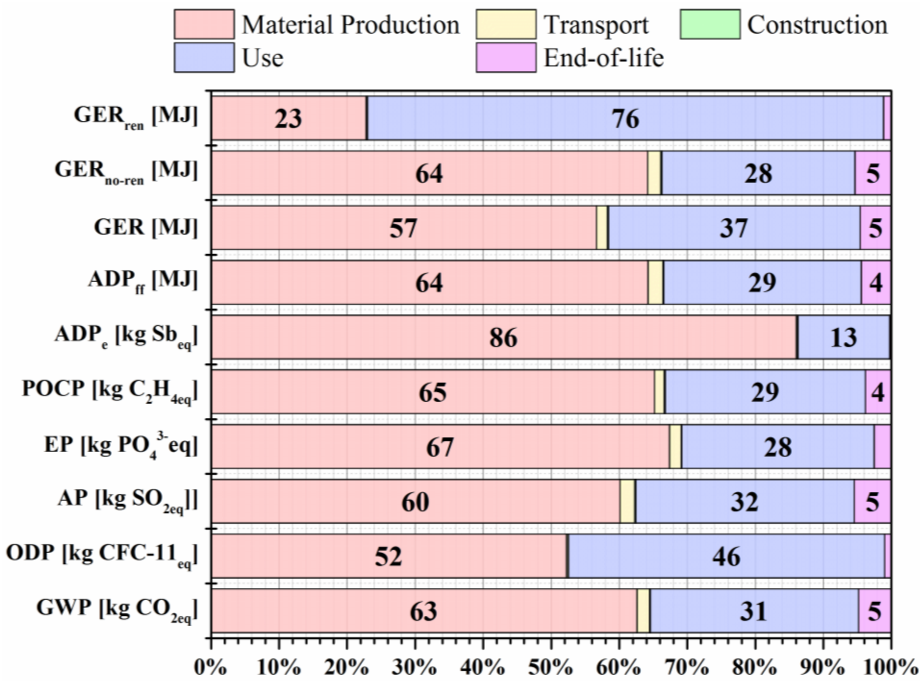

Fig. 8.1 -Share of each life cycle step on the total.

8.4 MATERIAL PRODUCTION STAGE (MODULE A1 – A3)

The boundary for material production stage (Modules A1 to A3) covers the 'cradle to gate' processes for the materials and services used in the construction. More details for this stage are given in Tab. 8.2 and in Fig. 8.2. The building envelope has a predominant weight in most of the indicators, reaching values above 80% in the case of GWP (29.3 kg CO_{2eq}/m^2year), AP (13 g SO_{2eq}/m^2year), POCP (6.66 g C_2H_{4eq}/m^2year), ADP_{ff} (385 MJ/m^2year), GER (509 MJ/m^2year) and GER_{no-ren} (482 MJ/m^2year).

Tab. 8.2 – Energy and environmental impacts due to the building envelope and plants.

Indicator	Unit	Building plants	Building envelope	Total
GWP	kg CO_{2eq}/m^{2}year	7.62E+00	2.93E+01	3.69E+01
ODP	kg CFC 11_{eq}/m^{2}year	3.01E-05	3.52E-06	3.37E-05
AP	kg SO_{2eq}/m^{2}year	3.07E-02	1.33E-01	1.64E-01
EP	kg $PO_4^{3-}{}_{eq}$/m^{2}year	2.02E-02	4.27E-02	6.29E-02
POCP	kg C_2H_{4eq}/m^{2}year	1.76E-03	6.66E-03	8.42E-03
ADPe	kg Sb_{eq}/m^{2}year	9.84E-04	5.35E-05	1.04E-03
ADP_{ff}	MJ/m^{2}year	8.20E+01	3.85E+02	4.67E+02
GER	MJ/m^{2}year	1.29E+02	5.09E+02	6.38E+02
GER_{no-ren}	MJ/m^{2}year	1.09E+02	4.82E+02	5.91E+02
GER_{ren}	MJ/m^{2}year	1.98E+01	2.69E+01	4.67E+01

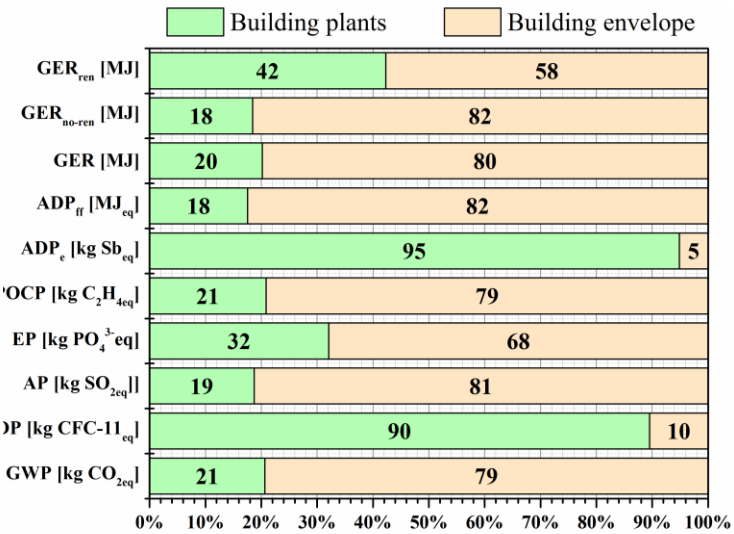

Fig. 8.2 - Share of the building envelope and the plants on the material production stage.

On the other hand, the plants are the most responsible for the impacts on the ODP (3.01E-5 kg CFC 11_{eq}/m^{2}year) and the ADPe (81.97 kg Sb_{eq}/m^{2}year), mainly caused by the thermal plant (94.5%) and the PV system (96.4%), as shown in Fig. 8.3. In particular, it is worth mentioning that by electric plant, author refer to all electrical components installed inside the building, such as lighting system or electric cables, while PV system refers to all the PV-related components, such as photovoltaic panels or inverters. From the analysis of the contribution of each element of the building envelope to the total impact, it is clear that, since the roof, the floor and the walls are made of the same materials, they contribute to each environmental indicator of a very similar impact. Finally, a contribution lower than 3% is caused by the electric plant, rainwater drainage system, windows and the foundation.

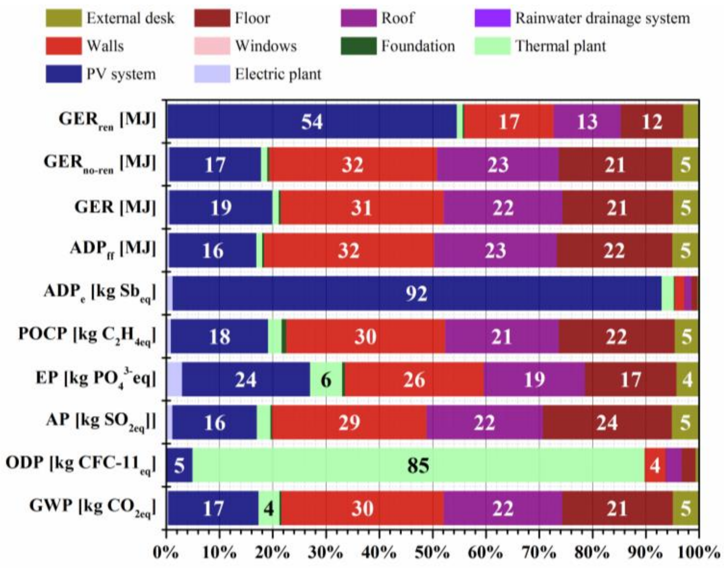

Fig. 8.3 - Share of the building systems on the material production stage.

More details for the material of the building envelope are given in Tab. 8.3. FRP material is the most impactful material but it is due to the fact that FRP is also the most used material in the building envelope (it constitutes about of 77% of the mass of the building envelope). In detail the FRP material has a predominant weight in all of the indicators, reaching values above 70% in the case of GWP (83%), AP (82%), EP (83%), POCP (77%), ADP_{ff} (82%) and ADPe (75%).

The second most impactful material is polyester fiber (the thermal insulation material and it constitutes about of 7% of the mass of the building envelope), reaching values above 17% in the case POPC. In detail, whit the exception of the POCP indicator, it has a contribution to the impacts variable from 13% (ADP_{ef}) to 2% (GER_{ren}). The Wood has a contribution to the impacts variable from 1.3% (ODP) to 48.8% (GER_{ren}), while the glass have a contribution to the impacts variable from 0.7% (GER_{ren}) to 3.2% (AP). Finally, a negligible impact is associated with all the others material (steel, rubber, polyurethane, HDPE and PVC plastics), due to the small amount of these materials in the building envelope.

Tab. 8.3 - Energy and environmental impacts due to building envelope material.

Indicator	FRP	Polyester fiber	Steel	Rubber	Polyurethane	Wood	HDPE	PVC	Glass
GWP	2.4E+1	3.6E+0	1.6E-1	7.2E-2	1.7E-2	5.5E-1	9.9E-2	1.4E-2	5.0E-1
ODP	3.1E-6	3.4E-7	7.0E-9	2.9E-9	8.6E-11	4.5E-8	3.5E-11	2.4E-11	4.5E-8
AP	1.1E-1	1.5E-2	6.3E-4	6.3E-4	6.8E-5	2.8E-3	3.2E-4	3.8E-5	4.3E-3
EP	3.5E-2	4.8E-3	3.7E-4	1.4E-4	1.5E-5	1.3E-3	2.7E-5	6.4E-6	5.4E-4
POCP	5.1E-3	1.1E-3	8.2E-5	2.2E-5	7.8E-6	1.7E-4	3.1E-5	2.2E-6	1.4E-4
ADPe	4.0E-5	6.5E-6	1.9E-6	2.5E-7	1.7E-8	3.4E-6	2.0E-9	7.5E-10	1.0E-6
ADP_{ff}	3.2E+2	5.1E+1	2.0E+0	7.4E-1	3.1E-1	7.0E+0	3.3E+0	3.1E-1	5.4E+0
GER	3.9E+2	5.3E+1	2.8E+0	9.9E-1	2.7E-1	1.4E+2	2.5E+1	4.3E-1	6.5E+0
GER_{no-ren}	3.8E+2	5.3E+1	2.6E+0	9.1E-1	2.6E-1	1.3E+2	2.4E+1	4.2E-1	6.3E+0
GER_{ren}	1.1E+1	3.8E-1	1.6E-1	8.5E-2	1.1E-2	1.2E+1	7.9E-1	6.6E-3	1.7E-1

Since the most impactful material is the FRP material more details are given in Tab. 8.4 and in Fig. 8.4 that show the impacts due to the production of a 1 kg of this material. In particular, the production of 1 kg of FRP material is responsible for the emissions of 3.8 kg of CO_{2eq}/kg and for the consumption of 64 MJ/kg of primary energy, of which 2 MJ/kg of renewable energy and 62 MJ/kg of non-renewable energy. Moreover it is responsible for the emissions of 17 g SO_{2eq}/kg and 5.5 g $PO_4^{3-}{}_{eq}$/kg.

Tab. 8.4 - Energy and environmental impacts due to the production of 1kg of FRP material.

		Reinforcing fiber	Thermosetting matrix	Catalysts	Paints	Energy	Production waste	Total
GWP	kg CO_{2eq}/kg	1.6E+0	1.4E+0	4.4E-2	7.6E-2	6.5E-1	2.0E-04	3.8E+0
ODP	kg CFC 11_{eq}/kg	1.4E-7	2.7E-7	3.9E-9	1.5E-8	5.6E-8	5.2E-11	4.9E-7
AP	kg SO_{2eq}/kg	9.6E-3	3.4E-3	2.0E-4	5.1E-4	3.2E-3	1.2E-06	1.7E-2
EP	kg $PO_4^{3-}{}_{eq}$/kg	2.7E-3	1.7E-3	1.1E-4	1.9E-4	7.7E-4	2.9E-07	5.5E-3
POCP	kg C_2H_{4eq}/kg	3.6E-4	2.6E-4	8.9E-6	2.5E-5	1.3E-4	4.2E-08	7.9E-4
ADPe	kg Sb_{eq}/kg	3.3E-06	1.5E-06	2.5E-07	2.7E-07	9.0E-07	2.9E-10	6.2E-6
ADPe	MJ/kg	2.0E+1	1.9E+1	5.9E-1	1.7E+0	8.0E+0	4.4E-03	4.9E+1
GER	kg CO_{2eq}/kg	2.8E+1	2.2E+1	7.9E-1	2.2E+0	1.1E+1	4.9E-03	6.4E+1
$GER_{non-ren}$	kg CFC 11_{eq}/kg	2.7E+1	2.2E+1	7.6E-1	2.0E+0	9.9E+0	4.9E-03	6.2E+1
GER_{ren}	kg SO_{2eq}/kg	8.8E-1	3.4E-1	2.6E-02	1.3E-1	8.9E-1	4.1E-05	2.3E+0

As shown in Fig. 8.4, the highest contribution to GHG emissions is due to the reinforcing fiber (43%) and the thermosetting matrix (37%). Moreover, except for ODP, the reinforcing fiber has a predominant weight in all of the indicators, reaching values above 50% in the case of AP (57%), EP (49%), POCP (46%) and ADPe (53%).

The second most impactful material is thermosetting matrix, reaching values above 56% in the case ODP. A contribution lower than 4% is caused by catalysts. The electric energy used during the production of FRP material has a contribution to the impacts variable from 39% (GER_{ren}) to 12% (ODP), while the paints have a contribution to the impacts variable from 2% (GWP) to 12% (GER_{ren}). Finally, a negligible impact is associated with the production waste.

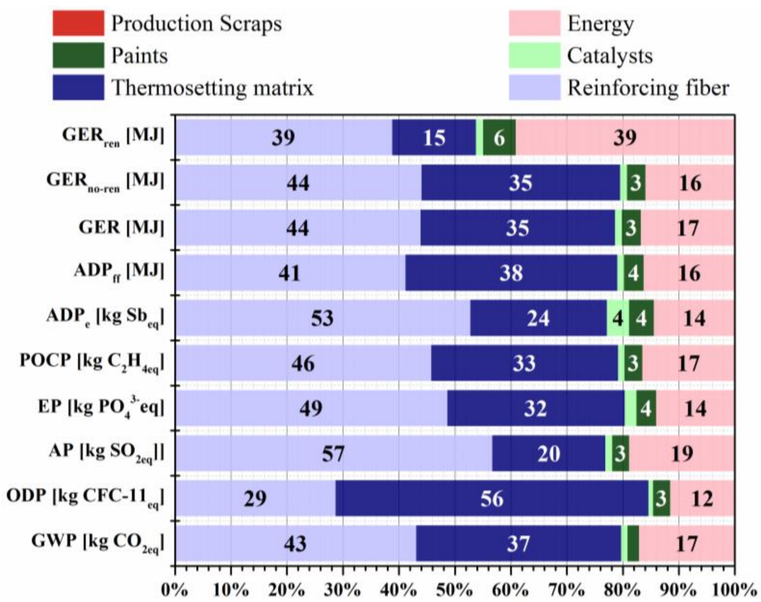

Fig. 8.4 - Share of the different materials on the production of 1kg of FRP material.

8.5 TRANSPORT STAGE (MODULE A4)

The boundary for the transport stage (Module A4) includes the transport of materials and components from the factory gate to the building site. Even if the building envelope materials are from production sites more than 1000 km far, this stage has a contribution lower than 2.3% on the building life cycle impacts.

As shown in Tab. 8.5, the GWP varies between 314 g CO_{2eq}/m^2year (walls) and 0.15 g CO_{2eq}/m^2year (rainwater system), while the GER varies between 5.86E GJ/m^2year (walls) and 2.72 MJ/m^2year (rainwater system). The same trend can be observed for all other indicators. This is due to the fact that the impacts due to the transport stage are only a function of the weight and the distances traveled. In particular, the walls are the most responsible for the impacts of the transport stage because they are also the heaviest system and the production site is distant from the construction site more than 1000 km. On the other hand, the rainwater system is the one that impacts less on the transports stage as it is the lighter system and comes from a production site near the building.

Since the plants materials are from much closer production site, the rainwater system, the electrical system, the photovoltaic system and the thermal system have a smaller contribution to the transport stage. Moreover, since the roof, the floor and the walls are made of the same materials, they contribute to each environmental indicator of a very similar impact.

Tab. 8.5 - Energy and environmental impacts due to the transport of the building envelope systems and the plants.

	Unit	**Roof**	**Floor**	**Wall**	**Window**	**External platform**
GWP	kg CO_{2eq}/m^{2}year	2.36E-01	2.15E-01	3.14E-01	1.77E-01	5.54E-02
ODP	kg CFC 11_{eq}/m^{2}year	3.64E-08	3.31E-08	4.84E-08	2.84E-08	8.54E-09
AP	kg SO_{2eq}/m^{2}year	1.33E-03	1.21E-03	1.76E-03	9.52E-04	3.11E-04
EP	kg $PO_4{}^{3-}{}_{eq}$/m^{2}year	3.54E-04	3.22E-04	4.70E-04	2.55E-04	8.30E-05
POCP	kg C_2H_{4eq}/m^{2}year	3.76E-05	3.42E-05	5.00E-05	2.95E-05	8.82E-06
ADPe	kg Sb_{eq}/m^{2}year	6.13E-07	5.57E-07	8.15E-07	5.14E-07	1.44E-07
ADP_{ff}	MJ/m^{2}year	3.43E+00	3.12E+00	4.56E+00	2.62E+00	8.05E-01
GER	MJ/m^{2}year	4.41E+03	4.01E+03	5.86E+03	3.37E+03	1.03E+03
GER_{no-ren}	MJ/m^{2}year	4.35E+03	3.96E+03	5.78E+03	3.33E+03	1.02E+03
GER_{ren}	MJ/m^{2}year	5.44E+01	4.95E+01	7.23E+01	4.26E+01	1.28E+01

	Unit	**Foundation**	**Rainwater system**	**Electrical system**	**Photovoltaic system**	**Thermal system**
GWP	kg CO_{2eq}/m^{2}year	1.03E-02	1.46E-04	1.83E-03	2.47E-02	4.49E-02
ODP	kg CFC 11_{eq}/m^{2}year	1.58E-09	2.25E-11	2.59E-10	3.86E-09	6.36E-09
AP	kg SO_{2eq}/m^{2}year	5.77E-05	8.15E-07	6.93E-06	1.29E-04	1.70E-04
EP	kg $PO_4{}^{3-}{}_{eq}$/m^{2}year	1.54E-05	2.17E-07	2.32E-06	3.51E-05	5.70E-05
POCP	kg C_2H_{4eq}/m^{2}year	1.63E-06	2.32E-08	6.82E-07	4.06E-06	1.67E-05
ADPe	kg Sb_{eq}/m^{2}year	2.66E-08	3.82E-10	4.64E-09	8.25E-08	1.14E-07
ADP_{ff}	MJ/m^{2}year	1.49E-01	2.12E-03	2.53E-02	3.57E-01	6.21E-01
GER	MJ/m^{2}year	1.92E+02	2.72E+00	3.57E+01	4.81E+02	8.76E+02
GER_{no-ren}	MJ/m^{2}year	1.89E+02	2.69E+00	3.48E+01	4.72E+02	8.53E+02
GER_{ren}	MJ/m^{2}year	2.36E+00	3.36E-02	9.11E-01	9.30E+00	2.24E+01

8.6 CONSTRUCTION STAGE (MODULE A5)

The energy and environmental impacts produced during the construction stage (Module A5) are due only to the electricity needed to power machinery and tools (during the construction of the building it was recorded an energy consumption of 150 MJ) and due to the disposal of waste and site scraps produced during the construction process. For these reasons, this stage give a marginal contribution to the total impacts (less than 0.5% in all indicators). As shown in Tab. 8.6, the disposal of waste and the site scraps, with the exception of the ADP_e and the EP, has a predominant weight in all of the indicators, reaching values above 75% in the case ODP (83%), AP (74%), GER (76%) and GERnn-ren (76%).

Tab. 8.6 - Energy and environmental impacts due to the energy consumption use during the building consumption and the site scraps.

Indicator	Unit	Energy consumption	Waste and site scraps	Total
GWP	kg CO_{2eq}/m^2year	2.38E-02	5.04E-02	7.41E-02
ODP	kg CFC $11_{eq}/m^2$year	2.07E-09	1.02E-08	1.23E-08
AP	kg SO_{2eq}/m^2year	1.18E-04	3.44E-04	4.61E-04
EP	kg $PO_4{}^{3-}{}_{eq}/m^2$year	2.84E-05	2.14E-05	4.99E-05
POCP	kg C_2H_{4eq}/m^2year	4.82E-06	1.24E-05	1.72E-05
ADPe	kg Sb_{eq}/m^2year	3.32E-08	1.37E-08	4.69E-08
ADP_{ff}	MJ/m^2year	2.95E-01	5.80E-01	8.75E-01
GER	MJ/m^2year	3.96E-01	1.23E+00	1.63E+00
GER_{no-ren}	MJ/m^2year	3.63E-01	1.15E+00	1.52E+00
GER_{ren}	MJ/m^2year	3.27E-02	7.75E-02	1.10E-01

8.7 USE STAGE (MODULES B4 AND B6)

This stage covers the period from the practical completion of the construction work to the point of time when the building is deconstructed/demolished. In particular, this stage includes replacement of some building components (Module B4) and the operational energy use (Module B6). According to the EN 15978 (UNI, 2011b), all impacts and aspects of the imported energy were assigned in module B6, while the net environmental benefits and/or loads of the energy exported beyond the building system boundary were reported in Module D.

Module B1 (installed products in use) that encompasses the impacts and aspects arising from the normal conditions of use of components of the building were neglected. Moreover, maintenance (Module B2), repair

(Module B3) and refurbishment (Module B5) were neglected, because the required service life for the building is the same as the estimated one for the plants and it guarantees a use of the building without any particular refurbishment or maintenance. Furthermore, since the building is not equipped with a water and sanitary supply system, the energy and materials data input due to the consumption of water during the use stage (Module B7) were also neglected.

The share of the Module B4 and the Module B6 on the use stage is shown in Tab. 8.7. The highest contribution to GHG emissions is due to the operational energy use (90%). Moreover, except for ODP and ADP_e, Module B6 has a predominant weight in all of the indicators, reaching values above 85% in the case AP (92%), POCP (87%), ADP_{ff} (96%), GER (97%), GER_{ren} (99%) and $GER_{nn\text{-}ren}$ (95%).

Tab. 8.7 - Energy and environmental impacts due to the building components replacement and the operational energy use.

Indicator	Unit	Module B4	Module B6	Total
GWP	kg CO_{2eq}/m^{2}year	1.70E+00	1.63E+01	1.80E+01
ODP	kg CFC 11_{eq}/m^{2}year	2.85E-05	1.42E-06	2.99E-05
AP	kg SO_{2eq}/m^{2}year	7.07E-03	8.06E-02	8.76E-02
EP	kg $PO_4{}^{3-}{}_{eq}$/m^{2}year	6.99E-03	1.94E-02	2.64E-02
POCP	kg C_2H_{4eq}/m^{2}year	5.02E-04	3.30E-03	3.80E-03
ADPe	kg Sb_{eq}/m^{2}year	1.40E-04	2.27E-05	1.63E-04
ADP_{ff}	MJ/m^{2}year	9.00E+00	2.01E+02	2.11E+02
GER	MJ/m^{2}year	1.30E+01	4.03E+02	4.16E+02
$GER_{no\text{-}ren}$	MJ/m^{2}year	1.29E+01	2.48E+02	2.61E+02
GER_{ren}	MJ/m^{2}year	8.23E-01	1.54E+02	1.55E+02

In detail, Module B4 include the replacement of the inverters of the photovoltaic system and the heat pump because a 15 year useful life was estimated for these components. The share of the replacement of the inverters and the heat pump on the Module B4 is shown in Fig. 8.5. The heat pump has a predominant weight in the GWP (81.8%), ODP (99.9%), AP (57.7%) and ADPff (58.3%) indicators. On the other hand, the inverters have a predominant weight in the POCP (56.9%) and ADPe (83.29%) indicators.

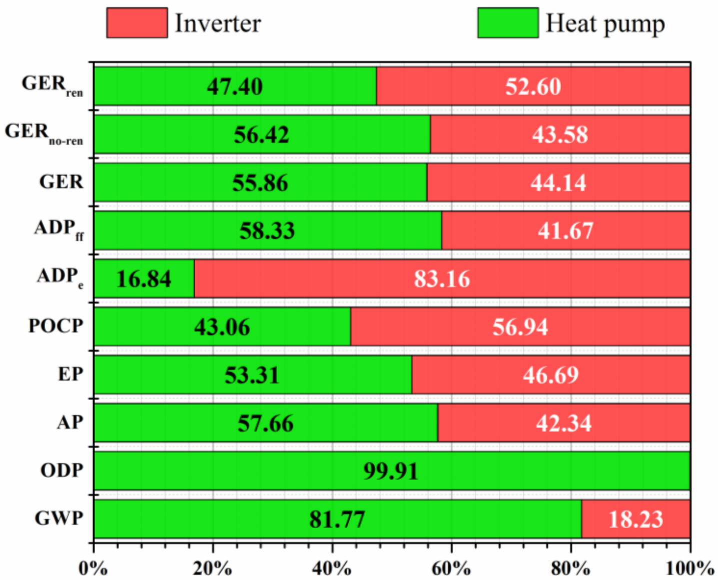

Fig. 8.5 - Share of the Module B4 and the Module B6 on the use stage.

8.8 END OF LIFE STAGE (MODULES C1-C4)

The end-of-life stage of a building starts when the building is decommissioned and is not intended to have any further use. At this point, the building's demolition/deconstruction is considered as a multi-output process that provides a source of materials, products and building elements that have to be discarded, recovered, recycled or reused. In detail, the end-of-life stage includes the following Modules:

- **C1:** deconstruction of the building (it was assumed that the same operations performed for the assembly of the housing module will occur, thus the energy consumption for the demolition was assumed equal to the construction stage (Module A5));
- **C2:** transportation of the discarded materials as part of the waste processing, e.g. to a recycling site, and transportation of waste to final disposal;
- **C3**: waste processing;
- **C4:** waste disposal.

As shown in Tab. 8.8, except for GER_{ren}, a negligible impact is associated with Module C1. The GWP varies between 1.48 kg CO_{2eq}/m^2year (Module C3) to 23.8 g CO_{2eq}/m^2year (Module C1). The EP is equal to about 2.3 g

$PO_4^{3-}{}_{eq}$/m^{2}year and it varies from about 2.8E-2 g $PO_4^{3-}{}_{eq}$/m^{2}year (Module C1) to 1.3 g $PO_4^{3-}{}_{eq}$/m^{2}year (Module C1). With regard to AP, it varies from 9.07 g SO_{2eq}/m^{2}year (Modules C3) to 0.2 g SO_{2eq}/m^{2}year (Module C1).

Tab. 8.8 - Energy and environmental impacts due to the Modules from C1 to C4.

Indicator	Unit	Module C1	Module C2	Module C3	Module C4	Total
GWP	kg CO_{2eq}/m^{2}year	2.38E-02	9.02E-01	1.48E+00	4.33E-01	2.84E+00
ODP	kg CFC 11_{eq}/m^{2}year	2.07E-09	1.40E-07	4.67E-07	1.92E-08	6.28E-07
AP	kg SO_{2eq}/m^{2}year	1.18E-04	5.03E-03	9.07E-03	6.25E-04	1.48E-02
EP	kg $PO_4^{3-}{}_{eq}$/m^{2}year	2.84E-05	1.34E-03	5.83E-04	3.80E-04	2.33E-03
POCP	kg C_2H_{4eq}/m^{2}year	4.82E-06	1.44E-04	3.20E-04	2.34E-05	4.92E-04
ADPe	kg Sb_{eq}/m^{2}year	3.32E-08	2.38E-06	7.79E-08	1.96E-07	2.69E-06
ADP_{ff}	MJ/m^{2}year	2.95E-01	1.31E+01	1.69E+01	1.78E+00	3.22E+01
GER	MJ/m^{2}year	3.96E-01	2.08E+02	1.30E+03	5.24E+03	6.74E+03
$GER_{no\text{-}ren}$	MJ/m^{2}year	3.63E-01	2.08E+02	1.30E+03	5.24E+03	6.74E+03
GER_{ren}	MJ/m^{2}year	3.27E-02	6.77E-03	1.08E-02	1.17E-03	5.14E-02

The share of the Modules from C1 to C4 on the end-of-life stage is shown in Fig. 8.6. The Module C3 has a predominant weight in the GWP (52%), ODP (74%), POCP (65%) and ADPff (53%) indicators. On the other hand, the module C2 has a predominant weight in the EP (58%), and ADPe (89%) indicators, while the Module C4 has a predominant weight in the GER (78%), and $GER_{no\text{-}ren}$ (78%) indicators.

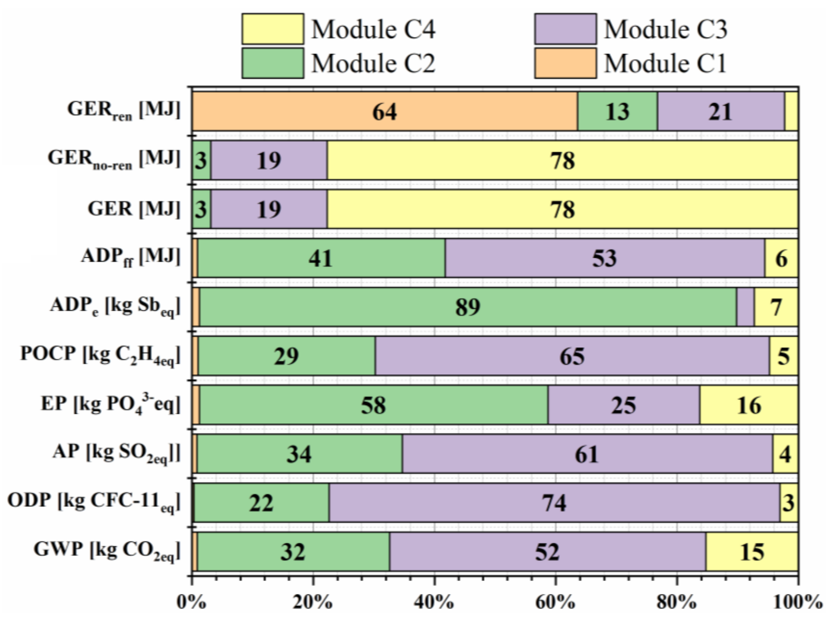

Fig. 8.6 - Share of the Modules from C1 to C4 on the end-of-life stage.

8.9 BENEFITS AND LOADS BEYOND THE SYSTEM BOUNDARY (MODULE D)

The benefits and loads beyond the system boundaries (Module D) include the environmental benefits and the loads due to the recycling of materials and the surplus energy fed into the electricity grid. In detail, Tab. 8.9 shows the benefits and loads beyond the system boundaries, moreover, it shows the environmental impacts due to the entire building life cycle both in the case where the module D is unconsidered within the system boundaries (total without Module D) and in the case where the Module D is considered in the system boundaries (total with Module D). If these benefits are included in the system boundaries, all the indicators show a significant reduction, the only exception being the GER_{ren}, which shows an increase of about 190%. This is due to the fact that this indicator takes into account the use of renewable energy, which is increased when Module D is considered within the boundaries of the systems.

In particular, these benefits, if included in the system boundaries, would allow to reduce the GWP and the GER respectively by 144.1% and 81.9%, compared to the case in which they are not included in the system boundaries. Moreover, they would allow to reduce the impacts for acidification (AP), eutrophication (EP) and photochemical ozone creation potential (POCP) of -157.88% (-0.43 kg SO_{2eq}/m^2year), 109.06% (-0.1 kg $PO_4{}^{3-}{}_{eq}/m^2$year) and 137.75% (-17.8 g C_2H_{4eq}/m^2year), respectively. However, the reduction potential of the indicators ODP and ADPe is equal only to 11.9% (-7.65E-06 kg CFC $11_{eq}/m^2$year) and -9.8% (-1.18E-04 kg Sb_{eq}/m^2year), respectively.

Therefore, except for ODP and ADPe indicators, the environmental benefits due to the recycling of materials and the surplus energy fed into the electricity grid are able to repay the primary energy use and environmental impacts produced during the entire building life cycle.

Tab. 8.9 - Benefits and loads beyond the system boundary stage.

Indicator	Unit	Total without Module D	Module D	Total with Module D
GWP	kg CO_{2eq}/m^{2}year	5.89E+01	-8.49E+01	-2.60E+01
ODP	kg CFC 11_{eq}/m^{2}year	6.44E-05	-7.65E-06	5.68E-05
AP	kg SO_{2eq}/m^{2}year	2.73E-01	-4.31E-01	-1.58E-01
EP	kg $PO_4{}^{3-}{}_{eq}$/m^{2}year	9.33E-02	-1.02E-01	-8.45E-03
POCP	kg C_2H_{4eq}/m^{2}year	1.29E-02	-1.78E-02	-4.87E-03
ADPe	kg Sb_{eq}/m^{2}year	1.21E-03	-1.18E-04	1.09E-03
ADP_{ff}	MJ/m^{2}year	7.27E+02	-1.08E+03	-3.50E+02
GER	MJ/m^{2}year	1.13E+03	-9.21E+02	2.05E+02
GER_{no-ren}	MJ/m^{2}year	9.21E+02	-1.33E+03	-4.10E+02
GER_{ren}	MJ/m^{2}year	2.05E+02	3.90E+02	5.95E+02

As shown in Fig. 8.7, the benefits beyond the system boundaries (Module D) are mainly due to the surplus energy fed into the electricity grid, with the exception of the ADP_e reduction, which is due only to the recycling of materials.

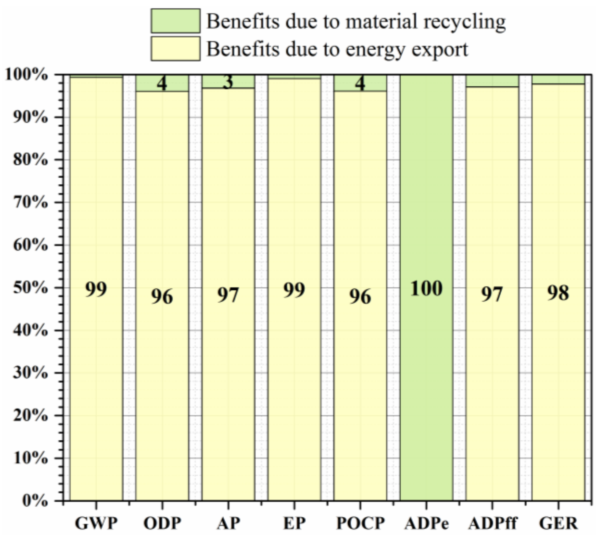

Fig. 8.7 – Benefits and loads beyond the system boundary stage due to the material recycling and energy export.

8.10 ENERGY AND ENVIRONMENTAL PAYBACK TIMES

Energy and environmental payback times has been calculated in order to compare the primary energy use and environmental impacts due to the entire building life cycle to the primary energy use and environmental impacts potentially avoided thanks to the renewable energy produced during the use stage. Tab. 8.10 and Fig. 8.8 show the energy (PBT_{GER}) and the environmental payback times, calculated without considering Module D (benefits and loads beyond the system boundaries) within the system boundaries. In particular they are between 12.4 years (PBT_{AP}) and 17.89 years (PBT_{EP}). The PBT_{GER} and the PBT_{GWP} of the system are estimated to be 15.36 years and 13.29 years, respectively, which are shorter than the hypothesized lifespan of building (25 years). However, the payback time for the ODP and ADP_e indicators estimated to be greater than the building useful life, while for all the others environmental impact categories the payback times are less than 25 years. This shows how the building, except for ODP and ADP_e indicators, is able to repay the primary energy use and environmental impacts produced during the entire building life cycle, from its production to its demolition, thanks to the primary energy use and environmental impacts potentially avoided due to the renewable energy produced during the use stage.

Tab. 8.10 - Energy and the environmental pay-back times.

	Unit	Payback time
PBT_{GWP}	years	13.29
PBT_{ODP}	years	>25
PBT_{AP}	years	12.40
PBT_{EP}	years	17.89
PBT_{POCP}	years	14.42
PBT_{ADPe}	years	>25
PBT_{ADPff}	years	13.21
PBT_{GER}	years	15.36

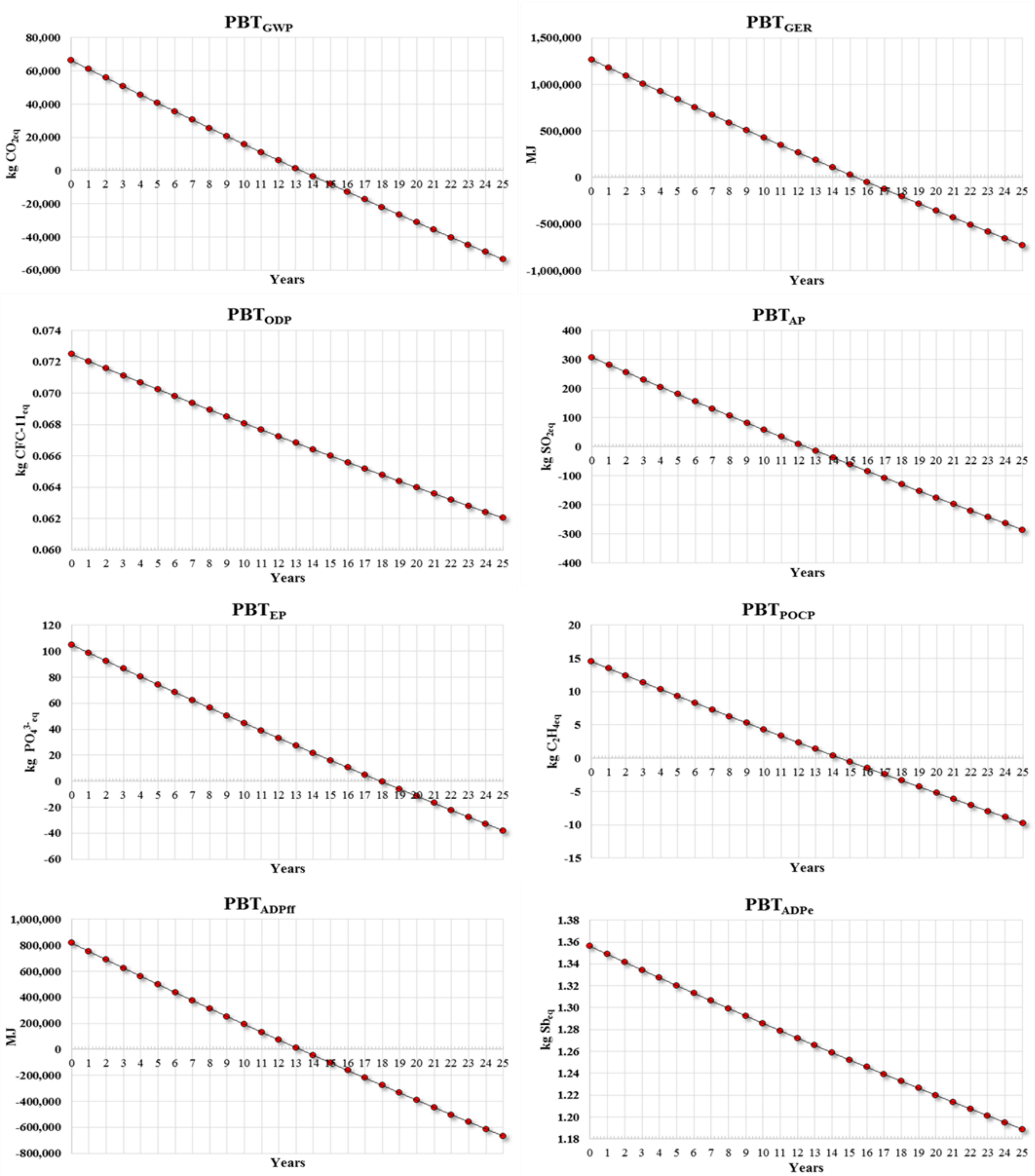

Fig. 8.8 - Energy and the environmental payback times.

8.11 CHAPTER CONCLUSIONS

The energy and environmental performances of a prefabricated housing module located in Messina (Italy) were analyzed in a life cycle perspective. All the life cycle stages, from the materials production (Modules A1 – A3) to the end-of-life (Modules C1 – C4), are examined according to a "from cradle to cradle" approach.

The material production stage (Modules A1 – A3) causes the highest impact for almost all the examined impact categories. For the products stage, FRP, that it is the main material used in the building envelope (about 77%), accounts for more than 40% of the impacts for almost all environmental and energy indicators, with the exception of the ODP and the ADPe.

The use stage (Modules B4 and B6) is the second most impactful stage. Since the overall PV generation (8,068 kWhe) in a year surpasses the electricity consumptions, the building achieves the NZEB target. However on-site generation and consumption are not contemporary and this causes a high grid dependency. The use of other types of systems fed by renewable energy sources and/or the use of electric energy storage systems might allow a higher load match. The detailed analysis of this stage allowed highlighting the "hot spots" of the design, identifying some aspects to improve. In particular, the large glazed openings in the two main facades of the building cause large solar gains.

The construction process (Module A5) and the end-of-life (Modules C1 – C4) stages give a marginal contribution to the total impacts. Since the main construction works are performed outside the construction site, the construction of the building is done with few easy operations that require a limited amount of inputs. Furthermore, the selective demolition of the building allows to obtain uniform and separated waste and this increases the possibility of recycling the wastes.

The results also demonstrated the importance of the environmental and energy benefits resulting from the recycling of materials and the surplus energy fed into the electricity grid (Module D). These benefits, although not directly included in the system boundaries but allocated in the benefits and loads beyond the system boundaries according to (UNI, 2011b), allow to avoid the emission of about 84.9 kg of CO_{2eq}/m^2year and the production of about 920.6 MJ/m^2year of total primary energy. Moreover they allow to avoid the emission of about 0.43 kg

SO_{2eq}/m^{2}year, 0.1 kg $PO_4^{3-}{}_{eq}$/m^{2}year and 17.8 g C_2H_{4eq}/m^{2}year. However, the reduction potential of the indicators ODP and ADPe is equal only to 11.9% (-7.65E-06 kg CFC 11_{eq}/m^{2}year) and -9.8% (-1.18E-04 kg Sb_{eq}/m^{2}year), respectively.

Finally, the energy and the environmental payback times show that thanks to environmental and energy benefits due to renewable energy produced during the use stage, with the exception of the ODP and the ADPe, the building is able to equal the primary energy use and the environmental impacts potentially produced during the entire life cycle in a time shorter than its useful life (25 years).

9 BUILDING REDESIGN RESULTS

9.2 INTRODUCTION

In this chapter, in order to improve the design of the module, a redesign of the building case study will be investigated. Since Net Zero Energy Buildings and – more in general – “prosumers” buildings are complex objects that cannot be studied from a single perspective, the redesign options were selected using a multidisciplinary approach.

In detail, all the redesign solutions were chosen while trying to reduce energy consumption and to increase building energy performances. In order to increase the self-consumption of electricity generated and to reduce the stress on the energy grids, load matching and grid interaction issues were also taken into account.

Moreover, since focusing only on the assessment of the energy consumption related to the use stage quantifies the reduction of the environmental burdens of this stage but it does not guarantee that the life cycle overall performances will be improved, the LCA methodology was used to investigate each of the proposed scenarios.

Finally, since to reach the target of NZEBs, the technical feasibility in general is not sufficient to help the diffusion of nZEBs into building current practice, a preliminary analysis of the economic feasibility of the different design option have been conducted.

Each scenario investigates some specific parameters that are closely related through wide applications of parametric analyses by analyzing the combined effects of all of them to the end results. The effect on other parameters not included as main focus of this thesis is also included when deemed necessary (e.g. visual comfort when investigating variation of window to wall ratio).

In detail, the following redesign scenarios were examined:

- Scenario 1: variation of the window-to-wall area ratios (WWRs) of the north and south façades and of the insulation thickness on all the exterior walls;
- Scenario 2: definition of a natural ventilation strategy;
- Scenario 3: integration of phase change materials (PCMs) into the building envelope;
- Scenario 4: variation of the PV system nominal power and sizing of an electric storage system.

The relationship between the set of parameters may not be simply understood due to the nonlinearity of the problem. As a result, the evaluation of the impact of alternative scenarios on the building performance requires exploring a large decision space (due to its combinatorial nature) which can be very time consuming and inefficient in a traditional iterative process. For these reasons, it was chosen to carry out a gradual redesign of the building case study, gradually implementing the solutions chosen by the different scenarios and finally obtaining the best case.

9.3 PRELIMINARY COST ANALYSIS

To identify the economic feasibility of the energy redesign scenarios, a preliminary cost analysis was performed, determining, for each different redesign option, the related cost. In detail, the preliminary cost analysis in the different cases was calculated, taking into account the following costs or gains:

- initial investment cost;

- gain due to the electricity fed into the grid;
- cost of the electricity purchased from the grid.

Finally, to verify the economic feasibility of the different scenario solutions, the net present value (NPV) was calculated using eq. 9.1. In detail, the NPV is the combination of the initial investment cost (I_0) and the difference between the present value of future money inflows and the present value of future money resulting from the initial investment (Doty & Turner, 2004). A positive NPV indicates a profitable investment, while a negative NPV indicates a net loss.

eq. 9.1
$$NPV = \sum_{t=1}^{T} \frac{C_i}{(1+r)^t} - \sum_{t=1}^{T} \frac{C_o}{(1+r)^t} - I_0$$

where:

I_0 = initial investment costs [€];

C_i = money inflow during the period t [€];

C_o = money inflow during the period t [€];

t = number of time periods [years];

r = discount rate [%].

In this work, instead of calculating the NPV for the base case and for the each solution investigated, it was chosen to calculate a relative NPV (NPV_r). NPV_r is the difference between the NPV of the redesign solution and the NPV of the base case. This was chosen since the goal is to investigate the economic feasibility of the redesign solution compared the base case. A positive NPV_r will indicate that the redesign solution compared to the base case produces an economic profit, while a negative NPV_r will indicate that the redesign solution is not economically feasible, because it produces an economic loss. The formula that was used to calculate the NPV_r is the following:

eq. 9.2
$$NPV_r = \sum_{t=1}^{T} \frac{\Delta C_i}{(1+r)^t} - \sum_{t=1}^{T} \frac{\Delta C_o}{(1+r)^t} - \Delta I_0$$

where:

ΔI_0 = Difference between the investment cost of the redesign solution and investment cost the base case [€].

ΔC_i = Difference between the money inflow of the redesign solution and the money inflow of the base case, during the period t [€].

ΔC_o = Difference between the money outflow of the redesign solution and the money outflow of the base case, during the period t [€].

The NPV results are sensitive to the choice of the discount rate (r). Choosing a high discount rate favors investments with lower initial cost, while a low discount rate favors investments with higher initial cost. If the discount rate is zero, timing has no importance whatsoever (Anna Joanna Marszal & Heiselberg, 2011; Ristimäki, Säynäjoki, Heinonen, & Junnila, 2013). For this reasons, in this work two different discount rate (2% and 4%) were used to execute a sensitivity analysis. In detail, the rate of 2.00% was tied to the European Central Bank inflation target (European Central Bank., 2018) and the discount rate of 4.00% (twice the European Central Bank forecasts) was assumed as the worst inflation limit case in the next 25 years.

9.3.1 Investment cost

The initial investment costs were calculated considering only materials and systems costs modified in the investigated scenario in comparison to the existing building, not taking into account the cost of the entire building. The installation cost - as well as the costs for design, etc. - were not considered since their values were assumed to be the same for all the candidate solutions. With the exception of the PCMs, for which literature values were used, the costs were obtained by means of market surveys.

9.3.2 Gain due to the electricity fed into the grid

The economic gains due to the electricity fed into the grid were calculated considering the current remuneration method in force in Italy. In particular, the Italian management authority of the electrical services (GSE) recognizes to the final user the contribution (C_s) due to the energy fed into the electricity grid through the following equation:

eq. 9.3
$$C_S = \min[O_E; C_{EI}] + CU_{Sf}^{reti} \cdot E_S$$

where:

- C_{EI} is the euro equivalent of electricity delivered, equal to the hourly summation of the quantitative of electricity delivered into the grid every year multiplied by different prices according to the geographic zone and the hour;
- O_{EI} represents the user's expenses (expressed in euro) to pay for the electricity withdrawn, and it is the electricity withdrawn multiplied by the National Single Price (PUN).
- CU_{Sf}^{reti}, common net-metering fixed contribution, is the algebraic addition according to the commercial principle of variable cost per unit, expressed in c€/kWh, of the prices of transmission and distribution of the dispatching equivalents.
- E_S is the electricity exchanged. It has the lowest value among the values of the energy withdrawn and delivered into the grid.

Basically GSE wants to repay the user with an equivalent of the price he paid to withdraw energy from the grid. Moreover there is a valorization of the surpluses that will be given back during the future solar years. The possible credit which can be settled C_{RL}, that is the amount paid out from the GSE to the producer is:

eq. 9.4

$$C_{RL} = \max\left[0; C_{EI} - O_E\right]$$

In other words, if there is a surplus having the same value of the difference between the energy delivered into the grid multiplied by the PUN, and the expenses of the user to withdraw the same amount of energy of the energy withdrawn for the National Single Price.

9.3.3 Cost of the electricity purchased from the grid

Besides the fixed quota, that is the fixed annual price to pay for the connection (a minimum portion of the final price), the cost of the electricity purchased from the grid involves:

- Retail services: energy, dispatching, commercialization sales price, equalization and dispatching components;

- Grid services: distribution, transportation and measurement;
- General expenses.

However, in this works a fixed average price 0.193 €/kWh$_e$ was considered. Thanks to the comparison between different retailers' offers, it is possible to notice that this is a competitive average price of energy for the year 2017.

9.4 Scenario 1: window to wall ratios and insulation thickness

Due to the high solar radiation transmitted through the large glass façades and the lightweight envelope, during summer the air temperature can be higher than 35 °C when free-floating. For these reasons, in this scenario, in order to vary the main features of the building envelope, it was decided to vary at the same time the window-to-wall area ratios (WWRs) of the south-east façade and of the north-west façade and the thickness of the insulating panels of the walls, the roof and the floor.

In particular, for this scenario, 1,125 different redesign solutions were analyzed, considering the following parameterization variables at the same time:

- WWR of the south-east façade, from the 15% to the 95% (step of variation equals to the 5%);
- WWR of the north-west façade, from the 15% to the 95% (step of variation equals to the 5%);
- insulation thickness: from 6 cm to 18 cm (step of variation equals to 3 cm).

9.4.1 Scenario 1: Selection of the redesign solution

Fig. 9.1 shows the overall building energy demand (Fig. 9.1a), the heating energy demand (Fig. 9.1b), the cooling energy demand (Fig. 9.1c) and the lighting energy demand (Fig. 9.1d) due to the variations at the same time of WWRs of the two façades and of the insulation thickness.

The building energy demand (Fig. 9.1a) varies between 2201.1 kWh$_e$ (WWRs of the two façades equal to the 15% and insulation thickness equals to 15 cm) and 2960.6 kWh$_e$ (WWRs of the two façades equal to the 95% and insulation thickness equals to 18 cm). For the first of the two previous cases, the building energy demand decrease by 18% (-476.1 kWh_e) compared to the base case, while the energy consumption for the heating, the cooling and the lighting, if compared to the base case, varies by -25% (-13.6 kWh_e), -52% (-457.6 kWh_e) and +55% (+35 kWh_e), respectively. On the other hand, for the second of the two previous cases, the building energy demand increase by 11% (+283.3 kWh_e) compared to the base case, while the energy consumption for the heating, the cooling and the lighting vary respectively by -52% (-28.5 kWh_e), +33% (+313.8 kWh_e) and -3%, (-2 kWh_e) respectively.

The lowest and highest heating energy demand, reported in Fig. 9.1b, are 21.7 kWh_e (reduction of 60% compared to the base case) and 104.3 kWh_e (increase of 90% compared to the base case), respectively, in the case of the WWR of the south-east façade equals to 95%, WWR of the north-west façade equals to 15% and insulation thickness equals to 18 cm and in the case of the WWRs of the two façades equal to 15% and the insulation thickness equals to 6 cm. For these two cases, the building energy demand shows a variation of -17% (-443.3 kWh_e) and -55% compared to the base case (-527.5 kWh_e), respectively.

The lowest and highest cooling energy demand (Fig. 9.1c) are 427.6 kWh_e (reduction of 55% compared to the base case) and 1268.9 kWh_e (increase of 33% compared to the base case) respectively in the two cases 1) WWR =15% and insulation thickness = 6 cm and 2) WWRs = 95% and insulation thickness = 18 cm. For these two cases, the building energy demand shows a variation of -17% (-443.3 kWh_e) and +11% (+283.3 kWh_e) compared to the base case, respectively.

The consumption of electricity for lighting varies between a minimum of 62 kWh_e (WWR = 95%) and a maximum of 100 kWh_e (WWR=15%). For these two cases, the building energy demand shows a variation of -3% (2 kWh_e) and -15% (35 kWh_e) compared to the base case, respectively.

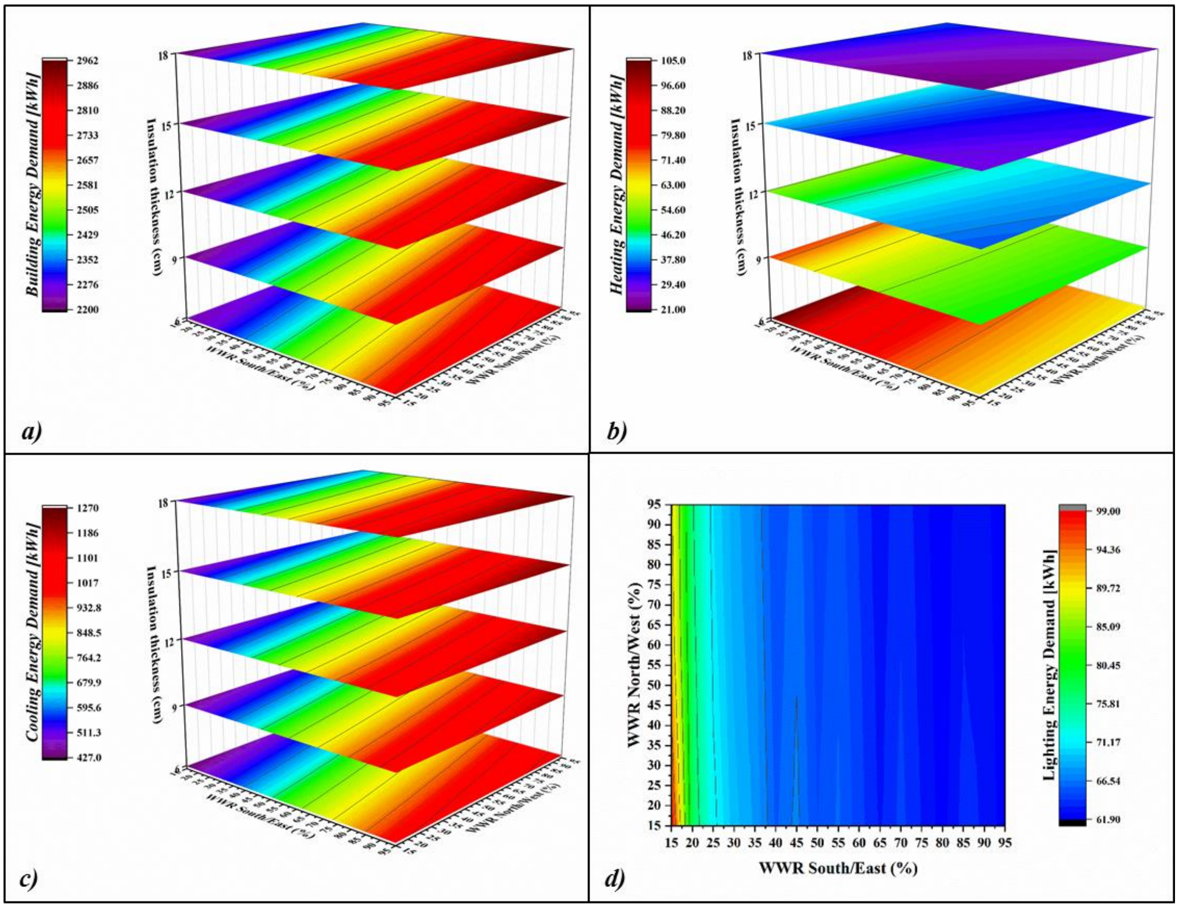

Fig. 9.1 - Building energy demand (a), heating energy demand (b), cooling energy demand (c) and lighting energy demand (d) due to the variations of WWRs of the two façades and due to variation of the insulation thickness.

Among all the redesign solutions analyzed in scenario 1 and shown in Fig. 9.1, the lowest building energy demand occurs in the case of WWRs of the two façades equal to 15% and insulation thickness equal to 15 cm, however in order to guarantee that the life cycle overall performances will be improved, it was decided to analyze in detail all the redesign solutions with WWRs of the two façades equal to 15%.

Tab. 9.1 shows the building energy demand, the heating energy demand, the cooling energy demand and the lighting energy demand due to the variation of the insulation thickness in the cases where the WWRs of the two façades are equal to 15%. In particular, the energy savings between 16.56% (Sc.1 Case 1) and 17.78% (Sc.1 Case 4). Moreover, all the cases shown in Tab. 9.1 show a reduction in cooling energy demand higher than 50%, while the variation in heating energy demand varies between -42% (Sc.1 Case 5) and + 90% (Sc. 1 Case1). Finally, the consumption of lighting show of increase of about 55% (+35 kWh_e).

Tab. 9.1 – Building energy demand due to the variation of the insulation thickness in the cases where the WWRs of the two façades are equal to 15%.

	Ins. Thickness [cm]	**Lighting [kWh_e]**	**Heating [kWh_e]**	**Cooling [kWh_e]**	**Building energy demand [kWh_e]**	**Energy saving [kWh_e]**	**Energy saving [%]**
Base case	9	63.98	55.02	955.14	2677.22	-	-
Sc.1 Case 1	6	98.98	104.34	427.56	2233.95	443.27	16.56
Sc.1 Case 2	9	98.98	74.65	436.03	2212.73	464.49	17.35
Sc.1 Case 3	12	98.98	54.67	446.95	2203.68	473.54	17.69
Sc.1 Case 4	15	98.98	41.41	457.64	2201.10	476.12	17.78
Sc.1 Case 5	18	98.98	31.75	467.99	2201.79	475.43	17.76

In order to choose the redesign solution that also ensures a reduction of the environmental impacts in a life cycle perspective Tab. 9.2 shows the life cycle impacts for all case investigated in Tab. 9.1. Since the cases shown in Tab. 9.1 have the same values of WWRs for the two façades but different insulation thickness, Tab. 9.2 shows the impacts due only to the variation of the insulation thickness. In particular, it shows the impacts due to the production, the transport from the production site to the construction site and the end of life of the insulation material. Furthermore, as the variation of the insulation also causes a variation in the energy use during the use stage, Tab. 9.2 also shows the impacts of the Module B6 of each of the redesign solutions selected.

As shown in Tab. 9.2, for all the indicators investigated the energy and environmental impacts due to the production, the transport and the end of life of the insulation material increase linearly with the increase in insulation thickness. On the other hand, as the building energy demand decreases as the insulation thickness increases, the impacts due to energy consumption during the use stage (Module B6) decrease with increasing insulation thickness. However, by summing the impacts due to the production, the transport and the end of life of the insulation material to the impacts due to Module B6, the results show that, for all the impact categories investigated, the case Sc.1 Case 2 (insulation thickness equals to 6 cm) shows the lowest energy and environmental impacts.

Tab. 9.2 – Life Cycle environmental impacts due to the variation of the insulation thickness in the cases where the WWRs of the two façades are equal to 15%.

	Production, transport and end of life of the insulation material				
	Sc.1 Case 1	**Sc.1 Case 2**	**Sc.1 Case 3**	**Sc.1 Case 4**	**Sc.1 Case 5**
GWP [kg CO_{2eq}/m^{2}year]	3.72E+00	5.59E+00	7.45E+00	9.31E+00	1.12E+01
ODP [kg CFC-11$_{eq}$/m^{2}year]	4.68E-07	7.02E-07	9.37E-07	1.17E-06	1.40E-06
AP [kg SO_{2eq}/m^{2}year]	1.31E+00	1.97E+00	2.62E+00	3.28E+00	3.93E+00
EP [kg $PO_4{}^{3-}{}_{eq}$/m^{2}year]	3.15E-01	4.72E-01	6.30E-01	7.87E-01	9.45E-01
POCP [kg C_2H_{4eq}/m^{2}year]	9.40E-04	1.41E-03	1.88E-03	2.35E-03	2.82E-03
ADP_e [kg Sb_{eq}/m^{2}year]	6.24E-06	9.36E-06	1.25E-05	1.56E-05	1.87E-05
ADP_{ff} [MJ/m^{2}year]	4.90E+01	7.35E+01	9.80E+01	1.23E+02	1.47E+02
GER [MJ/m^{2}year]	6.88E+01	1.03E+02	1.38E+02	1.72E+02	2.07E+02
	Module B6				
	Sc.1 Case 1	**Sc.1 Case 2**	**Sc.1 Case 3**	**Sc.1 Case 4**	**Sc.1 Case 5**
GWP [kg CO_{2eq}/m^{2}year]	1.62E+01	1.60E+01	1.59E+01	1.58E+01	1.58E+01
ODP [kg CFC-11$_{eq}$/m^{2}year]	1.41E-06	1.40E-06	1.39E-06	1.38E-06	1.38E-06
AP [kg SO_{2eq}/m^{2}year]	8.04E-02	7.93E-02	7.87E-02	7.84E-02	7.81E-02
EP [kg $PO_4{}^{3-}{}_{eq}$/m^{2}year]	1.94E-02	1.92E-02	1.90E-02	1.89E-02	1.89E-02
POCP [kg C_2H_{4eq}/m^{2}year]	3.29E-03	3.25E-03	3.22E-03	3.21E-03	3.20E-03
ADP_e [kg Sb_{eq}/m^{2}year]	2.27E-05	2.24E-05	2.22E-05	2.21E-05	2.20E-05
ADP_{ff} [MJ/m^{2}year]	2.01E+02	1.99E+02	1.97E+02	1.96E+02	1.96E+02
GER [MJ/m^{2}year]	3.64E+02	3.60E+02	3.58E+02	3.57E+02	3.57E+02
	Production, transport and end of life of the insulation material + Module B6				
	Sc.1 Case 1	**Sc.1 Case 2**	**Sc.1 Case 3**	**Sc.1 Case 4**	**Sc.1 Case 5**
GWP [kg CO_{2eq}/m^{2}year]	1.99E+01	2.16E+01	2.34E+01	2.51E+01	2.70E+01
ODP [kg CFC-11$_{eq}$/m^{2}year]	1.88E-06	2.10E-06	2.33E-06	2.55E-06	2.78E-06
AP [kg SO_{2eq}/m^{2}year]	1.39E+00	2.05E+00	2.70E+00	3.36E+00	4.01E+00
EP [kg $PO_4{}^{3-}{}_{eq}$/m^{2}year]	3.34E-01	4.91E-01	6.49E-01	8.06E-01	9.64E-01
POCP [kg C_2H_{4eq}/m^{2}year]	4.23E-03	4.66E-03	5.10E-03	5.56E-03	6.02E-03
ADP_e [kg Sb_{eq}/m^{2}year]	2.89E-05	3.18E-05	3.47E-05	3.77E-05	4.07E-05
ADP_{ff} [MJ/m^{2}year]	2.50E+02	2.73E+02	2.95E+02	3.19E+02	3.43E+02
GER [MJ/m^{2}year]	4.33E+02	4.63E+02	4.96E+02	5.29E+02	5.64E+02

In order to compare investment costs between the actual design and the proposed redesign solutions in the scenario 1, a preliminary cost analysis was conducted. In detail, the investment cost was estimated, through a market survey (Fibrenet, 2018; Freudenberg Politex, 2015; Ripamonti, 2018), which allowed to determine the cost of the materials involved in the redesign. The general assumptions are reported in Tab. 9.3.

Tab. 9.3 – Materials and components costs assumed for the scenario 1.

Material or components type	Cost [€/m²]	Reference
Insulation panel (thickness = 6 cm)	10.8	
Insulation panel (thickness = 9 cm)	16.1	
Insulation panel (thickness = 12 cm)	21.5	(Freudenberg Politex, 2015)
Insulation panel (thickness = 15 cm)	26.9	
Insulation panel (thickness = 18 cm)	32.3	
Glazed surfaces	200	(Ripamonti, 2018)
Opaque components	238	(Fibrenet, 2018)

Tab. 9.4 shows the preliminary cost analysis results for the base case and for the all the redesign solutions selected from the scenario 1. The results show that the only case in which the investment costs due to the purchase of materials are reduced is the case in which the insulation thickness is equal to 6 cm (-738 €), while for all other cases the investment costs show an increase between +223€ (Sc.1 Case 2) and +3,105€ (Sc.1 Case 5). On the other hand, since the building is equipped with a 5.76 kW PV system, the results are less sensitive to the costs and the gains due to the energy exchange with the electricity grid.

Tab. 9.4 – Preliminary cost analysis results for the scenario 1.

		Base Case	Sc.1 Case 1	Sc.1 Case 2	Sc.1 Case 3	Sc.1 Case 4	Sc.1 Case 5
Investment cost	Insulation panel [€]	2,624	1,921	2,881	3,842	4,802	5,763
	Transparent envelope [€]	4,814	1,028	1,028	1,028	1,028	1,028
	Opaque envelope [€]	2,407	6,159	6,159	6,159	6,159	6,159
	Tot. [€]	9,845	9,108	10,068	11,029	11,989	12,950
Yearly gain due to the electricity fed into the grid [€]		359	383	383	383	383	383
Yearly cost of the electricity purchased from the grid [€]		193	200	197	196	195	194

Tab. 9.5 shows the NPV_r values considering the two different discount rates for the all the redesign solutions selected from the scenario 1. The results show that the only two redesign solutions economically feasibility are the cases in which the insulation thickness are equal to 6 cm and 9 cm. Moreover, the case in which the insulation thickness is equal to 6 cm is the most economically advantageous because it is the one that shows the highest NPV_r

considering both the discount rates. In particular, considering a discount rate of 2%, the NPV_r for this case is equal to € 1,073, which means that, after 25 years, it has produced a profit of € 1,073 if compared to the base case.

Tab. 9.5 – NPV_r analysis for the redesign solutions of the scenario 1.

	Sc.1 Case 1 [€]	Sc.1 Case 2 [€]	Sc.1 Case 3 [€]	Sc.1 Case 4 [€]	Sc.1 Case 5 [€]
r = 2%	1,073	164	-765	-8,313	-2,649
r = 4%	1,006	87	-848	-9,048	-2,740

In order to verify if the cases selected in the scenario 1 (WWRs of two façades equal to 15%) are able to guarantee also the conditions of visual comfort (even if this is outside the scope of this work), the Daylight Autonomy (DA) for 5 points of the occupied area has been calculated by comparing the results with those obtained by the base case. In detail the DA, calculated using eq. 9.5 and eq. 9.6, is defined as the percentage of the occupied times of the year when the minimum illuminance requirement is met by daylight alone (Carlucci, Causone, De Rosa, & Pagliano, 2015; Reinhart, Mardaljevic, & Rogers, 2006). This metric was selected for this work due to the following reasons:

- DA is a long-term, one-tailed and local index referred to the amount of natural light available at a given point of the space during occupied hours
- It conceives the visual performance through a single value expressed as a percentage.
- DA takes into account the real weather conditions at the site.

eq. 9.5
$$DA = \frac{\sum_i \left(wf_i \cdot t_i \right)}{\sum_i t_i} \in [0,1]$$

eq. 9.6
$$wf_i = \begin{cases} 1 \ if \ E_{daylight} \geq E_{\text{limit}} \\ 0 \ if \ E_{daylight} < E_{\text{limit}} \end{cases}$$

Where:

wf_i = weighting factor;

t_i = building occupied hours when the simulated daylight illuminance ($E_{daylight}$)>0;

$E_{daylight}$ = horizontal illuminance at a given point due to the sole daylight;

E_{limit} = illuminance limit value (500 lux, as recommended by the UNI EN 12464-1 at the horizontal workplane in order to perform office tasks (UNI, 2011a)).

Using the time-varying illuminances derived from the weather file used for the simulation, DA during the occupation hours (i.e. between the hours 08:00 - 17:00, excluding weekends) was calculated for 5 points on a 0.8 m workplane. Fig. 9.2 the 5 points used to calculate the DA. In detail these points were chosen because they represent the most unfavorable points of the occupied zone.

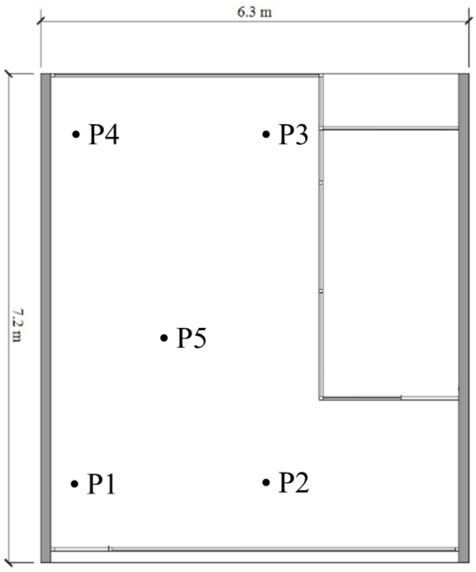

Fig. 9.2 – The 5 points used to calculate the DA.

The DA results for the base case and for the case selected from the Scenario 1 are shown in Tab. 9.6. In detail, for the base case the DA, due to the large glass façades, is greater than the 85% for all the considered points. On the other hand, for the selected redesign case the reduction of the windows surfaces causes a reduction of the DA between 1.6% (P1) and 16.7% (P3), with an average decrease of 8.6%. Moreover, the points subjected to a greater reduction of the DA are the points P3 (DA = 72.3%) and P4 (DA = 76.9%), due to the fact that these points are closer to the north-east façade which is most affected by the shading of the surrounding buildings. However, a maximum reduction of the DA of 16.7% was considered acceptable as the proposed solution allows a reduction in consumption due to cooling by 55.2%.

Tab. 9.6 – Daylight autonomy for the base case and for the selected case of the Scenario 1.

	DA	
	Base Case	**Case selected from scenario 1**
P1	88.5%	86.9%
P2	90.5%	89.4%
P3	89.0%	72.3%
P4	89.6%	76.9%
P5	86.5%	75.8%

Finally, it was decided to select the case Sc.1 Case 1 (WWRs of two façades equal to 15% and insulation thickness equals to 6 cm) as a redesign solution for the scenario 1, because, even if it is not the case with the lower reduction of energy consumption among all the solutions analyzed in scenario 1, this redesign solution ensures less environmental and economic impact than the other cases shown in Tab. 9.1.

The following sections show the energy performance and environmental impacts in a life cycle perspective of the case selected as the redesign solution of scenario 1.

9.4.2 Scenario 1: Building energy performances results

Results for monthly building energy demand, monthly heating energy demand, monthly cooling energy demand and monthly lighting energy demand for the base case and for the selected redesign solution are reported in Fig. 9.3. The yearly building energy demand of the proposed redesign solution compared to the base case decreases by 16.6% (-443.3 kWh_e), in particular the cooling consumption decreases by 55.2% (-527 kWh_e) while the consumption of lighting and heating, due to the reduction of the surface windows, increase by 54.7% (+35 kWh_e) and 88% (+48.7 kWh_e). At the monthly level the difference between the building energy demand of the proposed solution and the base case is between -17.5 kWh_e (February) and -94.7 kWh_e (August). In particular, the months of January, February and December show an increase in total consumption of +17 kWh_e, +17.5 kWh_e and +14.8 kWh_e, respectively. While the months showing a greater reduction in consumption are August (-94.7 kWh_e), July (-81.7 kWh_e) and June (-75.5 kWh_e).

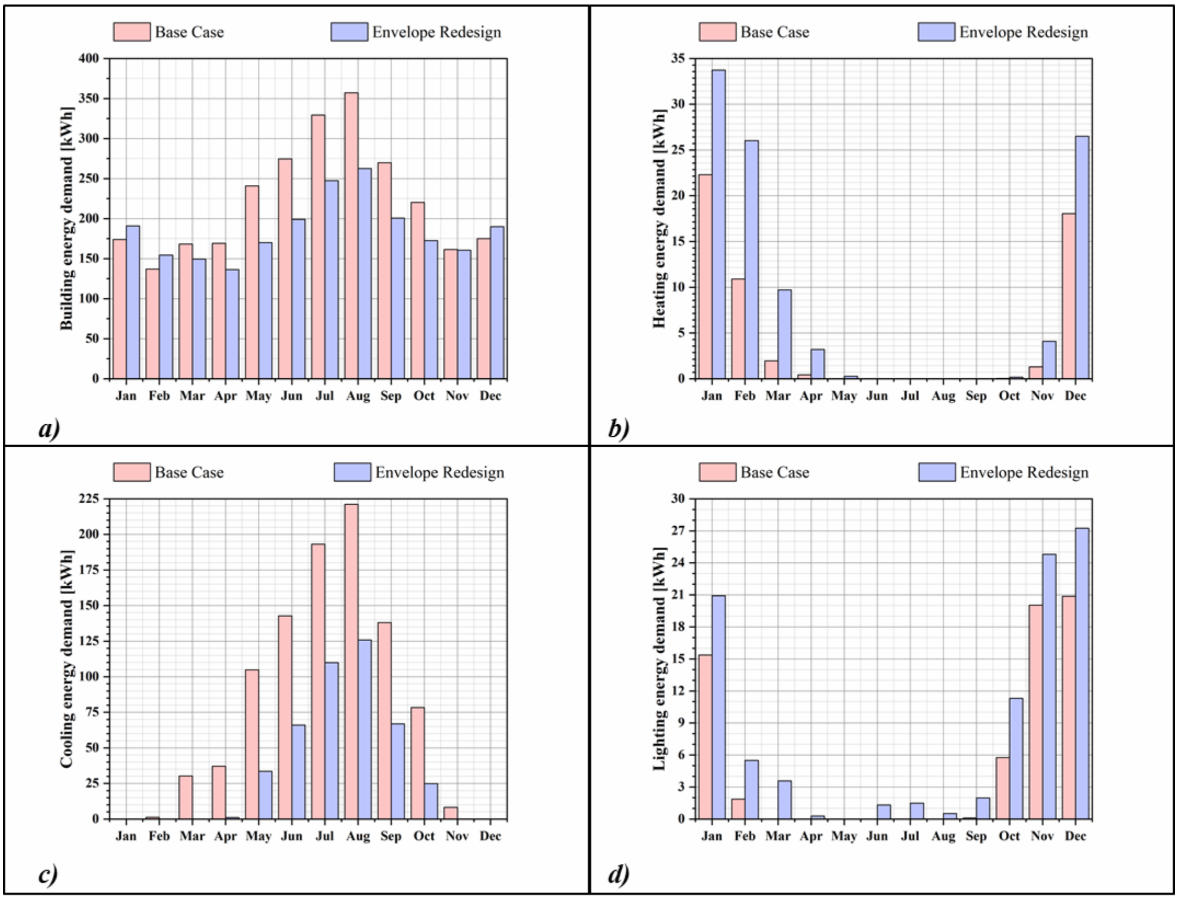

Fig. 9.3 – Monthly building energy demand (a), monthly heating energy demand (b), monthly cooling energy demand (c) and monthly lighting energy demand (d) for the base case and for the selected redesign solution.

In order to explore the impact of the proposed solution on the building-grid interaction, the net exported energy (ne), the monthly mean values of the load cover factor (γ_{load}), the supply cover factor (γ_{supply}), the loss of load probability (LOLP) and the no grid interaction probability ($P_{e\approx0}$) are calculated, as shown in Tab. 9.7. The yearly net exported energy has an increase of 443.3 kWh_e, at the monthly level the difference between the net exported of the proposed solution and the base case is between -17.5 kWh_e (February) and +94.7 kWh_e (August). In particular, during the winter months there is an increase in the imported energy, while in the summer months there is an increase in the exported energy. This is due to the fact that the reduction of window surfaces has led to an increase in heating demand and a decrease in cooling demand. However, the others indices shown in Tab. 9.7 (γ_{load}, γ_{supply}, LOLP and $P_{e\approx0}$) do not show significant changes. For example, the yearly mean value of the load cover factor and the supply cover factor vary from the values of 0.44 and 0.70 of the base case to the values of 0.43 and 0.69 of the proposed solutions, respectively.

Tab. 9.7 – Net exported energy (ne), load cover factor (γ_{load}), supply cover factor (γ_{supply}), loss of load probability (LOLP) and no grid interaction probability ($P_{e\approx0}$) – Scenario 1.

	ne [kWh$_e$]		γ_{load}		γ_{supply}		LOLP [%]		$P_{e\approx0}$ [%]	
	Base Case	**Envelope Redesign**	**Base Case**	**Envelope Redesign**	**Base Case**	**Envelope Redesign**	**Base Case**	**Envelope Redesign**	**Base Case**	**Envelope Redesign**
Jan	65.59	48.62	0.31	0.30	0.81	0.82	73.3	74.2	1.1	1.1
Feb	251.20	233.68	0.37	0.36	0.73	0.74	65.9	66.9	0.9	0.7
Mar	518.64	537.55	0.44	0.44	0.67	0.67	58.3	59.2	0.9	0.9
Apr	613.33	646.30	0.49	0.49	0.63	0.62	53.4	53.5	1.0	1.0
May	769.73	840.71	0.52	0.52	0.62	0.59	50.3	50.3	0.9	0.9
Jun	808.56	884.03	0.55	0.55	0.61	0.58	47.8	47.8	0.9	0.9
Jul	867.92	949.69	0.54	0.54	0.63	0.60	49.1	48.8	0.8	0.7
Aug	651.75	746.47	0.51	0.51	0.68	0.64	52.8	51.8	1.0	0.9
Sep	428.93	498.16	0.46	0.46	0.72	0.68	58.1	57.3	1.0	0.9
Oct	276.92	324.75	0.40	0.40	0.74	0.71	62.7	62.6	0.9	0.7
Nov	104.37	105.08	0.34	0.34	0.77	0.77	69.1	69.6	1.0	1.0
Dec	33.82	18.98	0.29	0.28	0.83	0.84	75.7	76.6	1.7	1.5
Year	5390.76	5834.03	0.44	0.43	0.70	0.69	59.7	59.8	1.0	0.9

9.4.3 Scenario 1: Life Cycle Assessment results

The life cycle impacts investigated for the base case and for the proposed solution from the scenario 1 (WWRs of two façades equal to 15% and insulation thickness equals to 6 cm) are shown in Tab. 9.8. These results exclude the environmental benefits and loads due to the exported energy and resulting from the recycling of materials since, according to the regulation UNI EN 15978 (UNI, 2011b), they are allocated outside the system boundaries (Module D). As shown in Tab. 9.8, for all the impact indicators investigated, if compared to the base case the proposed solution shows a reduction in the environmental and energy impacts. The total primary energy throughout the building's life cycle for the proposed solution is 1.07 GJ/m^{2}year, with a reduction compared to the base case equal to 4.53%. All other indicators show a reduction less than 2% compared to the base case: GWP (1.03%), ODP (0.26%), AP (1.69%), EP (0.38%), POCP (1.94%) and ADP_{ff} (0.15%).

Tab. 9.8 - Life Cycle environmental impacts for the base case and for the proposed solution in the scenario 1.

Indicator	Base Case	Redesign	Variation
GWP [kg CO_{2eq}/m^{2}year]	5.89E+01	5.83E+01	-1.03%
ODP [kg CFC-11$_{eq}$/m^{2}year]	6.44E-05	6.43E-05	-0.26%
AP [kg SO_{2eq}/m^{2}year]	2.73E-01	2.68E-01	-1.69%
EP [kg $PO_4^{3-}{}_{eq}$/m^{2}year]	9.33E-02	9.29E-02	-0.38%
POCP [kg C_2H_{4eq}/m^{2}year]	1.29E-02	1.27E-02	-1.94%
ADP_e [kg Sb_{eq}/m^{2}year]	1.21E-03	1.20E-03	-0.15%
ADP_{ff} [MJ/m^{2}year]	7.27E+02	7.20E+02	-1.01%
GER [MJ/m^{2}year]	1.13E+03	1.07E+03	-4.53%

The life cycle impacts, aggregated in the different building life cycle stages, for the base case and for the proposed solution are shown in Tab. 9.9. In detail, Module A5, Module B4 and Module C1 do not show any variation as these modules refer respectively to building construction stage, to the replacement of some building components during use stage and to the deconstruction of the building.

The materials production stage of the proposed solution (Modules A1 - A3), with the exception of the ODP which increased by 0.14%, if compared to the base case shows a reduction between 0.08% (EP) and 1.91% (POCP). The transport stage of the proposed solution (Module A4), which however has a contribution lower than 2.3% on the building life cycle impacts both for the base case and for the proposed solution, if compared to the base case shows a reduction between 6.75% (EP) and 8.15% (ADP_e). The use stage (Module B6), with the exception of the GER which decreased by 9.59%, if compared to the base case shows a reduction of 0.25% for all the impact categories investigated. Finally, the Modules C2 - C4, with the exception of the ADPe which increased by 4.33%, if compared to the base case shows a reduction between 6.69% (EP) and 32.16% (ODP).

Tab. 9.9 - Life Cycle environmental impacts, aggregated in the different building life cycle stages, for the base case and for the proposed solution in the scenario 1.

Indicator		LCA Modules						
		A1-A3	**A4**	**A5**	**B4**	**B6**	**C1**	**C2-C4**
GWP [kg CO_{2eq}/m^{2}year]	Base Case	3.69E+1	1.08	7.41E-2	1.70E+0	1.63E+1	2.38E-2	2.82E+0
	Redesign	3.68E+1	1.00	7.41E-2	1.70E+0	1.62E+1	2.38E-2	2.41E+0
	Variation	**-0.22%**	**-7.05%**	**0.00%**	**0.00%**	**-0.25%**	**0.00%**	**-14.51%**
ODP [kg CFC-11$_{eq}$/m^{2}year]	Base Case	3.37E-5	1.67E-7	1.23E-8	2.85E-5	1.42E-6	2.07E-9	6.26E-7
	Redesign	3.37E-5	1.54E-7	1.23E-8	2.85E-5	1.41E-6	2.07E-9	4.24E-7
	Variation	**0.14%**	**-7.47%**	**0.00%**	**0.00%**	**-0.25%**	**0.00%**	**-32.16%**
AP [kg SO_{2eq}/m^{2}year]	Base Case	1.64E-1	5.93E-3	4.61E-4	7.07E-3	8.06E-2	1.18E-4	1.47E-2
	Redesign	1.62E-1	5.52E-3	4.61E-4	7.07E-3	8.04E-2	1.18E-4	1.26E-2
	Variation	**-1.12%**	**-6.79%**	**0.00%**	**0.00%**	**-0.25%**	**0.00%**	**-14.77%**
EP [kg $PO_4^{3-}{}_{eq}$/m^{2}year]	Base Case	6.29E-2	1.59E-3	4.99E-5	6.99E-3	1.94E-2	2.84E-5	2.30E-3
	Redesign	6.29E-2	1.49E-3	4.99E-5	6.99E-3	1.94E-2	2.84E-5	2.15E-3
	Variation	**-0.08%**	**-6.75%**	**0.00%**	**0.00%**	**-0.25%**	**0.00%**	**-6.69%**
POCP [kg C_2H_{4eq}/m^{2}year]	Base Case	8.42E-3	1.83E-4	1.72E-5	5.02E-4	3.30E-3	4.82E-6	4.87E-4
	Redesign	8.25E-3	1.71E-4	1.72E-5	5.02E-4	3.29E-3	4.82E-6	4.18E-4
	Variation	**-1.91%**	**-6.77%**	**0.00%**	**0.00%**	**-0.25%**	**0.00%**	**-14.14%**
ADP_e [kg Sb_{eq}/m^{2}year]	Base Case	1.04E-3	2.87E-6	4.69E-8	1.40E-4	2.27E-5	3.32E-8	2.66E-6
	Redesign	1.04E-3	2.64E-6	4.69E-8	1.40E-4	2.27E-5	3.32E-8	2.77E-6
	Variation	**-0.16%**	**-8.15%**	**0.00%**	**0.00%**	**-0.25%**	**0.00%**	**4.33%**
ADP_{ff} [MJ/m^{2}year]	Base Case	4.67E+2	1.57E+1	8.75E-1	9.20E+0	2.02E+2	2.95E-1	3.19E+1
	Redesign	4.66E+2	1.46E+1	8.75E-1	9.20E+0	2.01E+2	2.95E-1	2.72E+1
	Variation	**-0.24%**	**-7.26%**	**0.00%**	**0.00%**	**-0.25%**	**0.00%**	**-14.51%**
GER [MJ/m^{2}year]	Base Case	6.38E+2	1.80E+1	1.63E+0	1.37E+1	4.03E+2	3.96E-1	5.11E+1
	Redesign	6.35E+2	1.67E+1	1.63E+0	1.37E+1	3.64E+2	3.96E-1	4.23E+1
	Variation	**-0.39%**	**-7.21%**	**0.00%**	**0.00%**	**-9.52%**	**0.00%**	**-17.25%**

Tab. 9.10 shows the energy and the environmental payback times, calculated without considering Module D (benefits and loads beyond the system boundaries) within the system boundaries for the base case and for the redesign case selected from the scenario 1. The results shows that the proposed solution, except for ODP and ADPe indicators, is able to repay the primary energy use and environmental impacts produced during the entire building life cycle in less time than in the base case. However, the differences are not very significant: the percentage variations between the payback time of the proposed solution and the base case are between -0.4% (PBT_{EP}) and -4.8% (PBT_{GER}).

Tab. 9.10 - Energy and the environmental pay-back times (Scenario 1).

	Unit	Base Case	Envelope Redesign
PBT_{GWP}	Years	13.29	13.15
PBT_{ODP}	Years	>25	>25
PBT_{AP}	Years	12.40	12.18
PBT_{EP}	Years	17.89	17.82
PBT_{POCP}	Years	14.42	14.13
PBT_{ADPe}	Years	>25	>25
PBT_{ADPff}	Years	13.21	13.07
PBT_{GER}	Years	15.36	14.63

9.4.4 Scenario 1 summary

In modern buildings the window area has grown and fully glazed façades are now frequently used to achieve high daylight levels inside and to obtain an attractive appearance of the buildings. This creates a problem of overheating, which can be partly prevented by different kinds of solar shading, but an acceptable indoor environment is in practice reached by air conditioning. For this reason, in the first scenario, to decrease the risk of overheating in summer and reduce the energy needed for cooling, the windows area of the south-east façade and of the north-west façade were varied.

Due to the outdoor climate features, the results show that the size of the windows does not have a major influence on the heating demand in the winter, but is relevant for the cooling need in the summer. Among all cases exanimated in this scenario, the minimum building energy demand (2201.1 kWh_e) occurs for the WWRs of the two façades equal to the 15% and insulation thickness equals to 15 cm. However, it was decided to select the case WWRs of the two façades equal to the 15% and insulation thickness equal to 6 cm as a redesign solution for the scenario 1, because, at the same WWRs values, this scenario ensures less environmental and economic impact than the other cases. The yearly building energy demand of the proposed redesign solution compared to the base case decreases by 17% (-443.3 kWhe), in particular the cooling consumption decreases by 55% (-527 KWhe) while the consumption of lighting and heating, due to the reduction of the surface windows, increase by 55% (+35 kWhe) and 88% (+48.7 kWhe).

The LCA results show that, for all the impact categories investigated, if compared to the base case the proposed solution shows a reduction in the environmental and energy impacts. However, except for GER (4.53% reduction compared to the base case), all indicators show a reduction less than 2% compared to the base case. On the other hand, the preliminary cost analysis results show that the proposed solution is economically feasible, as it allows to reduce the initial investment costs due to the purchase of materials of about € 738, while the gains and the costs due to the energy exchanged with the grid do not show significant variations.

9.5 SCENARIO 2: NATURAL VENTILATION STRATEGY

Natural ventilation that supplies and removes air to and from an indoor space without the use of mechanical systems shows great potential to reduce energy consumption and the cost of the HVAC system (Givoni, 2011; Santamouris & Kolokotsa, 2013). Especially in Mediterranean climate, controlled natural or hybrid ventilation is particularly effective in the reduction of cooling energy consumption and in the improvement of Indoor Air Quality (Givoni, 2011; Santamouris & Kolokotsa, 2013).

For these reasons, in this scenario a ventilation strategy to model occupant reactions to temperature variation was implemented in the case selected in section 9.4.1 (Sc.1 Case 1; WWRs of two façades equal to 15% and insulation thickness equals to 6 cm). In detail, temperature setpoints were fixed for the opening windows factors to model occupant reactions to temperature variation and airflow inside the building: Windows are open only during the occupation hours when indoor air temperature (T_i) is in the range of 20 < Ti < 26 °C, outdoor air temperature (T_o) is in the range of $18 < T_o < T_i$ and wind speed is lower than 2 m/s.

Fig. 9.4a shows the outdoor temperature and the Zone 1 air temperature in free-floating mode for the Sc.1 Case 1 and for the ventilation scenario in a week of May (15/05 – 20/05, on May 20 the ventilation strategy is not active because it is a Saturday and the building is not occupied). In particular, this week was chosen because it is the week in which the natural ventilation strategy shows the greatest cooling reduction potentials. The results show lower peak temperatures (up to 6.4 °C at the 17:00 of the 17/05) for the ventilation scenario. Moreover, the period between May 15 and May 19 shows an average temperature reduction of about 2.6 °C. As shown Fig. 9.4b, when the HVAC system is activated, the natural ventilation strategy allows to reduce cooling power demand. In particular, during the period between May 15 and May 17, the zone air temperature can remain in the range between 20 °C and 26 °C without requiring the activation of the HVAC system.

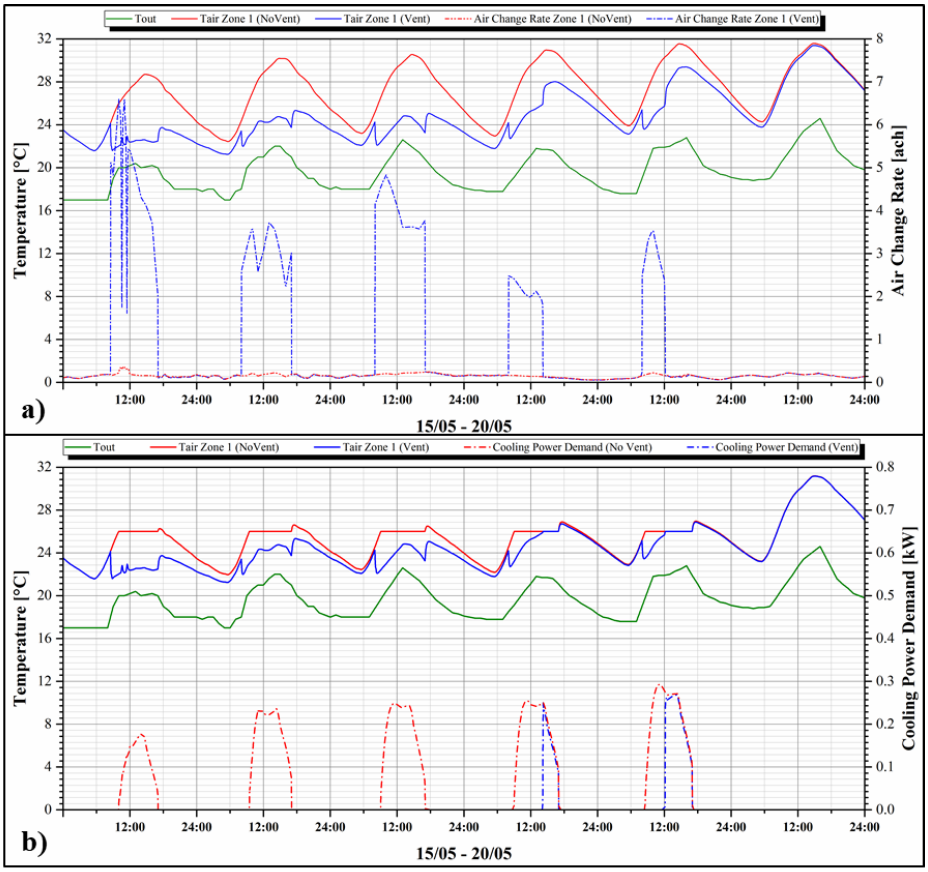

Fig. 9.4 - Outdoor dry-bulb temperature and zone air temperatures for the Sc.1 Case 1 and for the ventilation scenario in free-floating mode (a) and when the HVAC system is operating (b).

9.5.1 Scenario 2: Building energy performances results

The analysis on the building energy performances results has shown mixed results: although the proposed natural ventilation strategy could allow for around 5% of cooling electricity use reduction, such savings are mostly concentrated during May, June, September and October due to the features of the climate and to the very light structure of the building.

Tab. 9.11 shows the building energy demand, the heating energy demand and the cooling energy demand for both the Sc.1 Case 1 and the ventilation scenario. The proposed natural ventilation strategy does not involve any change in heating energy demand, while the yearly cooling energy demand is reduced by 4.8%. The most significant reductions in the cooling energy demand are available in mid-seasons, in particular in May (-30.2%) and in October (-17.3%). Limited benefits in terms of energy use for the cooling demand are available in June (-6.2%) and in September (-1.6%), while, and due to high temperatures during daytime, no reduction are available in July and in August.

Tab. 9.11 - Building energy demand, heating energy demand and cooling energy demand (Scenario 2)

	Heating			Cooling			Building energy demand		
	Sc.1 Case 1 [kWh$_e$]	**Vent. [kWh$_e$]**	**Saving [%]**	**Sc.1 Case 1 [kWh$_e$]**	**Vent. [kWh$_e$]**	**Saving [%]**	**Sc.1 Case 1 [kWh$_e$]**	**Vent. [kWh$_e$]**	**Saving [%]**
Jan	33.7	33.7	0	0	0	0	190.8	190.8	0
Feb	26.0	26.0	0	0	0	0	154.5	154.5	0
Mar	9.7	9.7	0	0	0	0	149.4	149.4	0
Apr	3.2	3.2	0	1.1	0.0	96.9	136.3	135.3	0.7
May	0.3	0.4	-25.0	33.6	23.4	30.2	170.0	159.9	5.9
Jun	0	0	0	66.0	61.9	6.2	199.1	195.0	2.1
Jul	0	0	0	109.9	109.9	0	247.5	247.5	0
Aug	0	0	0	125.9	125.9	0	262.6	262.6	0
Sep	0	0	0	66.9	65.9	1.6	200.7	199.6	0.5
Oct	0.2	0.2	0	24.9	20.6	17.3	172.5	168.2	2.5
Nov	4.1	4.1	0	0	0	0	160.7	160.7	0
Dec	26.5	26.5	0	0	0	0	189.9	189.9	0
Year	103.7	103.8	-0.1	428.2	407.5	4.8	2234.0	2213.4	0.9

As shown in Fig. 9.5 including the differences between indoor temperature in the Sc.1 Case 1 and in the ventilation scenario during May, temperature reductions of up to 6.6 °C can be achieved in the building during peak loads hours, while the monthly average temperature reduction is 1.1 °C.

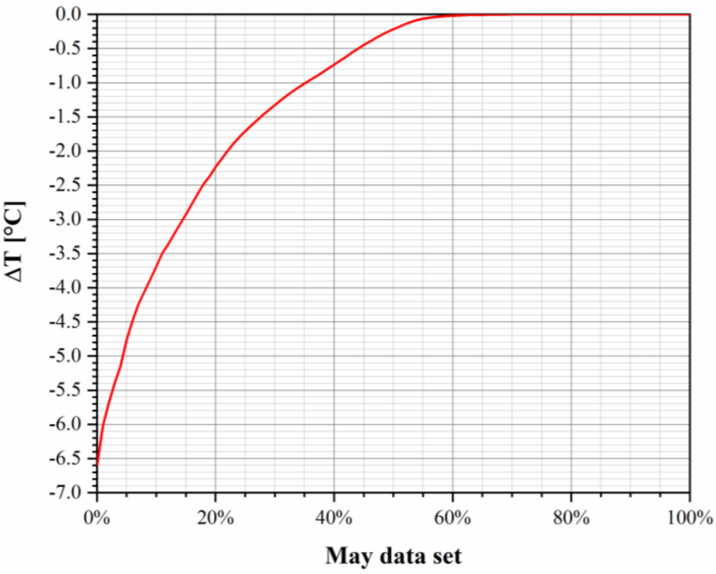

Fig. 9.5 - Percentile analysis of indoor temperature reductions for the month of May.

As shown in Tab. 9.12, the yearly net exported energy has an increase of only 20.5 kWh_e. In particular, the months in which the exported energy increases, due to the reduction in cooling, are May (+10.1 kWh_e), June (4.1 kWh_e) and October (4.3 kWh_e). However, the others indices shown in Tab. 9.12 (γ_{load}, γ_{supply}, LOLP and $P_{e\approx 0}$), at monthly level, do not show any changes. This is due to the fact that the reduction of total energy consumption is about 20 kWh_e, moreover the data presented in Tab. 9.12 are aggregated at monthly level.

Tab. 9.12 - Net exported energy (ne), load cover factor (γ_{load}), supply cover factor (γ_{supply}), loss of load probability (LOLP) and no grid interaction probability ($P_{e\approx 0}$) – Scenario 2.

	ne [kWh_e]		γ_{load}		γ_{supply}		**LOLP [%]**		$P_{e\approx 0}$ **[%]**	
	Sc.1 Case 1	**Vent.**	**Sc.1 Case 1**	**Vent.**	**Sc.1 Case 1**	**Vent.**	**Sc.1 Case 1**	**Vent.**	**Sc.1 Case 1**	**Vent.**
Jan	48.62	48.62	0.30	0.30	0.82	0.82	74.2	74.2	1.1	1.1
Feb	233.68	233.68	0.36	0.36	0.74	0.74	66.9	66.9	0.7	0.8
Mar	537.55	537.55	0.44	0.44	0.67	0.67	59.2	59.2	0.9	0.9
Apr	646.30	647.32	0.49	0.49	0.62	0.62	53.5	53.5	1.0	1.0
May	840.71	850.76	0.52	0.52	0.59	0.59	50.2	50.2	0.9	0.9
Jun	884.03	888.13	0.55	0.55	0.58	0.58	47.8	47.8	0.9	0.9
Jul	949.69	948.78	0.54	0.54	0.60	0.60	48.8	48.8	0.7	0.7
Aug	746.47	747.38	0.51	0.51	0.64	0.64	51.9	51.8	0.9	0.9
Sep	498.16	499.24	0.46	0.46	0.68	0.68	57.3	57.3	0.9	0.9
Oct	324.75	329.04	0.40	0.40	0.71	0.71	62.6	62.6	0.7	0.7
Nov	105.08	105.06	0.34	0.34	0.77	0.77	69.6	69.6	1.0	1.1
Dec	18.98	18.98	0.28	0.28	0.84	0.84	76.6	76.6	1.5	1.5
Year	5834.03	5854.54	0.43	0.43	0.69	0.69	59.85	59.85	0.94	0.94

9.5.2 Scenario 2: Life Cycle Assessment results

Since in this scenario the ventilation strategy aims to model occupant reactions to temperature variation, the only building life cycle stage to undergo a variation is the operational energy use during the use stage (Module B6), while the other life cycle stages remain unchanged. However, since the reduction in yearly building energy demand is equal to about 1% compare to the Sc.1 Case 1, the impacts due to the use stage do not show significant variations, as reported in Tab. 9.13.

Tab. 9.13 – Use stage (Module B6) energy and environmental impacts for the Sc.1 Case 1 and for the ventilation scenario.

Indicator	Sc.1 Case 1	Natural ventilation scenario	Variation
GWP [kg CO_{2eq}/m^{2}year]	1.62E+01	1.62E+01	0.06%
ODP [kg CFC-11$_{eq}$/m^{2}year]	1.41E-06	1.41E-06	0.06%
AP [kg SO_{2eq}/m^{2}year]	8.04E-02	8.03E-02	0.06%
EP [kg $PO_4^{3-}{}_{eq}$/m^{2}year]	1.94E-02	1.94E-02	0.06%
POCP [kg C_2H_{4eq}/m^{2}year]	3.29E-03	3.28E-03	0.06%
ADP_e [kg Sb_{eq}/m^{2}year]	2.27E-05	2.26E-05	0.06%
ADP_{ff} [MJ/m^{2}year]	2.01E+02	2.01E+02	0.06%
GER [MJ/m^{2}year]	3.64E+02	3.63E+02	0.21%

9.5.3 Scenario 2: Preliminary cost analysis results

Since in this scenario the ventilation strategy aims to model occupant reactions to temperature variation, there is no investment cost. Therefore the economic feasibility is linked only to the gain due to the electricity fed into the grid and to the cost of the electricity purchased from the grid. However, since the variations of the net energy exported between the Sc.1 Case 1 and the ventilation scenario, is equal to about 20 kWh$_e$, as shown in Tab. 9.14, the proposed solution in this scenario does not produce any variation in costs / gains due to the energy exchanged with the electricity grid. Therefore the NPV$_r$ is equal to € 0.

Tab. 9.14 - Preliminary cost analysis results for the scenario 2.

	Sc.1 Case 1	Natural ventilation scenario
Yearly gain due to the electricity fed into the grid	383	383
Yearly cost of the electricity purchased from the grid	200	200

9.5.4 Scenario 2 summary

Due to the low availability of thermal mass to be charged and discharged and due to the features of the climate, the analysis on the building energy performances has shown that the yearly cooling energy demand and the building energy demand are reduced by 4.8% and 0.9%, respectively. A so small reduction in the building energy demand is due to the fact that in the Sc.1 Case 1 the cooling energy demand is responsible for 19.2% of the total consumption, while 71.8% is due to the non-modifiable electricity consumption of the building. Moreover, since in this scenario the ventilation strategy aims to model occupant reactions to temperature variation and since the reduction in yearly building energy demand is equal to about 1% compare to the Sc.1 Case 1, the life cycle impacts and the economic feasibility do not show significant improvements. However, this redesign solution was selected among the possible solutions to include in the redesign for the case study building, because it guarantees, albeit slight, a reduction in energy consumption for cooling at basically no cost.

9.6 SCENARIO 3: PHASE CHANGE MATERIALS

One of the main disadvantage of the lightweight construction is having low thermal mass and the consequential risk of comfort issues due to high temperature swings during day and night and/or high solar radiation hours (e.g. overheating) (Koschenz & Lehmann, 2004; Osterman, Tyagi, Butala, Rahim, & Stritih, 2012). To overcome these problems, phase change materials (PCMs) can be incorporated in the building envelope allowing the building's thermal storage capacity to increase significantly. These materials provide a higher thermal capacity to the building that by absorbing the heat gains and reducing the heat flow. During daytime the PCM can absorb part of the heat through the melting process, and during night the heat is released by the solidification of the PCM, resulting in a lower heat flow from outdoors to indoors.

Since in the previous scenario, due to the low availability of thermal mass to be charged and discharged, the adopted natural ventilation strategy was not able to significantly reduce the cooling consumption, in this scenario PCMs were incorporated in the building envelope of the case study obtained in the previous scenario. In detail, the PCM panels are located on the inner faces of all the walls and ceiling, between the FRP panel and the insulation panel. The thickness of the PCM layer in the walls and in the ceiling were varied keeping all other parameters constant. In detail, the thickness was varied from 0.5 cm to 2 cm (0.5 cm variation step).

Based on the literature (Jiang, Wang, & Zhang, 2011; Memarian, Kari, Fayaz, & Asadi, 2018), that suggests to use PCMs with 24–28°C melting temperature for cooling applications, the PCM material selected for the present study was ClimSel C24 produced by Climator with a melting temperature of 27°C and a latent heat of about 140 kJ/kg (Climator, 2018). Data on the thermal properties of that PCM, provided by the manufacturer, are given in Tab. 9.15.

Tab. 9.15 - Thermo-physical properties of the used PCM (Climator, 2018).

Type of material	-	Salt hydrate
Specific latent heat	[kJ/kg]	140
Freezing temperature	[°C]	24
Melting temperature	[°C]	27
Thermal conductivity solid state	[W/(m K)]	0.74
Thermal conductivity liquid state	[W/(m K)]	0.93

The enthalpy profile of the selected PCM is shown in Fig. 9.6. Two curves are presented for the material: the melting curve (red line) and the solidification curve (blue line). These curves show that the melting and solidification peaks occur around 27 °C and 24 °C, respectively. Moreover, hysteresis can be observed; the melting peak occurs at a temperature lower than the solidification peak. This is a common effect of many phase change materials and has already been observed in literature (Mehling & Cabeza, 2008; You, Zhang, Wang, & Wang, 2009).

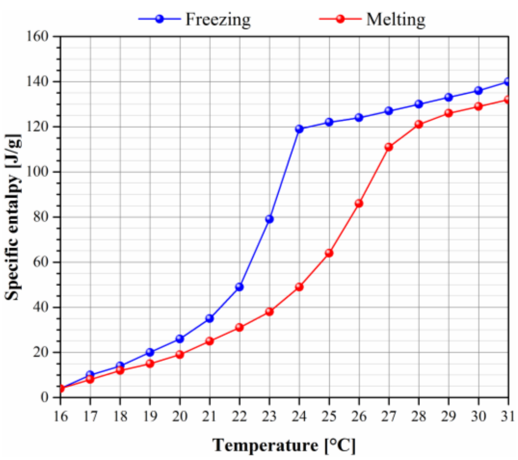

Fig. 9.6 - Enthalpy profile of the selected PCM (Climator, 2018).

PCM material was simulated in EnergyPlus environment using the conduction finite difference (CondFD) solution algorithm (DoE, 2010). In detail, CondFD discretizes walls, floors, and ceilings into several nodes and uses an implicit finite difference scheme to numerically solve the appropriate heat transfer equations (DoE, 2010). The CondFD algorithm in EnergyPlus uses an implicit finite difference scheme, where the user can select Crank-Nicholson or fully implicit (DoE, 2010). eq. 9.7 shows the calculation method for the fully implicit scheme for a homogeneous material with uniform node spacing.

eq. 9.7
$$C_p \cdot \rho \cdot \Delta x \cdot \frac{T_i^{j+1} - T_i^{1}}{\Delta t} = k_W \cdot \frac{T_{i+1}^{j+1} - T_i^{j+1}}{\Delta x} + k_E \cdot \frac{T_{i-1}^{j+1} - T_i^{j+1}}{\Delta x}$$

Where:

T = node temperature;

i = node being modeled;

i+1 = adjacent node to interior of construction;

i-1 = adjacent node to exterior of construction;

j+1 = new time step;

j = previous time step;

Δt = calculation time step;

Δx = finite difference layer thickness (always less than construction layer thickness);

C_p = specific heat of material;

k_w = thermal conductivity for interface between i node and i+1 node;

k_E = thermal conductivity for interface between i node and i-1 node;

ρ = density of material.

For the PCM algorithm, the CondFD method is coupled with an enthalpy-temperature function (eq. 9.8) that the user inputs to account for enthalpy changes during phase change (Pedersen, 2007). The enthalpy-temperature function is used to develop an equivalent specific heat at each time step (eq. 9.9). The resulting model is a modified version of the enthalpy method (Pedersen, 2007).

eq. 9.8 $$h = h(T)$$

eq. 9.9 $$C_p(T) = \frac{h_i^j - h_i^{j-1}}{T_i^j - T_i^{j-1}}$$

Fig. 9.7a shows the outdoor air temperature and the free-floating Zone 1 air temperature for all the 4 PCM scenarios and for the scenario without PCM in a week of June (15/06 – 20/06). All simulated PCM scenarios show similar trends clearly different from the scenario without PCM. The results show lower peak temperatures (up to 2.7 °C) and more constant conditions inside the occupied zone with PCM.

As shown in Fig. 9.7b, the effect of added by the PCM thermal mass in the walls and in the ceiling can be clearly seen by the dampened amplitude of the daily variation of wall's surface temperature (about 2 °C for the scenario PCM 2 cm) in comparison to the scenario without PCM (about 7°C).

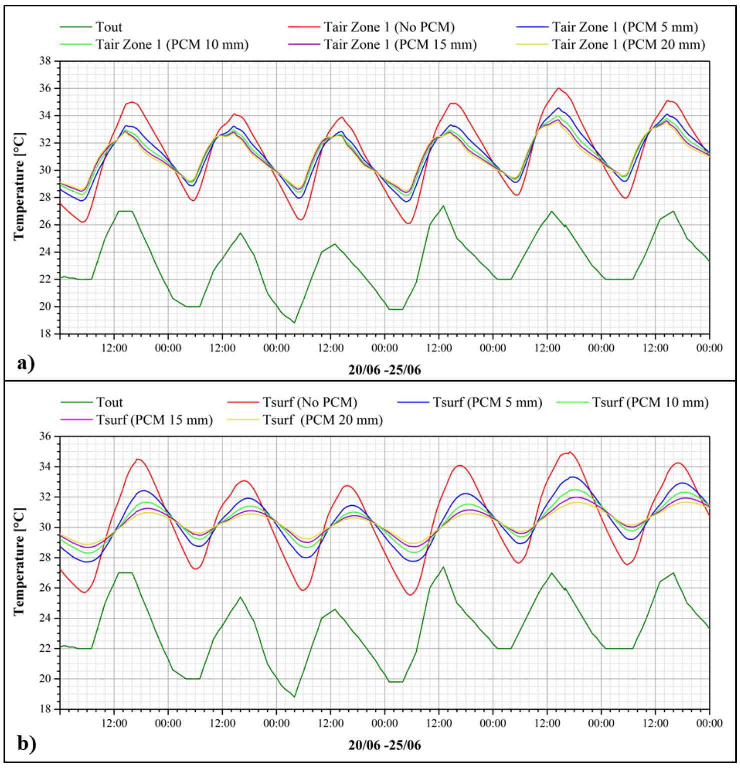

Fig. 9.7 - Outdoor air temperature, free-floating Zone 1 air temperature (a) and surface temperature for all the 4 PCM scenarios and for the scenario without PCM.

9.6.1 Scenario 3: Building energy performances results

Fig. 9.8 shows the heating energy demand and the cooling energy demand for all PCM scenarios and for the scenario without PCM. In particular, the yearly cooling demand shows a reduction between 8.9% (PCM 5 mm) and 5.1% (PCM 20 mm) compared to the scenario without PCM, while the heating shows an increase between 10.8% (PCM 5 mm) and 13.5% (PCM 15 mm). However, the increase in the heating energy demand by 13.5% corresponds to an increase of 14 kWh_e, while a reduction in the cooling energy demand by 8.9% corresponds to about 36 kWh_e. The months that show a greater reduction in the cooling energy demand are May and June. In particular, in May the cooling of the PCM scenarios shows a reduction between 28.1% (PCM 5 mm) and 39.8% (PCM 20 mm) if compared to the scenario without PCM, while in June the reduction is between 16% (PCM 5 mm) and 18.1% (PCM 20 mm). As seen in the Fig. 9.8, the energy savings are low during the peak winter and summer months suggesting the fact that the PCM remains either mostly at solid phase (winter) or at liquid phase (summer). For the other months, the climate is favorable to maintain the PCM in the solid-liquid transition phase for a longer duration and hence it has more heat storage capability and energy savings.

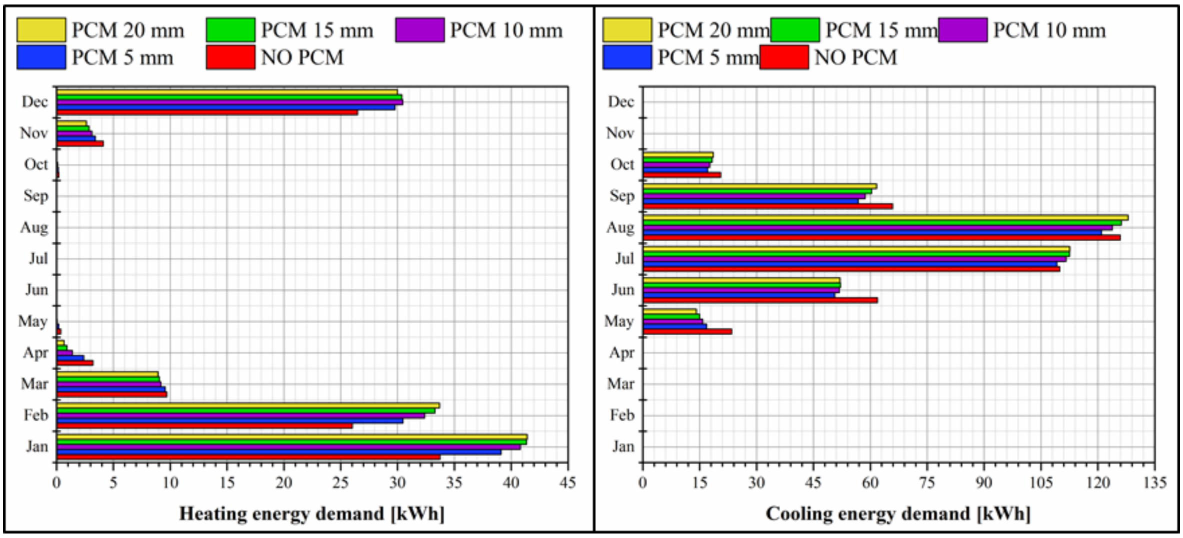

Fig. 9.8 - Heating energy demand and cooling energy demand for all PCM scenarios and for the scenario without PCM.

Fig. 9.9 shows the monthly heating peak power and cooling peak power with and without PCMs. In detail, in the scenario without PCM the monthly heating peak power and cooling peak power occur in February (3 kW) and in August (2.34 kW), respectively. PCMs prove to be impactful in reducing the peaks power of both heating and cooling. In particular, in December the reduction in peaks compared to the scenario without PCM is between 9.2% (PCM 5 mm) and 33.3% (PCM 20 mm). Since in July and in August, due to the high outdoor air temperature, the PCMs remain mostly at liquid phase, no variation in cooling peak power are shown. On the other hand, during the mid-seasons, since the climate is favorable to maintain the PCM in the solid-liquid transition phase for a longer duration, the PCMs showing the greatest energy savings. For example, in May cooling peak power shows a reduction between 46.2% (PCM 10 mm) and 50.3% (PCM 20 mm) compared to the scenario without PCM.

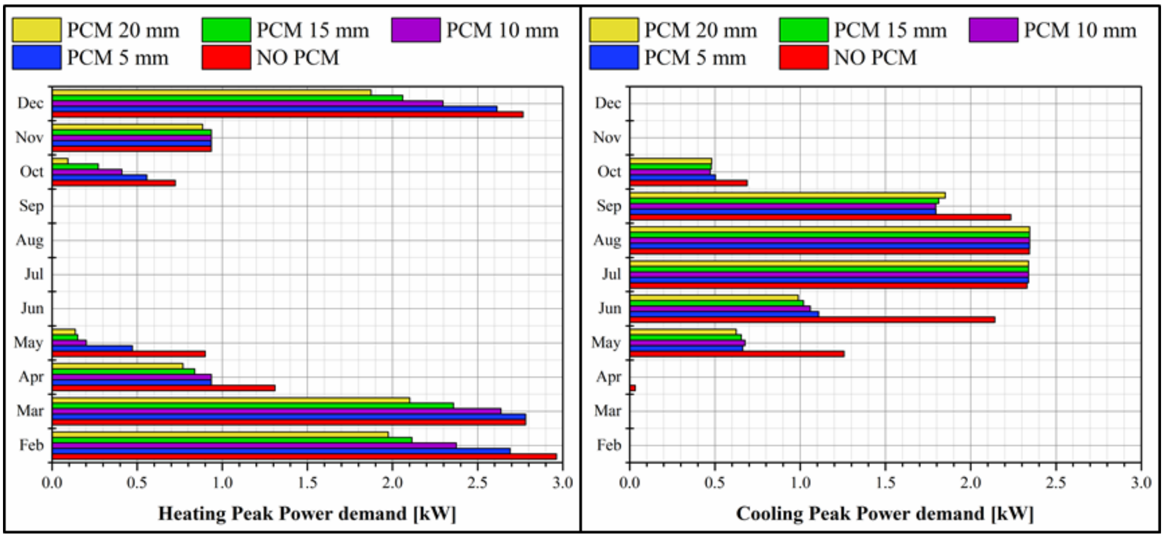

Fig. 9.9 – Heating peak power and cooling peak power for all PCM scenarios and for the scenario without PCM.

As shown in Fig. 9.10, the months that show the greatest building energy demand reduction are May, June and September. In particular, in May, compared to the scenario without PCM, the building energy demand reduction is between -6% (PCM 20 mm) and -4.2% (PCM 5 mm). The yearly building energy demand of the PCM scenarios shows a reduction between 1.1% (PCM 5 mm) and 0.3% (PCM 20 mm) when compared to the scenario without PCM. This is due to the fact that the proposed solution aims to reduce cooling energy demand, which for the scenario without PCM is responsible for 18% of the building energy demand.

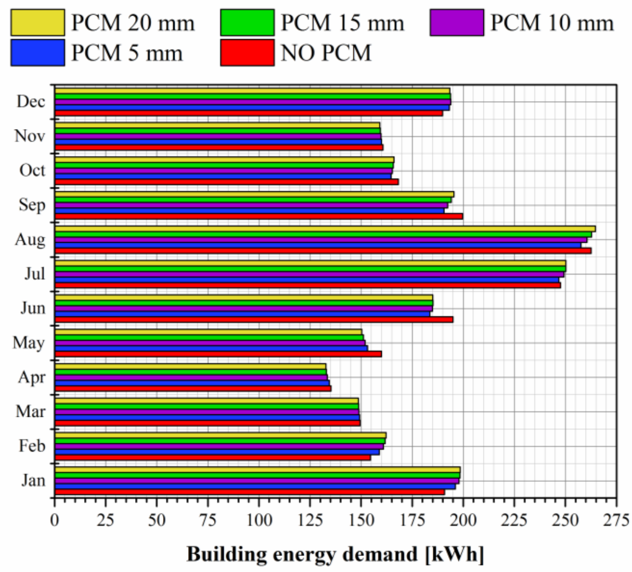

Fig. 9.10 - Building energy demand for all PCM scenarios and for the scenario without PCM.

Tab. 9.16 shows the monthly imported and exported energy with and without PCMs. In detail, in the scenario without PCM, the yearly imported and exported energy are equal to 1035.6 kWh_e and 6890.2 kWh_e, respectively. As shown in Tab. 9.16, exported and imported energy do not show significant variation in the scenarios with PCMs compared to the scenario without PCM. This is due to the fact that the building is equipped with a photovoltaic system with a peak power of 5.76 kW.

Tab. 9.16 – Imported energy and exported energy for all PCM scenarios and for the scenario without PCM.

	Imported energy [kWh]					**Exported energy [kWh]**				
	NO PCM	**PCM 5 mm**	**PCM 10 mm**	**PCM 15 mm**	**PCM 20 mm**	**NO PCM**	**PCM 5 mm**	**PCM 10 mm**	**PCM 15 mm**	**PCM 20 mm**
Jan	130.1	129.4	128.8	128.6	128.4	178.8	172.6	170.3	169.6	169.4
Feb	90.2	88.9	88.4	88.2	88.2	323.9	318.1	315.7	314.6	314.2
Mar	78.8	78.8	78.7	78.6	78.5	616.4	616.5	616.8	616.8	616.8
Apr	67.2	67.1	67.1	67.1	67.1	714.6	715.3	716.3	716.7	717.0
May	65.0	65.0	64.9	64.9	64.9	915.7	922.5	923.6	924.5	925.4
Jun	59.1	59.1	59.1	59.1	59.1	947.2	958.5	957.3	957.0	957.1
Jul	63.0	63.0	63.0	63.0	63.0	1012.7	1013.4	1011.0	1010.1	1010.1
Aug	67.7	67.5	67.5	67.6	67.6	814.2	818.9	816.1	813.8	812.0
Sep	73.7	73.2	73.3	73.3	73.3	572.9	581.6	579.7	578.0	576.7
Oct	92.9	92.2	92.2	92.2	92.2	421.9	424.8	424.2	423.6	423.3
Nov	112.3	111.8	111.7	111.7	111.6	217.3	217.6	217.8	218.0	218.2
Dec	135.6	135.2	134.8	134.5	134.2	154.6	150.9	149.8	149.6	149.6
Year	1035.6	1031.2	1029.5	1028.7	1028.1	6890.2	6910.6	6898.6	6892.4	6889.8

9.6.2 Scenario 3: Life Cycle Assessment results

It was not possible to model the eco-profile of the specific PCM used in this work using primary data, provided by the manufacturer. From this reason secondary data from literature (Aranda-Usón, Ferreira, López-Sabirón, Mainar-Toledo, & Zabalza Bribián, 2013; de Gracia et al., 2010; Kylili & Fokaides, 2016) were used. In particular, the study by Aranda-Usón et al. was used, where the environmental impacts of three commercial PCMs (including the one used in this study) were investigated using the LCA methodology (Aranda-Usón et al., 2013). In detail, all mass inputs of raw materials for PCMs manufacturing were obtained from (Aranda-Usón et al., 2013), while the eco-profiles of raw materials were modelled using the Ecoinvent database (Frischknecht et al., 2005). Due to the lack of data in (Aranda-Usón et al., 2013) it was not possible to model the PCM production process. Moreover, the transport of the raw materials up to the production plant of PCM was not included in the analysis, while that of the finished PCMs from manufactures to the building construction site was considered. Finally, due to the lack of data in the literature, it was not possible to estimate the impacts due to the end of life of the PCMs.

The life cycle impacts investigated, obtained through a simplified LCA of the phase change materials, for all PCM scenarios and for the scenario without PCM are shown in Tab. 9.17. These results exclude the environmental benefits and loads due to the exported energy and resulting from the recycling of materials. As shown in Tab. 9.17, for all the impact indicators investigated, energy and environmental impacts increase with the increase in PCM thickness. For example, the Scenario PCM 5 mm, if compared to the scenario without PCM, shows an increase of all indicators between +0.2% (ODP) and +3.9% (POCP), while the Scenario PCM 20 mm shows an increase of all indicators between +0.4% (ODP) and +5.5% (POCP).

Tab. 9.17 – Life Cycle environmental impacts for all PCM scenarios and for the scenario without PCM.

	No PCM	**PCM 5 mm**		**PCM 10 mm**		**PCM 15 mm**		**PCM 20 mm**	
Indicator	**Impacts**	**Impacts**	**Var.**	**Impacts**	**Var.**	**Impacts**	**Var.**	**Impacts**	**Var.**
GWP [kg CO_{2eq}/m^{2}year]	5.83E+1	5.97E+1	+2.4%	6.01E+1	+3.0%	6.04E+1	+3.5%	6.07E+1	+4.1%
ODP [kg CFC-11$_{eq}$/m^{2}year]	6.43E-5	6.44E-5	+0.2%	6.44E-5	+0.2%	6.45E-5	+0.3%	6.45E-5	+0.4%
AP [kg SO_{2eq}/m^{2}year]	2.68E-1	2.75E-1	+2.6%	2.77E-1	+3.3%	2.79E-1	+4.1%	2.81E-1	+4.8%
EP [kg $PO_4^{3-}{}_{eq}$/m^{2}year]	9.29E-2	9.54E-2	+2.7%	9.60E-2	+3.3%	9.66E-2	+4.0%	9.72E-2	+4.6%
POCP [kg C_2H_{4eq}/m^{2}year]	1.27E-2	1.31E-2	+3.9%	1.32E-2	+4.4%	1.33E-2	+5.0%	1.33E-2	+5.5%
ADP_e [kg Sb_{eq}/m^{2}year]	1.20E-3	1.21E-3	+0.3%	1.21E-3	+0.4%	1.21E-3	-0.5%	1.21E-3	+0.5%
ADP_{ff} [MJ/m^{2}year]	7.20E+2	7.35E+2	+2.1%	7.40E+2	+2.8%	7.44E+2	-3.4%	7.49E+2	+4.0%
GER [MJ/m^{2}year]	1.07E+3	1.09E+3	+1.8%	1.10E+3	+2.5%	1.10E+3	-1.9%	1.11E+3	+3.6%

9.6.3 Scenario 3: Preliminary cost analysis results

It was not possible to determine the cost of the specific PCM used in this work, therefore the literature values shown in Tab. 9.18 were used. In detail, the cost of PCMs varies widely according to their type, melting temperature and purity (which affects melting temperature range and latent heat of fusion) (Kosny, Shukla, & Fallahi, 2013). Unfortunately, it is impossible to take all of these factors into account to accurately estimate the cost of PCM. An average cost was thus estimated from values reported in the literature, using the values for the inorganic PCMs, as it is the type of PCM used in this work. In detail, from the costs reported in Tab. 9.18, an average cost of 57.9 €/m^2/cm was chosen.

Tab. 9.18 – PCM cost.

PCM Type	**€/kg**	**€/m^2/cm**	**Reference**
Organic, paraffins			
Paraffin wax	1.75	13.32	(Kosny et al., 2013)
Eicosan, Laboratory-grade (>99%)	48.69	428.45	(Kosny et al., 2013)
Eicosan, Technical-grade (90%-95%)	6.36	52.96	(Kosny et al., 2013)
Rubitherm RT20	14.74	110.56	(Chaiyat, 2015)
Rubitherm RT (23 - 25 - 27 °C) in CSM	0.62	5.46	(Saffari, de Gracia, Ushak, & Cabeza, 2016)
Smartboard BASF	-	33.33	(Mustaparta, Silva, & Leitão, 2013)
Dupont Energain	-	115.00	(Soares, Reinhart, & Hajiah, 2017)
Organic, fatty acids			
Oleic acid	1.55	13.79	(Kosny et al., 2013)
Biodiesel crude glicerine	0.23	2.88	(Kosny et al., 2013)
PureTemp (min)	1.49	12.82	(Kosny et al., 2013)
PureTemp (max)	4.97	42.73	(Kosny et al., 2013)
BioPCM	1.18	10.13	(Baniassadi, Sajadi, Amidpour, & Noori, 2016)
Inorganic, salt hydrates			
PCM Energy P. Ltd (min)	2.78	41.73	(Kosny et al., 2013)
PCM Energy P. Ltd (max)	4.47	67.07	(Kosny et al., 2013)
Delta-Cool	-	65.00	(Mustaparta et al., 2013)

As shown in Tab. 9.19, investment costs increase linearly with the increase in PCM thickness. Since the energy exchanged with the power grid does not show significant changes compared to the scenario without PCM, these costs / gains of the PCM scenarios do not show appreciable change.

Tab. 9.19 – Preliminary cost analysis results for the scenario 3.

	NO PCM [€]	**PCM 5 mm [€]**	**PCM 10 mm [€]**	**PCM 15 mm [€]**	**PCM 20 mm [€]**
Investment cost	-	3,200	6,400	9,600	12,800
Yearly gain due to the electricity fed into the grid	382.9	382.6	382.7	382.5	382.4
Yearly cost of the electricity purchased from the grid	199.9	199.6	198.6	198.4	198.3

Tab. 9.20 shows the NPV_r values considering the two different discount rates for the all the redesign solutions selected from the scenario 3. The results show that all PCM scenarios are not economically feasibility because all the NPV_r are negative.

Tab. 9.20 – NPV_r analysis for the redesign solutions of the scenario 3.

	PCM 5 mm[€]	**PCM 10 mm[€]**	**PCM 15 mm[€]**	**PCM 20 mm[€]**
r = 2%	-3200	-6379	-9579	-12779
r = 4%	-3200	-6383	-9583	-12783

9.6.4 Scenario 3 summary

Research on PCMs has considered many applications to the building sector during the last two decades, resulting in a considerable amount of literature about successful PCM applications, such as indoor temperature stabilization potential and peak load reduction potential. In particular, the results shows PCMs prove to be impactful in reducing the peaks power of both heating and cooling. In detail, during the mid-seasons, since the climate is favorable to maintain the PCM in the solid-liquid transition phase for a longer duration, the PCMs showing the greatest energy savings. For example, in May cooling peak power shows a reduction between 46.2% (PCM 10 mm) and 50.3% (PCM 20 mm) compared to the scenario without PCM. Furthermore, a reduction in the peaks power translates into a lower nominal power of the HVAC system and therefore also in lower initial and maintenance costs. However, phase change materials were not been selected among the possible solutions to include in the redesign for the case study building for the following reasons:

- For the case study, the PCM selected allow to reduce the yearly building energy demand of only about 1.1% in the best case (PCM 5 mm) if compared to the scenario without PCM.

- The large-scale use of PCMs in the building sector is linked to some challenges to be overcome, such as the high cost of the materials. In detail the preliminary cost analysis showed that, due to the high investment cost, the benefit derived from the decrease of the building energy consumption is not such as to make economically feasible the inclusion of these materials in building envelope the case study.

- The simplified LCA of the PCMs, conducted using only secondary data from literature, showed that the environmental impacts of the building life cycle increase by less than 5.5% in the worst case. However, due to the lack of literature data, some life cycle stages of these materials, such as the production and end-of-life phases, which could result particularly impactful, were not included in the analysis. For these reasons, the simplified LCA analysis may have underestimated the life cycle impacts of these materials.

9.7 Scenario 4: PV system and electric storage system

The building is equipped with a grid-connected photovoltaic system (PV) for the production of electricity. The photovoltaic system has a peak power of 5.76 kW_p, made up of 24 modules of 240 W_p. Even though the overall PV energy generation (8,068 kWh_e) in a year surpasses the electricity consumption (2,677), about 47% of the electricity consumption is supplied by electricity imported from the network. Moreover, since the PV system is oversized about 79% of the energy produced is fed into the grid. The yearly mean value of γ_{load} is equal to 0.44, while the yearly mean value of LOLP and $P_{e\approx 0}$ are equal to 59.69% and 1.01%, respectively, which means that the building needs a continuous interaction with the power grid.

For these reasons, in order to optimize the self-consumption of generated electricity and to reduce the stress on the energy grids, load matching and grid interaction issues were also taken into account in the redesign of module. In this context, a parametric study on the case study selected from the scenario 2 was performed considering the following parameterizations variables:

- PV system nominal power, from 240 W_p to the 5.76 kW_p (step of variation equals to 240 W);

- electric storage system (EES) nominal capacity, from the 0 kWh to 9.6 kWh (step of variation equals to 960 Wh).

The range and the step of PV variation were set according to technical feasibility requirements. In particular, the PV was changed with a 240 W step because the modules already installed have the same nominal power, while the maximum power of installed PV was set to 5.76 kW_p as this corresponds a total area of about 43.3 m^2 (roof area equal to 45 m^2).

The installation of an electric storage system (EES) was investigated to optimize the self-consumption and the degree of self-sufficiency of the building enabling different modes of operation (grid connected, battery-buffered and occasionally stand-alone). In particular, the EES use was aimed at matching the electricity demand of the building with its own solar energy generation. In particular, the maximum EES capacity was set to 9.6 kWh, because for a higher EES capacity the load match and the grid interaction indicators did not show significant improvements.

The energy storage system considered in this study was a sodium / nickel chloride battery, including the battery management interface system. In detail, Tab. 9.21 shows the technical characteristics of the battery for an EES system whit a nominal capacity equals to 9.6 kWh.

Tab. 9.21 – Technical characteristics of the EES system.

Characteristics	**Value**
Nominal voltage [V]	4.80E+01
Open circuit voltage [V]	5.16E+01
Nominal capacity [Ah]	2.00E+02
Nominal energy [Wh]	9.60E+03
Gravimetric energy density [Wh/kg]	9.10E+01
Thermal loss in operation [W]	1.05E+02
Operating temperature range [°C]	−20 to +60
Mass [kg]	1.05E+02
Dimensions [mm]	558 × 496 × 320

9.7.1 Scenario 4: Building energy performances results

Fig. 9.11 shows the variation of the γ_{load} (a), of the γ_{supply} (b), of the LOLP (c), of the $P_{e\approx0}$ (d), of the imported energy (e) and of the exported energy (f) due to the variation of the installed EES and installed PV.

As depicted in Fig. 9.11a, for a fixed EES, an increase of installed PV corresponds to an increase of the yearly mean value of γ_{load}. For example for an EES equals to 0 kWh, with the increase of installed PV, γ_{load} increases exponentially reaching the maximum value of about 0.43 in the case of installed PV equal to 5.76 kW_p, however, for installed power greater than 2.88 kW_p the percentage increase is less than 1%. On the other hand, for an EES equals to 9.6 kWh, it grows much faster as the PV increases reaching the asymptotic value of about 0.98 for a 5.76 PV system, percentage variation compared to the base case (installed PV = 5.76 kW_p and EES = 0 kWh) equal to +126.9%.

For a fixed PV system, load cover factor is considerably higher when the system is equipped with an EES, but the yearly mean value never reach the unit value. For example, whit PV = 5.76 kW_p, 2.88 kWh EES can increase γ_{load} by 103% (to 0.88) compared to the base case (γ_{load} = 0.43) while a capacity of 5.76 kWh increase γ_{load} by 123.8% (0.97). However, this corresponds to doubling the battery size to gain only 9% greater γ_{load}.

As shown in Fig. 9.11c and Fig. 9.11d, the LOLP varies between 0.16 (PV = 5.76 kW_p and EES = 9.6 kWh) and 1 (PV = 0.24 kW_p and EES =0 kWh), while $P_{e\approx0}$ varies between 0 (PV = 0 kW_p and EES = 0 kWh) and 0.73 (PV = 4.32 kW_p and EES = 9.6 kWh). Therefore, between the examined configurations, the installation of 4.32 kW_p PV system and a 9.6 kWh EES system is the one that minimizes the interaction between the building and the grid.

Finally, the exported energy (Fig. 9.11e) varies between 0 kWh_e (PV = 0.24 kW_p and EES = 0 kWh) and 6,885.8 kWh_e (PV = 5.76 kW_p and EES =0 kWh), on the other hand the imported energy (Fig. 9.11e) varies between 38.75 kWh_e (PV = 5.76 kW_p and EES = 9.6 kWh) and 1,883 kWh_e (PV = 0.24 kW_p and EES =0 kWh).

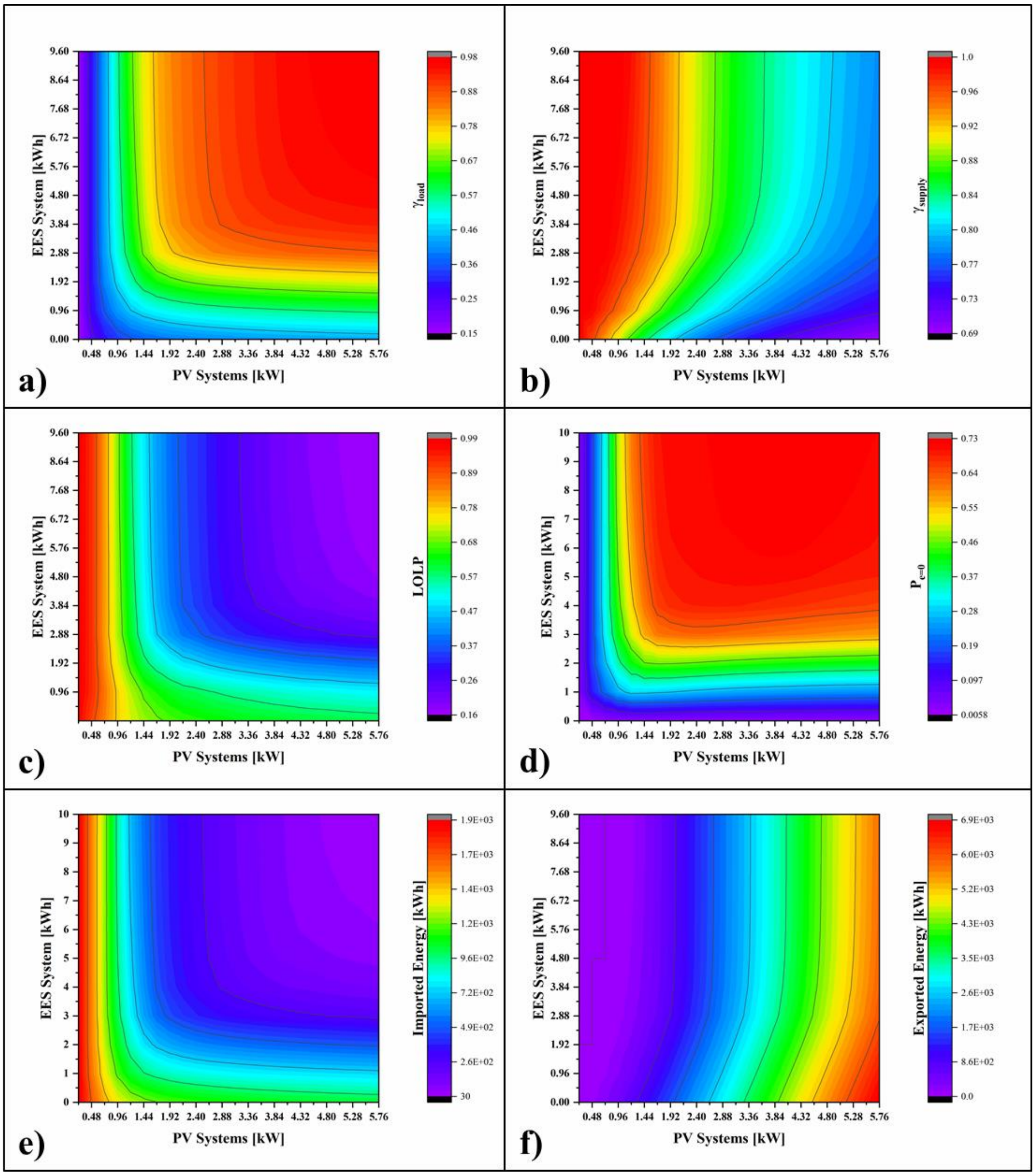

Fig. 9.11 - Variation of the γ_{load} (a), of the γ_{supply} (b), of the LOLP (c), of the $P_{e\approx0}$ (d), of the imported energy (e) and of the exported energy (f) due to the variation of the installed EES and installed PV.

Fig. 9.12 shows the variation of the γ_{load} (a), of the γ_{supply} (b), of the LOLP (c), of the $P_{e\approx0}$ (d), of the imported energy (e) and of the exported energy (f) due to the variation of the installed EES for the following cases selected from Fig. 9.11:

- Case 1: PV = 1.44 kW_p;
- Case 2: PV = 1.68 kW_p;
- Case 3: PV = 1.92 kW_p;
- Case 4: PV = 5.76 kW_p.

In particular, Case 2 was selected because 1.68 kW_p is the lowest nominal power of PV system for which it occurs that the PV energy generation (2,353 kWh_e) in a year surpasses the electricity consumption (2,213 kWh_e). Case 1 (PV = 1.44 kW_p) and case 3 (PV = 1.92 kW_p) were selected because they are the cases in which the nominal power of the PV is slightly lower and higher, respectively, than the case 2. Finally, case 4 (PV = 5.76 kW_p) was selected because it is the case with the greatest yearly PV energy generation (8,068 kWh_e).

Since one of the goals of this scenario was to reduce the stress on the energy grid, among the cases shown in Fig. 9.12, the case PV = 1.92 kW_p and EES = 3.84 kWh (Point A in Fig. 9.12) was chosen as the redesign solution, because, for the same nominal capacity of the batteries included in the 2.88 kWh and 5.76 kWh range, it is the one that shows the higher $P_{e\approx 0}$ index and therefore less interaction with the grid. In particular, a nominal capacity of 3.84 kWh was chosen for the EES system, because for a higher EES capacity the load match and the grid interaction indicators did not show significant improvements. For example, for EES = 4.8 kWh compared to EES = 3.84 kWh, all indices show a variation of less than 4.5% (γ_{load} = + 1.2%; γ_{supply} = 0.27%; LOLP = -1.82%; $P_{e\approx 0}$ = 2.43%; imported energy = -4.21% and Exported energy = -2.4%).

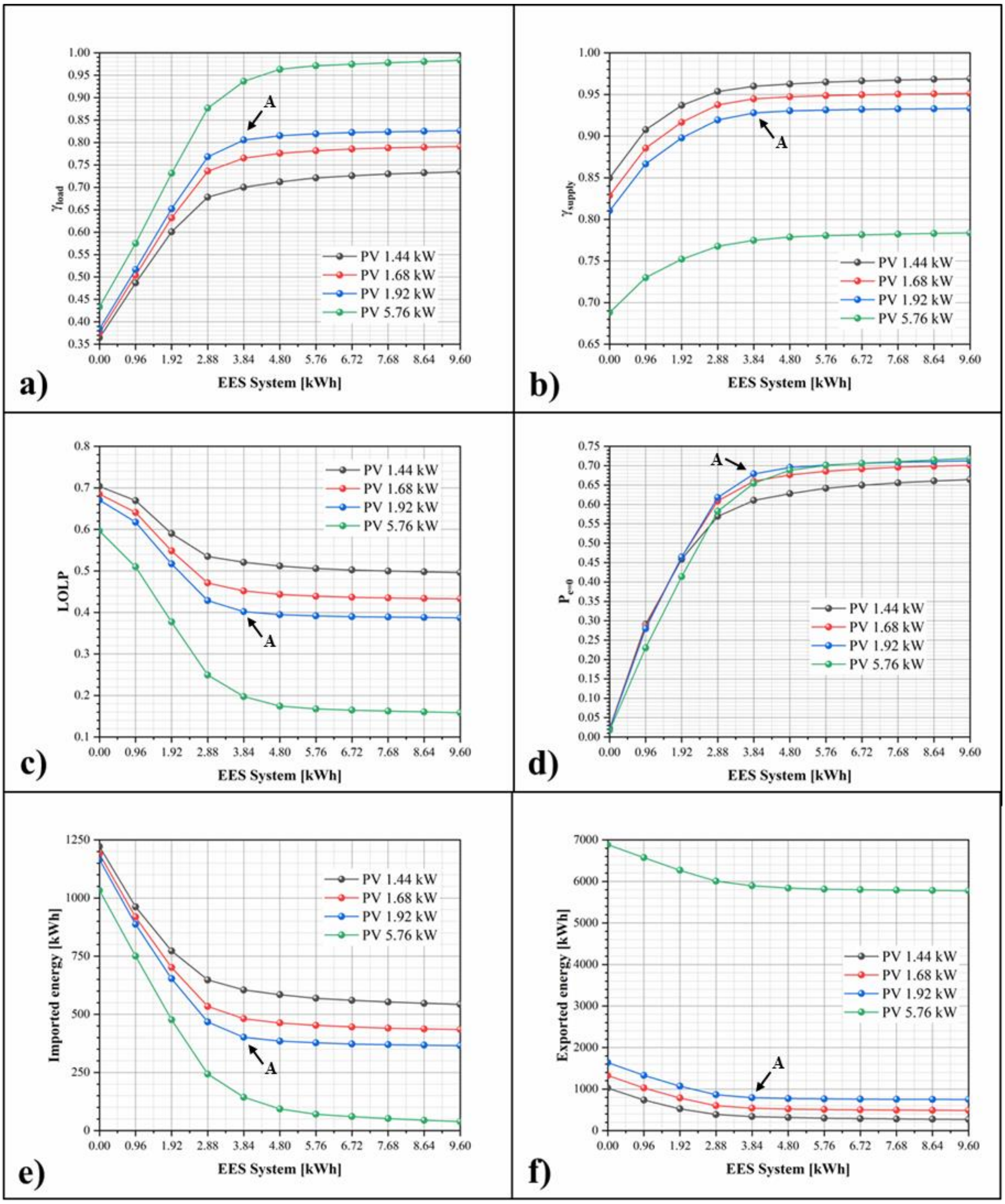

Fig. 9.12 - Variation of the γ_{load} (a), of the γ_{supply} (b), of the LOLP (c), of the $P_{e\approx0}$ (d), of the imported energy (e) and of the exported energy (f) due to the variation of the installed EES for installed PV equal to 1.44 kW_p, 1.68 kW_p, 1.92 kW_p and 5.76 kW_p.

Tab. 9.22 shows the net exported energy (ne) and the monthly mean values of the load cover factor (γ_{load}), the supply cover factor (γ_{supply}), the loss of load probability (LOLP) and the no grid interaction probability ($P_{e\approx0}$) for the case selected in the scenario 2 (PV = 5.76 kW_p, EES = 0 kWh) and for the case selected in this scenario (PV = 1.92 kW_p, EES = 3.84 kWh). As the case selected in this scenario is also the best case chosen as the final redesign solution of the building case study, more details on its energy performance will be given in section 9.8, where the energy, the environmental and the economic performance of the final redesign solution are compared to real building case study.

Due to the reduction of the nominal power of the PV system, the yearly net exported energy shows a decrease of 5,464 kWh_e, at the monthly level the difference between the net exported of the case selected in the scenario 2 and the redesign solution is between -142.4 kWh_e (December) and -805.2 kWh_e (August). Since the EES system allows to match the building energy demand with the PV energy generation, the others indices shown in Tab. 9.22 (γ_{load}, γ_{supply}, LOLP and $P_{e\approx0}$) show significant changes. The yearly mean value of the load cover factor and the supply cover factor vary from the values of 0.43 and 0.69 of the case selected in the scenario 2 to the values of 0.81 and 0.93 of the proposed solution, respectively. In particular, γ_{load} equal to 0.81 means that on yearly basis the 81% of the building electric demand is covered by on-site electricity generation, while γ_{supply} equal to 0.93 means that on yearly basis the 93% of the PV generation is used on-site. However, as the PV system fails to cover the peaks of the building energy demand, due to the building's heating and cooling, the LOLP shows an annual reduction of 19.5%. The difference between the LOLP of the case selected in scenario 2 and that of the redesign solution varies between -8% (December) and +34.4% (July and August). Finally, as shown by the index $P_{e\approx0}$, which on an annual basis has varied from 0.94% of the case selected in the scenario 2 to 67.9% of the redesign solution, the battery allows to greatly reduce interactions with the electricity grid.

Tab. 9.22 – Net exported energy (ne), load cover factor (γ_{load}), supply cover factor (γ_{supply}), loss of load probability (LOLP) and no grid interaction probability ($P_{e\approx0}$) – Scenario 4.

	ne [kWh$_e$]		**γ_{load}**		**γ_{supply}**		**LOLP [%]**		**$P_{e\approx0}$ [%]**	
	Case Sc. 2	**Case Sc. 4**	**Case Sc. 2**	**Case Sc. 4**	**Case Sc. 2**	**Case Sc. 4**	**Case Sc. 2**	**Case Sc. 4**	**Case Sc. 2**	**Case Sc. 4**
Jan	48.62	-115.37	0.30	0.40	0.82	1.00	73.3	76.8	1.1	35.2
Feb	233.68	-32.51	0.36	0.81	0.74	0.99	65.9	42.7	0.8	76.2
Mar	537.55	68.85	0.44	0.94	0.67	0.89	58.3	27.5	0.9	78.7
Apr	647.32	117.51	0.49	0.99	0.62	0.86	53.4	24.4	1.0	80.0
May	850.76	169.40	0.52	0.98	0.59	0.83	50.3	23.1	0.9	73.7
Jun	888.13	158.75	0.55	0.99	0.58	0.84	47.8	21.5	0.9	74.6
Jul	948.78	143.58	0.54	1.00	0.60	0.86	49.1	19.7	0.7	78.1
Aug	747.38	64.67	0.51	0.98	0.64	0.93	52.8	22.4	0.9	84.9
Sep	499.24	24.90	0.46	0.93	0.68	0.95	58.1	27.7	0.9	82.1
Oct	329.04	-9.26	0.40	0.85	0.71	0.98	62.7	38.5	0.7	78.9
Nov	105.06	-76.92	0.34	0.49	0.77	1.00	69.1	74.3	1.1	45.8
Dec	18.98	-123.39	0.28	0.33	0.84	1.00	75.7	83.7	1.5	27.7
Year	5854.54	390.23	0.43	0.81	0.69	0.93	59.7	40.2	0.94	67.9

9.7.2 Scenario 4: Life Cycle Assessment results

Due to the lack of data in the Ecoinvent database (Frischknecht et al., 2005), the environmental impact due to the production and to the end-of-life of the electrical energy storage systems were calculated using literature values. In particular, the study by Longo et al. was used, where the environmental and energy impacts of a sodium / nickel chloride battery with a nominal capacity of 9.6 kWh were investigated using the LCA methodology (Longo, Antonucci, Cellura, & Ferraro, 2013). Tab. 9.23 shows the results obtained from the authors referring to the functional unit of this work (1 m^2 of building useful floor area with reference to 1 year). Moreover, since the authors analyze an EES with a nominal capacity of 9.6 kWh, the impacts for an EES system with a lower capacity than 9.6 kWh were reduced linearly.

Tab. 9.23 – Energy and environmental impacts of an EES = 9.6 kWh (Longo et al., 2013).

Indicator	**Impacts**
GWP [kg CO_{2eq}/m^2year]	1.46E+00
ODP [kg CFC-11_{eq}/m^2year]	1.61E-07
AP [kg SO_{2eq}/m^2year]	2.76E-02
EP [kg $PO_4^{3-}{}_{eq}$/m^2year]	1.05E-02
POCP [kg C_2H_{4eq}/m^2year]	1.17E-03
ADP_e [kg Sb_{eq}/m^2year]	4.49E-05
ADP_{ff} [MJ/m^2year]	1.78E+01
GER [MJ/m^2year]	2.29E+01

The life cycle impacts for all case investigated in this scenario are shown in Fig. 9.13 and in Fig. 9.14. In detail, Fig. 9.13 shows the variation of the GWP (a), of the ODP (b), of the AP (c) and of the EP (d) due to the variation of the installed EES and installed PV, while Fig. 9.14 shows the variation of the ADP_e (a), of the ADP_{ff} (b), of the POCP (c) and of the GER (d). As for the previous scenarios, these results exclude the environmental benefits and loads due to the exported energy and resulting from the recycling of materials since.

As shown in Fig. 9.13a, the GWP varies between 43.1 kg CO_{2eq}/m^2year (PV = 3.84 kW_p and EES = 5.76 kWh) and 67.2 kg CO_{2eq}/m^2year (PV = 0.24 kW_p and EES = 9.6 kWh). In particular, the minimum and maximum values of the GWP show changes in impacts compared to the case selected in scenario 2 (PV = 5.76 kW_p, EES = 0 and GWP = 58.29 kg CO_{2eq}/m^2year) of -26.1% and + 23.5%, respectively.

The ODP (Fig. 9.13b) varies between 6.23E-05 kg CFC-11_{eq}/m^2year (PV = 2.16 kW_p and EES = 4.8 kWh) and 6.42E-05 kg CFC-11_{eq}/m^2year (PV = 5.76 kW_p and EES = 0 kWh). The maximum value of the ODP shows a variation with respect to the case selected in scenario 2 of -2.96%.

As depicted in Fig. 9.13c, the AP varies between 206.2 g SO_{2eq}/m^2year (PV = 4.08 kW_p and EES = 4.8 kWh) and 338.7 g SO_{2eq}/m^2year (PV = 0.24 kW_p and EES = 9.6 kWh). The minimum and maximum values of the AP show changes in impacts compared to the case selected in scenario 2 (AP = 268.19 g SO_{2eq}/m^2year) of -23.1% and +26.3%, respectively.

Finally, the EP (Fig. 9.13d) varies between 7.52E-02 kg $PO_4^{3-}{}_{2eq}$/m^2year (PV = 2.64 kW_p and EES = 4.8 kWh) and 1.07E-01 kg $PO_4^{3-}{}_{2eq}$/m^2year (PV = 0.24 kW_p and EES = 9.6 kWh). The minimum and maximum values of the EP show changes in impacts compared to the case selected in scenario 2 (EP = 9.29E-02 kg $PO_4^{3-}{}_{eq}$/m^2year) of -22.6% and +26.3%, respectively.

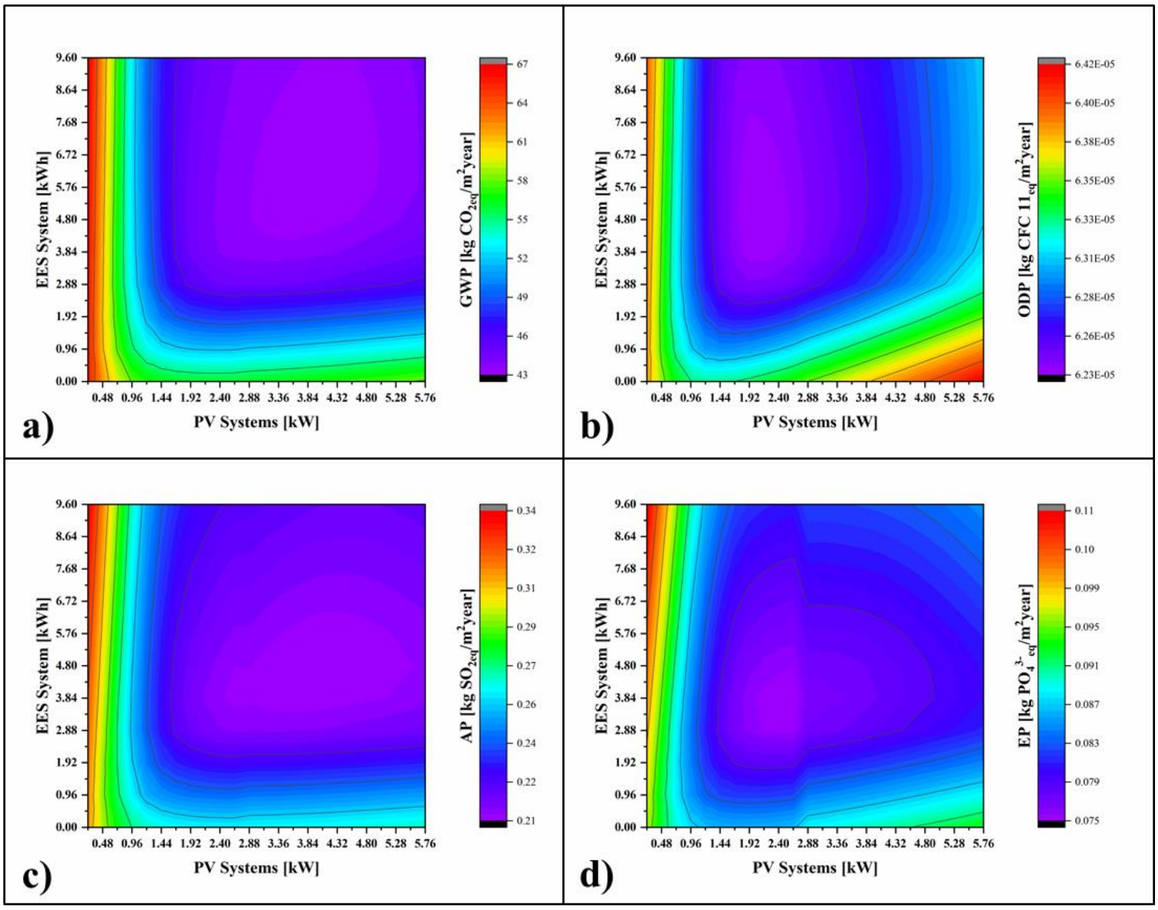

Fig. 9.13 - Variation of the GWP (a), of the ODP (b), of the AP (c) and of the EP (d) due to the variation of the installed EES and installed PV.

As shown in Fig. 9.14a, the ADP_e varies between 0.37 g Sb_{eq}/m^2year (PV = 0.24 kW_p and EES = 0 kWh) and 1.28 g Sb_{eq}/m^2year (PV = 5.76 kW_p and EES = 9.6 kWh). The minimum and maximum values of the ADP_e show changes in impacts compared to the case selected in scenario 2 (ADP_e = 1.20 g Sb_{eq}/m^2year) of -69.5% and +1.9%, respectively.

The ADP_{ff} (Fig. 9.14b) varies between 531.4 MJ/m^2year (PV = 3.84 kW_p and EES = 5.76 kWh) and 831.8 MJ/m^2year (PV = 0.24 kW_p and EES = 9.6 kWh). The minimum and maximum values of the ADP_{ff} show changes in impacts compared to the case selected in scenario 2 (ADP_{ff} = 719.2 MJ/m^{2}year) of -26.1% and +15.7%, respectively.

As depicted in Fig. 9.14c, the POCP varies between 9.9 g C_2H_{4eq}/m^{2}year (PV = 2.64 kW$_p$ and EES = 3.84 kWh) and 15.2 g C_2H_{4eq}/m^{2}year (PV = 0.24 kW$_p$ and EES = 9.6 kWh). The minimum and maximum values of the POCP show changes in impacts compared to the case selected in scenario 2 (POCP = 12.7 g C_2H_{4eq}/m^{2}year) of -21.4% and +20.3%, respectively.

Finally, the GER (Fig. 9.14d) varies between 892.8 MJ/m^{2}year (PV = 2.64 kW$_p$ and EES = 4.8 kWh) and 1127.9 MJ/m^{2}year (PV = 0.24 kW$_p$ and EES = 9.6 kWh). The minimum and maximum values of the EP show changes in impacts compared to the case selected in scenario 2 (GER = 1074 MJ/m^{2}year) of -16.9% and +5.0%, respectively.

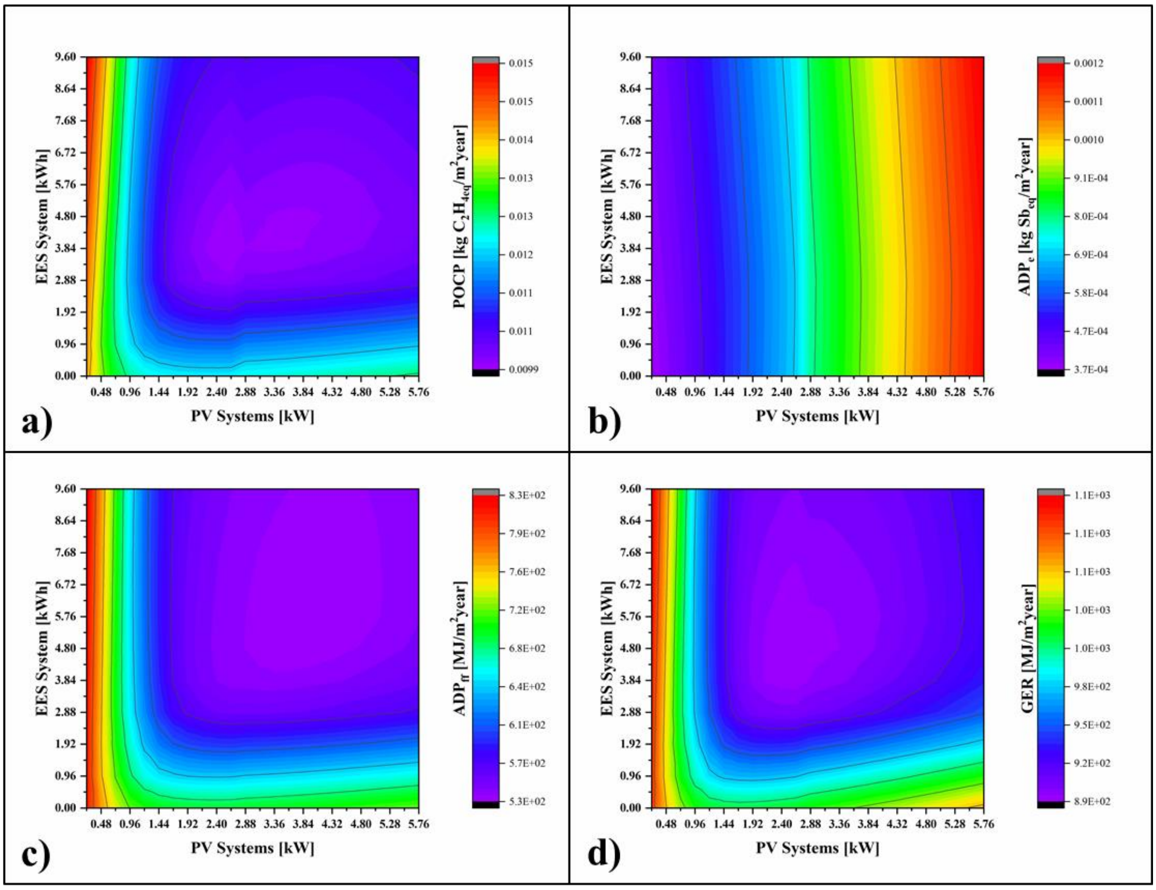

Fig. 9.14 - Variation of the ADP_e (a), of the ADP_{ff} (b), of the POCP (c) and of the GER (d) due to the variation of the installed EES and installed PV.

The life cycle impacts for the case selected in the scenario 2 and for the proposed solution in this scenario are shown in Tab. 9.24. In detail, for all the impact indicators investigated, if compared to the case selected in the scenario 2, the proposed solution in this scenario shows a reduction in the environmental and energy impacts between 2.8% (ODP) and 55.4% (ADP_e). Moreover, except for ODP, all indicators show a reduction greater than 15% compared to the base case: GWP (23.4%), AP (20.8%), EP (20%), POCP (20.8%), ADP_{ff} (23.2%) and GER (16.6%).

Tab. 9.24 – Life Cycle environmental impacts for the case selected in the scenario 2 and for the case selected in the scenario 4.

Indicator	Case selected in Scenario 2	Case selected in Scenario 4	Variation
GWP [kg CO_{2eq}/m^2year]	5.83E+01	4.47E+01	-23.38%
ODP [kg CFC-11_{eq}/m^2year]	6.42E-05	6.24E-05	-2.83%
AP [kg SO_{2eq}/m^2year]	2.68E-01	2.13E-01	-20.81%
EP [kg $PO_4^{3-}{}_{eq}$/m^2year]	9.29E-02	7.44E-02	-19.98%
POCP [kg C_2H_{4eq}/m^2year]	1.26E-02	1.00E-02	-20.79%
ADP_e [kg Sb_{eq}/m^2year]	1.20E-03	5.37E-04	-55.39%
ADP_{ff} [MJ/m^2year]	7.19E+02	5.53E+02	-23.21%
GER [MJ/m^2year]	1.07E+03	8.96E+02	-16.59%

Tab. 9.25 shows the comparison between the life cycle impacts for the proposed solution in this scenario, selected trying to reduce the stress on the electricity, and the absolute minimum values of all the impact categories investigated. As shown in Tab. 9.25, there is no a unique system configuration that allows to minimize all the examined impact categories at the same time. Moreover, although the case selected in this scenario does not ensure the lowest impacts among all the configurations examined in this scenario, except for ADP_e, shows variations with respect to the optimal configurations below 4.5%, reaching values below 1% in the case of ODP and GER.

Tab. 9.25 – Comparison between the life cycle impacts for the proposed solution in this scenario and the absolute minimum values.

Indicator	Minimum impact	PV system [kW_p]	EES System [kWh]	**Case selected in Scenario 4**	**Variation**
GWP [kg CO_{2eq}/m^2year]	4.85E+04	3.84	5.76	5.05E+04	4.16%
ODP [kg CFC-$11_{eq}/m^2year$]	7.01E-02	2.16	4.8	7.01E-02	0.01%
AP [kg SO_{2eq}/m^2year]	2.32E+02	4.08	4.8	2.41E+02	3.84%
EP [kg $PO_4^{3-}{}_{eq}/m^2year$]	8.46E+01	2.64	4.8	8.55E+01	1.08%
POCP [kg C_2H_{4eq}/m^2year]	1.12E+01	2.64	3.84	1.14E+01	2.32%
ADP_e [kg Sb_{eq}/m^2year]	4.13E-01	0.24	0	6.69E-01	62.20%
ADP_{ff} [MJ/m^2year]	5.98E+05	3.84	5.76	6.24E+05	4.39%
GER [MJ/m^2year]	1.00E+06	2.64	4.8	1.01E+06	0.81%

9.7.3 Scenario 4: Preliminary cost analysis results

In order to verify the economic feasibility of the proposed redesign solution, a preliminary cost analysis was conducted. In detail, the investment cost was estimated, through a literature survey, which allowed to determine the cost of the systems involved in the redesign. The general assumptions are summed up in Tab. 9.26 (Baumann et al., 2017; Peters, Baumann, Zimmermann, Braun, & Weil, 2017). In particular, for the PV system an investment cost of 1500 €/kW was considered, while for the EES system the investment cost of 500 €/kWh was used. The installation cost were not considered since their value was assumed to be the same for both the base case and the redesign solution. Moreover, the costs / gains due to the energy exchange with the network were estimated as explained in 9.3.2 and 9.3.3.

Tab. 9.26 – Systems costs assumed for the scenario 4.

	Cost
PV system [€/kW_p]	1500
EES system [€/kWh]	500

Fig. 9.15 shows the variation of the investment costs due to the variation of the installed EES and installed PV, while Fig. 9.16 shows the variation of the costs (a) and of the gains (b) of the energy exchange with the electricity grid. As shown in Fig. 9.15, the investment cost varies between € 360 (PV = 0.24 kW_p and EES = 0 kWh) and €

13,440 (PV = 5.76 kW_p and EES = 9.6 kWh). In particular, the minimum and maximum values of the investment cost show changes compared to the case selected in scenario 2 (investment cost = 8,640 €) of -95.8% and +55.6%, respectively. The yearly cost of energy imported from the grid (Fig. 9.16a) varies between € 7.5 (PV = 5.76 kW_p and EES = 9.6 kWh) and € 363.4 (PV = 0.24 kW_p and EES = 0 kWh). The minimum and maximum values of the investment cost show changes compared to the case selected in scenario 2 (cost of imported energy = 199.3 €) of -96.2% and +82.3%, respectively. Finally, as depicted in Fig. 9.16b, the economic gain due to the energy fed into the electricity grid varies between € 0 (PV = 0.24 kW_p and EES = 0.96 kWh) and € 371.5 (PV = 5.76 kW_p and EES = 0 kWh).

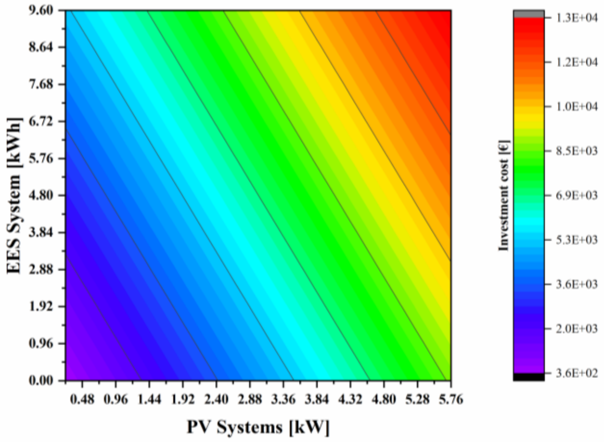

Fig. 9.15 - Variation of the investment costs due to the variation of the installed EES and installed PV.

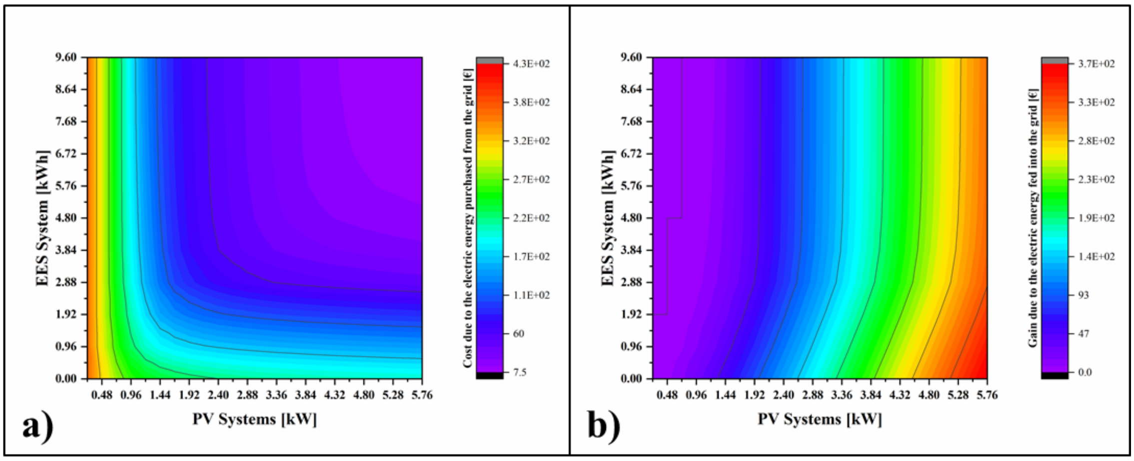

Fig. 9.16 - Variation of the costs (a) and of the gains (b) of the energy exchange with the electricity grid due to the variation of the installed EES and installed PV.

Tab. 9.27 shows the preliminary cost analysis results for the case selected from the scenario 2 and for the redesign case selected from the scenario 4. The results show that the proposed solution allows to reduce the initial investment costs due to the reduction of the nominal power of the PV system of about € 3,840. Moreover, since the storage capacity allows to match the electricity demand of the building with its own solar energy generation, the yearly costs of energy imported from the grid decrease of about € 122. However, since the nominal power of the photovoltaic system compared to the base case was reduced by 3.84 kW_p, the yearly gains due to the energy fed into the electricity grid decrease of about € 340.

Tab. 9.27 – Preliminary cost analysis results for the scenario 4.

		Base Case [€]	Envelope Redesign [€]
Investment cost	PV system	8,640	2,880
	EES system	-	1,920
	Tot.	8,640	4,800
Yearly gain due to the electricity fed into the grid		383	43
Yearly cost of the electricity purchased from the grid		200	78

9.7.4 Scenario 4 summary

The results show that oversizing the PV system shows that the building self-sufficiency does not undergo significant improvements. For example, in the case of installed PV equal to 1.92 kWp (EES = 0 kWh), the yearly γ_{load} variation compared to the base case (PV = 5.76 kW_p and EES = 0kWh) is only equal to 0.05. However, this corresponds to three times the size of the PV system. Therefore, in order to reach the nZEB target, the challenge to be faced is not only limited to reaching a balance between a building's energy consumption and renewable energy production, because a poorly-designed building could even achieve the goal of net zero energy per year simply by means of oversizing the PV system. However, an oversized PV system may not be particularly efficient for the building load match and grid interaction.

On the other hand, the degree of self-sufficiency of the building is improved by increasing storage capacity that allows to match the electricity demand of the building with its own solar energy generation. The greater the storage, the greater the load cover factor, because the storage system is able to supply the loads even when generation is not taking place. However, as the storage is an environmentally impactful and costly element of the system, it should be as small as possible.

Among all cases exanimated in this scenario, the case PV = 1.92 kW_p and EES = 3.84 kWh was chosen as the redesign solution. The yearly mean value of the load cover factor and the supply cover factor vary from the values of 0.44 and 0.70 of the base case to the values of 0.81 and 0.93 of the proposed solution, respectively. In particular, γ_{load} equal to 0.81 means that on yearly basis the 81% of the building electric demand is covered by on-site electricity generation, while γ_{supply} equal to 0.93 means that on yearly basis the 93% of the PV generation is used on-site. Moreover, as shown by the index $P_{e\approx 0}$, which on an annual basis has varied from 0.9% of the base case to 67.9% of the redesign solution, the battery allows to greatly reduce interactions with the electricity grid.

The preliminary cost analysis results show that the redesign solution is economically feasibility, the NPV_r after 25 years is positive by either a 2.00% (NPV_r = € 740) discount rate or a 4% discount rate (NPV_r = € 1,507).

The LCA results show that, for all the impact categories investigated, if compared to the base case the proposed solution shows a reduction in the environmental and energy impacts between 3.1% (ODP) and 50.5% (ADP_e). In detail, the operational energy use (Module B6), due to the reduction of the imported energy, shows the highest impacts reduction followed by the Modules C2 –C4 and the materials production stage (Modules A1 –A3).

9.8 THE REDESIGN SOLUTION

In this section, based on the redesign choices made in the previous sections, the results on building energy performances, the Life Cycle Assessment and cost analysis of the final redesign solution (obtained from scenarios 1, 2 and 4) are compared to those of the base case. In detail, compared to the base case this solution includes:

- variation of the WWRs of the north façade from 65% case to 15%
- variation of the WWRs of the south façade from 90% to 15%
- variation of the insulation thickness on all the exterior walls from 9 cm to 6 cm;
- definition of a natural ventilation strategy;
- variation of the PV system nominal power from the 5.76 kWp to 1.92 kWp;

- sizing of a 3.84 kWh electric storage system.

9.8.1 Building energy performances results

Results on a monthly base for building energy demand, heating energy demand, cooling energy demand, lighting energy demand and the PV generation for the base case and for the redesign solution are reported in Tab. 9.28.

The yearly building energy demand of the redesign solution compared to the base case decreases by 17.3% (-463.8 kWh_e), in particular the cooling consumption decreases by 57.3% (-547.6 KWh_e) while the consumption of lighting and heating, due to the reduction of the surface windows, increase by 54.7% (+35 kWh_e) and 88% (+48.7 kWh_e). A 17.3% reduction in the building energy demand compared to the 57.3% reduction of the cooling energy demand is due to the fact that in the redesign scenario, the cooling energy demand is responsible for 18.41% of the total consumption, while 72.4% is due to the non-modifiable electricity consumption of the building. At the monthly level the difference between the building energy demand of the redesign solution and the base case is between +17.5 kWh_e (February) and -94.7 kWh_e (August). In particular, the months of January, February and December show an increase in total consumption of +17 kWh_e, +17.5 kWh_e and +14.8 kWh_e, respectively. While the months showing a greater reduction in consumption are August (-94.7 kWh_e), July (-81.8 kWh_e) and May (-81.1 kWh_e). These months are also the months that show the most significant reductions in the cooling energy demand, in particular: -81.1% in May and -43.1% in July and in August.

Due to the reduction of the nominal power of the PV system from 5.76 kW_p to 1.92 kW_p, the yearly PV generation of the redesign solution shows a decrease of 5,379 kWh_e, at the monthly level the difference between the PV generation of the base case and the redesign solution is between -139.3 kWh_e (December) and -798.1 kWh_e (August).

Tab. 9.28 – Building energy demand, heating energy demand, cooling energy demand, lighting energy demand and PV generation for the base case and for the redesign solution.

	Heating		**Cooling**		**Lighting**		**Tot**		**PV**	
	Base	**Redesign**	**Base**	**Redesign**	**Base**	**Redesign**	**Base**	**Redesign**	**Base**	**Redesign**
	kWh_e	**kWh_e**	**kWh_e**	**kWh_e**	**kWh_e**	**kWh_e**	**kWh_e**	**kWh_e**	**kWh_e**	**kWh_e**
Jan	22.3	33.7	0	0	15.4	20.9	173.8	190.8	239.4	79.8
Feb	10.9	26.0	12	0	1.9	5.5	137	154.5	388.2	129.4
Mar	2.0	9.7	30.2	0	0	3.6	168.4	149.4	687	229.0
Apr	0.4	3.2	37.1	0	0	0.3	169.3	135.3	782.6	260.9
May	0	0.4	104.8	23.4	0	0	241	159.9	1010.7	336.9
Jun	0	0	142.8	61.9	0	1.3	274.5	195.0	1083.1	361.0
Jul	0	0	193.2	109.9	0	1.5	329.3	247.5	1197.2	399.1
Aug	0	0	221.1	125.9	0	0.5	357.3	262.6	1009.0	336.3
Sep	0	0	138.1	65.9	0.10	2	269.9	199.6	698.8	232.9
Oct	0	0.2	78.4	20.6	5.8	11.3	220.3	168.2	497.3	165.8
Nov	1.3	4.1	8.3	0	20.0	24.8	161.4	160.7	265.8	88.6
Dec	18.1	26.5	0	0	20.8	27.3	175.1	189.9	208.9	69.6
Year	55.0	103.8	955.1	407.5	64	99	2677.2	2213.4	8068	2689.3

Tab. 9.29 shows the monthly exported energy and the monthly imported energy for a year as well as the net exported energy for the base case and for the redesign solution. Due to the reduction of the nominal power of the PV system, the yearly exported energy shows a decrease of 6,140.3 kWh_e, at the monthly level the difference between the exported energy of the base and the redesign solution is between 159.9 kWh_e (December) and 787.8 kWh_e (July). Moreover, during the winter months (January, November and December), the redesign solution does not feed energy into the grid. On the other hand, since the EES system allows to match the building energy demand with the PV energy generation, the yearly imported energy decreases of 599.8 kWh_e, while at the monthly level the difference between the imported energy of the base and the redesign solution is between 2.64 kWh_e (December) and 67.2 kWh_e (October).

Tab. 9.29 – Delivered, exported and net exported energy for the case study for the base case and for the redesign solution.

	Imported energy		Exported energy		Net exported energy	
	Base	Redesign	Base	Redesign	Base	Redesign
	kWh_e	kWh_e	kWh_e	kWh_e	kWh_e	kWh_e
Jan	120.78	115.37	186.37	0.00	65.59	-115.37
Feb	83.41	36.24	334.62	3.73	251.20	-32.51
Mar	76.87	10.06	595.51	78.91	518.64	68.85
Apr	67.09	1.44	680.43	118.95	613.33	117.51
May	65.04	3.03	834.77	172.44	769.73	169.40
Jun	59.27	0.97	867.83	159.73	808.56	158.75
Jul	63.49	0.00	931.41	143.58	867.92	143.58
Aug	69.70	3.13	721.45	67.80	651.75	64.67
Sep	74.21	9.81	503.13	34.70	428.93	24.90
Oct	88.48	21.24	365.40	11.98	276.92	-9.26
Nov	107.01	76.92	211.38	0.00	104.37	-76.92
Dec	126.03	123.39	159.85	0.00	33.82	-123.39
Year	1001.38	401.60	6392.14	791.82	5390.76	390.23

Fig. 9.17 shows the instantaneous γ_{load} for the whole year for the base case and for the redesign. In detail, as shown in Fig. 9.17a for the base case, the instantaneous γ_{load} strictly follow the on-site PV generation. It reaches the unit values during the day as generation reaches its peak, decreases during low solar radiation hours while during the night it is equal to zero. On the other hand, as shown in Fig. 9.17b for the redesign solution, if the building is equipped with 3.84 kWh EES system and 1.92 kW PV system, γ_{load} varies largely, mostly during no occupation hours. This is due to the fact that the storage system allows to accumulate the energy during the maximum hours of insolation and use it at night to cover the base load.

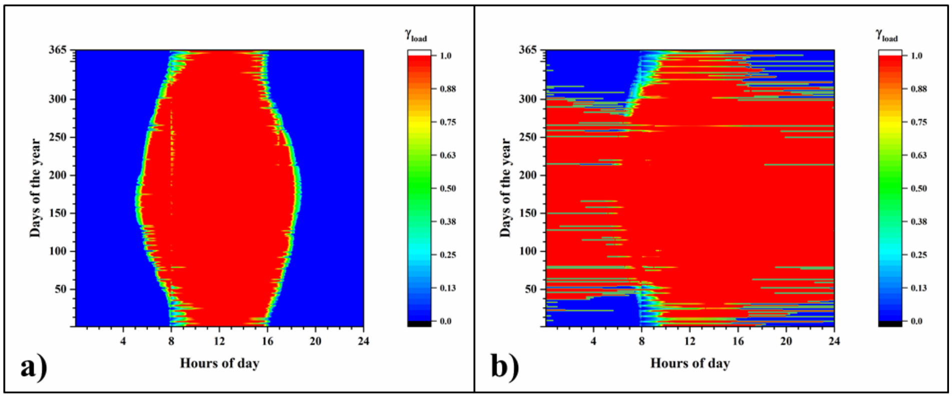

Fig. 9.17 - Instantaneous γ_{load} for the whole year for the base case and for the redesign solution.

To further explore the impact of the proposed solution on the building-grid interaction, Tab. 9.30 shows the monthly mean values of the load cover factor (γ_{load}), the supply cover factor (γ_{supply}), the loss of load probability (LOLP) and the no grid interaction probability ($P_{e\approx0}$) for the base case and for the redesign solution.

The yearly mean value of the load cover factor and the supply cover factor vary from the values of 0.44 and 0.7 of the base case to the values of 0.81 and 0.93 of the proposed solution, respectively. As the PV system fails to cover the peaks of the building energy demand, due to the building's heating and cooling, the LOLP shows an annual reduction of 19.5%. The difference between the LOLP of the base case and that of the redesign solution varies between -8% (December) and +34.4% (July and August). Finally, as shown by the index $P_{e\approx0}$, which on an annual basis has varied from 0.9% of the base case to 67.9% of the redesign solution, the battery allows to greatly reduce interactions with the electricity grid.

Tab. 9.30 – Load cover factor (γ_{load}), supply cover factor (γ_{supply}), loss of load probability (LOLP) and no grid interaction probability ($P_{e\approx0}$).

	γ_{load}		γ_{supply}		**LOLP [%]**		**$P_{e\approx0}$ [%]**	
	Base Case	**Redesign**	**Base Case**	**Redesign**	**Base Case**	**Redesign**	**Base Case**	**Redesign**
Jan	0.31	0.40	0.81	1.00	73.3	76.8	1.1	35.2
Feb	0.37	0.81	0.73	0.99	65.9	42.7	0.9	76.2
Mar	0.44	0.94	0.67	0.89	58.3	27.5%	0.9	78.7
Apr	0.49	0.99	0.63	0.86	53.4	24.4	1.0	80.0
May	0.52	0.98	0.62	0.83	50.3	23.1	0.9	73.7
Jun	0.55	0.99	0.61	0.84	47.8	21.5	0.9	74.6
Jul	0.54	1.00	0.63	0.86	49.1	19.7	0.8	78.1
Aug	0.51	0.98	0.68	0.93	52.8	22.4	1.0	84.9
Sep	0.46	0.93	0.72	0.95	58.1	27.7	1.0	82.1
Oct	0.40	0.85	0.74	0.98	62.7	38.5	0.9	78.9
Nov	0.34	0.49	0.77	1.00	69.1	74.3	1.0	45.8
Dec	0.29	0.33	0.83	1.00	75.7	83.7	1.7	27.7
Year	0.44	0.81	0.70	0.93	59.7	40.2	1.0	67.9

9.8.2 Life Cycle Assessment results

The life cycle impacts investigated for the base case and for the building redesign solution are shown in Tab. 9.31. These results exclude the environmental benefits and loads due to the exported energy and resulting from the recycling of materials since, according to the regulation UNI EN 15978 (UNI, 2011b), they are allocated outside the system boundaries (Module D).

In particular, the redesign solution is responsible for the emissions of 44.7 kg of CO_{2eq}/m^2year and for the consumption of 896.2 MJ/m^2year of primary energy, moreover it is responsible for the emissions of 0.21 kg SO_{2eq}/m^2year, 6.24E-5 kg CFC-$11_{eq}/m^2$year and 10.2 g $PO_4{}^{3-}{}_{eq}/m^2$year. As shown in Tab. 9.31, for all the impact indicators investigated, if compared to the base case the proposed solution shows a reduction in the environmental and energy impacts between 3.1% (ODP) and 50.5% (ADP_e). In particular, a reduction of 3.1% of the ODP is due to the fact that the greatest impact on this indicator is due to the thermal plant that has remained unchanged in the redesign solution. On the other hand the 50.5% reduction of the ADP_e is due to the fact that the greatest contribution to this impact category is given by the photovoltaic system that was reduced from 5.76 kW_p to 1.92 kW_p. Moreover, except for ODP, all indicators show a reduction greater than 20% compared to the base case: GWP (24.2%), AP (22.2%), EP (20.3%), POCP (22.3%), ADP_{ff} (23.9%) and GER (20.4%).

Tab. 9.31 – Life Cycle environmental impacts for the base case and for the redesign solution.

Indicator	**Base Case**	**Redesign Solution**	**Variation**
GWP [kg CO_{2eq}/m^2year]	5.89E+01	4.47E+01	-24.16%
ODP [kg CFC-$11_{eq}/m^2$year]	6.44E-05	6.24E-05	-3.09%
AP [kg SO_{2eq}/m^2year]	2.73E-01	2.13E-01	-22.15%
EP [kg $PO_4{}^{3-}{}_{eq}/m^2$year]	9.33E-02	7.44E-02	-20.29%
POCP [kg C_2H_{4eq}/m^2year]	1.29E-02	1.00E-02	-22.33%
ADP_e [kg Sb_{eq}/m^2year]	1.21E-03	5.37E-04	-55.46%
ADP_{ff} [MJ/m^2year]	7.27E+02	5.53E+02	-23.99%
GER [MJ/m^2year]	1.13E+03	8.96E+02	-20.37%

The life cycle impacts, aggregated in the different building life cycle stages, for the base case and for the redesign solution are shown in Tab. 9.32. In detail, Module A5 and Module C1 do not show any variation as these modules refer respectively to construction stage and to the deconstruction stage of the building. The operational energy use (Module B6), due to the reduction of the imported energy, shows the highest impacts reduction followed by the Modules C2 –C4 and the materials production stage (Modules A1 –A3). In detail, the use stage, with the exception of the GER, which decreased by 36.1%, if compared to the base case shows a reduction of 61.4% for all the impact categories investigated. The materials production stage of the redesign solution (Modules A1 - A3) if compared to the base case shows a reduction between 2.7% (ODP) and 57.5% (ADP_e). Moreover, except for ADP_e and GER (11.2%), all indicators show a reduction lower than 10% compared to the base case: GWP (9.6%), AP (4.4%), EP (8.2%), POCP (7.6%) and ADP_{ff} (9.3%). The transport stage of the redesign solution (Module A4), which however has a contribution lower than 2.3% on the building life cycle impacts both for the base case and for the redesign solution, if compared to the base case shows a reduction between 6.75% (EP) and 8.15% (ADP_e). Since the photovoltaic system of the redesign solution includes only one inverter, unlike the base case that includes 2 inverters, Module B4, which include the replacement of the inverters of the photovoltaic system and the heat pump during the building use stage, shows reductions of between -0.04% (ODP) and -41.55% (ADPe). Finally, the Modules C2 - C4 if compared to the base case shows a reduction between 5.9% (EP) and 31.9% (ODP).

Tab. 9.32 - Life Cycle environmental impacts, aggregated in the different building life cycle stages, for the base case and for the redesign solution.

Indicator		LCA Modules						
		A1-A3	**A4**	**A5**	**B4**	**B6**	**C1**	**C2-C4**
GWP [kg CO_{2eq}/m^{2}year]	Base Case	3.69E+1	1.08	7.41E-2	1.76E+0	1.63E+1	2.38E-2	2.82E+0
	Redesign Solution	3.34E+1	1.00	7.41E-2	1.60E+0	6.29E+0	2.38E-2	2.33E+0
	Variation	**-9.58%**	**-7.05%**	**0%**	**-8.88%**	**-61.37%**	**0%**	**-17.20%**
ODP [kg CFC-11$_{eq}$/m^{2}year]	Base Case	3.37E-5	1.67E-7	1.23E-8	2.85E-5	1.42E-6	2.07E-9	6.26E07
	Redesign Solution	3.28E-5	1.54E-7	1.23E-8	2.85E-5	5.48E-7	2.07E-9	4.26E-7
	Variation	**-2.66%**	**-7.47%**	**0%**	**-0.04%**	**-61.37%**	**0%**	**-31.85%**
AP [kg SO_{2eq}/m^{2}year]	Base Case	1.64E-1	5.93E-3	4.61E-4	7.07E-3	8.06E-2	1.18E-4	1.47E-2
	Redesign Solution	1.57E-1	5.52E-3	4.61E-4	5.61E-3	3.11E-2	1.18E-4	1.27E-2
	Variation	**-4.38%**	**-6.79%**	**0%**	**-20.66%**	**-61.37%**	**0%**	**-13.51%**
EP [kg $PO_4^{3-}$$_{eq}$/m^{2}year]	Base Case	6.29E-2	1.59E-3	4.99E-5	6.99E-3	1.94E-2	2.84E-5	2.30E-3
	Redesign Solution	5.78E-2	1.49E-3	4.99E-5	5.37E-3	7.51E-3	2.84E-5	2.17E-3
	Variation	**-8.16%**	**-6.75%**	**0%**	**-23.15%**	**-61.37%**	**0%**	**-5.92%**
POCP [kg C_2H_{4eq}/m^{2}year]	Base Case	8.42E-3	1.83E-4	1.72E-5	5.02E-4	3.30E-3	4.82E-6	4.87E-4
	Redesign Solution	7.78E-03	1.71E-4	1.72E-5	3.64E-4	1.27E-3	4.82E-6	4.19E-4
	Variation	**-7.60%**	**-6.77%**	**0%**	**-27.52%**	**-61.37%**	**0%**	**-14.07%**
ADP$_e$ [kg Sb$_{eq}$/m^{2}year]	Base Case	1.04E-3	2.87E-6	4.69E-8	1.40E-4	2.27E-5	3.32E-8	2.66E-6
	Redesign Solution	4.41E-04	2.64E-6	4.69E-8	8.18E-5	8.77E-6	3.32E-8	2.83E-6
	Variation	**-57.50%**	**-8.15%**	**0%**	**-41.55%**	**-61.37%**	**0%**	**6.40%**
ADP$_{ff}$ [MJ/m^{2}year]	Base Case	4.67E+2	1.57E+1	8.75E-1	9.20E+0	2.02E+2	2.95E-1	3.19E+1
	Redesign Solution	4.24E+2	1.46E+1	8.75E-1	7.41E+0	7.80E+1	2.95E-1	2.75E+1
	Variation	**-9.26%**	**-7.26%**	**0%**	**-19.43%**	**-61.37%**	**0%**	**-13.72%**
GER [MJ/m^{2}year]	Base Case	6.38E+2	1.80E+1	1.63	1.37E+01	4.03E+2	3.96E-1	5.11E+1
	Redesign Solution	5.66E+2	1.67E+1	1.63	1.09E+01	2.58E+2	3.96E-1	4.27E+1
	Variation	**-11.20%**	**-7.21%**	**0%**	**-20.82%**	**-36.05%**	**0%**	**-16.52%**

In detail, Tab. 9.33 shows the benefits and loads beyond the system boundaries (Module D) for the base case and the redesign solution. Since, as shown in chapter 8, the benefits beyond the system boundaries are mainly due to the surplus energy fed into the electricity grid and since the exported energy in the redesign solution was reduced by 87.6% (from 6392 kWh$_e$ to 732 kWh$_e$), the Module D of the redesign shows a significant reduction if compared to the Module D of the base case. In detail, the benefits beyond the system boundaries of the redesign solution if compared to those of the base case shows a reduction higher than 70% in all the indicators investigated.

Tab. 9.33 - Benefits and loads beyond the system boundary stage for the base case and for the redesign solution.

Indicator	Unit	Base Case	Redesign Solution	Variation
GWP	kg CO_{2eq}/m^2year	-8.49E+01	-1.10E+01	-87.1%
ODP	kg CFC $11_{eq}/m^2year$	-7.65E-06	-1.21E-06	-84.2%
AP	kg SO_{2eq}/m^2year	-4.31E-01	-5.24E-02	-87.9%
EP	kg $PO_4{}^{3-}{}_{eq}/m^2year$	-1.02E-01	-2.62E-02	-74.3%
POCP	kg C_2H_{4eq}/m^2year	-1.78E-02	-2.81E-03	-84.2%
ADPe	kg Sb_{eq}/m^2year	-1.18E-04	-1.45E-05	-87.6%
ADP_{ff}	MJ/m^2year	-1.08E+03	-1.61E+02	-85.1%
GER	MJ/m^2year	-9.21E+02	-1.12E+02	-87.9%

Tab. 9.34 shows the environmental impacts due to the entire building life cycle both in the case where the module D is unconsidered within the system boundaries (total without Module D) and in the case where the Module D is considered in the system boundaries (total with Module D) for the base case and for the redesign solution. If these benefits are included in the system boundaries, all the indicators show a significant reduction in both cases.

In particular, for the base case, except for ODP and ADP_e indicators, the environmental benefits due to the recycling of materials and the surplus energy fed into the electricity grid are able to repay the primary energy use and environmental impacts produced during the entire building life cycle.

For the redesign scenario, even if these benefits, if included in the system boundaries, are not able to repay the primary energy use and environmental impacts produced during the entire building life cycle, would allow to reduce the GWP and the GER respectively by 24.6% and 12.5%, compared to the case in which they are not included in the system boundaries. Moreover, they would allow to reduce the impacts for acidification (AP), eutrophication (EP) and photochemical ozone creation potential (POCP) of 24.6% (-5.24E-2 kg SO2eq/m2year), 35.2% (-2.62E-02 kg PO43-eq/m2year) and 28.1% (-2.81E-3 kg C2H4eq/m2year), respectively. However, the reduction potential of the indicators ODP and ADPe is equal only to 1.94% (-1.21E-06 kg CFC 11eq/m2year) and 2.7% (-1.45E-05 kg Sbeq/m2year), respectively.

Tab. 9.34 – Benefits and loads beyond the system boundary stage for the base case and for the redesign solution.

Indicator	Unit	Total without Module D		Total with Module D	
		Base Case	Redesign Solution	Base Case	Redesign Solution
GWP	kg CO_{2eq}/m^2year	5.89E+01	4.47E+01	-2.60E+01	3.37E+01
ODP	kg CFC $11_{eq}/m^2year$	6.44E-05	6.24E-05	5.68E-05	6.12E-05
AP	kg SO_{2eq}/m^2year	2.73E-01	2.13E-01	-1.58E-01	1.61E-01
EP	kg $PO_4{}^{3-}{}_{eq}/m^2year$	9.33E-02	7.44E-02	-8.45E-03	4.82E-02
POCP	kg C_2H_{4eq}/m^2year	1.29E-02	1.00E-02	-4.87E-03	7.19E-03
ADPe	kg Sb_{eq}/m^2year	1.21E-03	5.37E-04	1.09E-03	5.23E-04
ADP_{ff}	MJ/m^2year	7.27E+02	5.53E+02	-3.50E+02	3.92E+02
GER	MJ/m^2year	1.13E+03	8.96E+02	2.05E+02	7.84E+02

Fig. 9.18 shows the energy and the environmental payback times, calculated without considering Module D (benefits and loads beyond the system boundaries) within the system boundaries for both the base case and the redesign solution. In particular, for the base case, except for ODP and ADP_e, the payback times are lower than 25 years (the service life of the case study). On the other hand, for the redesign solution, since the yearly PV generation was reduced from 8068 kWh_e (base case) to 2689 kWh_e (redesign) and thus due to the reduction energy export towards the grid, the energy and the environmental payback times are greater than the building useful life.

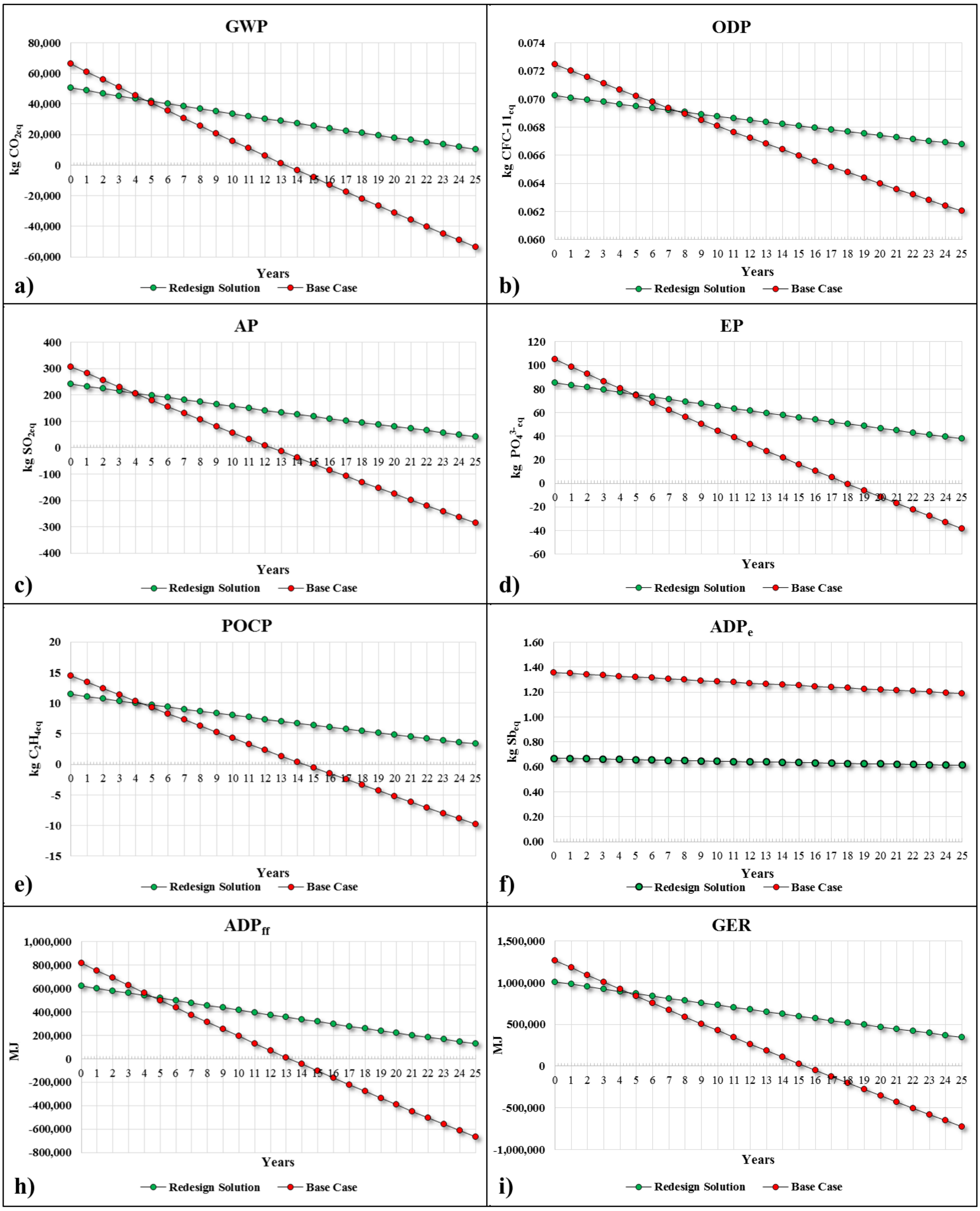

Fig. 9.18 - Energy and the environmental payback times for the base case and for the redesign solution.

The LCA results show that, for all the impact categories investigated, if compared to the base case the proposed solution shows a reduction in the environmental and energy impacts between 3.1% (ODP) and 50.5% (ADP_e). However, since the benefits beyond the system boundaries are mainly due to the surplus energy fed into the electricity grid and since the exported energy in the redesign solution was reduced by 87.6% (from 6392 kWhe to 732 kWh_e), the Module D of the redesign shows a significant reduction if compared to the Module D of the base case. Moreover, since the energy generation in the redesign solution was reduced by 66.7%, while for the base case the energy and the environmental payback times, except for PBT_{ODP} and PBT_{ADPe}, are less than the building required service life, the renewable energy produced during the useful life of the redesign solution is not able to repay the primary energy use and environmental impacts produced during the entire building life cycle.

However, the large scale diffusion of sustainable buildings in a life cycle perspective cannot simply be achieved by oversizing the renewable energy production systems integrated into the building so that the exported energy could compensate the primary energy use and environmental impacts produced during the entire of the building life cycle. In particular, even if PV systems offer a clean, renewable, and domestic energy source, and are essential components of a sustainable energy future, the PV energy surplus may represent an important issue:

1) for the electricity transmission grid operators: the unpredictable presence in the grid of PV generated energy can increase the difficulties in dealing with short-term transients, electricity load, non-dispatchable power and intermittency. Moreover, there are however some challenges needed to be solved to achieve a high penetration of intermittent electricity production in the electric power system, such as frequency regulation, the ability to rapidly start and ramp the remaining electric power generation and better match the consumption with the intermittent generation to avoid exceeding voltage limits.

2) for the PV system owners: with decreased subsidies for PV electricity in several countries, oversizing the PV systems almost always makes them unprofitable, because the selling price of electricity is generally less than the purchase price. If only a very small part of the PV generation is used to supply the local load, benefits may not compensate disbursements. Moreover, instead of giving a benefit to the community, an amount of surplus electricity generated by a great number of PV systems may represent a significant problem for the grid operators. On the other hand, self-consumption, optimized through the use of energy

storage systems and demand side management, could raise the profit of PV systems, because it is very gainful for both the self-producing consumer, whose energy bills will lower, and the electrical manufacturers and grid operators that will reduce costs for transmission and distribution.

3) for the environment: an energy policy that economically supports the PV electricity generated may be responsible of high levels of greenhouse gas emission and fossil fuel importation. Moreover, traditional electric power systems are designed in large part to utilize large base load power plants, with limited ability to rapidly ramp output or reduce output below a certain level. From the point of view of fuel utilization, this type plants generally are much less efficient, and therefore more environmental impacts are produced, when they do not work in nominal conditions. Finally, the increase in demand variability created by intermittent sources such as photovoltaic could increase the GHG emissions as the peak power will be supplied by rapid startup power plants which are very impacting in terms of GHG emissions.

9.8.3 Preliminary cost analysis results

Tab. 9.35 shows the preliminary cost analysis results for the base case and for the redesign solution. The results show that the redesign solution allows to reduce the initial investment costs of about € 4577. The yearly economic gain due to the decrease of the exported energy is reduced to only around € 24, while the costs of energy imported from the grid decrease by around € 115.

Tab. 9.35 – Preliminary cost analysis results for the redesign solution.

		Base Case [€]	**Envelope Redesign [€]**
Investment cost	Insulation panel	2,624	1,921
	Transparent envelope	4,814	1,028
	Opaque envelope	2,407	6,159
	PV system	8,640	2,880
	EES system	-	1,920
	Tot.	18,485	13,908
Yearly gain due to the electricity fed into the grid		359	43
Yearly cost of the electricity purchased from the grid		193	78

Fig. 9.19 shows the trend of the NPV_r considering the different discount rates, it also shows the trend of the NPV_r considering a discounted rate of 0.55%. This represents the limit case in which the redesign solution is economically feasible (NPV_r after 25 years equals 0). The trend of the NPV_r is decreasing because, due to the reduction in exported energy, the yearly net cash inflow of the redesign solution (-35€) is lower than that of the base case (+166 €). However, the results show that the redesign solution is economically feasibility by either a 2% discount rate or a 4% discount rate. In particular, considering a discount rate of 2%, NPV_r is equal to € 740 after 25 years, which means that the redesign solution has produced a profit of € 740. Using a higher discount rate make the reduction of the investment cost of the redesign solution more profitable. In detail, by increasing the rate to 4 %, the NPV_r is increase by 103%, from € 740 to € 1,507.

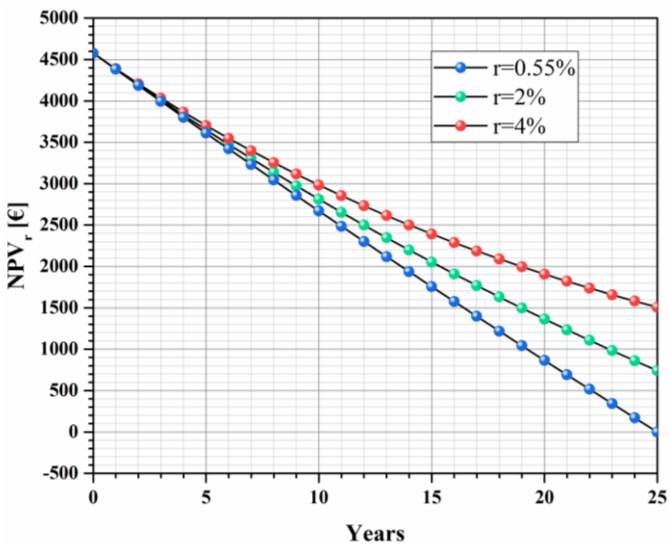

Fig. 9.19 – NPV_r analysis for the redesign solution.

9.9 CHAPTER CONCLUSIONS

The building energy analysis revealed that the main issue that the building must face, from a thermo-physical point of view, is overheating in summer. In fact, due to the high solar radiation transmitted through the large glass façades and the lightweight envelope, during summer the air temperature can be higher than 35 °C when free-floating. For this reason, to decrease the risk of overheating in summer and reduce the energy needed for cooling, into the building redesign the windows area of the south-east façade and of the north-west façade were reduced to the 15%, the thickness of the insulation panels of the walls, the roof and the floor was also changed from 9 cm to 6 cm, and a simple ventilation strategy to model occupant reactions to temperature variation was implemented allowing a reduction of the building energy demand of about 17% if compared to the existing building, with a decrease of the cooling consumption of about 57.3%.

Moreover, even though the overall PV energy generation (about 8,000 kWhe) in a year surpasses the electricity consumption (2,700), about 79% of the energy produced is fed into the grid and about 47% of the electricity consumption is supplied by electricity imported from the electricity grid. For these reasons, in order to optimize the self-consumption of generated electricity, in the redesign the building was equipped with 3.84 kWh electric storage system, which allows to match the building energy demand with the PV energy generation, while, in order to reduce the stress on the power grids, the nominal power of the PV system was varied from 5.76 kWp to the 1.92 kWp. The downsizing of the PV system coupled with the sizing of the electrical storage system show that on yearly basis the 81% of the building electric demand is covered by on-site electricity generation. Moreover, as shown by the index $Pe \approx 0$, that shows the probability that the building is acting autonomously of the grid and which on an annual basis varied from 0.9% of the base case to 67.9% of the redesign solution, the battery allows to greatly reduce interactions with the electricity grid.

The LCA results show that, for all the impact categories investigated, if compared to the base case the redesign solution shows a reduction in the environmental and energy impacts between 3.1% (ODP) and 50.5% (ADPe) reaching values above 20% in the case of GWP (24%), AP (22%), EP (20%), POCP (22%), ADPff (24%) and GER (20%).

The preliminary cost analysis results show that the redesign solution is economically feasibility, the relative Net present value (NPV_r) after 25 years is positive by either a 2.00% (NPV_r = € 740) discount rate or a 4% discount rate (NPV_r = € 1,507), which means that, after 25 years, it has produced a profit of € 740 if compared to the base case in the worst case scenario (discount rate equals to 2%).

10 CONCLUSIONS

The energy and environmental performances of a Net Zero Energy housing module located in Messina (Italy) were analyzed in a life cycle perspective. All the life cycle stages, from the materials production to the end-of-life, are examined according to a "from cradle to cradle" approach. Moreover, several building redesign options were investigated, through a multidisciplinary approach towards the entire building life cycle.

This research builds on earlier studies that have considered the reduction or the mitigation of global and local environmental impacts of the building sector (Attia, 2016, 2018). In agreement with these studies, it is possible to state that the operational stage usually can contribute by more than 80–85% share in the total life cycle impacts of conventional buildings (Beccali, Cellura, Fontana, Longo, & Mistretta, 2013; Luisa F Cabeza et al., 2014; Ramesh et al., 2010; Sharma et al., 2011). However, for the case study, the results of life cycle assessment showed that the materials production is the most impactful stage. These findings are in line with the previous studies on the energy and environmental performances of Net Zero Energy Buildings (Blengini & Di Carlo, 2010; Maurizio Cellura et al., 2014; P Chastas, Theodosiou, Bikas, & Kontoleon, 2017; Paleari et al., 2013). Therefore, a greater knowledge of materials and of the incorporated energy is needed, in order to generate a more conscious attitude towards the choice of materials and energy resources during the early design stage (Meex, Hollberg, Knapen, Hildebrand, & Verbeeck, 2018).

Moreover, the design of any type of building, even modular building, requires an integrated and multidisciplinary design approach (Karlessi et al., 2017; Torgal, Mistretta, Kaklauskas, Granqvist, & Cabeza, 2013), covering a number of key aspects such as energy saving, life cycle environmental impacts (Blengini & Di Carlo, 2010), economic feasibility (Goggins, Moran, Armstrong, & Hajdukiewicz, 2016; Sesana & Salvalai, 2013) and many others, to create the conditions for a significant decarbonisation of the building sector.

Finally, while energy performance and environmental effects of traditional buildings have been previously studied in detail, only a limited number of works about prefabricated constructions and more in particular about modular buildings are available in literature. In this context, this research contributes to the current body of knowledge by providing a deeper insight into the environmental performance of modular buildings by investigating the importance of the design of a building to its whole life cycle sustainability performances.

Although the outcomes of the study are based on the specific conditions of the assessed building, the results can be used and extrapolated in wider context. In detail, the main points of conclusions arisen from the results of the case study are reported below:

- The results show that the materials production stage alone accounted for about 50 - 80% of the total environmental impacts caused by the building, so in future projects, in order to follow an eco-design approach, it will be important to choose constructions materials and installations options with lower environmental impacts during this phase. The use stage is the second most impactful stage (about the 31% on average of the total life cycle impacts). The construction process and the end-of-life stages give a marginal contribution to the total impacts. Since the main construction works are performed outside the construction site, the construction of the building is done with few easy operations that require a limited amount of inputs. Furthermore, the selective demolition of the building allows to obtain uniform and separated waste and this increases the possibility of recycling the wastes. This last feature of the building can contribute to the transition to a circular building sector, where the value of products and materials is maintained for as long as possible, and when a product reaches the end of its life, it is used again to create further value through reuse, recycling, remanufacturing, refurbishment, cascading use, reducing the need of primary materials use and the waste production.

- Decisions made during a building's early design stage heavily influence its environmental impacts. Moreover, a mere focus on the use stage performances cannot give the whole picture that is required in the context of a paradigm shift towards decarbonisation policies. Focusing only on the assessment of the energy consumptions related to the use stage quantifies the reduction of the environmental burdens of this stage but it does not guarantee that the life cycle overall performances will be improved. Thus, the integration of the LCA methodology in the design choices is of paramount importance to support the development of sustainable buildings.

  In this context, LCA was used to enable better early stage decision-making by providing feedback on the environmental impacts. In particular, the integration of the LCA into the building design highlights that, for all the impact categories investigated, if compared to the base case, the redesign solution shows a reduction in the environmental and energy impacts between 3.1% (ODP) and 50.5% (ADPe), reaching values above 20% in the case of GWP (24%), AP (22%), EP (20%), POCP (22%), ADPff (24%) and GER (20%).

- Even though the overall PV energy generation (about 8,000 kWhe) in a year surpasses the electricity consumption (2,700), about 79% of the energy produced is fed into the grid and the building imports from the grid about 47% of the electricity needed. Thus, the case study is not independent from the grid (this could be an important feature for a modular building that could be used in areas where, due to several causes, ranging from natural disasters to temporary working needs, it is not possible to connect the building to the electricity grid), but at the current state it needs a continuous bidirectional interaction with the electricity grid. The use of other types of systems fed by renewable energy sources and/or the use of electric energy storage systems might allow a higher load match.

  In this context, the results show that a successful design and construction of a NZEB includes not only energy efficient measures and adoption of renewable energy sources targeting to the minimization of the energy needs, but also an effective grid integration and the optimization of the time coincidence between demand and supply.

The redesign analysis shows that, oversizing the PV system, the building self-sufficiency does not undergo significant improvements. On the other hand, the degree of self-sufficiency of the building is improved by increasing storage capacity that allows to match the electricity demand of the building with its own solar energy generation. The greater the storage, the greater the load cover factor, because the storage system is able to supply the loads even when generation is not taking place. However, as the storage is an environmentally impactful and costly element of the system, it should be as small as possible. Therefore, in order to reach the NZEB target, the challenge is not only limited to reaching a balance between a building's energy consumption and renewable energy production, because a poorly-designed building could even achieve the goal of net zero energy per year simply by means of oversizing the PV system.

- The results also demonstrated the importance of the environmental and energy benefits resulting from the surplus energy fed into the electricity grid. These benefits, although not directly included in the system boundaries but allocated in the benefits and loads beyond the system boundaries, allow to avoid the emission of about 84.9 kg of CO_{2eq}/m^2year and the production of about 920.6 MJ/m^2year of total primary energy.

  However, high penetration of intermittent energy sources technologies such as photovoltaic systems, will impact the operations of the remaining generators on the power system. In detail, wind and solar renewable energy sources may cause fossil-fueled generators to cycle on and off and ramp down to part load more frequently and potentially more rapidly. Increased cycling on and off and ramping down to partial load of fossil-fueled generators also affect emissions and may result in higher emissions rates than steady-state operation. Therefore, the analysis of the overall benefits of replacing fossil-fueled generation with variable renewable generation should also take these aspects into account.

  Moreover, the PV energy surplus fed into the grid may represent an important issue for the management of grids, such as frequency regulation issues. On the other hand, self-consumption, optimized through the use of energy storage systems and demand side management, could raise the profit of PV systems, because it is very gainful for both the self-producing consumer, whose energy bills will lower, and the electrical manufacturers and grid operators that will reduce costs for energy transmission and distribution.

- Generally, the minimization of use stage energy consumption and related polluting emissions is the main objective of the public perspective. On the other hand, when the optimization of building energy performance is faced, it is fundamental to consider also the cost-effectiveness of the design solutions, which is the principal aim of the private perspective. Moreover, while the current technologies related to energy savings, energy efficiency and renewable energies are sufficient to reach, in combination, the NZEB target, one of the primary barriers to the adoption of NZEBs and to energy efficient buildings is linked to economic issues. Whereby, it is indispensable that, staring from very preliminary phase of the building project, a synergy between the energy performance targets and the economic dimension is set up.

  In this context, a preliminary analysis of the economic feasibility of the different design option have been conducted. In particular, the integration of the cost dimension into the building design allowed to integrate into the final building design only cost-effective solutions. For these reason, for example, even if the integration of PCMs into the building envelope shows some benefit, such as indoor temperature stabilization potential and peak load reduction potential, due to the high investment cost, this solution was not selected among the possible solutions to include in the redesign for the case study. Moreover, the preliminary results of the cost analysis show that the final redesign solution is more cost-effective than the base case, as it produce a profit between € 700 and € 1500 compared to the base case after 25 year.

To conclude, the NZEBs assessment methods are often sets of economic, energy and environmental indicators assessed in isolation to each other without any connection. However, it was found that, in order to reach NZEB target in a conflating domains environment, all these aspects, plus many others not directly considered in this work, such as the social aspect and the comfort of the occupants, must be assessed together. The optimization of building design is a complex multi-objective problem with a huge domain of design variables and several potential objective functions. Therefore, the need to address multiple and often contradicting objectives emphasizes the necessity of a holistic approach during all stages of the design process.

In context, the research proposes a multidisciplinary methodical framework which allows to integrate into the building design and investigate at the same time the use stage energy performances, the load matching and the grid interaction issues, the life cycle overall performances and the economic feasibility. It can be used to explore and improve the low sustainability performing areas over the life cycle of new modular building designs. Moreover, the methodological approach can also be adopted for sustainability assessment of other type of constructions.

REFERENCES

Abegg, B. (2011). Energy self-sufficient regions in the European Alps. *Mountain Research and Development*, *31*(4), 367–371.

Action, E. (2011). Implementing the Energy Performance of Buildings Directive (EPBD), Featuring country reports. EU Publications Office.

Adalberth, K., Almgren, A., & Petersen, E. H. (2001). Life cycle assessment of four multi-family buildings. *International Journal of Low Energy and Sustainable Buildings*, *2*(1), 1–21.

Aditya, L., Mahlia, T. M. I., Rismanchi, B., Ng, H. M., Hasan, M. H., Metselaar, H. S. C., … Aditiya, H. B. (2017). A review on insulation materials for energy conservation in buildings. *Renewable and Sustainable Energy Reviews*, *73*, 1352–1365. https://doi.org/https://doi.org/10.1016/j.rser.2017.02.034

Aelenei, L., Paduos, S., Petran, H., Tarrés, J., Ferreira, A., Corrado, V., … Murano, G. (2015). Implementing Cost-optimal Methodology in Existing Public Buildings. *Energy Procedia*, *78*, 2022–2027. https://doi.org/https://doi.org/10.1016/j.egypro.2015.11.197

Al-Hussein, M., Manrique, J. D., & Mah, D. (2009). North Ridge CO2 Analysis Report: Comparison between Modular and On-Site Construction. *University of Alberta, Canada*.

Alanne, K., Salo, A., Saari, A., & Gustafsson, S.-I. (2007). Multi-criteria evaluation of residential energy supply systems. *Energy and Buildings*, *39*(12), 1218–1226. https://doi.org/https://doi.org/10.1016/j.enbuild.2007.01.009

Allen, M. R., Barros, V. R., Broome, J., Cramer, W., Christ, R., Church, J. A., … Dubash, N. K. (2014). IPCC fifth assessment synthesis report-climate change 2014 synthesis report.

Alonso, M. J., & Mathisen, H. M. (2017). Analysis of reduction of energy demands for Zero Emission Renovated Office Building by using thermal mass and ventilative cooling. *Energy Procedia*, *132*, 592–597. https://doi.org/https://doi.org/10.1016/j.egypro.2017.09.750

Ambler, S. (2013). Briefing: Off-site construction of a new nuclear laboratory at Dounreay, Scotland. *Proceedings of the Institution of Civil Engineers - Energy*, *166*(2), 49–52. https://doi.org/10.1680/ener.11.00036

Amiri, A., Caddock, P., & Whitehead, M. (2013). Accounting for the greenhouse gas emissions of construction: a UK case study. *Proceedings of the Institution of Civil Engineers - Civil Engineering*, *166*(2), 82–88. https://doi.org/10.1680/cien.12.00040

Annunziata, E., Frey, M., & Rizzi, F. (2013). Towards nearly zero-energy buildings: The state-of-art of national regulations in Europe. *Energy*, *57*, 125–133.

Aranda-Usón, A., Ferreira, G., López-Sabirón, A. M., Mainar-Toledo, M. D., & Zabalza Bribián, I. (2013). Phase change material applications in buildings: An environmental assessment for some Spanish climate severities. *Science of The Total Environment*, *444*(0), 16–25. https://doi.org/http://dx.doi.org/10.1016/j.scitotenv.2012.11.012

Asadi, E., da Silva, M. G., Antunes, C. H., & Dias, L. (2012). A multi-objective optimization model for building retrofit strategies using TRNSYS simulations, GenOpt and MATLAB. *Building and Environment*, *56*, 370–378. https://doi.org/https://doi.org/10.1016/j.buildenv.2012.04.005

Ascione, F., Cheche, N., Masi, R. F. De, Minichiello, F., & Vanoli, G. P. (2015). Design the refurbishment of historic buildings with the cost-optimal methodology: The case study of a XV century Italian building. *Energy and Buildings*, *99*, 162–176. https://doi.org/https://doi.org/10.1016/j.enbuild.2015.04.027

ASHRAE. (2014). Guideline 14-2014--Measurement of Energy, Demand, and Water Savings. *American Society of Heating, Refrigerating, and Air Conditioning Engineers*.

ASHRAE. (2017). *ASHRAE HANDBOOK: FUNDAMENTALS*. (M. S. Owen, Ed.). Atlanta, GA, USA.

ASHRAE, A. G. (2002). Guideline 14-2002: Measurement of Energy and Demand Savings. *American Society of Heating, Refrigerating and Air-Conditioning Engineers, Atlanta*.

Atanasiu, B., Kouloumpi, I., Thomsen, K. E., Aggerholm, S., Enseling, A., Loga, T., & Witczak, K. (2013). Implementing the cost-optimal methodology in EU countries. BPIE - Buildings Performance Institute Europe.

Athienitis, A., & O'Brien, W. (2015). *Modeling, design, and optimization of net-zero energy buildings*. John Wiley & Sons.

Atmaca, N. (2017). Life-cycle assessment of post-disaster temporary housing. *Building Research & Information*, *45*(5), 524–538.

Attia, S. (2010). Zero Energy Retrofit Case Study of a Chalet in Ain-Sukhna, EGYPT. In *Conference proceedings of American Solar Energy Society-2010*. Arizona.

Attia, S. (2016). Towards regenerative and positive impact architecture: A comparison of two net zero energy buildings. *Sustainable Cities and Society*, *26*, 393–406. https://doi.org/https://doi.org/10.1016/j.scs.2016.04.017

Attia, S. (2018). *Regenerative and positive impact architecture: Learning from case studies*. Springer.

Attia, S., Evrard, A., & Gratia, E. (2012). Development of benchmark models for the Egyptian residential buildings sector. *Applied Energy*, *94*, 270–284.

Aye, L., Ngo, T., Crawford, R. H., Gammampila, R., & Mendis, P. (2012). Life cycle greenhouse gas emissions and energy analysis of prefabricated reusable building modules. *Energy and Buildings*, *47*, 159–168.

Ayoub, J., Aelenei, L., Aelenei, D., & Scognamiglio, A. (2017). *Solution sets for net zero energy buildings: feedback from 30 buildings worldwide*. John Wiley & Sons.

Azari, R. (2014). Integrated energy and environmental life cycle assessment of office building envelopes. *Energy and Buildings*, *82*, 156–162. https://doi.org/https://doi.org/10.1016/j.enbuild.2014.06.041

Baetens, R., de Coninck, R., Helsen, L., & Saelens, D. (2010). The impact of load profile on the grid-interaction of building integrated photovoltaic (BIPV) systems in low-energy dwellings. *Journal of Green Building*, *5*(4), 137–147. Retrieved from http://www.scopus.com/inward/record.url?eid=2-s2.0-

79251516107&partnerID=40&md5=90be3e81bd63b58740dcdfa7a2763783

Baetens, R., De Coninck, R., Van Roy, J., Verbruggen, B., Driesen, J., Helsen, L., & Saelens, D. (2012). Assessing electrical bottlenecks at feeder level for residential net zero-energy buildings by integrated system simulation. *Applied Energy*, *96*, 74–83.

Bağcı, B. (2009). Towards a zero energy island. *Renewable Energy*, *34*(3), 784–789.

Bakis, C. E., Bank, L. C., Brown, Vl., Cosenza, E., Davalos, J. F., Lesko, J. J., … Triantafillou, T. C. (2002). Fiber-reinforced polymer composites for construction—State-of-the-art review. *Journal of Composites for Construction*, *6*(2), 73–87.

Baniassadi, A., Sajadi, B., Amidpour, M., & Noori, N. (2016). Economic optimization of PCM and insulation layer thickness in residential buildings. *Sustainable Energy Technologies and Assessments*, *14*, 92–99.

Barthelmes, V. M., Becchio, C., Bottero, M. C., & Corgnati, S. P. (2014). The influence of energy targets and economic concerns in design strategies for a residential nearly-zero energy building. *Buildings*, *4*(4), 937–962.

Basbagill, J. P., Lepech, M. D., & Ali, S. M. (2012). Human health impact as a boundary selection criterion in the life cycle assessment of pultruded fiber reinforced polymer composite materials. *Journal of Industrial Ecology*, *16*(2), 266–275.

Baumann, M., Peters, J., Weil, M., Marcelino, C., Almeida, P., & Wanner, E. (2017). Environmental impacts of different battery technologies in renewable hybrid micro-grids. In *2017 IEEE PES Innovative Smart Grid Technologies Conference Europe (ISGT-Europe)* (pp. 1–6). https://doi.org/10.1109/ISGTEurope.2017.8260137

Beccali, M., Cellura, M., Fontana, M., Longo, S., & Mistretta, M. (2013). Energy retrofit of a single-family house: Life cycle net energy saving and environmental benefits. *Renewable and Sustainable Energy Reviews*, *27*, 283–293. https://doi.org/10.1016/j.rser.2013.05.040

Becchio, C., Bottero, M. C., Corgnati, S. P., & Ghiglione, C. (2015). nZEB Design: Challenging between Energy and Economic Targets. *Energy Procedia*, *78*, 2070–2075. https://doi.org/https://doi.org/10.1016/j.egypro.2015.11.226

Becchio, C., Corgnati, S. P., Orlietti, L., & Spigliantini, G. (2015). Proposal for a Modified Cost-optimal Approach by Introducing Benefits Evaluation. *Energy Procedia*, *82*, 445–451. https://doi.org/https://doi.org/10.1016/j.egypro.2015.11.835

Becchio, C., Dabbene, P., Fabrizio, E., Monetti, V., & Filippi, M. (2015). Cost optimality assessment of a single family house: Building and technical systems solutions for the nZEB target. *Energy and Buildings*, *90*, 173–187. https://doi.org/https://doi.org/10.1016/j.enbuild.2014.12.050

Beim, A., Nielsen, J., & Vibæk, K. S. (2010). *Three ways of assembling a house*.

Bergdoll, B., Christensen, P., Christensen, P. H., & Oshima, K. (2008). *Home delivery: fabricating the modern dwelling*. The Museum of Modern Art.

Berggren, B., Hall, M., & Wall, M. (2013). LCE analysis of buildings – Taking the step towards Net Zero Energy Buildings. *Energy and Buildings*, *62*, 381–391. https://doi.org/https://doi.org/10.1016/j.enbuild.2013.02.063

Biaou, A. L., & Bernier, M. A. (2008). Achieving total domestic hot water production with renewable energy. *Building and Environment*, *43*(4), 651–660.

Blengini, G. A., & Di Carlo, T. (2010). The changing role of life cycle phases, subsystems and materials in the LCA of low energy buildings. *Energy and Buildings*, *42*(6), 869–880. https://doi.org/https://doi.org/10.1016/j.enbuild.2009.12.009

Bojić, M., Miletić, M., & Bojić, L. (2014). Optimization of thermal insulation to achieve energy savings in low energy house (refurbishment). *Energy Conversion and Management*, *84*, 681–690. https://doi.org/https://doi.org/10.1016/j.enconman.2014.04.095

Bojić, M., Nikolić, N., Nikolić, D., Skerlić, J., & Miletić, I. (2011). Toward a positive-net-energy residential building in Serbian conditions. *Applied Energy*, *88*(7), 2407–2419.

Bonoli, V., & Fabbri, K. (2013). Prestazione energetica e livello ottimale in funzione dei costi, in PONTE. Architettura Tecnica e Legislazione per Costruire. *DEI Tipografia Del Genio Civile*, *4*, 51–67.

Bourrelle, J. S. (2014). Zero energy buildings and the rebound effect: A solution to the paradox of energy efficiency? *Energy and Buildings*, *84*, 633–640.

Boyd, N., Khalfan, M. M. A., & Maqsood, T. (2013). Off-Site Construction of Apartment Buildings. *Journal of Architectural Engineering*, *19*(1), 51–57. https://doi.org/10.1061/(ASCE)AE.1943-5568.0000091

Brandão de Vasconcelos, A., Pinheiro, M. D., Manso, A., & Cabaço, A. (2016). EPBD cost-optimal methodology: Application to the thermal rehabilitation of the building envelope of a Portuguese residential reference building. *Energy and Buildings*, *111*, 12–25. https://doi.org/https://doi.org/10.1016/j.enbuild.2015.11.006

Burman, E., Mumovic, D., & Kimpian, J. (2014). Towards measurement and verification of energy performance under the framework of the European directive for energy performance of buildings. *Energy*, *77*, 153–163.

Butcher, K., & Craig, B. (2015). *Environmental Design: CIBSE Guide A*. Chartered Institution of Building Services Engineers.

Butera, F. M. (2013). Zero-energy buildings: the challenges. *Advances in Building Energy Research*, *7*(1), 51–65.

Cabeza, L. F., Castell, A., & Pérez, G. (2014). 13 - Life cycle assessment (LCA) of phase change materials (PCMs) used in buildings. In F. Pacheco-Torgal, L. F. Cabeza, J. Labrincha, & A. de Magalhães (Eds.), *Eco-Efficient Construction and Building Materials* (pp. 287–310). Woodhead Publishing. https://doi.org/http://dx.doi.org/10.1533/9780857097729.2.287

Cabeza, L. F., Rincón, L., Vilariño, V., Pérez, G., & Castell, A. (2014). Life cycle assessment (LCA) and life cycle energy analysis (LCEA) of buildings and the building sector: A review. *Renewable and Sustainable Energy Reviews*, *29*(0), 394–416. https://doi.org/http://dx.doi.org/10.1016/j.rser.2013.08.037

Cao, S., Hasan, A., & Sirén, K. (2013). On-site energy matching indices for buildings with energy conversion, storage and hybrid grid connections. *Energy and Buildings*, *64*, 423–438.

Cao, X., Li, X., Zhu, Y., & Zhang, Z. (2015). A comparative study of environmental performance between prefabricated and traditional residential buildings in China. *Journal of Cleaner Production*, *109*, 131–143.

Carletti, C., Cellai, G., Pierangioli, L., Sciurpi, F., & Secchi, S. (2017). The influence of daylighting in buildings with parameters nZEB: application to the case study for an office in Tuscany Mediterranean area. *Energy Procedia*, *140*, 339–350. https://doi.org/https://doi.org/10.1016/j.egypro.2017.11.147

Carlisle, N., Van Geet, O., & Pless, S. (2009). *Definition of a'Zero Net Energy'Community*. National Renewable Energy Laboratory (NREL), Golden, CO.

Carlucci, S., Causone, F., De Rosa, F., & Pagliano, L. (2015). A review of indices for assessing visual comfort with a view to their use in optimization processes to support building integrated design. *Renewable and Sustainable Energy Reviews*, *47*, 1016–1033. https://doi.org/https://doi.org/10.1016/j.rser.2015.03.062

Carstens, H., Xia, X., & Yadavalli, S. (2017). Low-cost energy meter calibration method for measurement and verification. *Applied Energy*, *188*, 563–575.

Cartz, J.-P., & Crosby, M. (2007). Building high-rise modular homes. *Structural Engineer*, *85*(1), 20–21. Retrieved from https://www.scopus.com/inward/record.uri?eid=2-s2.0-33846446427&partnerID=40&md5=28467f753c9751cd1423e01e2f0c1f77

Castillo Cagigal, M., Matallanas de Avila, E., Masa Bote, D., Caamaño Martín, E., Gutiérrez Martín, Á., Monasterio-Huelin Maciá, F., & Jiménez Leube, F. J. (2010). Self-consumption enhancement with storage system and demand-side management: GeDELOS-PV system.

Cellura, M., Guarino, F., Longo, S., & Mistretta, M. (2014). Energy life-cycle approach in Net zero energy buildings balance: Operation and embodied energy of an Italian case study. *Energy and Buildings*, *72*(0), 371–381. https://doi.org/10.1016/j.enbuild.2013.12.046

Cellura, M., Guarino, F., Longo, S., & Mistretta, M. (2015). Different energy balances for the redesign of nearly net zero energy buildings: An Italian case study. *Renewable and Sustainable Energy Reviews*, *45*, 100–112. https://doi.org/10.1016/j.rser.2015.01.048

Cellura, M., Guarino, F., Longo, S., & Mistretta, M. (2017). Modeling the energy and environmental life cycle of buildings: A co-simulation approach. *Renewable and Sustainable Energy Reviews*, *80*, 733–742. https://doi.org/https://doi.org/10.1016/j.rser.2017.05.273

CEU, E. P. &. (2004). Directive 2004/18/EC of the European Parliament and of the Council of 31 March 2004 on the coordination of procedures for the award of public works contracts, public supply contracts and public service contracts. *Official Journal of the European Union*, *47*(L134), 114–233.

Chaiyat, N. (2015). Energy and economic analysis of a building air-conditioner with a phase change material (PCM). *Energy Conversion and Management*, *94*, 150–158.

Charron, R., & Athienitis, A. (2006). Design and optimization of net zero energy solar homes (Vol. 112 PART 2, pp. 285–295). Quebec City, QC. Retrieved from http://www.scopus.com/inward/record.url?eid=2-s2.0-33750299097&partnerID=40&md5=a5faf4610e4c711c1d48a748f18bde1c

Chastas, P., Theodosiou, T., & Bikas, D. (2016). Embodied energy in residential buildings-towards the nearly zero energy building: A literature review. *Building and Environment*, *105*, 267–282. https://doi.org/https://doi.org/10.1016/j.buildenv.2016.05.040

Chastas, P., Theodosiou, T., Bikas, D., & Kontoleon, K. (2017). Embodied Energy and Nearly Zero Energy Buildings: A Review in Residential Buildings. *Procedia Environmental Sciences*, *38*, 554–561. https://doi.org/https://doi.org/10.1016/j.proenv.2017.03.123

Chen, S.-Y., Chu, C.-Y., Cheng, M., & Lin, C.-Y. (2009). The autonomous house: a bio-hydrogen based energy self-sufficient approach. *International Journal of Environmental Research and Public Health*, *6*(4), 1515–1529.

Chiang, Y.-H., Hon-Wan Chan, E., & Ka-Leung Lok, L. (2006). Prefabrication and barriers to entry—a case study of public housing and institutional buildings in Hong Kong. *Habitat International*, *30*(3), 482–499. https://doi.org/10.1016/j.habitatint.2004.12.004

Clarke, P., Ailshire, J., Melendez, R., Bader, M., & Morenoff, J. (2010). Using Google Earth to conduct a neighborhood audit: reliability of a virtual audit instrument. *Health & Place*, *16*(6), 1224–1229.

Climator. (2018). Product data sheet Climsel C24. Retrieved November 8, 2018, from https://www.climator.com/en/pcm-climsel/product-data-sheets

Coakley, D., Raftery, P., & Keane, M. (2014). A review of methods to match building energy simulation models to measured data. *Renewable and Sustainable Energy Reviews*, *37*, 123–141. https://doi.org/https://doi.org/10.1016/j.rser.2014.05.007

Cole, R. J., & Fedoruk, L. (2015). Shifting from net-zero to net-positive energy buildings. *Building Research & Information*, *43*(1), 111–120.

Commissie, E. (2004). *Proposal for a Directive of the European Parliament and of the Council amending Directive 2002/22/EC on universal service and users' rights relating to electronic communications networks*. Directive 2002/58/EC concerning the processing of personal data and the protection of privacy in the electronic communications sector and Regulation (EC).

Commission, E. U. (2012). Commission Delegated Regulation (EU) No 244/2012 of 16 January 2012 supplementing Directive 2010/31. *EU of the European Parliament and of the Council on the Energy Performance of Buildings*.

Committee, I. (2001). *International Performance Measurement and Verification Protocol: Concepts and options for determining energy and water savings, Volume I*. National Renewable Energy Lab., Golden, CO (US).

Copiello, S. (2017). Building energy efficiency: A research branch made of paradoxes. *Renewable and Sustainable Energy Reviews*, *69*, 1064–1076. https://doi.org/https://doi.org/10.1016/j.rser.2016.09.094

Corrado, V., Ballarini, I., & Paduos, S. (2014). Assessment of Cost-optimal Energy Performance Requirements for the Italian Residential Building Stock. *Energy Procedia*, *45*, 443–452. https://doi.org/https://doi.org/10.1016/j.egypro.2014.01.048

Crawford, R. H., Bartak, E. L., Stephan, A., & Jensen, C. A. (2016). Evaluating the life cycle energy benefits of energy efficiency regulations for buildings. *Renewable and Sustainable Energy Reviews*, *63*, 435–451. https://doi.org/https://doi.org/10.1016/j.rser.2016.05.061

Crawley, D. B., Hand, J. W., Kummert, M., & Griffith, B. T. (2008). Contrasting the capabilities of building energy performance simulation programs. *Building and Environment*, *43*(4), 661–673. https://doi.org/http://dx.doi.org/10.1016/j.buildenv.2006.10.027

Crawley, D. B., Lawrie, L. K., Pedersen, C. O., & Winkelmann, F. C. (2000). Energy plus: energy simulation program. *ASHRAE Journal*, *42*(4), 49–56.

Crawley, D., Pless, S., & Torcellini, P. (2009). *Getting to net zero*. National Renewable Energy Lab.(NREL), Golden, CO (United States).

Czerwinska, D. (World G. B. C. (2017). Green building: Improving the lives of billions by helping to achieve the UN Sustainable Development Goals. Retrieved September 13, 2018, from http://www.worldgbc.org/news-media/green-building-improving-lives-billions-helping-achieve-un-sustainable-development-goals

D'Agostino, D., Zangheri, P., & Castellazzi, L. (2017). Towards nearly zero energy buildings in Europe: A focus on retrofit in non-residential buildings. *Energies*, *10*(1), 117.

D'Agostino, D., Zangheri, P., Cuniberti, B., Paci, D., & Bertoldi, P. (2016). Synthesis Report on the National Plans for Nearly Zero Energy Buildings (NZEBs). *Joint Research Center (JRC) Publications*.

Dalhammar, C. (2014). Promoting energy and resource efficiency through the Ecodesign Directive. *Scand Stud Law*, *59*, 147–179.

Dalton, G. J., Lockington, D. A., & Baldock, T. E. (2008). Feasibility analysis of stand-alone renewable energy supply options for a large hotel. *Renewable Energy*, *33*(7), 1475–1490.

Dar, U. I., Sartori, I., Georges, L., & Novakovic, V. (2014). Advanced control of heat pumps for improved flexibility of Net-ZEB towards the grid. *Energy and Buildings*, *69*, 74–84. https://doi.org/10.1016/j.enbuild.2013.10.019

Dawes, R. (2010). Building to improve energy efficiency in England and Wales. *Environmental Law Review*, *12*(4), 266–281.

De Almeida, A., Fonseca, P., Schlomann, B., & Feilberg, N. (2011). Characterization of the household electricity consumption in the EU, potential energy savings and specific policy recommendations. *Energy and Buildings*, *43*(8), 1884–1894.

De Coninck, R., & Helsen, L. (2016). Quantification of flexibility in buildings by cost curves–Methodology and application. *Applied Energy*, *162*, 653–665.

de Gracia, A., Rincón, L., Castell, A., Jiménez, M., Boer, D., Medrano, M., & Cabeza, L. F. (2010). Life Cycle Assessment of the inclusion of phase change materials (PCM) in experimental buildings. *Energy and Buildings*, *42*(9), 1517–1523. https://doi.org/https://doi.org/10.1016/j.enbuild.2010.03.022

Del Río, P. (2010). Analysing the interactions between renewable energy promotion and energy efficiency support schemes: The impact of different instruments and design elements. *Energy Policy*, *38*(9), 4978–4989.

Delsante, A. (2004). A Validation of the AccuRate simulation engine using BESTEST. *Canberra, Australia: CSIRO*.

Deng, S., Dai, Y. J., Wang, R. Z., Matsuura, T., & Yasui, Y. (2011). Comparison study on performance of a hybrid solar-assisted CO2 heat pump. *Applied Thermal Engineering*, *31*(17–18), 3696–3705.

Deng, S., Dalibard, A., Martin, M., Dai, Y. J., Eicker, U., & Wang, R. Z. (2011). Energy supply concepts for zero energy residential buildings in humid and dry climate. *Energy Conversion and Management*, *52*(6), 2455–2460. https://doi.org/http://dx.doi.org/10.1016/j.enconman.2010.12.054

Deng, S., Wang, R. Z., & Dai, Y. J. (2014). How to evaluate performance of net zero energy building – A literature research. *Energy*, *71*(0), 1–16. https://doi.org/http://dx.doi.org/10.1016/j.energy.2014.05.007

DoE, U. S. (2010). Energyplus engineering reference. *The Reference to Energyplus Calculations*.

Dokka, T. H., Sartori, I., Thyholt, M., Lien, K., & Lindberg, K. B. (2013). A Norwegian zero emission building definition. *Passivhus Norden*.

Dolmans, D. (2011). Change is going to come. A new mandate: nearly zero energy buildings. *Eur HVAC Rehva J*, *48*(6), 34–37.

Dong, L., Wang, Y., Li, X. H., Jiang, B., & Al-Hussein, M. (2018). Carbon Reduction Measures-Based LCA of Prefabricated Temporary Housing with Renewable Energy Systems. *Sustainability*. https://doi.org/10.3390/su10030718

Doty, S., & Turner, W. C. (2004). *Energy management handbook*. CRC Press.

Doub, E. (2009). Solar Harvest: City of Boulder's First Zero Energy Home. *Ecofutures Building Inc., Boulder, CO, USA*.

Economidou, M., Atanasiu, B., Despret, C., Maio, J., Nolte, I., & Rapf, O. (2011). Europe's buildings under the microscope. A country-by-country review of the energy performance of buildings. *Buildings Performance Institute Europe (BPIE)*, 35–36.

Edenhofer, O., Pichs-Madruga, R., Sokona, Y., & Minx, J. C. (2014). Change 2014: Mitigation of Climate Change. Contribution of Working Group III to the Fifth Assessment Report of the Intergovernmental Panel on Climate Change.

EED. (2012). Directive 2012/27/EU of the European Parliament and of the Council of 25 October 2012 on energy efficiency. Brussels.

Elrayies, G. M. (2017). Thermal Performance Assessment of Shipping Container Architecture in Hot and Humid Climates. *International Journal on Advanced Science, Engineering and Information Technology*, *7*(4), 1114–1126.

EN, B. S. (2011). Sustainability of construction works–Assessment of environmental performance of buildings–Calculation method. *European Committee for Standardisation*.

EPBD, D. (2002). 20 02/91. *EC of the European Parliament and of the Council of*, *16*.

EPBD Recast. (2018). Directive 2018/844/UE of the European Parliament and of Council, 30 May 2018 on the energy performance of buildings (recast) Official Journal of the European Union.

Esbensen, T. V, & Korsgaard, V. (1977). Dimensioning of the solar heating system in the zero energy house in Denmark. *Solar Energy*, *19*(2), 195–199. https://doi.org/https://doi.org/10.1016/0038-092X(77)90058-5

Escamilla, E. Z., & Habert, G. (2015). Global or local construction materials for post-disaster reconstruction? Sustainability assessment of twenty post-disaster shelter designs. *Building and Environment*, *92*, 692–702.

European Central Bank. (2018). European central bank, monetary policy strategy. Retrieved November 16, 2018, from https://www.ecb.europa.eu/mopo/intro/html/index.en.html

European Commission. (2011). A Roadmap for moving to a competitive low carbon economy in 2050. *Brussels, 8.3.2011 COM(2011) 112 Final*. Brussels,.

European Committee for Standardization. (2008). EN 15603: 2008 Energy performance of buildings - Overall energy use and definition of energy ratings.

Faludi, J., Lepech, M. D., & Loisos, G. (2012). USING LIFE CYCLE ASSESSMENT METHODS TO GUIDE ARCHITECTURAL DECISION-MAKING FOR SUSTAINABLE PREFABRICATED MODULAR BUILDINGS. *Journal of Green Building*, *7*(3), 151–170. https://doi.org/10.3992/jgb.7.3.151

Favre, B., & Peuportier, B. (2014). Application of dynamic programming to study load shifting in buildings. *Energy and Buildings, 82,* 57–64.

Feist, W., Peper, S., Kah, O., & von Oesen, M. (2005). Climate neutral passive house estate in Hannover-Kronsberg: construction and measurement results. *PEP Project Information*, (1), 72.

FEMP, M. V. (2008). Guidelines: Measurement and Verification for Federal Energy Projects, Version 3.0. *Energy Efficiency and Renewable Energy*.

Ferrara, M., Fabrizio, E., Virgone, J., & Filippi, M. (2014). A simulation-based optimization method for cost-optimal analysis of nearly Zero Energy Buildings. *Energy and Buildings*, *84*, 442–457. https://doi.org/https://doi.org/10.1016/j.enbuild.2014.08.031

Fibrenet. (2018). Archivi Products - Fibrenet. Retrieved November 5, 2018, from https://www.fibrenet.it/product/

Fokaides, P. A., & Papadopoulos, A. M. (2014). Cost-optimal insulation thickness in dry and mesothermal climates: Existing models and their improvement. *Energy and Buildings*, *68*, 203–212.

Freudenberg Politex. (2015). *EcoZero Insulation panel*. Retrieved from www.environdec.com

Frischknecht, R., Heath, G., Raugei, M., Sinha, P., & de Wild-Scholten, M. (2016). *Methodology guidelines on life cycle assessment of photovoltaic electricity*. National Renewable Energy Lab.(NREL), Golden, CO (United States).

Frischknecht, R., Jungbluth, N., Althaus, H.-J., Doka, G., Dones, R., Heck, T., … Rebitzer, G. (2005). The ecoinvent database: overview and methodological framework (7 pp). *The International Journal of Life Cycle Assessment*, *10*(1), 3–9.

Frischknecht, R., Jungbluth, N., Althaus, H.-J., Hischier, R., Doka, G., Bauer, C., … Humbert, S. (2007). *Implementation of life cycle impact assessment methods. Data v2. 0 (2007). Ecoinvent report No. 3*. Ecoinvent Centre.

Fthenakis, V., Frischknecht, R., Raugei, M., Kim, H. C., Alsema, E., Held, M., & de Wild-Scholten, M. (2011). Methodology guidelines on life cycle assessment of photovoltaic electricity. *IEA PVPS Task*, *12*.

Ganiç, N., & Yılmaz, A. Z. (2014). Adaptation of the cost optimal level calculation method of Directive 2010/31/EU considering the influence of Turkish national factors. *Applied Energy*, *123*, 94–107. https://doi.org/https://doi.org/10.1016/j.apenergy.2014.02.045

Gibb, A. (2007). Offsite Construction Industry Survey–2006. *Build Offsite, London*.

Gil-Baez, M., Barrios-Padura, Á., Molina-Huelva, M., & Chacartegui, R. (2017). Natural ventilation systems in 21st-century for near zero energy school buildings. *Energy*, *137*, 1186–1200. https://doi.org/https://doi.org/10.1016/j.energy.2017.05.188

Gilijamse, W. (1995). Zero-energy houses in the Netherlands. *Proceedings of Building Simulation '95. Madison, Wisconsin, USA*, 276–283.

Givoni, B. (2011). Indoor temperature reduction by passive cooling systems. *Solar Energy*, *85*(8), 1692–1726. https://doi.org/http://dx.doi.org/10.1016/j.solener.2009.10.003

Goggins, J., Moran, P., Armstrong, A., & Hajdukiewicz, M. (2016). Lifecycle environmental and economic performance of nearly zero energy buildings (NZEB) in Ireland. *Energy and Buildings*, *116*, 622–637.

Gu, L. (2007). Airflow network modeling in EnergyPlus. In *Building Simulation* (Vol. 10).

Guinée, J. B. (2002). Handbook on life cycle assessment operational guide to the ISO standards. *The International Journal of Life Cycle Assessment*, *7*(5), 311.

Gustavsson, L., & Joelsson, A. (2010). Life cycle primary energy analysis of residential buildings. *Energy and Buildings*, *42*(2), 210–220. https://doi.org/10.1016/j.enbuild.2009.08.017

Hamada, Y., Nakamura, M., Ochifuji, K., Nagano, K., & Yokoyama, S. (2001). Field performance of a Japanese low energy home relying on renewable energy. *Energy and Buildings*, *33*(8), 805–814.

Hamada, Y., Ochifuji, K., Nagano, K., & Nakamura, M. (2000). Low energy house with ground source heat pump in Hokkaido. In *Proc. World Geothermal Congress* (pp. 3427–3432). Citeseer.

Hamdy, M., Hasan, A., & Siren, K. (2013). A multi-stage optimization method for cost-optimal and nearly-zero-energy building solutions in line with the EPBD-recast 2010. *Energy and Buildings*, *56*, 189–203. https://doi.org/https://doi.org/10.1016/j.enbuild.2012.08.023

Handbook, E. E. D. (2013). EU Energy Efficiency Directive Guidebook for Good Implementation. *The Coalition for Energy Savings*.

Hasan, A., Vuolle, M., & Sirén, K. (2008). Minimisation of life cycle cost of a detached house using combined simulation and optimisation. *Building and Environment*, *43*(12), 2022–2034. https://doi.org/https://doi.org/10.1016/j.buildenv.2007.12.003

Helm, D. (2014). The European framework for energy and climate policies. *Energy Policy*, *64*, 29–35.

Henninger, R. H., & Witte, M. J. (2004). EnergyPlus testing with ANSI/ASHRAE standard 140-2001 (BESTEST). *GARD Analytics*.

Heo, Y., Choudhary, R., & Augenbroe, G. A. (2012). Calibration of building energy models for retrofit analysis under uncertainty. *Energy and Buildings*, *47*, 550–560. https://doi.org/https://doi.org/10.1016/j.enbuild.2011.12.029

Hernandez, P., & Kenny, P. (2010). From net energy to zero energy buildings: Defining life cycle zero energy buildings (LC-ZEB). *Energy and Buildings*, *42*(6), 815–821. https://doi.org/https://doi.org/10.1016/j.enbuild.2009.12.001

Hong, J., Shen, G. Q., Mao, C., Li, Z., & Li, K. (2016). Life-cycle energy analysis of prefabricated building components: an input–output-based hybrid model. *Journal of Cleaner Production*, *112*, 2198–2207.

Hootman, T. (2012). *Net zero energy design: a guide for commercial architecture*. John Wiley & Sons.

Huang, C.-H. J. (2008). *Using internet and query approach of customizing prefabricated houses*. Illinois Institute of Technology.

International Energy Agency. (2017). *Energy Efficiency 2017*. Paris.

Iqbal, M. T. (2004). A feasibility study of a zero energy home in Newfoundland. *Renewable Energy*, *29*(2), 277–289. https://doi.org/https://doi.org/10.1016/S0960-1481(03)00192-7

Islam, H., Zhang, G., Setunge, S., & Bhuiyan, M. A. (2016). Life cycle assessment of shipping container home: A sustainable construction. *Energy and Buildings*, *128*, 673–685.

ISO, E. N. (2005). 13789. *Thermal Performance of Buildings-Transmission and Ventilation Heat Transfer Coefficients-Calculation Method*.

ISO, E. N. (2006a). 14040: 2006. *Environmental Management-Life Cycle Assessment-Principles and Framework. European Committee for Standardization*.

ISO, E. N. (2006b). ISO 14044: 2006. *Environmental management–Life Cycle assessment–Requirements and Guidelines. European Committee for Standardization.*

Jaillon, L. C. (2009). The evolution of the use of prefabrication techniques in Hong Kong construction industry. Hong Kong Polytechnic University.

Jaillon, L., & Poon, C. (2010). Design issues of using prefabrication in Hong Kong building construction. *Construction Management and Economics*, *28*(10), 1025–1042.

https://doi.org/10.1080/01446193.2010.498481

Jiang, F., Wang, X., & Zhang, Y. (2011). A new method to estimate optimal phase change material characteristics in a passive solar room. *Energy Conversion and Management*, *52*(6), 2437–2441. https://doi.org/10.1016/J.ENCONMAN.2010.12.051

Kamal, M. A. (2010). A study on shading of buildings as a preventive measure for passive cooling and energy conservation in buildings. *International Journal of Civil & Environmental Engineering*, *10*(6), 19–22.

Kamali, M., & Hewage, K. (2016). Life cycle performance of modular buildings: A critical review. *Renewable and Sustainable Energy Reviews*, *62*, 1171–1183. https://doi.org/https://doi.org/10.1016/j.rser.2016.05.031

Kamali, M., Hewage, K., & Milani, A. S. (2018). Life cycle sustainability performance assessment framework for residential modular buildings: Aggregated sustainability indices. *Building and Environment*, *138*, 21–41. https://doi.org/https://doi.org/10.1016/j.buildenv.2018.04.019

Karlessi, T., Kampelis, N., Kolokotsa, D., Santamouris, M., Standardi, L., Isidori, D., & Cristalli, C. (2017). The concept of smart and NZEB buildings and the integrated design approach. *Procedia Engineering*, *180*, 1316–1325.

Kawecki, L. R. (2010). *Environmental performance of modular fabrication: Calculating the carbon footprint of energy used in the construction of a modular home*. Arizona State University.

Kilkis, S. (2007). A new metric for net-zero carbon buildings. In *ASME 2007 Energy Sustainability Conference* (pp. 219–224). American Society of Mechanical Engineers.

Kim, D. (2008). Preliminary Life Cycle Analysis of Modular and Conventional Housing in Benton Harbor, MI.

Kim, J.-H., Kim, H.-R., & Kim, J.-T. (2015). Analysis of photovoltaic applications in zero energy building cases of IEA SHC/EBC task 40/annex 52. *Sustainability*, *7*(7), 8782–8800.

Kılkış, Ş. (2012). A net-zero building application and its role in exergy-aware local energy strategies for sustainability. *Energy Conversion and Management*, *63*, 208–217.

Klein, K., Herkel, S., Henning, H.-M., & Felsmann, C. (2017). Load shifting using the heating and cooling system of an office building: Quantitative potential evaluation for different flexibility and storage options. *Applied Energy*, *203*, 917–937. https://doi.org/https://doi.org/10.1016/j.apenergy.2017.06.073

Klein, K., Langner, R., Kalz, D., Herkel, S., & Henning, H.-M. (2016). Grid support coefficients for electricity-based heating and cooling and field data analysis of present-day installations in Germany. *Applied Energy*, *162*, 853–867. https://doi.org/https://doi.org/10.1016/j.apenergy.2015.10.107

Knaack, U., Chung-Klatte, S., & Hasselbach, R. (2012). *Prefabricated systems: Principles of construction*. Walter de Gruyter.

Koschenz, M., & Lehmann, B. (2004). Development of a thermally activated ceiling panel with PCM for application in lightweight and retrofitted buildings. *Energy and Buildings*, *36*(6), 567–578. https://doi.org/http://dx.doi.org/10.1016/j.enbuild.2004.01.029

Kosny, J., Shukla, N., & Fallahi, A. (2013). *Cost analysis of simple phase change material-enhanced building envelopes in southern US climates*. Fraunhofer CSE, Cambridge, MA (United States).

Kottek, M., Grieser, J., Beck, C., Rudolf, B., & Rubel, F. (2006). World map of the Köppen-Geiger climate classification updated. *Meteorologische Zeitschrift*, *15*(3), 259–263.

Kozlovská, M., Kaleja, P., & Struková, Z. (2014). Sustainable Construction Technology Based on Building Modules. *Advanced Materials Research*, *1041*, 231–234. https://doi.org/10.4028/www.scientific.net/AMR.1041.231

Kurnitski, J., Saari, A., Kalamees, T., Vuolle, M., Niemelä, J., & Tark, T. (2011). Cost optimal and nearly zero (nZEB) energy performance calculations for residential buildings with REHVA definition for nZEB national implementation. *Energy and Buildings*, *43*(11), 3279–3288.

Kylili, A., & Fokaides, P. A. (2016). Life Cycle Assessment (LCA) of Phase Change Materials (PCMs) for building applications: A review. *Journal of Building Engineering*, *6*, 133–143. https://doi.org/https://doi.org/10.1016/j.jobe.2016.02.008

Laski, J. (World G. B. C., & Burrows, V. (World G. B. C. (2017). *From Thousands to Billion. Coordinated Action toward 100% Net Zero Carbon Buildings by 2050.* London. Retrieved from http://www.worldgbc.org/sites/default/files/From Thousands To Billions WorldGBC report_FINAL issue 310517.compressed.pdf

Laustsen, J. (2008). Energy efficiency requirements in building codes, energy efficiency policies for new buildings. *International Energy Agency (IEA)*, *2*(8), 477–488.

Lawson, R. M., & Ogden, R. G. (2008). "Hybrid" light steel panel and modular systems. *Thin-Walled Structures*, *46*(7), 720–730. https://doi.org/10.1016/j.tws.2008.01.042

Lawson, R. M., & Ogden, R. G. (2010). Sustainability and process benefits of modular construction. In *Proceedings of the 18th CIB World Building Congress, TG57-Special Track, Salford, UK* (pp. 10–13).

Lawson, R. M., Ogden, R. G., & Bergin, R. (2012). Application of Modular Construction in High-Rise Buildings. *Journal of Architectural Engineering*, *18*(2), 148–154. https://doi.org/10.1061/(ASCE)AE.1943-5568.0000057

Le Dreau, J., & Heiselberg, P. (2016). Energy flexibility of residential buildings using short term heat storage in the thermal mass. *Energy*, *111*, 991–1002.

Leckner, M., & Zmeureanu, R. (2011). Life cycle cost and energy analysis of a Net Zero Energy House with solar combisystem. *Applied Energy*, *88*(1), 232–241. https://doi.org/https://doi.org/10.1016/j.apenergy.2010.07.031

Li, X. X., & Li, G. L. (2013). Exploration of Modular Build of Architectural Space. *Applied Mechanics and Materials*, *357–360*, 338–344. https://doi.org/10.4028/www.scientific.net/AMM.357-360.338

Lindkvist, C., Karlsson, A., Sørnes, K., & Wyckmans, A. (2014). Barriers and Challenges in nZEB Projects in Sweden and Norway. *Energy Procedia*, *58*, 199–206. https://doi.org/https://doi.org/10.1016/j.egypro.2014.10.429

Longo, S., Antonucci, V., Cellura, M., & Ferraro, M. (2013). Life cycle assessment of storage systems: the case study of a sodium/nickel chloride battery. *Journal of Cleaner Production*. https://doi.org/10.1016/j.jclepro.2013.10.004

Lu, N. (2007). Investigation of the designers' and general contractors' perceptions of offsite construction techniques in the United States construction industry. Clemson University.

Lu, N. (2009). The current use of offsite construction techniques in the United States construction industry. In *Construction Research Congress 2009: Building a Sustainable Future* (pp. 946–955).

Lu, N., & Korman, T. (2010). Implementation of building information modeling (BIM) in modular construction: Benefits and challenges. In *Construction Research Congress 2010: Innovation for Reshaping Construction Practice* (pp. 1136–1145).

Lund, H., Marszal, A., & Heiselberg, P. (2011). Zero energy buildings and mismatch compensation factors. *Energy and Buildings*, *43*(7), 1646–1654.

Lützkendorf, T., Foliente, G., Balouktsi, M., & Wiberg, A. H. (2015). Net-zero buildings: incorporating embodied impacts. *Building Research & Information*, *43*(1), 62–81.

Mao, C., Shen, Q., Pan, W., & Ye, K. (2013). Major barriers to off-site construction: the developer's perspective in China. *Journal of Management in Engineering*, *31*(3), 4014043.

Mao, C., Shen, Q., Shen, L., & Tang, L. (2013). Comparative study of greenhouse gas emissions between off-site prefabrication and conventional construction methods: Two case studies of residential projects. *Energy and Buildings*, *66*, 165–176.

Marszal, A. J., & Heiselberg, P. (2011). Life cycle cost analysis of a multi-storey residential net zero energy building in Denmark. *Energy*, *36*(9), 5600–5609.

Marszal, A. J., Heiselberg, P., Bourrelle, J. S., Musall, E., Voss, K., Sartori, I., & Napolitano, A. (2011). Zero Energy Building - A review of definitions and calculation methodologies. *Energy and Buildings*, *43*(4), 971–979. https://doi.org/10.1016/j.enbuild.2010.12.022

Martinez, S., Jardon, A., Navarro, J. M., & Gonzalez, P. (2008). Building industrialization: robotized assembly of modular products. *Assembly Automation*, *28*(2), 134–142. https://doi.org/10.1108/01445150810863716

Masy, G., Georges, E., Verhelst, C., Lemort, V., & André, P. (2015). Smart grid energy flexible buildings through the use of heat pumps and building thermal mass as energy storage in the Belgian context. *Science and Technology for the Built Environment*, *21*(6), 800–811.

Maxa. (2018). High efficiency heat pumps | Products | Maxa. Retrieved November 5, 2018, from https://www.maxa.it/en/prodotti/high-efficiency-heat-pumps-20

Maxoulis, C. N. (2012). The challenges of implementing the EPBD recast (2010/31/EC) effectively, in order to untap its true potential. *Advances in Building Energy Research*, *6*(2), 259–271.

Meex, E., Hollberg, A., Knapen, E., Hildebrand, L., & Verbeeck, G. (2018). Requirements for applying LCA-based environmental impact assessment tools in the early stages of building design. *Building and Environment*, *133*, 228–236. https://doi.org/https://doi.org/10.1016/j.buildenv.2018.02.016

Mehling, H., & Cabeza, L. F. (2008). *Heat and cold storage with PCM*. Berlin, Heidelberg: Springer Berlin Heidelberg. https://doi.org/10.1007/978-3-540-68557-9

Memarian, S., Kari, B. M., Fayaz, R., & Asadi, S. (2018). Single and combined phase change materials: Their effect on seasonal transition period. *Energy and Buildings*, *169*, 453–472. https://doi.org/10.1016/J.ENBUILD.2018.03.085

merimp. (2019). data sheet mis 240. Retrieved January 28, 2019, from http://www.merimp.com/wp-content/uploads/2017/09/data-sheet-mis-230-235-240-w.pdf

Merrigan, T. (2001). *On the path to zero energy homes*. National Renewable Energy Lab., Golden, CO (US).

Mertz, G. a., Raffio, G. S., & Kissock, K. (2007). +ù. In *ASME 2007 Energy Sustainability Conference* (pp. 477–487). American Society of Mechanical Engineers. https://doi.org/10.1115/ES2007-36077

Mertz, G. A., Raffio, G. S., & Kissock, K. (2007). Cost optimization of net-zero energy house. In *ASME 2007 Energy Sustainability Conference* (pp. 477–487). American Society of Mechanical Engineers.

Miller, W., & Buys, L. (2010). Post-occupancy analysis of a Zero Energy Hojme (ZEH).

Ministero dello Sviluppo Economico. (2015). Decreto interministeriale 26 giugno 2015 - Applicazione delle metodologie di calcolo delle prestazioni energetiche e definizione delle prescrizioni e dei requisiti minimi degli edifici. Gazzetta Ufficiale della Repubblica italiana 2015.

Mlecnik, E., Visscher, H., & Van Hal, A. (2010). Barriers and opportunities for labels for highly energy-efficient houses. *Energy Policy*, *38*(8), 4592–4603.

Monahan, J., & Powell, J. C. (2011). An embodied carbon and energy analysis of modern methods of construction in housing: A case study using a lifecycle assessment framework. *Energy and Buildings*, *43*(1), 179–188.

Moon, C. (2014). Three dimensions of sustainability and floating architecture. *International Journal of Sustainable Building Technology and Urban Development*, *5*(2), 123–127. https://doi.org/10.1080/2093761X.2014.908809

Mrkonjic, K. (2006). Autonomous Lightweight Houses: Learning from Yurts. In *PLEA2006–the 23rd Conference on Passive and Low Energy Architecture* (pp. 6–8).

Murdock, K. L. (2009). *Google SketchUp and SketchUp Pro 7 Bible* (Vol. 606). John Wiley & Sons.

Musall, E., Weiss, T., Lenoir, A., Voss, K., Garde, F., & Donn, M. (2010). Net Zero energy solar buildings: an overview and analysis on worldwide building projects. In *EuroSun conference* (pp. 7–8).

Mustaparta, O., Silva, S. M., & Leitão, D. (2013). Potentialities of using PCM in residential buildings in Portugal. *Portugal SB13-Contribution of Sustainable Building to Meet EU 20-20-20 Targets*, 229–236.

Nielsen, P. V., Lin, C.-H., Phillips, D., Al-Alusi, T., Chen, Y., Srebric, J., … Musser, A. (2005). *Indoor Environmental Modelling: Chapter 34 in ASHRAE Handbook, Fundamentals*. American Society of Heating, Refrigerating and Air-Conditioning Engineers, Inc.

Noguchi, M., Athienitis, A., Delisle, V., Ayoub, J., & Berneche, B. (2008). Net zero energy homes of the future: A case study of the EcoTerraTM house in Canada. In *Renewable Energy Congress, Glasgow, Scotland* (pp. 2008–2112).

O'Brien, W., Kesik, T., & Athienitis, A. (2014). Solar Design Days: A Tool for Passive Solar House Design. *ASHRAE Transactions*, *120*(1).

O'Brien, W. T., Athienitis, A. K., & Kesik, T. (2011). Parametric analysis to support the integrated design and performance modeling of net zero energy houses (PART 1, Vol. 117, pp. 945–960). Las Vegas, NV. Retrieved from http://www.scopus.com/inward/record.url?eid=2-s2.0-82055183938&partnerID=40&md5=efc547622210374d9df05d8919e866c1

O'Connor, J. T., O'Brien, W. J., & Choi, J. O. (2015). Industrial project execution planning: Modularization versus stick-built. *Practice Periodical on Structural Design and Construction*, *21*(1), 4015014.

O'Neill, D., & Organ, S. (2016). A literature review of the evolution of British prefabricated low-rise housing. *Structural Survey*, *34*(2), 191–214.

Oberthur, S., & Oberthür, S. (2010). *The new climate policies of the European Union: internal legislation and climate diplomacy*. ASP/VUBPRESS/UPA.

Optimality, C. (2010). Discussing methodology and challenges within the recast Energy Performance of Buildings Directive. *Buildings Performance Institute Europe (BPIE): Brussels, Belgium*.

Orme, M., & Leksmono, N. (2002). Ventilation modelling data guide. *AIVC Guide*, *5*(2002), 80.

Osterman, E., Tyagi, V. V, Butala, V., Rahim, N. A., & Stritih, U. (2012). Review of PCM based cooling technologies for buildings. *Energy and Buildings*, *49*(0), 37–49. https://doi.org/http://dx.doi.org/10.1016/j.enbuild.2012.03.022

Paleari, M., Lavagna, M., & Campioli, A. (2013). Life cycle assessment and zero energy residential buildings. In *PLEA*.

Paleari, M., Lavagna, M., & Campioli, A. (2016). The assessment of the relevance of building components and life phases for the environmental profile of nearly zero-energy buildings: life cycle assessment of a multifamily building in Italy. *The International Journal of Life Cycle Assessment*, *21*(12), 1667–1690.

Pan, Y., Wong, F. K. W., & Hui, E. C. M. (2011). Application of Industrialized Housing System in China: A Chongqing Study (pp. 161–168). https://doi.org/10.1007/978-3-642-15243-6_19

Panagiotidou, M., & Fuller, R. J. (2013). Progress in ZEBs—A review of definitions, policies and construction activity. *Energy Policy*, *62*, 196–206.

Pardo, N., & Thiel, C. (2012). Evaluation of several measures to improve the energy efficiency and CO2 emission in the European single-family houses. *Energy and Buildings*, *49*, 619–630. https://doi.org/https://doi.org/10.1016/j.enbuild.2012.03.006

Parejo-Navajas, T. (2015). A Legal Approach to the Improvement of Energy Efficiency Measures for the Existing Building Stock in the United States Based on the European. *Seattle J. Envtl. L.*, *5*, i.

Park, J., & Kim, S. (2014). A Comparative study of housing life-cycle carbon emissions for the characteristics of structural materials. In *Proceedings of 2014 World Sustainable Building Conference* (pp. 172–179).

Barcelona, Spain.

Parker, D. S. (2009). Very low energy homes in the United States: Perspectives on performance from measured data. *Energy and Buildings*, *41*(5), 512–520.

Parsons, J. (2017). Charting the unfulfilled expectations of prefab. *ENR (Engineering News-Record)*, *278*(14), 14–15. Retrieved from https://www.scopus.com/inward/record.uri?eid=2-s2.0-85019714925&partnerID=40&md5=b524becb35c7779a784f4924ba7e2b8b

Paya-Marin, M. A., Lim, J., & Sengupta, B. (2013). Life-Cycle Energy Analysis of a Modular/Off-Site Building School. *American Journal of Civil Engineering and Architecture*, *1*(3), 59–63. https://doi.org/10.12691/ajcea-1-3-2

Pedersen, C. O. (2007). Advanced zone simulation in EnergyPlus: incorporation of variable properties and phase change material (PCM) capability. In *Building simulation* (pp. 1341–1345).

Perez, R., Seals, R., Ineichen, P., Stewart, R., & Menicucci, D. (1987). A new simplified version of the Perez diffuse irradiance model for tilted surfaces. *Solar Energy*, *39*(3), 221–231.

Perez, R., Stewart, R., Arbogast, C., Seals, R., & Scott, J. (1986). An anisotropic hourly diffuse radiation model for sloping surfaces: description, performance validation, site dependency evaluation. *Solar Energy*, *36*(6), 481–497.

Peters, J. F., Baumann, M., Zimmermann, B., Braun, J., & Weil, M. (2017). The environmental impact of Li-Ion batteries and the role of key parameters–A review. *Renewable and Sustainable Energy Reviews*, *67*, 491–506.

Pietila, A., Beausoleil-Morrison, I., & Newsham, G. R. (2012). Zero peak housing: Exploring the possibility of eliminating electrical draws from houses during periods of high demand on the electrical grid. *Building and Environment*, *58*, 103–113. https://doi.org/10.1016/j.buildenv.2012.06.019

Pikas, E., Thalfeldt, M., & Kurnitski, J. (2014). Cost optimal and nearly zero energy building solutions for office buildings. *Energy and Buildings*, *74*, 30–42. https://doi.org/https://doi.org/10.1016/j.enbuild.2014.01.039

Pinna, R., Costanzo, E., & Romano, S. (2018). Pathways to ZEED. *TECHNE-Journal of Technology for Architecture and Environment*, (1), 40–44.

Pless, S., & Torcellini, P. (2010). *Net-zero energy buildings: A classification system based on renewable energy supply options*. National Renewable Energy Lab.(NREL), Golden, CO (United States).

Pons, O., & Wadel, G. (2011). Environmental impacts of prefabricated school buildings in Catalonia. *Habitat International*, *35*(4), 553–563.

PRè Consultant. (2010). Simapro 8. *PRè Consultant: Amersfoort, The Netherlands*.

Presidente della Repubblica. (2013). Legge 3 agosto 2013, n. 90, Conversione in legge, con modificazioni, del decreto-legge 4 giugno 2013, n. 63. Gazzetta Ufficiale della Repubblica italiana 2013.

Prindle, B., Eldridge, M., Eckhardt, M., & Frederick, A. (2007). The twin pillars of sustainable energy: synergies between energy efficiency and renewable energy technology and policy. *Washington, DC: American Council for an Energy-Efficient Economy*.

Pylsy, P., & Kalema, T. (2008). Concepts for low-energy single-family houses. *Tampereen Teknillinen Yliopisto. Konstruktiotekniikan Laitos. Tutkimusraportti*.

Quale, J., Eckelman, M. J., Williams, K. W., Sloditskie, G., & Zimmerman, J. B. (2012). Construction Matters: Comparing Environmental Impacts of Building Modular and Conventional Homes in the United States. *Journal of Industrial Ecology*, *16*(2), 243–253. https://doi.org/10.1111/j.1530-9290.2011.00424.x

Rahman, M. M. (2013). Barriers of implementing modern methods of construction. *Journal of Management in Engineering*, *30*(1), 69–77.

Ramaji, I. J., & Memari, A. M. (2015). Information exchange standardization for BIM application to multi-story modular residential buildings. In *AEI 2015* (pp. 13–24).

Ramesh, T., Prakash, R., & Shukla, K. K. (2010). Life cycle energy analysis of buildings: An overview. *Energy and Buildings*, *42*(10), 1592–1600. https://doi.org/https://doi.org/10.1016/j.enbuild.2010.05.007

Recast, E. (2010). Directive 2010/31/EU of the European Parliament and of the Council of 19 May 2010 on the energy performance of buildings (recast). *Official Journal of the European Union*, *18*(6), 2010.

Reilly, A., & Kinnane, O. (2017). The impact of thermal mass on building energy consumption. *Applied Energy*, *198*, 108–121. https://doi.org/https://doi.org/10.1016/j.apenergy.2017.04.024

Reinhart, C. F., Mardaljevic, J., & Rogers, Z. (2006). Dynamic daylight performance metrics for sustainable building design. *Leukos*, *3*(1), 7–31.

Reynders, G., Diriken, J., & Saelens, D. (2015). A generic quantification method for the active demand response potential of structural storage in buildings. In *14th International Conference of the International Building Performance Simulation Association, Hyderabad, India*.

Ries, C., Jenkins, J., & Wise, O. (2009). *Improving the energy performance of buildings: Learning from the European Union and Australia* (Vol. 728). Rand Corporation.

Rifkin, J. (2011). *The third industrial revolution: how lateral power is transforming energy, the economy, and the world*. Macmillan.

Ripamonti. (2018). Doors and windows. Retrieved November 5, 2018, from http://www.ripamontiserramenti.it/eng/finestre.aspx

Ristimäki, M., Säynäjoki, A., Heinonen, J., & Junnila, S. (2013). Combining life cycle costing and life cycle assessment for an analysis of a new residential district energy system design. *Energy*, *63*, 168–179.

Rodriguez-Ubinas, E., Rodriguez, S., Voss, K., & Todorovic, M. S. (2014). Energy efficiency evaluation of zero energy houses. *Energy and Buildings*, *83*, 23–35.

Rogelj, J., Den Elzen, M., Höhne, N., Fransen, T., Fekete, H., Winkler, H., … Meinshausen, M. (2016). Paris Agreement climate proposals need a boost to keep warming well below 2 C. *Nature*, *534*(7609), 631.

Rosenow, J., Cowart, R., Bayer, E., & Fabbri, M. (2017). Assessing the European Union's energy efficiency policy: Will the winter package deliver on "Efficiency First"? *Energy Research & Social Science*, *26*, 72–79.

Rosta, S., Hurt, R., Boehm, R., & Hale, M. J. (2008). Performance of a zero-energy house. *Journal of Solar Energy Engineering*, *130*(2), 21006.

Rovers, R. (2014). Zero-energy and beyond: A paradigm shift in assessment. *Buildings*, *5*(1), 1–13.

Ruiz, G. R., & Bandera, C. F. (2017). Validation of Calibrated Energy Models: Common Errors. *Energies*, *10*(10), 1587.

Saari, A., Kalamees, T., Jokisalo, J., Michelsson, R., Alanne, K., & Kurnitski, J. (2012). Financial viability of energy-efficiency measures in a new detached house design in Finland. *Applied Energy*, *92*, 76–83. https://doi.org/https://doi.org/10.1016/j.apenergy.2011.10.029

Sachs, J. D. (2012). From millennium development goals to sustainable development goals. *The Lancet*, *379*(9832), 2206–2211.

Sachs, J. D. (2015). *The age of sustainable development*. Columbia University Press.

Saffari, M., de Gracia, A., Ushak, S., & Cabeza, L. F. (2016). Economic impact of integrating PCM as passive system in buildings using Fanger comfort model. *Energy and Buildings*, *112*, 159–172.

Sajn, N. (2016). Energy efficiency of buildings: A nearly zero-energy future.

Salom, J., Marszal, A. J., Widén, J., Candanedo, J., & Lindberg, K. B. (2014). Analysis of load match and grid interaction indicators in net zero energy buildings with simulated and monitored data. *Applied Energy*, *136*(0), 119–131. https://doi.org/http://dx.doi.org/10.1016/j.apenergy.2014.09.018

Salom, J., Widén, J., Candanedo, J., Sartori, I., Voss, K., & Marszal, A. (2011). Understanding net zero energy buildings: Evaluation of load matching and grid interaction indicators. In *12th Conference of International Building Performance Simulation Association Building Simulation 2011, BS 2011* (pp. 2514–2521). Sydney, NSW. Retrieved from http://www.scopus.com/inward/record.url?eid=2-s2.0-84870163278&partnerID=40&md5=a6158590149d916b2f2e612a675ac175

Santamouris, M., & Kolokotsa, D. (2013). Passive cooling dissipation techniques for buildings and other structures: The state of the art. *Energy and Buildings*, *57*(0), 74–94. https://doi.org/http://dx.doi.org/10.1016/j.enbuild.2012.11.002

Sartori, I., & Hestnes, A. G. (2007). Energy use in the life cycle of conventional and low-energy buildings: A review article. *Energy and Buildings*, *39*(3), 249–257. https://doi.org/10.1016/j.enbuild.2006.07.001

Sartori, I., Napolitano, A., & Voss, K. (2012). Net zero energy buildings: A consistent definition framework. *Energy and Buildings*, *48*, 220–232. https://doi.org/10.1016/j.enbuild.2012.01.032

Sass, L. (2007). Synthesis of design production with integrated digital fabrication. *Automation in Construction*, *16*(3), 298–310.

Schiavo, G. Lo. (2013). The new EU Directive on Energy Efficiency: A critical view. *Maastricht J. Eur. & Comp. L.*, *20*, 321.

Schiavoni, S., Sambuco, S., Rotili, A., D'Alessandro, F., & Fantauzzi, F. (2017). A nZEB housing structure derived from end of life containers: Energy, lighting and life cycle assessment. In *Building Simulation* (Vol. 10, pp. 165–181). Springer.

Schimschar, S., Hermelink, A., Boermans, T., Pagliano, L., Zangheri, P., Voss, K., & Musall, E. (2013). Towards nearly zero-energy buildings—Definition of common principles under the EPBD. *Ecofys, Politecnico Di Milano, University of Wuppertal (Unpublished) for European Commission Google Scholar*.

Schoenborn, J. (2012). A case study approach to identifying the constraints and barriers to design innovation for modular construction. Virginia Tech.

Schulze, T., Gürlich, D., & Eicker, U. (2018). Performance assessment of controlled natural ventilation for air quality control and passive cooling in existing and new office type buildings. *Energy and Buildings*. https://doi.org/https://doi.org/10.1016/j.enbuild.2018.03.023

Sesana, M. M., & Salvalai, G. (2013). Overview on life cycle methodologies and economic feasibility for nZEBs. *Building and Environment*, *67*, 211–216. https://doi.org/https://doi.org/10.1016/j.buildenv.2013.05.022

Sharma, A., Saxena, A., Sethi, M., Shree, V., & Varun. (2011). Life cycle assessment of buildings: A review. *Renewable and Sustainable Energy Reviews*, *15*(1), 871–875. https://doi.org/https://doi.org/10.1016/j.rser.2010.09.008

Simona, P. L., Spiru, P., & Ion, I. V. (2017). Increasing the energy efficiency of buildings by thermal insulation. *Energy Procedia*, *128*, 393–399. https://doi.org/https://doi.org/10.1016/j.egypro.2017.09.044

Smith, R. E. (2010). *Prefab architecture: A guide to modular design and construction*. John Wiley & Sons.

Soares, N., Reinhart, C. F., & Hajiah, A. (2017). Simulation-based analysis of the use of PCM-wallboards to reduce cooling energy demand and peak-loads in low-rise residential heavyweight buildings in Kuwait. In *Building Simulation* (Vol. 10, pp. 481–495). Springer.

Song, Y., Mithraratne, N., & Zhang, H. (2016). Life-time performance of post-disaster temporary housing: A case study in Nanjing. *Energy and Buildings*, *128*, 394–404. https://doi.org/https://doi.org/10.1016/j.enbuild.2016.07.019

Sorrell, S. (2009). Jevons' Paradox revisited: The evidence for backfire from improved energy efficiency. *Energy Policy*, *37*(4), 1456–1469.

Stefanović, A., Bojić, M., & Gordić, D. (2014). Achieving net zero energy cost house from old thermally non-insulated house using photovoltaic panels. *Energy and Buildings*, *76*, 57–63.

Steinhardt, D. A., & Manley, K. (2016). Adoption of prefabricated housing–the role of country context. *Sustainable Cities and Society*, *22*, 126–135.

Stephan, A., & Stephan, L. (2014). Reducing the total life cycle energy demand of recent residential buildings in Lebanon. *Energy*, *74*, 618–637. https://doi.org/https://doi.org/10.1016/j.energy.2014.07.028

Stocker, E., Tschurtschenthaler, M., & Schrott, L. (2015). Cost-optimal renovation and energy performance: Evidence from existing school buildings in the Alps. *Energy and Buildings*, *100*, 20–26. https://doi.org/https://doi.org/10.1016/j.enbuild.2015.04.005

Stocker D. Qin, G., K. Plattner, M. Tignor, S.K. Allen, J. Boschung, A. Nauels, Y. Xia, V. Bex and P.M. Midgley (eds.), T. F. (2013). *IPCC, Climate Change 2013: The Physical Science Basis. Contribution of Working Group I to the Fifth Assessment Report of the Intergovernmental Panel on Climate Change*. Cambridge, United Kingdom and New York, NY, USA, : Cambridge University Press,.

Szalay, Z., & Zöld, A. (2014). Definition of nearly zero-energy building requirements based on a large building sample. *Energy Policy*, *74*, 510–521.

Tabares-Velasco, P. C., Christensen, C., & Bianchi, M. (2012). Verification and validation of EnergyPlus phase change material model for opaque wall assemblies. *Building and Environment*, *54*(0), 186–196. https://doi.org/http://dx.doi.org/10.1016/j.buildenv.2012.02.019

Tadeu, S. F., Alexandre, R. F., Tadeu, A. J. B., Antunes, C. H., Simões, N. A. V, & Silva, P. P. da. (2016). A comparison between cost optimality and return on investment for energy retrofit in buildings-A real options perspective. *Sustainable Cities and Society*, *21*, 12–25. https://doi.org/https://doi.org/10.1016/j.scs.2015.11.002

Thevenard, D. J., & Brunger, A. P. (2002). The development of typical weather years for international locations: part I, algorithms. *ASHRAE Transactions*, *108*, 376.

Thiers, S., & Peuportier, B. (2012). Energy and environmental assessment of two high energy performance residential buildings. *Building and Environment*, *51*, 276–284. https://doi.org/https://doi.org/10.1016/j.buildenv.2011.11.018

Thomas, W. D., & Duffy, J. J. (2013). Energy performance of net-zero and near net-zero energy homes in New England. *Energy and Buildings*, *67*, 551–558.

Torcellini, P. A., & Crawley, D. B. (2006). Understanding zero-energy buildings. *ASHRAE Journal*, *48*(9), 62.

Torcellini, P., Pless, S., Deru, M., & Crawley, D. (2006). *Zero Energy Buildings: A Critical Look at the Definition; Preprint*. National Renewable Energy Laboratory (NREL), Golden, CO.

Torgal, F. P., Mistretta, M., Kaklauskas, A., Granqvist, C. G., & Cabeza, L. F. (2013). *Nearly Zero Energy Building Refurbishment: A Multidisciplinary Approach*. Springer Science & Business Media.

Tse, H., & Fung, A. S. (2007). Feasibility of low-rise Net-Zero Energy Houses for Toronto. In *2nd Canadian Solar Buildings Conference, Calgary*. Citeseer.

Uddin, N. (2013). *Developments in fiber-reinforced polymer (FRP) composites for civil engineering*. Elsevier.

Ulloa, C., Arce, M. E., Rey, G., Míguez, J. L., & Hernández, J. (2017). Recycling COR-TEN® Sea Containers into Service Modules for Military Applications: Thermal Analysis. *Energies* . https://doi.org/10.3390/en10060820

UN. (2015). Transforming our world: The 2030 agenda for sustainable development.

UN Environment and International Energy Agency. (2017). *Towards a zero-emission, efficient, and resilient buildings and construction sector. Global Status Report 2017*.

UNI, E. N. (2011a). 12464-1: 2011. *Light and Lighting. Lighting of Work Places. Part, 1*.

UNI, E. N. (2011b). 15978. Sustainability of construction works. *Assessment of Environmental Performance of Buildings*.

UNI, E. N. (2014). 15804, 2014: Sostenibilità delle costruzioni-Dichiarazioni ambientali di prodotto-Regole quadro di sviluppo per categoria di prodotto. *Ente Nazionale Italiano Di Unificazione, 23*.

Union, I. (2014). *Communication from the Commission to the European Parliament, the Council, the European Economic and Social Committee and the Committee of the Regions*. Brussels.

US DOE. (2008). Building Technologies Program. Planned Program Activities for 2008-2012.

Vale, B., & Vale, R. (2006). Zero energy housing retrofit. In *2006) Clever design, affordable comfort: a challenge for low energy architecture and urban planning PLEA 2006 23rd International Conference on Passive and Low Energy Architecture, Geneva* (pp. 6–8).

Vale, B., & Vale, R. J. D. (1975). *The Autonomous House: design and planning for self-sufficiency*. Thames and Hudson.

Vale, B., & Vale, R. J. D. (2000). *The new autonomous house: Design and planning for sustainability*. Thames & Hudson.

Van Oers, L. (2015). CML-IA database, characterisation and normalisation factors for midpoint impact category indicators. *Version*, *4*, 5.

Verbeke, S., & Audenaert, A. (2018). Thermal inertia in buildings: A review of impacts across climate and building use. *Renewable and Sustainable Energy Reviews*, *82*, 2300–2318. https://doi.org/https://doi.org/10.1016/j.rser.2017.08.083

Verbruggen, B., De Coninck, R., Baetens, R., Saelens, D., Helsen, L., & Driesen, J. (2011). Grid impact indicators for active building simulation. In *Innovative Smart Grid Technologies (ISGT), 2011 IEEE PES* (pp. 1–6). IEEE.

Vogt, M., Remmen, P., Lauster, M., Fuchs, M., & Müller, D. (2018). Selecting statistical indices for calibrating building energy models. *Building and Environment*, *144*, 94–107.

Voss, K. (2012). Nearly-zero, net zero and plus energy buildings. *REHVA Journal, Dec*.

Voss, K., Goetzberger, A., Bopp, G., Häberle, A., Heinzel, A., & Lehmberg, H. (1996). The self-sufficient solar house in Freiburg—Results of 3 years of operation. *Solar Energy*, *58*(1–3), 17–23.

Voss, K., & Musall, E. (2013). *Net zero energy buildings: International projects of carbon neutrality in buildings*. Walter de Gruyter.

Voss, K., Musall, E., & Lichtmeß, M. (2011). From low-energy to Net Zero-Energy Buildings: status and perspectives. *Journal of Green Building*, *6*(1), 46–57.

Voss, K., Sartori, I., Napolitano, A., Geier, S., Gonçalves, H., Hall, M., … Musall, E. (2010). Load matching and grid interaction of net zero energy buildings. In *EUROSUN 2010 International Conference on Solar Heating, Cooling and Buildings*.

Wang, L., Gwilliam, J., & Jones, P. (2009). Case study of zero energy house design in UK. *Energy and Buildings*, *41*(11), 1215–1222.

Webster, L., Bradford, J., Sartor, D., Shonder, J., Atkin, E., Dunnivant, S., … Schiller, S. (2015). *M&V Guidelines: Measurement and Verification for Performance-Based Contracts*. Version 4.0, Technical Report.

Weston, M. (2010). Memory Mesh: Conformationally Adaptive Solar Shading. In *Proceedings of the 14th Congress of the Iberoamerican Society of Digital Graphics, pp. Bogotá, Colombia, November* (pp. 17–19).

Wilford, C., & Ramos, M. (2009). Zero Carbon Compendium Who's Doing What in Housing Worldwide. *NHBC Foundation, Amsterdam*.

Wong, I. L. (2017). A review of daylighting design and implementation in buildings. *Renewable and Sustainable*

Energy Reviews, *74*, 959–968. https://doi.org/https://doi.org/10.1016/j.rser.2017.03.061

You, M., Zhang, X., Wang, J., & Wang, X. (2009). Polyurethane foam containing microencapsulated phase-change materials with styrene–divinybenzene co-polymer shells. *Journal of Materials Science*, *44*(12), 3141–3147. https://doi.org/10.1007/s10853-009-3418-7

Zacà, I., D'Agostino, D., Congedo, P. M., & Baglivo, C. (2015). Assessment of cost-optimality and technical solutions in high performance multi-residential buildings in the Mediterranean area. *Energy and Buildings*, *102*, 250–265. https://doi.org/https://doi.org/10.1016/j.enbuild.2015.04.038

Zhu, L., Hurt, R., Correa, D., & Boehm, R. (2009). Comprehensive energy and economic analyses on a zero energy house versus a conventional house. *Energy*, *34*(9), 1043–1053.